Modelling and design optimisation of renewable energy communities to support the energy transition aspirations of rural and islanded populations

A Thesis Submitted for the Degree of Doctor of Philosophy

Ву

**Robert Garner** 

Department of Mechanical and Aerospace Engineering, Brunel University London

2025

#### Abstract

The market for distributed Renewable Energy Systems has increased considerably in recent decades, driven by the necessity for a reduction in global carbon emissions in an effort to combat climate change.

While the focus on decarbonising the energy sector in Europe has been successful in recent years, it has disproportionately benefited urban population centres. Those who live in built-up environments will likely have better access to newer, greener technology, with islanded communities often relying on a weaker grid with fossil fuel reliant infrastructure. These communities are therefore at high risk of being left behind in the energy transition towards net-zero emissions.

This study presents a novel solution to the problem of decarbonising remote, islanded populations by means of Renewable Energy Communities (RECs). The test location, Formentera, was chosen due to its unique set of challenges and opportunities regarding energy security and access to clean energy. A generalised, modular model was developed in Python, allowing the integration of generation (wind and solar), storage (battery and hydrogen), and real-world data from the test location. The model simulates the dynamic dispatch of the system over hourly increments to evaluate the annual performance.

The system is optimised using the Non-dominated Sorting Genetic Algorithm (NSGA-II), which identified an inherent trade-off relationship between cost reduction and decarbonisation of the REC. Results show that the deployment in the case study location can deliver improvements in both cost and emissions relative to a grid-only scenario. A comparison of storage configurations shows a considerable benefit to co-locating batteries and a regenerative hydrogen storage system due to the latter's ability to act as a seasonal storage buffer. Findings suggest that a 'friendly' local trading policy outperforms a market-based regime on cost savings, and ensures better energy equity between members.

The analysis incorporates Monte Carlo simulations of estimated assumption ranges and a variance-based Sobol sensitivity analysis. These methods reveal the range of variability in the result arising from uncertainty in the input assumptions, including those which most impact performance, thus identifying high-risk areas for project monitoring and intervention. These can not only support the design stage of the REC but also contribute to risk-aware planning and policy development.

The model's development in Python allows for a scalable foundation on which future research can be built, and contribute to the commercialisation of an REC-focused planning tool. The outcome of this work provides a novel, quantitative guide for energy developers, government entities, and network operators on REC development. The model framework can be used to trade-off system cost and emissions reduction, design for and navigate potential future energy policy, assess energy equity, and ensure a clearer route to realising the net-zero aspirations of rural, islanded communities.

## Acknowledgements

I would like to thank the following people who have helped me carry out and complete this research thesis:

Firstly, Dr Zahir Dehouche for guiding me through the project and for your enthusiasm and subject matter knowledge. Secondary, Dr Carola König for your tireless support through the second half of my research time, during the write-up phase and some of the most challenging moments - I could not thank you enough.

I would also like to thank all those part of the VPP4ISLANDS project, particularly Sergi at the Consel Insular de Formentera, for providing input data and extending their valuable knowledge and insight.

Finally I would like to thank my family and friends for cheering me on, especially my fiancé, Nina, for encouraging me to pursue the PhD and supporting through all the late nights and weekends.

I declare that the research within this thesis is the original work of the author. The research has not been previously submitted as part of the requirement for an award or higher degree in this or any other university. The research work was conducted by the author except where specified, or where acknowledgments are made and by references. I do not authorise Brunel University to reproduce this thesis by any means or to share the work with other institutions or individuals for the purpose of scholarly research or for any other purpose apart from the requirement to assess the research.

Signature:

Date: 08/05/2025

#### **Publications and Dissemination**

- Robert Garner. "Renewable Energy Community VPP Design and Modelling for Sustainable Islands" (poster presentation), International Conference on Evolving Cities, Southampton, 2021
- Robert Garner, Gerard Jansen, Zahir Dehouche. "Analysis of Obstacles to Innovation in Islands" (report), [online] available at: https://cordis.europa.eu/project/id/957852/results, 2021
- Robert Garner, Gerard Jansen, Zahir Dehouche. "Report on the VPP4ISLANDS concept" (report), [online] available at: https://cordis.europa.eu/project/id/957852/results, 2021
- Robert Garner, Zahir Dehouche. "Renewable Energy Community VPP Design and Modelling for Sustainable Islands" (book chapter), in VPP2021: Virtual Power Plant Solution for Future Smart Energy Communities, Taylor and Francis Group, 2022
- Robert Garner, Zahir Dehouche. "Optimal Design and Analysis of a Hybrid Hydrogen Energy Storage System for an Island-Based Renewable Energy Community" (article), in energies 2023, 16, 7363
- Robert Garner, Abdelaziz Abualshawareb. "Modelling and Design of a Hybrid Fuel Cell and Metal Hydride Storage for VPPs" (poster presentation), Brunel Research Festival, 2022
- "VPP4ISLANDS: Virtual Power Plant For Smart and Interoperable Islands", (presentation), Brunel PGR Symposium, 2023

## Contents

| 1 | Intr               | oducti  | on   | 16         |
|---|--------------------|---------|--|------------|
|   | 1.1                | Backg   | round  | 16         |
|   | 1.2                | Aims a  | and Research Questions                                 | 21         |
|   | 1.3                | Projec  | t Approach   | 22         |
|   | 1.4                | Resear  | ch Methods   | 22         |
| 2 | ${ m Lit}\epsilon$ | erature | Review   | <b>2</b> 6 |
|   | 2.1                | Overv   | iew and Structure                                      | 26         |
|   | 2.2                | Virtua  | l Power Plant Definition                               | 28         |
|   |                    | 2.2.1   | VPP Policy and Regulation                              | 28         |
|   |                    | 2.2.2   | Technology, Reliability and Services                   | 33         |
|   |                    | 2.2.3   | Environmental Considerations and Societal Value        | 37         |
|   | 2.3                | Virtua  | l Power Plant and Microgrid Case Studies               | 39         |
|   | 2.4                | Renew   | rable Energy Communities                               | 50         |
|   | 2.5                | Asset   | Modelling, Control, and Design Optimisation            | 60         |
|   |                    | 2.5.1   | Renewable Energy Assets                                | 61         |
|   |                    | 2.5.2   | Energy Storage Systems                                 | 68         |
|   |                    | 2.5.3   | Optimisation Approaches                                | 76         |
|   | 2.6                | Review  | v Summary  | 84         |
| 3 | Cas                | e Stud  | y Definition and Modelling Methods                     | 86         |
|   | 3.1                | Overv   | iew  | 86         |
|   | 3.2                | Field ' | Test Location  | 88         |
|   |                    | 3.2.1   | Location Overview, Geography, and Climate              | 88         |
|   |                    | 3.2.2   | Energy Community Definition and Building Load Profiles | 93         |
|   | 3.3                | Energy  | y Community Asset Models                               | 99         |
|   |                    | 3.3.1   | PV Solar Array   | 00         |
|   |                    | 3.3.2   | Wind Turbine   | 03         |
|   |                    | 3.3.3   | Battery Storage System                                 | 05         |
|   |                    | 3.3.4   | Regenerative Hydrogen Storage System                   | 06         |

|   | 3.4                                   | System Control Logic and Trading   | )7 |  |
|---|---------------------------------------|--|----|--|
|   |                                       | 3.4.1 Energy Management Strategy   | )7 |  |
|   |                                       | 3.4.2 Community Energy Trading   | )8 |  |
|   | 3.5                                   | Design Optimisation and Performance Analysis                             | .2 |  |
|   |                                       | 3.5.1 Economic and Environmental Objective Functions                     | .3 |  |
|   |                                       | 3.5.2 Genetic Algorithm Implementation                                   | .6 |  |
|   | 3.6                                   | Model Assumptions  | 20 |  |
|   | 3.7 Technical Structure and Execution |  |    |  |
| 4 | Res                                   | m ults   | 25 |  |
|   | 4.1                                   | Asset Model Validation   | 26 |  |
|   |                                       | 4.1.1 PV Solar   | 27 |  |
|   |                                       | 4.1.2 Wind Turbine   |    |  |
|   | 4.2                                   | Multi-Objective Optimisation of the Renewable Energy Community System 13 |    |  |
|   |                                       | 4.2.1 Optimal System Design  |    |  |
|   |                                       | 4.2.2 REC System Performance at the Extrema                              |    |  |
|   | 4.3                                   | Sensitivity Scenarios  |    |  |
|   |                                       | 4.3.1 Scenario Set 1: Battery and Hydrogen Storage Comparison 14         | 17 |  |
|   |                                       | 4.3.2 Scenario Set 2: REC Energy Trade Policies                          |    |  |
|   | 4.4                                   | Results Uncertainty Analysis   | 53 |  |
|   |                                       | 4.4.1 Parameter Uncertainty Propagation                                  | 54 |  |
|   |                                       | 4.4.2 Sensitivity Analysis   |    |  |
| 5 | Disc                                  | cussion 16   | 3  |  |
|   | 5.1                                   | Research Context and Objectives  |    |  |
|   | 5.2                                   | Multi-Objective Design Results   |    |  |
|   | 5.3                                   | System Performance and Renewable Asset Sizing                            |    |  |
|   | 5.4                                   | Additional Scenarios   |    |  |
|   | 5.5                                   | Uncertainty and Sensitivity Analysis                                     |    |  |
|   | 5.6                                   | Synthesis and Broader Implications of RECs                               | ′2 |  |
| 6 | Con                                   | clusions 17  | '6 |  |
|   | 6.1                                   | Main Conclusions of this Study   | 76 |  |
|   | 6.2                                   | Recommendations for Further Work   |    |  |
| A | Sun                                   | plementary Analysis 19   | 7  |  |
|   | _                                     | Solution Deployment and Test   |    |  |
| В | Inp                                   | ıt data tables 20  | 2  |  |
|   | •                                     |  |    |  |

| $\mathbf{C}$ | Sam | ple Model Code                       | <b>20</b> 4 |  |  |
|--------------|-----|--------------------------------------|-------------|--|--|
|              | C.1 | Energy System Model Classes          | . 204       |  |  |
|              | C.2 | Multi-objective Optimisation Routine | . 213       |  |  |

# List of Figures

| Europe power sector generation mix (Eurostat)                                    | 17   |
|--|--|
| Renewable energy community system architecture (Environmental Investigation      |  |
| Agency 2017)   | 18   |
| The percentage of the European population living in rural and decentralised      |  |
| communities (source: World Bank database of as 2024)                             | 19   |
| A simple schematic of a typical Virtual Power Plant configuration                | 20   |
| A flow diagram illustrating the content of this thesis                           | 24   |
| A simplified view of the traditional energy market structure                     | 29   |
| Proposed local micro-market concept and services provision                       | 31   |
| Potential services of VPPs   | 33   |
| The FENIX VPP concept  | 41   |
| The Edison VPP concept   | 43   |
| VPP concepts developed as part of the TWENTIES project                           | 45   |
| Con Edison VPP location  | 46   |
| Internal Rate of Return (IRR) of the hybrid VPP fleet                            | 47   |
| AGL hybrid end user system   | 48   |
| Location of VPP in Australia   | 48   |
| Example dispatch response from the VPP battery fleet compared to the             |  |
| target response  | 49   |
| Approximate number of community energy initiatives from nine countries           |  |
| within Europe  | 52   |
| Locations of the 24 council and community ECSC PV solar installations            | 54   |
| small-scale hydroelectric generator located on the Isle of Eigg $\ldots\ldots$   | 55   |
| Example solar Energy Community created as part Repsol Solmatch                   | 57   |
| The applications of solar cells and panels have progressed significantly over    |  |
| the past 50 years, from space exploration to energy production at scale. $$      | 61   |
| The electrical field induced by free electrons in the n-type layer $\dots \dots$ | 62   |
| A lumped model diagram showing the mathematically modelled components            |  |
| of the solar cell $\dots$  | 62   |
|  | Renewable energy community system architecture (Environmental Investigation Agency 2017) |

| 2.19 | A PV solar IV curve showing the impact of changing the series resistance                        |     |
|------|---|-----|
|      | on the output power voltage and current   | 64  |
| 2.20 | Diagram showing some types of wind turbines and their rotor power coefficient                   |     |
|      | and tip speed ratio   | 66  |
| 2.21 | Suitability of various ESS technologies for grid applications                                   | 69  |
| 2.22 | The charge in discharge characteristics of lithium ion batteries $\dots \dots$                  | 70  |
| 2.23 | Li-ion battery equivalent circuit diagram under charging condition $\dots$                      | 71  |
| 2.24 | Diagram showing the working principle of a hydrogen fuel cell                                   | 72  |
| 2.25 | Diagram displaying the operating principles of PEM and Alkaline electrolysis                    | 74  |
| 2.26 | A typical polarisation curve of a PEM electrolyser  | 75  |
| 2.27 | Example of a constrained LP problem illustrating the feasible region                            | 78  |
| 2.28 | The classification of metaheuristic algorithms  | 80  |
| 2.29 | Components of a Genetic Algorithm   | 81  |
| 2.30 | A 2D search plane illustrating the existence of both a local and global minimum $$              | 82  |
| 3.1  | Map showing the location of Formentera in relation to the Iberian peninsula.                    | 88  |
| 3.2  | The meteorological conditions by hour of day and day of year for the proposed                   |     |
|      | EC location   | 90  |
| 3.3  | The interconnections between the mainland and Formentera, illustrating                          |     |
|      | the increase in emissions intensity of the island communities                                   | 91  |
| 3.4  | ${\bf Historical\ emissions\ intensity\ on\ the\ Island\ of\ Formentera\ 2017-2020,\ obtained}$ |     |
|      | from REE  | 92  |
| 3.5  | Daily and annual average emissions in 2020 for Formentera, obtained from                        |     |
|      | REE   | 93  |
| 3.6  | Locations of the individual buildings   | 93  |
| 3.7  | Proposed REC location on the island of Formentera   | 94  |
| 3.8  | A simplified overview of the Energy Community design highlighting key assets.                   | 95  |
| 3.9  | Map displaying the classification of Köppen climate regions in Europe $$                        | 96  |
| 3.10 | The composite components of the load input assumptions for EC members.                          | 97  |
| 3.11 | Illustration of the spline function used to fit the daily and monthly measured                  |     |
|      | load profiles into the annual total load expectation  | 98  |
| 3.12 | Heat map illustrating the total daily load for all buildings in the REC $$                      | 99  |
| 3.13 | The impact of different irradiance measures on the power output of a solar                      |     |
|      | module  | 100 |
| 3.14 | Graph showing the performance characteristics of the IEC classes                                | 104 |
| 3.15 | Flowchart with a simplified view of the energy management control logic $1$                     | 107 |
| 3.16 | Simple energy trading concept of the EC, showing (left) an example with                         |     |
|      | low generation and (right) high generation.   | 110 |

| 3.17 | Graph illustration of how the marginal price is set under the simple decentralised energy market scheme |
|------|---|
| 3.18 | Hybrid energy system model approach with multi-objective optimisation                                   |
|      | algorithm NSGA-II solving process   |
| 3.19 | Resulting Pareto optimality fronts used to find the best NSGA-II settings $$ . 119                      |
| 3.20 | Convergence of the optimisation pareto front as shown by an aggregated                                  |
|      | scalar objective function minimising towards a single value   |
| 3.21 | The object-based architecture of the system model implemented in Python 123                             |
| 4.1  | NREL PV solar test set up in Golden, Colorado   |
| 4.2  | A portion of the solar validation data compared to the modelled result. $$ 128                          |
| 4.3  | Histogram illustrating the error distribution and variance over the validation                          |
|      | time horizon (one year)   |
| 4.4  | The Gökçeada installation site of the wind turbines used for model validation. $130$                    |
| 4.5  | An example section of wind validation data compared to the modelled outcome. $131$                      |
| 4.6  | The set of Pareto optimal solutions for the REC system design $\dots \dots 133$                         |
| 4.7  | The change in renewable asset size with specific performance target $134$                               |
| 4.8  | Energy generation hour-by-hour breakdown by source. Example shown                                       |
|      | includes a typical summer (August 2023) and winter (February 2023) week. $136$                          |
| 4.9  | The annual weekly-averaged daily operation of the hybrid combined storage,                              |
|      | and PV solar and wind generation  |
| 4.10 | A comparison of the state of charge between the hydrogen and battery                                    |
|      | storage systems on an hourly basis  |
|      | Present value curve for the central scenario compared to grid-only use 142                              |
| 4.12 | The absolute change in power import volume between the lowest cost and                                  |
|      | lowest emissions scenarios  |
| 4.13 | Percentage of demand delivered by each of the renewable asset classes over                              |
|      | the three scenarios   |
| 4.14 | A Pareto front comparison between battery-only, hydrogen-only, and the                                  |
|      | hybrid storage system set up  |
| 4.15 | The optimal system sizing with binary storage choice ranging from best cost                             |
|      | to best decarbonisation performance   |
|      | Reduced set of community buildings to test trading impacts  |
| 4.17 | The impact on system sizing and LCOE performance under different local                                  |
|      | trading regimes   |
| 4.18 | REC system NPV graph with the included maximum impact of parameter                                      |
|      | uncertainty   |
| 4.19 | Uncertainty distribution of system LCOE and payback period resulting from                               |
|      | the Monte Carlo assessment  |

| 4.20 Uncertainty distribution of system LCOE and payback period resulting from |   |  |
|--|---|--|
|  | the Monte Carlo assessment  |  |
| 4.21   | Average monthly solar irradiance and wind speed data by year from $2014-2023.158$ |  |
| 4.22   | Resulting variation by weather year in the system LCOE and emissions              |  |
|  | intensity   |  |
| 4.23   | Ranking of the most sensitive variables contributing to the system LCOE           |  |
|  | derived via SOBOL method  |  |
| 4.24   | Most sensitive variables contributing to the system emissions intensity           |  |
|  | derived via SOBOL method  |  |
| 5.1  | Pareto front resulting from the REC system multi-objective optimisation . 166     |  |
| A.1  | REC asset schematic for the installation on Formentera                            |  |
| A.2  | Solar and battery installations for the REC in Formentera 199                     |  |
| A.3  | The hydrogen system installation showing the cabinet and storage tank $200$       |  |
| A.4  | The 15kVA three-phase inverter and 48V DC bus to manage the DC power              |  |
|  | generation and battery storage for the REC system                                 |  |
| A.5  | Example REC system operation for the month of July 2024 201                       |  |

## List of Tables

| 2.1  | Table of reviewed VPP and microgrid projects in Europe and globally 39       |  |  |
|------|--|--|--|
| 2.2  | Table Renewable Energy Community projects reviewed in detail 52              |  |  |
| 2.3  | Simplified example of the renumeration process of the NEOOM Energy           |  |  |
|      | Communities  |  |  |
| 2.4  | Values of surface roughness length for various types of terrain 67           |  |  |
| 2.5  | A comparison table displaying the key characteristics of different hydrogen  |  |  |
|      | fuel cell variants   |  |  |
| 2.6  | Comparison of key performance and usability considerations between the       |  |  |
|      | two model and optimisation approaches  |  |  |
| 3.1  | A summary of load data available for each of the Energy Community            |  |  |
|      | Buildings in Formentera  |  |  |
| 3.2  | Building load statistics for the different members of the REC 98             |  |  |
| 3.3  | Wind turbine IEC class for corresponding average wind speeds used in         |  |  |
|      | modelling turbine power output   |  |  |
| 3.4  | Spread of parameters values tested to determine the best operation of the    |  |  |
|      | NSGA-II  |  |  |
| 3.5  | Table showing the main NSGA-II algorithm control setting used in determining |  |  |
|      | the design solution  |  |  |
| 3.6  | Table of the global model assumptions  |  |  |
| 3.7  | PV technical parameters and assumptions                                      |  |  |
| 3.8  | Wind Turbine technical parameters and assumptions                            |  |  |
| 3.9  | Battery technical parameters and assumptions                                 |  |  |
| 3.10 | Hydrogen Storage Energy technical parameters and assumptions 122             |  |  |
| 4.1  | The technical cell parameters of the PV solar test set-up                    |  |  |
| 4.2  | The technical parameters required for the wind turbine model 130 $$          |  |  |
| 4.3  | NSGA-II optimisation settings  |  |  |
| 4.4  | Optimal decentralised asset sizing for the Formentera REC                    |  |  |
| 4.5  | Optimal REC system design key technoeconomic results                         |  |  |

| 4.6 | Comparison REC configurations for extreme cases for net savings and             |
|-----|---|
|     | decarbonisation potential compared with the central optimal case 144            |
| 4.7 | Energy community asset sizing at the optimisation extrema                       |
| 4.8 | Summary of key performance parameters considering the maximum degree            |
|     | of uncertainty propagation in the REC model                                     |
| 5.1 | Thesis research questions with how each objective has been addressed and        |
|     | the key outcomes  |
| 5.2 | Comparison of the levelised cost of electricity results of similar hybrid       |
|     | hydrogen smart grid systems within the literature                               |
| 5.3 | Comparison REC configurations for extreme cases for net savings and             |
|     | decarbonisation potential compared with the chosen nominal case $168$           |
| B.1 | Adopted building power load profiles for the hourly simulation [normalised] 202 |
| B.2 | Wind turbine performance profiles by IEC classification                         |

## List of Abbreviations

| Term                                     | Abbreviation         |
|--|----------------------|
| Anion Exchange Membrane                  | AEM                  |
| Balancing Responsible Party              | BRP                  |
| Basic Feasible Solution                  | BFS                  |
| Battery Energy Storage System            | BESS                 |
| California Independent System Operator   | CISO                 |
| Clean Energy Community                   | CEC                  |
| Closed Cycle Gas Turbine                 | CCGT                 |
| Combined Heat and Power                  | CHP                  |
| Commercial Virtual Power Plant           | CVPP                 |
| Demand Response                          | DR                   |
| Distributed Energy Resource              | DER                  |
| Distributed Ledger Technology            | DLT                  |
| Distribution System Operator             | DSO                  |
| Electric Vehicle                         | ${ m EV}$            |
| Energy Storage System                    | ESS                  |
| Feed-in-Tariff                           | $\operatorname{FiT}$ |
| Frequency Control Ancillary Services     | FCAS                 |
| Fuel Cell                                | FC                   |
| Genetic Algorithm                        | GA                   |
| Global Warming Potential                 | GWP                  |
| Guarantees of Origin                     | GoO                  |
| Heating Ventilation and Air Conditioning | HVAC                 |
| Internal Rate of Return                  | IRR                  |
| Levelised Cost Of Electricity            | LCOE                 |
| Linear Programming                       | LP                   |
| Loss of Load Probability                 | LLP                  |
| Mixed Integer Linear Programming         | MILP                 |
| National Renewable Energy Laboratory     | NREL                 |
| Nationally Determined Contribution       | NDC                  |
| Nominal Operating Cell Temperature       | NOCT                 |
| Non-Dominating Sorted Genetic Algorithm  | NSGA                 |
| Open Cycle Gas Turbine                   | OCGT                 |
| Peer-to-Peer                             | P2P                  |
| Photovoltaic                             | PV                   |
| Power Purchase Agreement                 | PPA                  |
| Present Value                            | PV                   |

| Proton Exchange Membrane                              | PEM    |
|---|--------|
| Regenerative Hydrogen Fuel Cell                       | RHFC   |
| Renewable Energy Community                            | REC    |
| Renewable Energy Directive                            | RED    |
| Renewable Energy System                               | RES    |
| Sun Peak Hour   | SPH    |
| System Average Interruption Duration Index            | SAIDI  |
| System Average Interruption Frequency Index           | SAIFI  |
| Technical Virtual Power Plant                         | TVPP   |
| Transmission System Operator                          | TSO    |
| United Nations Framework Convention on Climate Change | UNFCCC |
| Virtual Power Plant                                   | VPP    |

## Chapter 1

## Introduction

#### 1.1 Background

The market for distributed Renewable Energy Systems (RESs) has increased considerably in recent decades, driven by the need for a reduction in global emissions to combat climate change. The European Council for Climate Action set out a target of at least 27% share of renewable energy usage within the EU by the year 2030, and a total of 40% domestic reduction in greenhouse gas emissions compared to 1990 [1]. These targets were agreed upon to comply with the objectives of the 2015 Paris Agreement on Climate Change following the 21st Conference of the Parties to the United Nations Framework Convention on Climate Change (UNFCCC). The central aim is to prevent global average temperatures from rising by 1.5°C, with a contingency to keep 'well under' 2°C compared to pre-industrial levels [2]. With a 1.5°C increase surpassed for the first time in 2024, and, according to the International Energy Agency (IEA), a rise of 2.4-3°C is far more likely [3]. The impacts of such warming would be understandably devastating to the global ecological system.

In 2023, the UNFCCC conducted the first of many global stocktake exercises to measure decarbonisation performance against individual countries' Nationally Determined Contributions (NDC). NDCs are commitments that countries make to reduce their greenhouse gas emissions as part of the climate change mitigation plan. Conclusions from the technical report released ahead of the 28th Conference of Parties (COP28) confirmed that, while many nations have made strides to reduce carbon emissions, an accelerated effort is needed to keep global temperature rise below 2°C [4]. The UK has committed to a NDC target of reducing emissions by 65% from 1990 levels, and having met a 52.7% reduction in 2023, are considered on track to meet its target [5]. Other European countries, like Poland, for example, have committed to the EU target of 55% reduction by 2030. However, for Poland, a fossil fuel heavy market with a large, primarily rural population [6], the country has reduced emissions by just 19% in 2023 compared to 1990 [7].

A key assumption for many economies is that decarbonisation of the energy system will be achieved through electrification. In the UK, 104.2Mtonnes of CO<sub>2</sub> equivalent emissions were produced from power generation alone in 2018, accounting for 23.2% of the total greenhouse gas production, only being surpassed by the transport industry with 27.6% share [8]. Assuming that the emissions share values are similar for other European countries, there is scope for further reductions in the emissions from power production, helping to catalyse the transition to a low carbon world. In Europe, renewable energies increased their share of power generation to 35% as of 2022, equal to over 50% in the previous 10 years, as seen in Figure 1.1, reducing the requirement for fossil fuel power.

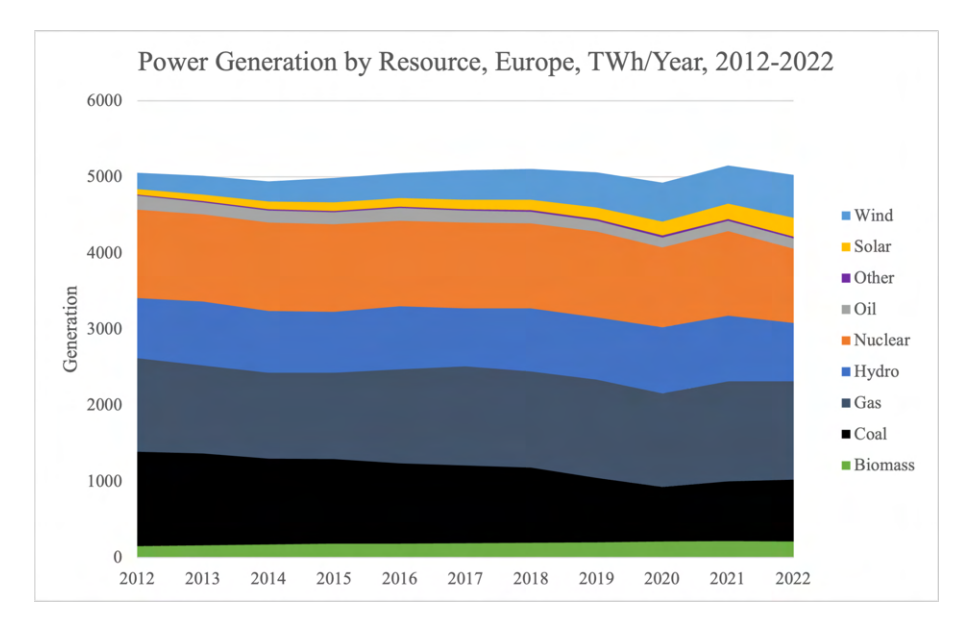


Figure 1.1: Europe power sector generation mix (Eurostat).

While RES are excellent at cutting emissions from power generation, there is still the challenge of their intermittency during unfavourable weather conditions. Situations of high energy production will create an energy surplus on the grid, leading to grid congestion and negative price signals in a free energy market, and damaging the energy economy [9]. Conversely, intermittent or too little RES production will cause grid instabilities and the potential for black-outs. The increasing uptake of roof-top mounted solar panels and other consumer-level generation will add further difficulty to the control and management of the power grid. Figure 1.2 is an illustrative example from the California Independent System Operator (CISO) of how the increasing penetration of solar power produces a considerable portion of surplus energy, and therefore a negative market pricing signal between 7:00-15:00. The ability to temporarily store the excess power generated would go some way to limiting these negative impacts, though comes with its own set of technical challenges. The uncertainty of the final cost to the consumer for upgrades required to transition to 'green' power generation also raises concerns for developing, as well as developed, economies.

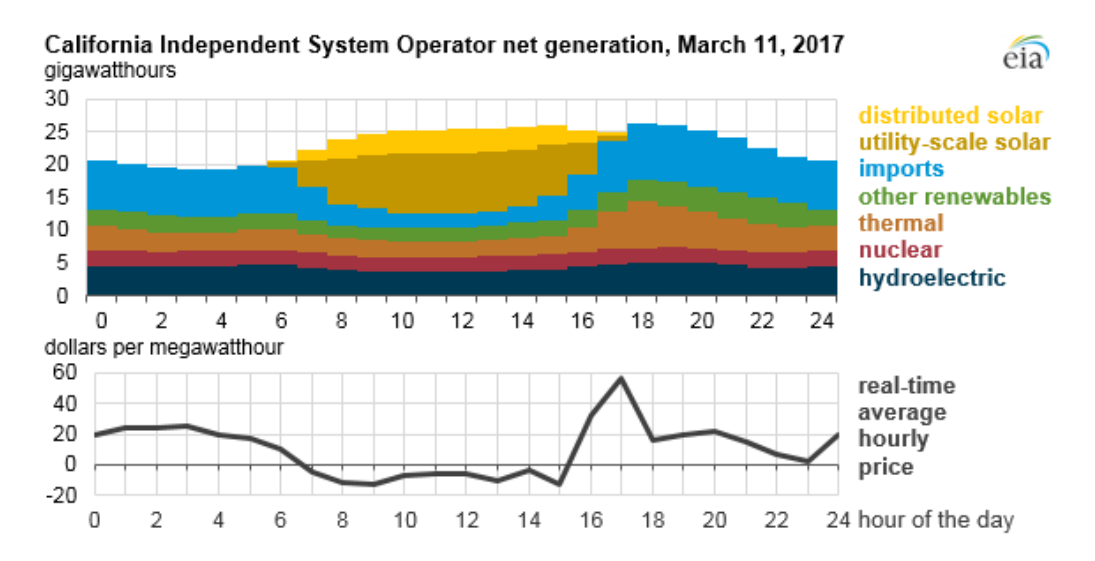


Figure 1.2: Renewable energy community system architecture (Environmental Investigation Agency 2017).

Considering consumer uncertainty is vital when analysing the impact of renewables on the supply of power, particular those in islanded locations or remote communities. Rural populations account for 43% of the total global population, that is, citizens who live outside of larger towns and metropolitan areas. Figure 1.3 shows the percentage of the rural population, highlighting particular countries such as Ireland and Romania as having higher numbers of decentralised rural community living.

While those who live in built-up environments will likely have better access to newer, greener technology, rural communities often rely on a weaker grid with aging, fossil fuel reliant infrastructure. Local energy prices can vary significantly, based on the availability of generation and the cost of infrastructure. Because rural and islanded populations often have limited connection to the grid, this puts them at high risk of grid congestion and curtailment, pushing up operational costs. For many remote locations, such as Scotland in the UK and the Nordics, the location emissions are actually lower than populated areas due to the increased space for renewables. However, rural islands, such as Malta or the Balearic Islands, have a higher emissions intensity as limited space for renewable power leads to additional gas and coal power stations to keep up with demand. Rural and remote populations are also more likely to be impacted by renewable development projects which will, in many cases, have a physical impact on the local area, resource availability, and other societal factors many fear would damage the local economy. A number of European countries, including Poland, France and parts of the UK currently have, or have previously had, some form of onshore wind generation ban in place. This line of reasoning indicates that rural communities are therefore at higher risk in energy transition. Firstly, by being stranded without means to access a clean, secure energy, and secondly, facing possible disruption to local systems and economies due to the increasing land use for renewable

development programs. One of the key findings from the first UNFCCC global stocktake states that "systems transformations open up many opportunities, but rapid change can be disruptive. A focus on inclusion and equity can increase ambition in climate action and support." [4]. The report calls on action for all parties, including subnational authorities and local communities to ensure a just transition.

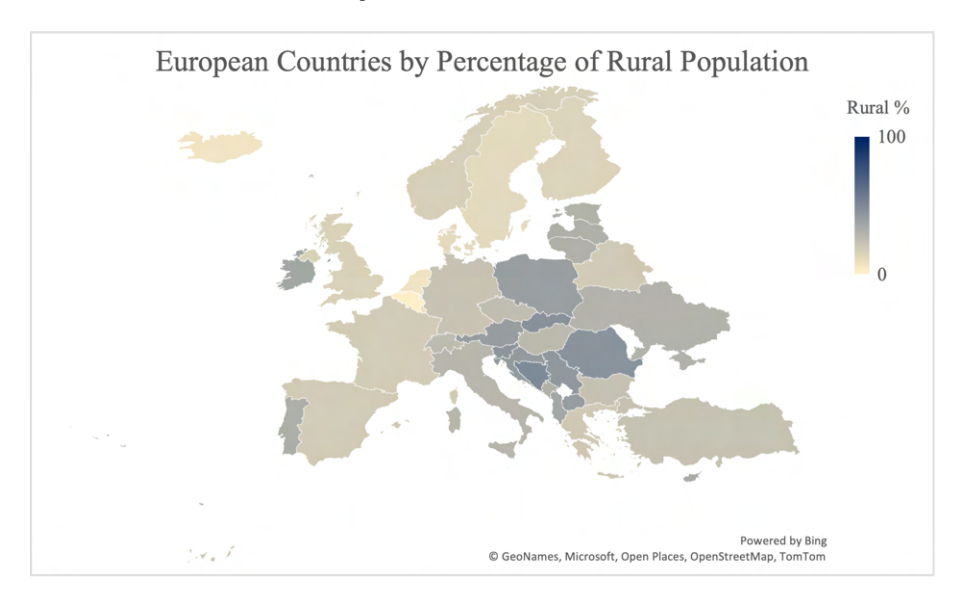


Figure 1.3: The percentage of the European population living in rural and decentralised communities (source: World Bank database of as 2024).

These considerations in combination with the imposed net-zero energy grid targets bring up the following objectives that must be addressed:

- 1. Allow increased RES installation without impacting grid stability.
- 2. Increase visibility of decentralised renewables as the consumer market grows.
- 3. Allow for the optimal deployment and usage of Energy Storage Systems (ESS).
- 4. Minimise the economic and societal impact of the 'green' power transition on rural and islanded populations.
- 5. Assess the optimal system sizing and operation of decentralised renewables for best economic and environmental performance.

Previous efforts have gone to some length to find individual, feasible solutions to these problems, but many lack a connection of these somewhat wide-ranging aspects through a single, technical solution.

A potential answer to the growing problem described is utilising decentralised RES with ESS capability, that can automate and control the process of energy production, storage, and distribution within their respective markets while minimising grid distortion. It would

negate the requirement for support power to be supplied by fossil fuels by producing an aggregated, controllable power supply, also known a Virtual Power Plant (VPPs).

A VPP essentially combines the power outputs of several heterogeneous energy generating sources, along with ESS, to function as a single energy source. This is usually described as consisting of dispatchable and non-dispatchable sources, as shown in Figure 1.4. Non-dispatchable sources including PV solar and wind turbines form the base power generation, then hydro power, battery ESS, and other dispatchable sources can be ramped up and down to balance the supply requirement. Certain VPP topologies are not necessarily aimed at providing the lowest possible energy price, and may equally prioritise positive societal impacts, such as displacing fossil fuel emissions, whilst providing local security of supply benefits. The definition of a VPP covers a number of different decentralised energy delivery architectures.

In this research, the depth and breath of potential configurations is reviewed in detail, assessing the obstacles and challenges to implementation. From this process, it was determined that the direction of this work would primarily focus on the concept of a Renewable Energy Community (REC); a type of VPP that is instead operated for the direct benefit of a localised community with shared objectives [10]. The justification for this narrowing of the research scope is described in detail in Chapter 2. Comprehensive research and understanding of ESS technologies are central to the functionality of the REC definition as presented. This thesis reviews the options for decentralised energy storage, before applying this process to a reduced set of optimal technology; namely electrochemical batteries and Regenerative Hydrogen Fuel Cells (RHFCs).

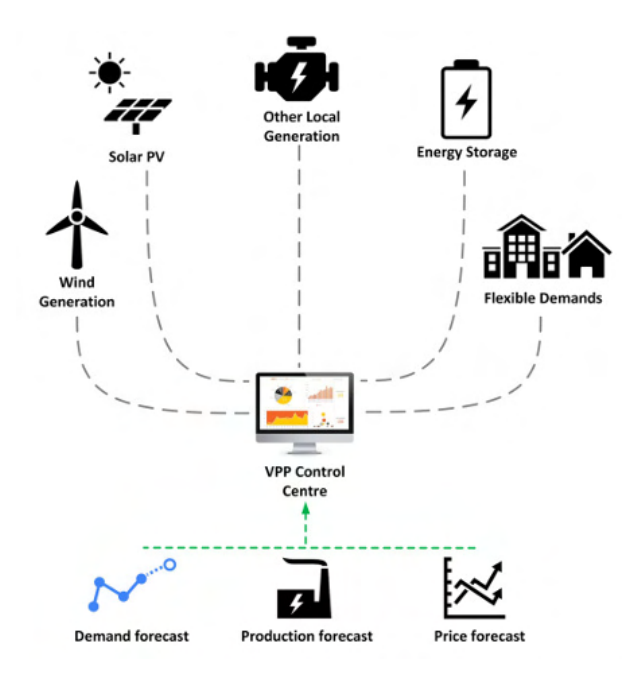


Figure 1.4: A simple schematic of a typical Virtual Power Plant configuration.

Ever increasing computational capability has enabled complex energy systems to be modelled in high fidelity. This research effort culminates in a comprehensive multi-domain energy systems model to provide the optimal design and deployment pathway for a decentralised REC. The model takes into account the local conditions of the deployment location, constraints on asset sizes, emissions, and the final cost to the community members. The modelling capability would allow local stakeholders and policymakers to view and assess the impacts of a proposed REC configuration, and gives the ability to observed the trade-off in abatement cost of reducing emissions through renewable energy investment.

This work, as part of a wider European effort to accelerate the energy transition, uses the case of geographical islands to illustrate and validate the solutions proposed. Using islands as test locations, an in-depth assessment remote island communities' current state of renewable energy access was performed, highlighting weaknesses and risks to achieving effective decarbonisation.

One of the biggest challenges of emissions reduction of European countries is in the development of renewable energies on geographical islands. Some more remote islands often rely on low capacity sea cables to receive energy from the mainland or use on site diesel generators for additional power in remote areas, both of which are unsustainable. The risk of increased cost and decreased security of supply is therefore very likely for these communities in the near future, particularly those without the space and resources required to develop renewable energy sites locally. European island countries such as Malta and Cyprus already report some of the highest energy and network costs in Europe [11], likely due to the requirement for mainland energy trade and fuel imports, with fossil fuel levies and emissions trading schemes exacerbating problems. Geographical islands also often lack the necessary facilities and expertise to develop potential smart grid concepts to increase sustainability and reduce reliance on imported energy. Sustained energy independence is therefore a critical goal for these islands.

### 1.2 Aims and Research Questions

Based on the problem set out, the overall aim is to design and assess routes to commercial deployment of REC systems on geographical islands, taking into account the impacts on policy and regulation, technological requirements, as well as the social and environmental impacts. The formulated research questions to answer are therefore as follows:

- 1. How can the deployment of VPP-based RECs be most effective in serving the energy transition needs of rural and islanded locations?
- 2. How can an energy system model be used to design and simulate the dynamics of a REC, considering the specific needs and demands of an islanded community?

- 3. What is the system design benefit of integrating a multi-objective optimisation methodology considering specific cost and decarbonisation targets?
- 4. What are the potential benefits of co-locating battery and hydrogen storage systems on the performance and resilience of the REC?
- 5. How can sensitivity and uncertainty analysis be implemented in the modelling approach, be used to guide risk-related REC design, and inform potential policy frameworks?

#### 1.3 Project Approach

The approach of this project is as follows. In the first phase, a literature review of community-based Virtual Power Plant systems was conducted to provide the framework for the research methodology and gaps in the state-of-the-art. This is accompanied by an obstacles to innovation review, where the critical opportunities and challenges to the technical deployment and commercialisation of such a system is explored in detail. The decision to analyse a hybrid battery and regenerative hydrogen fuel cell storage system are also presented. The modelling methodologies for decentralised power generation and storage assets is also consolidated within the literature review, as well as design, control and optimisation techniques used to solve the prominent challenges facing Energy Communities.

What follows is the approach and research methods used to answer the overall research questions of this work.

#### 1.4 Research Methods

The methods used to answer the research questions laid out can be broadly categorised into the following pillars:

- 1. Define the operational, geographic and socioeconomic landscape in which the REC case study sits, ensuring that the system design is anchored in a real world scenario and accompanying data.
- Create an energy system and multi-objective optimisation model to simulate and optimise the design of the proposed REC configuration, with a focus on the trade-off between economic and decarbonisation performance.
- 3. Use known uncertainty and sensitivity analysis methods to assess the robustness of the model results, understanding the range of performance under variability, and identify critical input parameters.

Contextual analysis and REC case study: The island of Formentera, Spain, is used as a representative case of a rural, isolated energy community candidate. A quantitative analysis is conducted on the input data, including hourly electric load profiles of the included buildings, hourly meteorological data (wind speed, temperature), and the local grid emissions intensity, all of which are used in the parameterisation of the system model. A qualitative assessment of land availability, suitability of renewable deployment, and regional planning restrictions in the context of renewable energy communities is also conducted. The outcome of these methods is a robust, real-world data-driven foundation for the REC case study on which to base the design and simulation model, and fulfills the objectives of research question one.

REC system modelling and multi-objective optimisation: A model is then developed, including all REC buildings and multiple renewable generation and storage assets, and is built on the strong data foundation provided by the previous pillar. In particular, the wind and solar modelled performance is directly related to the local weather conditions of the site. The Non-dominating Sorting Genetic Algorithm (NSGA-II) multi-objective optimisation method is then used to explore the trade-off arrangement between cost and decarbonisation of the system, and the benefit to the local community. The system is also tested under a number of scenarios, the first of which is a comparison between co-located battery and hydrogen storage compared to standalone, and the second is a comparison of friendly and competitive energy trading policies. The key outcome of this is a comprehensive understanding of the system dynamics, and under different operational designs and constraints.

Uncertainty and sensitivity analysis: Once the system modelling methodology is complete and analysis of cost and emissions performance has been conducted, an uncertainty and sensitivity analysis of the model then follows. First is a Monte Carlo assessment, in which different input parameters including technology costs and efficiencies are varied across realistic ranges from literature. The resulting simulation data provides an understanding of the range of possible performance outcomes. Secondly, the variance-based Sobol sensitivity analysis was chosen to attribute variance in model performance to specific input parameters. This methodology aided in the understanding of which inputs are most uncertainty, therefore needing close monitoring and potential policy control to reduce project risk. The aim of the methods described is an insight into the overall stability of the recommended REC design under uncertainty, including assets risk hold high investment risk, potentially providing the basis for future policy support frameworks.

Figure 1.5 contains the content of each chapter to guide the reader through this work.

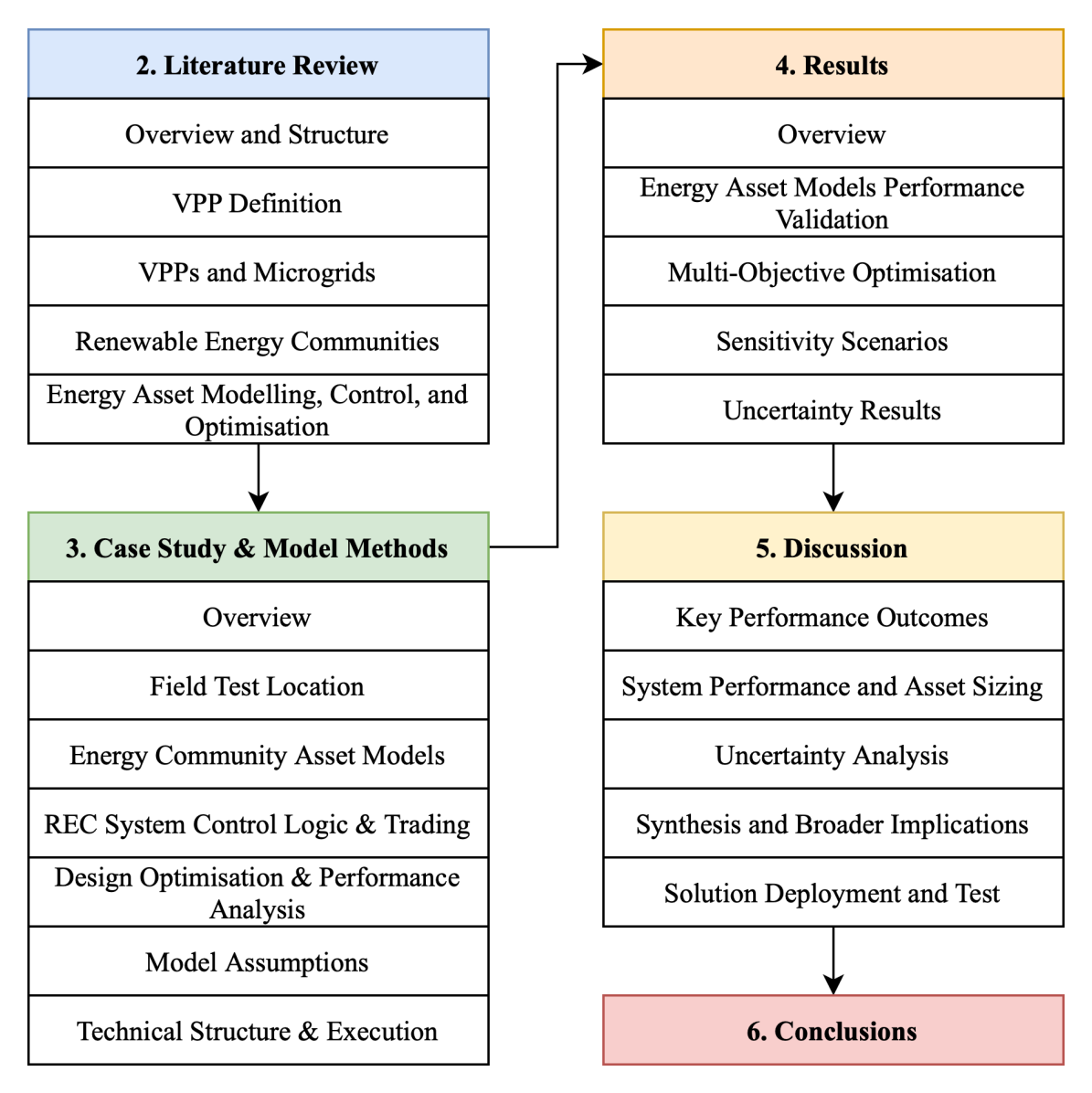


Figure 1.5: A flow diagram illustrating the content of this thesis.

The review of the existing literature reaffirms the novelty of this work, in that it is addressing a number of gaps in existing research:

- The focus of this work is on bespoke design and modelling of RECs for islanded and rural communities, who have specific challenges regarding energy security, high energy costs, and asset stranding in the future. This relates to the themes of an inclusive energy transition, energy equity, and local community support.
- Multi-objective optimisation via the NSGA-II algorithm, whilst explored among energy system models, has a particular degree of novelty when applied specifically to energy community-based VPPs, and more specifically balancing the design of a system that is both as economically effective and environmentally sustainable as

possible.

• The novel comparison of battery and a combined hybrid battery and hydrogen storage system applied to decentralised locations to evaluate the performance benefits of hydrogen in both the cost and the decarbonisation dimensions.

### Chapter 2

### Literature Review

#### 2.1 Overview and Structure

Before defining the system concept for this study, it is important to first evaluate the history of Virtual Power Plants (VPPs) in detail, understanding the balance of strengths and weaknesses, and how the performance can be maximised. Since the technology is still in its early adoption stage, most examples within the literature point to technical showcases that have been tested on a small scale in partnership with Transmission System Operators (TSOs) and Distribution System Operators (DSOs) of the host countries. The concepts often require fundamental modifications to the method in which energy generation is handled and value is redistributed among aggregators and participants.

The key VPP characteristic were categorised into the three main sections:

- Policy and regulatory landscape
- Technology and service enablers
- Societal value and climate impact

As with all new technologies or services, there are a range of market and regulatory challenges that may impact the VPP's ability to provide the maximum benefit to a localised community. The review considers the possibility of providing different services to a local population through, primarily, reduced dependence on the national-level grid. The environmental impacts and barriers to REC based VPP deployment were also reviewed, including the impact of energy generation activities, and relevant policy restrictions. The challenges and opportunities assessed have been based on a number of resources, covering published research, international directives, environmental reports, and local news articles.

The second part of the chapter links the challenges and opportunities to existing VPPs, microgrids and Renewable Energy Community (REC) systems. A critical analysis follows, assessing how these concepts have used the opportunities available to their advantage, and

where they may have fallen foul of the challenges facing these nascent but growing services. The motivation for why an REC based system may be more achievable than a traditional VPP is presented.

The final sub-section brings together the analysis of community-based VPPs, and presents the notion that with comprehensive energy system modelling and design optimisation, positive project outcomes can be maximised, whilst minimising, or at least provide an understanding of, downside risk for a rural, islanded population. This would be achieved through comprehensive energy system modelling and design optimisation to intelligently plan the REC system for a given local environment, climate, and policy landscape. A review of related energy system modelling approaches is presented, navigating through technology asset models, control systems logic, and design optimisation. The chosen methodology of this work is outlined, highlighting the successes and challenges of similar works within the literature.

With a high-level of modelled understanding if its operation, a VPP-based renewable energy community can not only reduce cost, but also eliminate a large amount of embedded carbon emissions from the system, aligning islanded, rural communities with the climate action objectives at a national and global level.

#### 2.2 Virtual Power Plant Definition

#### 2.2.1 VPP Policy and Regulation

It is important to outline what is meant by *Virtual Power Plant* before continuing to identify the key barriers and obstacles related to deployment. A VPP is a relatively new concept, being the object of study for the past 15 to 20 years. Over time, different sources have expanded upon its potential uses within the energy grid, and documented the many benefits. The definitions of a VPP therefore vary widely across the literary landscape, depending on the objectives of the system and the available resources. A generally accepted definition of the VPP is:

"A flexible representation of a portfolio of Distributed Energy Resources (DERs), not only aggregating the capacity of many diverse resources, but also creating a single operating profile from a composite of the parameters characterizing each DER and incorporating spatial constraints." [12]

This definition, while including the fundamental structure of the VPP, does not consider the additional information that defines the other complex operational aspects. The definition also needs to place importance on these virtual connections and control to ensure the successful interoperation between multiple distributed assets.

The VPP structure is often confused with the microgrid concept as both integrate a number of distributed generators. A microgrid, however, describes a physical system of connected generators such as Photovoltaic (PV) solar, wind, and battery storage that can act as an islanded system to service a very localised area. A VPP, however, is much more reliant on a network of data connections and smart metering equipment to control the remote generators as a single entity, and to export this energy to the grid to serve a larger area than a traditional microgrid. Artificial Intelligence algorithms such as Artificial Neural Networks (ANN) and Neural Fuzzy (NF) are becoming crucial to the performance of VPP concepts [13], so should also be incorporated into the VPP definition.

#### VPPs in the power market

A key barrier identified within the literature which hampers the successful implementation of the VPP is the position of the system within the structure of the energy market. The VPP needs to not only improve efficiency and the reliability of the system at a local level, but also be visible to the TSO/DSO such that can to participate in the energy market on a distribution or national level.

The price-based mechanisms that allow for profitability of distributed Renewable Energy Systems (RES) vary between technology and location. Many European countries have adopted Feed-In Tariffs (FITs) or Contracts for Difference (CFDs) set by government regulators to receive remuneration for the energy generated by RES. The tariffs are often fixed or floor values, or are set as a percentage premium combined with the market value

[14]. Another option to unlocking value in renewable energies is via Power Purchasing Agreements (PPAs). A PPA is a long-term contract that a power generator has with a supplier or direct consumer to pay a certain fixed amount for that energy over the given period. PPAs are a good method of ensuring financial security for both, the supplier and consumer, as parties trade a fixed value for the energy. This means that market participation is not required, negating the associated financial risk [15]. Both, FITs and PPAs could work well as a preliminary mechanism, with the potential downside of applying a pre-agreed pricing structure.

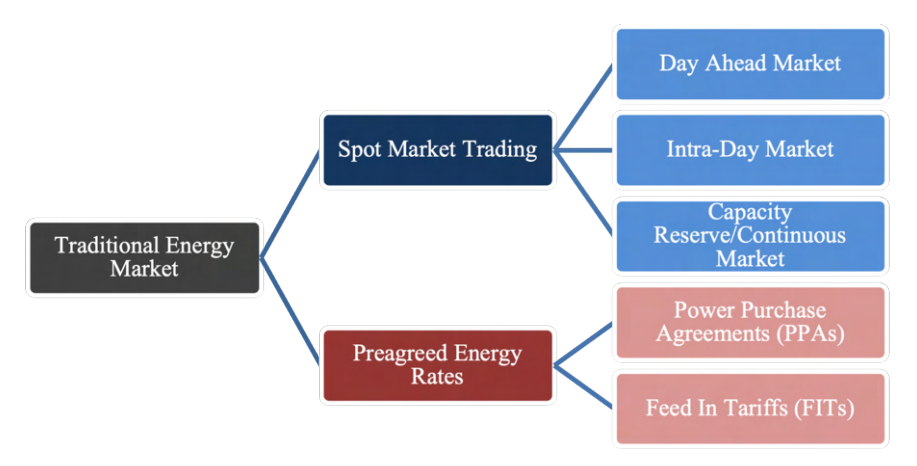


Figure 2.1: A simplified view of the traditional energy market structure.

Another other option for power generation companies is to participate in the wholesale spot market. In most European markets, players can opt to take part in the day ahead, intra-day, and continuous/capacity market auctions. The day-ahead market consists of energy generators and suppliers bidding for energy values hourly for the next day, after which the market operator calculates the power price through the clearing process. The intraday bidding occurs in often hourly or quarter-day intervals, with reserve markets responding to offers from minute responses to up to one hour in order to keep the system balanced [1].

Analysis conducted in the EU project 'MASSIG' suggested that DER suitability for participation within the spot market relies heavily on whether they qualify for both, the day ahead and reserve markets, and if the generation forecasting is accurate [16]. The traditional market also does not provide mechanisms that value the potential merits of a flexible VPP system at a local level, and any changes to the market would be a challenge due to regulatory barriers to be discussed.

A number of studies have been conducted into the potential value to be gained by VPPs by participating in wholesale trade despite the current regulatory hurdles. The paper by [17] addresses an optimal bidding strategy for what is known as a Commercial Virtual Power Plant (CVPP), which is considered as a separate entity to the actual aggregated VPP. The model also assumed all DERs, when combined in the VPP, are able to participate

openly in all markets and that there are no minimum energy bid limitations, which as discussed in [18, 19], are not strictly true for all European markets.

Over many decades, additional layers of regulation and complexity have produced a market that is largely unsuited for new renewable technologies and services to participate. As an example of this problem, it has been a challenge to implement a system of demand response capability – one of the key services offered by the VPP concept. The 2016 EU demand response policy report revealed that "many national regulators see the process of opening markets to demand response as complex and confusing" [20].

A method needs to be devised for the regulatory bodies to recognise the additional value that the VPP can create within the energy system, without making a large quantity of reforms to the current national and international markets [21].

#### Local markets and Energy Communities

A possible mitigation strategy for the market barriers is to operate a small-scale 'deregulated' market in parallel to the existing spot market and PPAs. The Flexible Congestion House (FLECH) originally suggested by [22] stipulates a local energy market within the DSO level that specialises in the unique services offered by the VPP, including responding to demand changes, storing excess RES, and supporting critical loads during interruptions. The parallel local market theory lends itself well to the applications on islands, as are usually connected through a single sea cable interconnector to the mainland, so any activity within the island can be monitored and controlled.

Local ancillary services markets have been explored with the use of Peer-to-Peer (P2P) trading as presented in [23]. The research implements a novel bidding and optimisation strategy for a selection of 20 consumers and prosumers with varying PV installation and Electric Vehicle (EV) charging facility, assumed to be equipped with smart metering. The results show that the creation of a local energy market where customers can participate in community energy balancing and ancillary services can increase the individual profits considerably, as well as the social welfare of the customers.

The concept of so-called Clean Energy Communities (CECs), definitionally similar to RECs, is a continuation on the development of local market theory. An exploration into the structure and challenges of CECs conducted by [24] states that a CEC differs from a system of local RES in that it details the specific relationship between the end users and their energy management. In this way, all end users are considered key stakeholders in the development and management of the CEC to continuously promote and improve their sustainable energy usage. Parallel local markets therefore play a key role in shaping the economic feasibility of island-based RECs, as the revenue generated by the energy community activities such as providing ancillary services to the DSO and peer-to-peer trading is then fed back into the portfolio of community investments.

The requirement for changes in the traditional energy market structure is being

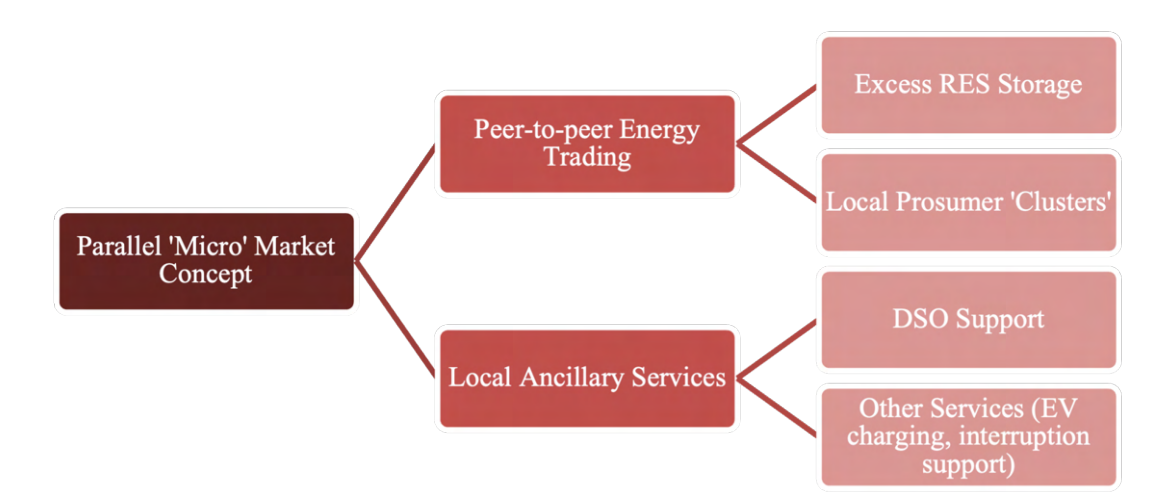


Figure 2.2: Proposed local micro-market concept and services provision.

recognised by the EU, who recently released regulation (EU) 2019/943 'on the internal market of electricity' [25]. This report highlights the state of the current energy market and how it is not suited to the fast-transforming nature of modern energy generation via prosumer participation. Emphasis is placed on new technologies and services such as distributed generation, flexible generation, demand response, and energy storage, as well as how these should be incentivised further. Like the local parallel market theory, Article 24 of the document suggests the use of short-term markets to improve liquidity by allowing more participants within the market, which may reduce the entry requirements for small generators. The related directive (EU) 2019/944 also recognises the reforms that are required to move towards a decarbonised energy grid, and that the renewable energy targets would be most effectively met through the creation of "a market framework that rewards flexibility and innovation" [26]. The directive also defined new industry terms such as 'active customer', 'citizen energy community', 'aggregation', and 'interoperability'.

#### Modelling energy policy mechanisms

It is clear that one of the key challenges blocking Energy Commmunity-based VPPs is in the uncertainty related to local policy design in particular countries, as it can pose a threat to the economic and societal success of the project. Because of this uncertainty, the ability to design and model a system before investing real capital would be an enormous benefit. Research conducted in [27] presents a multi-period investment and system planning model to minimise project risk through changing regulation of deploying a PV solar and battery system. The results showed that the optimal temporal build of RES can reduce the investment risk and ensure maximum impact. Results from [28] consider the regulatory uncertainty in energy grid planning for Australia, and highlight that uncertainty in investment outcomes tends towards flexible assets, such as battery storage in the long term.

These are both critical findings that will need to be considered when exploring the optimal design of a VPP system. This investigation will also fill a potentially valuable knowledge gap in the planning and regulatory structures as distributed RES become increasingly prominent.

#### 2.2.2 Technology, Reliability and Services

The increase in small-scale distributed generation has had a dramatic effect on the energy landscape and has produced a potential market for equally local ancillary services and renewable energy grid support. The regulatory barriers discussed in section 2.2.1 have a considerable effect on the variety of services that can be implemented, and their value added to the VPP concept. Table 2.3 summarises the identified services that could be provided, ranging from instantaneous response to grid fluctuations, down to long-term, seasonal grid storage to balance renewable generation. This is followed by a detailed discussion of commonly researched and implemented services in Europe and the USA. A review of Energy Storage Systems (ESS) service barriers presented in [29] provides an excellent foundation, from which an extension into VPP services provision is discussed.

| Application Time<br>Frame | Services for Flexible VPP Dispatch                                 |   |   |  |
|---------------------------|--|---|---|--|
| 0-30 Seconds              | Voltage and frequency control                                      | Voltage/VAR support   | Power quality   |  |
| 3 Minutes                 | Spinning reserve   | RES generati  | on smoothing  |  |
|                           |  | Voltage sag   |   |  |
|                           |  | Rapid demand support  |   |  |
|                           | R  | eal-time energy balancir  | ng  |  |
| 20 Minutes                | RE   | S ramp and voltage supp   | ort   |  |
|                           | Back-up power  | Blackou   | t support   |  |
| 2 Hours                   | Peak load shaving  | Consumer incentives<br>for quick load<br>reduction                                      | Energy cost management  |  |
|                           | Congestion relief  | RES energy store during interruption  |   |  |
| 8 Hours                   | Time-shifting  | Price arbitrage   | Consumer time-of-<br>use incentives   |  |
| Days                      | Weekday-weekend load smoothing and carry over                      |   |   |  |
| Weeks                     |  | Smoothing weather and environmental conditions  |   |  |
| Seasonal                  | RES seasonal storage   | Annual load   | l smoothing   |  |
| Years                     | Outage mitigation  | Grid upgrade deferral   | Reliability   |  |
|                           |  |   | improvements  |  |
| Other Energy<br>Services  | Smart EV-charging  | CHP district heating and industrial processes   |   |  |
| Data mining and sharing   | Shared energy data could be used for grid performance improvements | Transparency with 3 <sup>rd</sup> parties to increase project visibility and investment | Shared with communities to create additional cost saving measures and carbon emissions reductions |  |

Figure 2.3: Potential services that can be implemented through VPPs [29]

#### **Demand Response**

Demand Response (DR) has been noted as one of the key services to be provided by

VPPs. DR can be seen as a competitor to the traditional reserve markets, except that it can be effective at a community level. Due to the increase in distributed generation, it is becoming increasingly important to respond to sudden supply changes and consumer demand. For example, shaving the peak solar generation from rooftop solar generations would be of enormous benefit to grid stability, providing cost reductions to the consumer as this energy can then be used at another time of day. DR concepts, like those presented in [30] and [31], consist of an aggregated grouping of small renewable generators, a consumer fixed load, consumer variable load, and an ESS. These models consider the optimal approach to controlling the VPP energy community to meet the DR objectives in the most robust and cost-efficient manner.

A potential technical barrier with the DR method is in understanding the range of operating conditions and connection requirements of the distributed resources, and how to coordinate the appropriate response to the grid. This barrier can be grouped under the larger IT considerations to be applied to the VPP such as sensing, computing, and communication of the DR assets [32]. Unfortunately, the route to inclusion of DR within the European energy market is currently mixed, as noted in the regulatory landscape analysis of the previous section.

The review of services provision from VPPs is vital in shaping the modelling approach of this thesis, including which are most practical and valuable from a community perspective, such as peak load shifting and demand balancing. Additionally, the current policy support outlined in the Renewable Energy Directive (RED-II) framework also narrowed the scope of the service provision, since VPPs and RECs generally cannot yet participate in power markets and provide ancillary services. Finally, the potential for future policy exploration, such as self-consumption incentives and community energy trading have also been considered based on this review.

#### Price Arbitrage

The potential flexibility of the VPP concept combined with an appropriate ESS could take advantage of price variations on the energy spot market, known as price arbitrage. Price arbitrage is the practice of buying energy from the grid while the price and demand are low, such as at night or early afternoon, and selling it when the price and demand are high. This process also complements DR as the use of arbitrage can produce excess stored energy that can be made available for other services. As mentioned in the previous section, the practicality of price arbitrage would depend on whether small-scale, aggregated generators qualify for participation in power spot markets, which is known to vary between EU countries. While providing potential profits through promoting renewable energies, price arbitrage could increase overall carbon emissions in the system due to efficiency losses in operating an ESS. Research presented in [33] analyses the prospect of market price arbitrage participation for individual prosumers with small Battery Energy Storage Systems (BESS). A forecasting sensitivity analysis and its effects on the scheduling performance is

also modelled in detail, and outcomes show that the profits using this method rely heavily on the quality and accuracy of the forecasting technique. Most notably, arbitrage can have a negative effect on both, the price and environmental sustainability of the stored energy if forecasting is proven to be inaccurate. As a mitigation strategy, analysis of the capital and maintenance of the ESS should be considered when calculating market arbitrage viability, as well as the risks associated with generation forecasting.

#### **System Performance Targets**

The system performance targets for the VPP will provide crucial objectives and constraints for the conceptual design and specification. As mentioned in the previous section, the performance objectives will vary depending on the objectives of the 'fostering entity' - the stakeholder who is responsible for the practical investment and integration of the VPP systems into the community grid.

For each case the objectives and constraints will be different, as well as the costs and benefits of the VPP. It should also be noted that the objectives defined may conflict with each other, so must be considered as a multi-objective optimisation problem. The performance objectives can be approximately grouped into three categories.

#### Carbon emissions reduction

Given the current climate situation, and stress placed on national energy bodies to reduce the climate impact of the distribution grid, this will be one of the key performance objectives for most fostering entities. Considering the local governing body, they may have incentives placed on them by national government to provide evidence of emissions reduction with the community, as well as penalisation to those who do not participate. The same carbon levies may not apply to local DSOs, who also may not have as much of an interest in carbon emissions reduction over other prioritised objectives. The VPP concept presents a method of curbing carbon emissions from energy production in a local area with a large amount of RES generation capacity. RES that must be curtailed due to over-production or sudden generations peaks would be ideal to exploit in this scenario, either through export to the grid, local energy trading, or ancillarly services supply.

#### Energy cost reduction

The reduction of electricity cost for the participants with the VPP is one of the key motivators with research. A number of methods have been presented [19, 23, 34, 35] that consider the economic impacts and potential benefits of the aggregation of DERs into a VPP-style system. Cost reduction is seen as a major future driving force to the implementation of such futuristic and disruptive technologies, even more so than the other objectives discussed. Cost reduction also applies to the widest audience of potential fostering entities, as all will look to reduce the operational cost and even produce a profit from the implementation of a VPP. It can be noted, however, that increasing cost effectiveness may conflict with the objective of carbon reduction, as it may be most beneficial economically

to operate a system that produces increased emissions. When the previously discussed example service of price arbitrage is considered, it has been shown to increase profits for an installed ESS, but the disadvantage is that efficiency losses which will inevitably increase the carbon impact, even before the manufacture and lifespan of the ESS is considered.

#### Reliability improvements

The reliability of the local energy system is closely linked to the ultimate cost of operation and frequency of maintenance, as the TSO and DSO are rewarded and penalised based on the reliability performance within which they operate. Reliability can also consider the quality and comfort of the energy consumers, which can be approximated with the reliability indexes System Average Interruption Duration Index (SAIDI) and the System Average Interruption Frequency Index (SAIFI). Loss of Load Probability (LLP) is also used to define the fraction of time which loss of load may be expected to occur during a period in the future [36], usually expressed as hours or days of the year or a percentage. The probability density function is determined based on data from previous plant outages, which can then be used to estimate when a power station may experience an outage and how much capacity is lost.

As discussed previously, geographical islands are generally connected to the mainland or another island through a single medium voltage sea cable and may not have additional ancillary services on the island to respond to demand variation. The introduction of ancillary balancing services through the VPP may have the ability to considerably increase the robustness of the system.

#### 2.2.3 Environmental Considerations and Societal Value

It is well understood that a key objective of a community-based VPP system is to provide tangible societal and environmental value for the local participants. The general concept, as suggested by comprehensive review of Energy Community business models in [37], is to provide these benefits in addition to the clear economic reasoning, which would be a requirement for the uptake of community-based VPPs in the long-term. Although public opinion on new RES technology is generally positive, there may also be both, public and regulatory concern over the implementation of a VPP. The local acceptance within the community, in addition to adoption of the new technology and additional RESs will be key to its success. How these factors impact the current view of VPPs is presented below, highlighting some of the methods that could be implemented to maximise societal value proposition for islanded and rural populations.

#### Resource Limits and Protected Areas

Within this analysis, it is important to consider limitations of the physical implementation of VPP components including future potential energy generation, particularly when a key objective of most VPP systems is to maximise renewable energy penetration.

Rural locations, particularly those on geographical islands, may have space and resource limitations that could stifle future growth of certain RESs. Unpredictable weather conditions for PV and wind turbines, as well as limited freshwater supply for hydro power to be feasible are examples of these limitations. Different resource availabilities of the different islands will change the nature of the RESs generation mix, and therefore flexibility of services offered through the community-based VPP.

Nature reserves and parks have similar laws prohibiting RES development. This barrier is another important consideration for the REC, as it will again limit the amount of RESs that are permitted. Hydro power and the requirement for building dams and reservoirs can also pose a significant threat to freshwater species such as fish and waterfowl [38]. The dammed rivers can also limit communities' access to fresh water further downstream. Other location-based restrictions could include built up urban centres, airports, and military bases.

#### Local acceptance of the new RES and VPP systems

While there is little specific analysis of public sentiment towards VPP systems due to the novelty of the technology, the impact that RES technologies have on the local environment has been researched at length. Since a key objective of any VPP is to facilitate the increase in distributed RESs, any related barriers need to be considered. The continuation of generalised public antipathy as documented in [39] has become less of a concern than it was a decade prior, but still affects the installation of RESs in certain locations. For

geographical islands with strong community values towards the aesthetics of their local area, there may be a degree of public opposition to the implementation of new RES technologies.

Excellent research presented in [40] provides an assessment of the lessons learned from engaging local, small-island communities in the discussion over renewable energy projects, including those projects that could also support VPPs. The article concludes that island communities are concerned with ensuring any engagement in developing such a project should give active priority to securing the localised benefits, and provide credible policy mechanisms for providing intra-community conflict resolution. This article also suggests that island locations are also excellent test locations for new renewable technologies and systems, so must be engaged with effectively. The sentiment aligns well with the objectives of this thesis, in that providing local, islanded communities with clear, measurable benefits will not only improve the energy supply conditions for the citizens, but also provide continued opportunity and support for more development of future renewable power.

# 2.3 Virtual Power Plant and Microgrid Case Studies

This review of VPPs and Microgrids was conducted to identify the technical, regulatory, and social design features relevant to rural and islanded contexts. A structured selection of case studies and peer-reviewed research was used to explore recurring challenges and successful strategies in existing projects. The review considered small- to medium-scale implementations across Europe and internationally, with a particular focus on studies that reported on real-world deployment and operational performance. Sources were identified using Scopus, as well as policy reports, EU project summaries, and technical documentation from VPP pilot programmes. Key selection criteria included contextual similarity to the target system (e.g. European location, decentralised generation, citizen participation), availability of system performance or economic data, and relevance to the integration model proposed in this thesis. Lessons learned from these cases informed the design decisions and assumptions of this work, with particular attention paid to the scale, storage integration and trading arrangements. Table 2.1 details the key aspects of the VPPs in the literature, including a summary, provided services, and stakeholder involvement. The list also includes examples of P2P trading based microgrids, which by definition are subtly different to VPPs.

Table 2.1: Table of reviewed VPP and microgrid projects in Europe and globally.

| Name        | Type | Location | Summary                  | Services            |
|-------------|------|----------|--------------------------|---------------------|
| Fenix       | VPP  | UK &     | One of the first         | -DERs can be        |
| (2005-2008) |      | Spain    | VPPs to address          | made visible to     |
| [41]        |      |          | increasing visibility by | network operators   |
|             |      |          | aggregating DER and      | -Contribution of    |
|             |      |          | pass information to      | DERs to grid        |
|             |      |          | the TSO to assist in     | management          |
|             |      |          | planning infrastructure  | activities -Optimal |
|             |      |          | upgrades, transmissions  | use of DER in       |
|             |      |          | and assessing congestion | ancillary services  |
|             |      |          | problems                 |                     |

|                | TYDE      | -         | (D + + + + + + + + + + + + + + + + + + + |                       |
|----------------|-----------|-----------|--|-----------------------|
| TWENTIES       | VPP       | Europe    | 'Power Hub' proposed                     | -Ancillary services   |
| (2010-2013)    |           | various   | as part of the project                   | (voltage and          |
| [42]           |           |           | to provide VPP style                     | frequency control)    |
|                |           |           | flexibility services from                | -Optimise outputs     |
|                |           |           | large scale offshore wind                | from available        |
|                |           |           | farms and other DERs.                    | resources -Provide    |
|                |           |           |  | cost reductions       |
|                |           |           |  | through increased     |
|                |           |           |  | energy security       |
| Con Edison     | VPP       | New York, | Aggregation of 1.8 MW                    | -Network resiliency   |
| (2016-2017)    |           | US        | capacity DERs with                       | (outage support)      |
| [43]           |           |           | energy output of 4                       | -Power delivery       |
|                |           |           | MWh.                                     | smoothing -Load       |
|                |           |           |  | shedding and shifting |
| AGL VPP        | VPP       | South     | The creation of 5 MW                     | -Voltage control      |
| (2018-present) |           | Australia | generation from a                        | -Frequency balancing  |
| [44]           |           |           | combination of 1000                      | -DER visibility       |
|                |           |           | prosumer residents (PV                   |                       |
|                |           |           | solar and batteries,                     |                       |
|                |           |           | during trail period)                     |                       |
| Piclo          | VPP       | UK        | Online energy trading                    | -Demand side          |
| (2018-present) |           |           | platform for flexible                    | response -System      |
| [45]           |           |           | capacity auctions                        | regulation -Energy    |
|                |           |           | for independent                          | marketplace           |
|                |           |           | DER generators to                        | (primary, secondary   |
|                |           |           | participate, allowing                    | response) -DER        |
|                |           |           | small players to                         | visibility            |
|                |           |           | participate in the                       |                       |
|                |           |           | energy marketplace.                      |                       |
| Brooklyn       | Microgrid | Brooklyn, | A P2P platform for                       | -P2P energy trades    |
| Microgrid      |           | New York, | a local energy market                    | -Grid support         |
| (2016-present) |           | US        | to support weak energy                   | 11.                   |
| [46]           |           | · ·-      | grid and produce value                   |                       |
| [ -1           |           |           | from DER.                                |                       |
| [              |           |           |  |                       |

# Fenix VPP

It is well understood that the increase in penetration of DER into the traditional energy grid reduces the amount of visibility and therefore ability of network operators to be able

to plan supply and demand balancing effectively. As one of the first ever VPP concepts to present pilot demonstrations, the 'FENIX Future' aimed to represent the increased system capabilities on DER whilst removing barriers and negative impacts. The project began in 2005 and consisted of 20 partners from research and industrial EU partners, largely from the UK and Spain, to meet the challenge of future DER integration.

As noted in [41], the objective of FENIX was to design and demonstrate technical and commercial architectures that would increase the viability of increased DER in Europe as a solution for the approaching green energy future. The key aim, in alignment with the simple definition of a VPP to represent DER as a single system which generators and consumes energy, as shown in Figure 2.4. The concept is categorised into a Technical Virtual Power Plant (TVPP) and a CVPP.

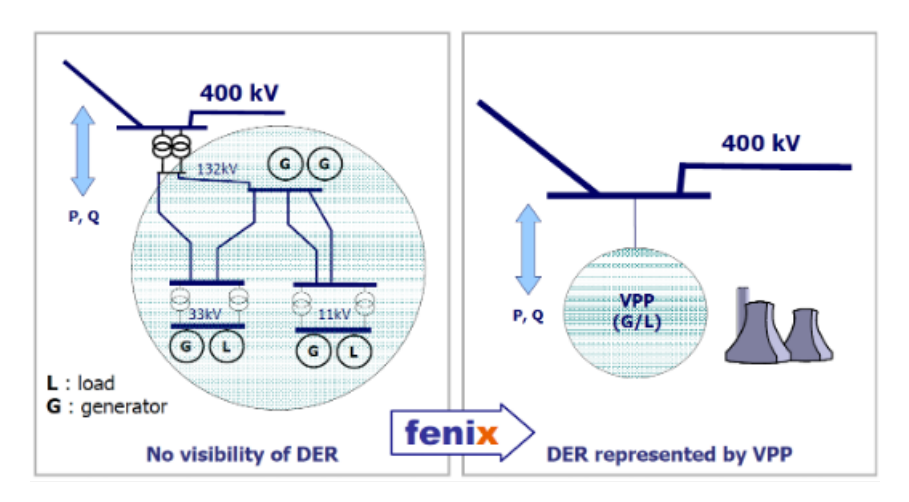


Figure 2.4: The FENIX VPP concept [41]

**TVPP:** represents the physical DER as installed in the geographical location, including records of the real time influence of the aggregated system, as well as cost and operational characteristics. The main purpose is to allow for DER visibility, from which other functions include local grid system management and informed decision making for system balancing. In addition, the aggregation of many DER reduces the risk of unavailability from any one unit within the system, and therefore can smooth the output of the VPP. The operator could be the DSO but may face regulatory challenges as particularly in the UK, the DSO is not able to operate generation units [47].

CVPP: represents the higher-level commercial services and function of the VPP portfolio, such as wholesale market participation and balancing services provision, and maximising the DER participation. It is known that these services face more stringent regulatory challenges due to the structure of the traditional energy market. The CVPP performs only commercial services and does not consider technical aspects.

Given that FENIX was one of the first VPP projects to present a pilot study, many of the technical requirements and enablers were first outlined within this project which could be built upon by others. It can be seen that the main architectural property was in separating the physical components such as generators, consumers, and storage from the virtual and commercial aspects of services support, data management and market participation with the TVPP and the CVPP. This is an important process in that it clearly highlights the challenge of combining these two domains using the VPP and can be more easily understood and engaged with. Critically, the Fenix VPP was one of the first to highlight the difficulties, at least in Europe, of entering a series of virtually connected generators in to the traditional electricity market structure, as outlined in the previous section. Overall, the FENIX VPP is relatively simple in design, likely due to the regulatory constraints of the time, so was not able to fully realise the potential of a virtually connected system. Now, with the new RED III policy definitions for VPPs and RECs, it is more likely that the Fenix VPP would have been more successful in achieving the objectives of the project.

#### **Edison VPP**

The Edison project was launched as part of the smart energy system drive on the island of Bornholm, Denmark. The project investigated how a large number of Electric Vehicles (EVs) could be integrated such that grid support can be offered for the mutual benefits of the EV owners and grid operators. The motivation for the project was that with the projected rise in EVs in Europe will increase the demand on the grid during certain times of the day, which could have an adverse effect on the reliability of the system when heavily loaded. Like the following WEB2ENERGY VPP, the Edison project builds upon the recommended set of IEC 61850 communication protocols and security measures.

The EVs connected within the Edison EVPP can be considered as a large power consumer which are also able to provide balancing at peak demand. This operates by modulating the rate of charge entering the EV such that the grid demand can be shifted to reduce stress. Like other projects, Edison uses a two-level environmental approach, with the 'electrical layer' consisting of physical components (EVs, DSO metering, generation) which can be represented with physical laws and constraints, and the 'electricity market' layer consisting of the commodity trading systems and various stakeholders involved in the clearing and billing processes.

The concept defined allows for two defined architectures to be presented. An integrated architecture approach requires an existing Balancing Responsible Party (BRP) such as power-generation or utility company to perform the interactions with the TSO and sport market on behalf of the EVPP, as shown in Figure 2.5. The BRP can use all the collected data from the systems metering and EV charging locations such as demand, generation,

state-of-charge, and available flexibility to make decisions about when to perform the market interactions. By contrast, a standalone architecture absorbs the role of the BRP into the function of the EVPP such that it can interact with the market as an individual player.

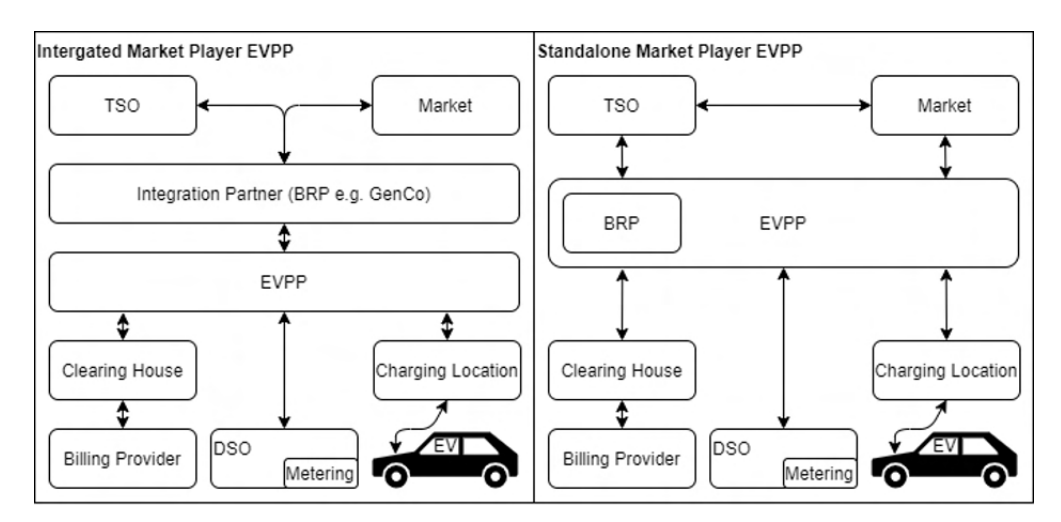


Figure 2.5: The Edison VPP concept [48]

There are advantages and disadvantages to both methods presented, however, it would be more sustainable long term for the VPP to be able to act as a standalone entity for the purposes of cost saving and reducing the required stakeholder interaction. In terms of previously observed VPP characteristics, it is clear that this project aligned closely with the concept of maximising flexible services provision, such as demand response, which has previously been identified as one of the key value drivers of VPPs. In addition, the use of EVs as a flexible load and storage fleet is also commonly viewed as integral to the future operational of such a system.

The project was in many ways ahead of its time, chiefly in that it anticipated the increase in EV usage before true widespread adoption. It is not known if the Edison VPP concept was successfully tested in the field, likely due to lack of requirement at the time of research, and other regulatory challenges. Continued research into an EV based fleet VPP system was still ongoing in Denmark as of 2018 [48]. The VPP design also lends itself much more towards the community-based design, due to the involvement of citizen actors through EV flexibility. Allowing the system participants to actively benefit from the VPP through additional storage and rooftop solar, then allowing renumeration for these actions could have increased effectiveness of the system.

#### WEB2ENERGY

Web2Energy is a European project started in 2008 with the objective of implementing what is described as the main pillars of 'Smart Distribution'. These pillars are described

as follows [49]:

- Smart Metering: the project implemented hundreds of consumer smart meters in the field to provide a number of innovative functions, including management of price signals, interruptions and failures, loads, generation, and demand profiles. This would allow the other pillar to function.
- Smart Energy Management: Following the definition of a VPP, this pillar requires a large number of small independent DERs which are cooperatively controlled such that scheduled power can be manipulated for the given requirement in real time.

In the Web2Energy project, over one hundred smart meters were connected in five locations, with non-dispatchable generators such as wind turbines and PV solar connected to dispatched generators including Combined Heat and Power (CHP), pumped hydro storage, and controllable industrial loads. The generators can be scheduled for greater overall dispatch efficiency and reduce power losses within the system.

The project consisted of 5 CHP plants, 12 storage batteries (1200 kWh total), 12 PV solar farms, 3 wind farms, 2 hydro plants, 3 large industrial loads, and involved 200 residential consumers in a 1-year Demand Side Management study. Outcomes of the project highlighted the requirement of a standardised communication system for the smart systems to interact effectively, as well as the restrictions and market regulations that, like other VPP projects, hinder the realisation of many revenue streams that would otherwise be available. The project was also one of the first studies to explore the requirements of a commercially viable VPP system including communication tools, energy management, and smart distributed generation. Critically, the exact technical specifications for this project is not known, and little information is shared about potential commercialisation of the concept. During the time of the project, regulation and market barriers would have presented severe limitations.

#### **TWENTIES**

The aim of the EU TWENTIES project was to advance new technologies that would assist in integrating the ever-increasing penetration of onshore and offshore wind generation. Specifically, the demonstration project 2 invested in a large-scale integration of a VPP 'Power Hub' to reliability deliver ancillary services such as voltage control and frequency balancing through intelligent control of the wind farms. The Power Hub was able to optimise the outputs of the different wind turbine units to provide the highest value of energy generation. The results from this project also indicate that the introduction of biomass and heat pumps could reduce the CO<sub>2</sub> emissions by 3.46% in comparison to the main German power system [42]. Figure 2.6 below shows the VPP concept as visualised in the TWENTIES project, showing the variety of potential assets that could be implemented.

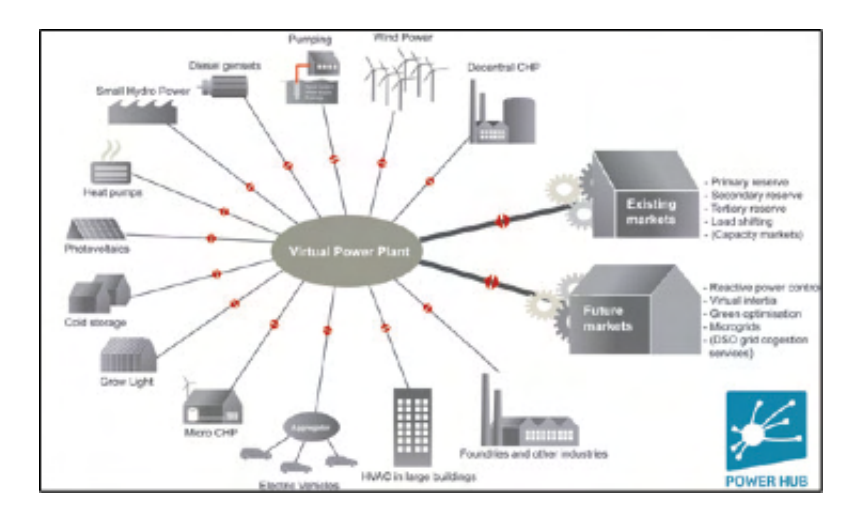


Figure 2.6: The VPP concepts developed as part of the TWENTIES project. [42]

The main findings for the project were that the field tested 'Power Hub' was able to reliably deliver ancillary services such as voltage control and continuous reserves, as well as provide an optimised output to maximise value to all included generator units. Although the results were economically feasible, technical challenges were also identified. One of the challenges is the initial incentivisation for generator and industrial units to take part in the scheme and expand the size of the VPP. Another key challenge was in scaling up the VPP commercially due to the market and regulatory design in the test countries of Denmark, Germany and Spain. The latter is certainly a common barrier that has been identified by multiple other VPP projects. While it is not confirmed, a speculative, critical view could be that the engagement with locals, including prosumers that may have been unable to understand the potential benefits of the TWENTIES project could have helped it gain traction and support from community stakeholders.

#### Con Edison (2016-2017)

The Consolidated Edison Company of New York, Inc. ('Con Edison') VPP was a project to create an aggregated RES platform created in partnership with SunPower for managing and dispatching distributed generation in the most efficient and cost-effective way. The motivation of the pilot project was to demonstrate a method in which combining PV battery systems in hundreds of homes could be reliably and remotely operated to fully realise the monetisable benefits. The project plan in [50] highlights the areas of New York that experience peak demand during the day and during the night. It is clear from the map in Figure 2.7 that as most of the high demand occurs at night, the PV solar generation should be shifted through the use of battery storage.

The pilot was categorised into three consecutive phases that each build upon the successes of the previous steps: customer adoption of resiliency services, VPP integration,

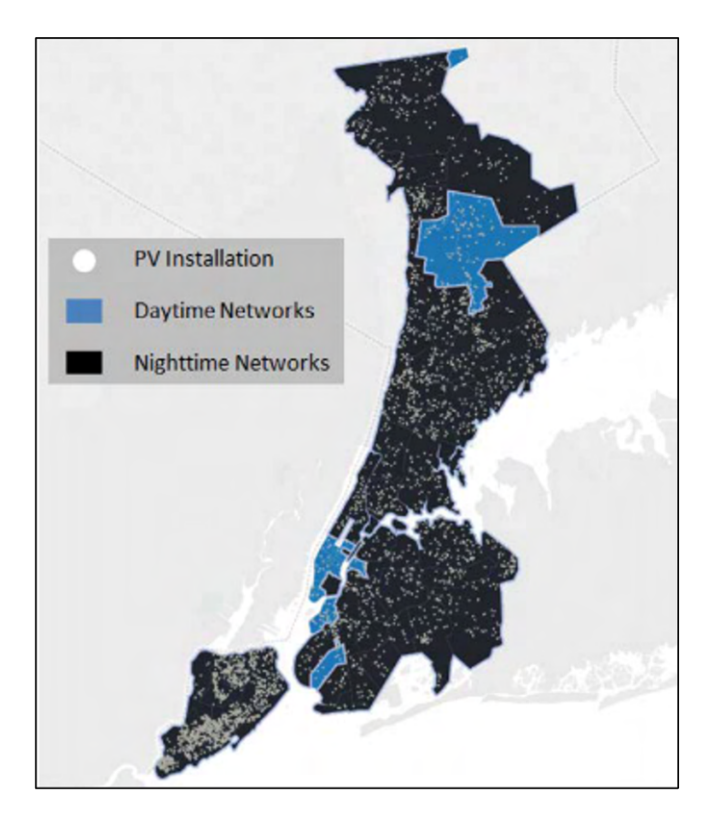


Figure 2.7: The Con Edison VPP location with PV installations and indication of peak demand time of day [43]

and market participation.

Phase 1: Customer Adoption of Resiliency Services This phase consisted of SunPower presenting an inclusive PV and storage package to residential customers to expand the capacity of the VPP. The chosen economic model stipulated that no upfront cost would be imposed on the customer, instead returns would be made back over the usage life of the system. The project estimated that with a market firm capacity value of 20 \$/kW per month, the inclusion of resilience fees would bring the Internal Rate of Return (IRR) to approximately 3 years before profit generation, as shown in Figure 2.8. These values were based on 2014 storage system costs, the report suggested that by 2021 the system would be economically viable.

Phase 2: Virtual Power Plant Integration After the initial customer installations phase, the project would then move to produce a communication network of each end user's PV storage system. This process required upgrading Con Edison's existing communication system (SCADA) with smart meters so that services and control requirements can be communicated effectively. The system could also be performance tested to check the VPP response to certain operation inputs so that risk can be analysed before entering the capacity and spot markets.

Phase 3: Market Participation and Rate Design Once the VPP integration with Con

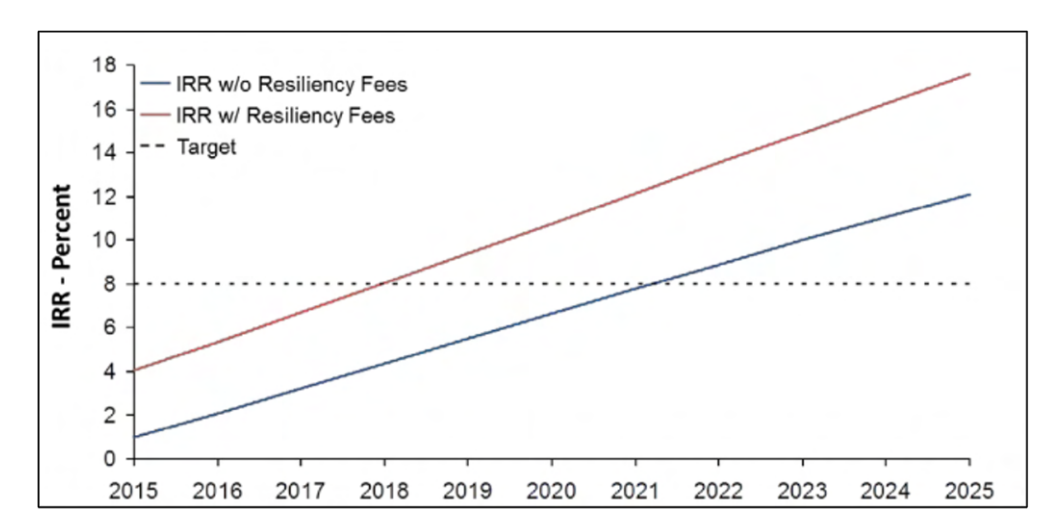


Figure 2.8: Internal Rate of Return (IRR) of the hybrid VPP fleet based on value of firm capacity value [50]

Edison's SCADA system was successful, the energy company would then explore method of market participation, although it was noted at the time of planning that there were currently no methods to do so given the regulatory barriers. In addition, alternative residential rate design such as Time of Use (TOU) cost was to be explored in order to incentivise participants in the VPP to maximise their flexibility for the aggregated system.

The project had a promising background of stakeholders at the time, including the DSO Con Edison and two large renewable energy companies SunPower and Sunverge. Unfortunately, significant challenges arose when seeking approval from local regulatory and community bodies to have access to the required buildings and install the equipment. It is believed that the complexities of the installation, uncertainties and risk associated with the untested design meant that it was unfavourable with end users. The delay caused the termination of lead industrial partner SunPower's contract, and the project has been on hold since Q1 2017. This highlights one of the fundamental barriers that affect many VPP pilot studies and commercial rollouts.

One of the critical reasons why this project failed could have been in the assumptions about the routes to commercialise the project. It is known that little support is often available to receive renumeration from VPP activities at the market level, which may have led to the eventual uncertainty in profits for the final system. As discussed in the previous section, deep understanding of the policy mechanisms and local regulatory environment, as well as the correct technology and service enablers are vital to the success of a VPP.

## AGL VPP

The AGL VPP is a large-scale distributed PV solar and battery hybrid system which has been in successful commercial operation in Australia since its trial period in 2018. The

system consisted of 1000 end users from residential, commercial, and industrial sectors, and is now expanding to cover 50,000 households as of 2019 to produce 250 MW of flexible demand, which is approximately 20% of the demand of South Australia [44]. The installation of the PV battery hybrid system in AC and DC coupled modes are shown in Figure 2.9.

The main service of the VPP is to provide balancing services to the grid that would otherwise be provided by traditional synchronous generators. In partnership with Tesla, installed wall batteries can be remotely operated to inject, hold, or absorb energy to keep a balance between supply and demand. Results showed that the VPP could react to dispatch 'events' such as frequency fluctuations in as little as 6 seconds, theoretically allowing participation in Australia's contingency Frequency Control Ancillary Services (FCAS) market [51]. The map in Figure 2.10 shows the distributions of VPP PV battery sales in terms of citizen demographics in Adelaide, Australia.

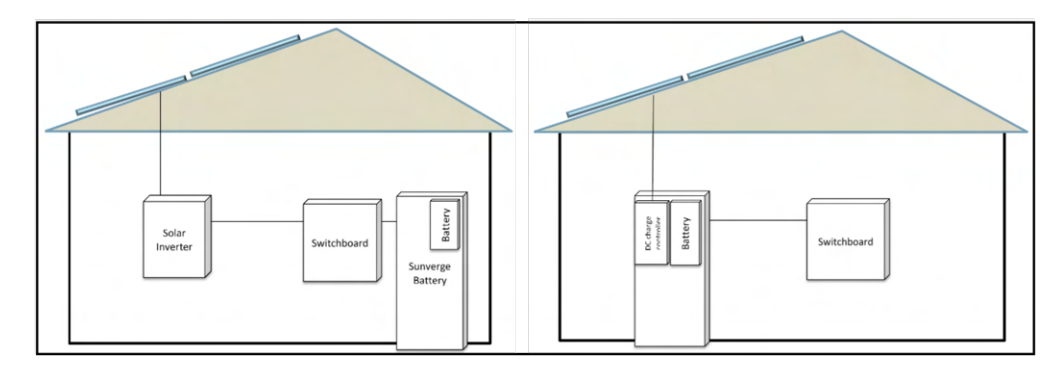


Figure 2.9: with AC coupled (left) and DC coupled (right) modes [44]

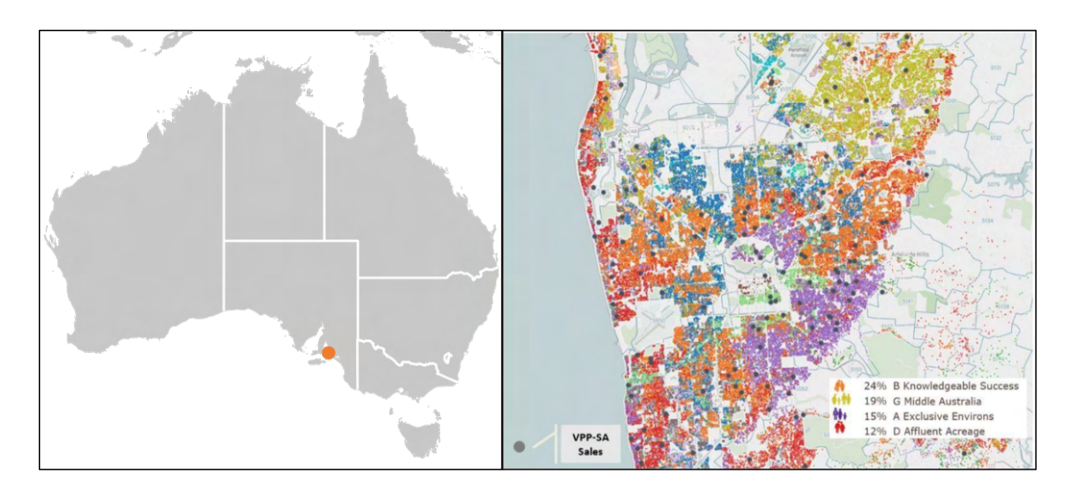


Figure 2.10: Location of VPP in Australia (left) and Distribution of VPP sales map of Adelaide (right) [51]

During the trial phase, the VPP showed successful ability to track the required power dispatch during a simulation frequency fluctuation event. In the example shown in Figure

2.11, the system power response from battery storage is displayed and compared with the target power output on a 6 second time frame. It can be seen that even on a modulation scale as small as this that the system is successfully able to track the required output.

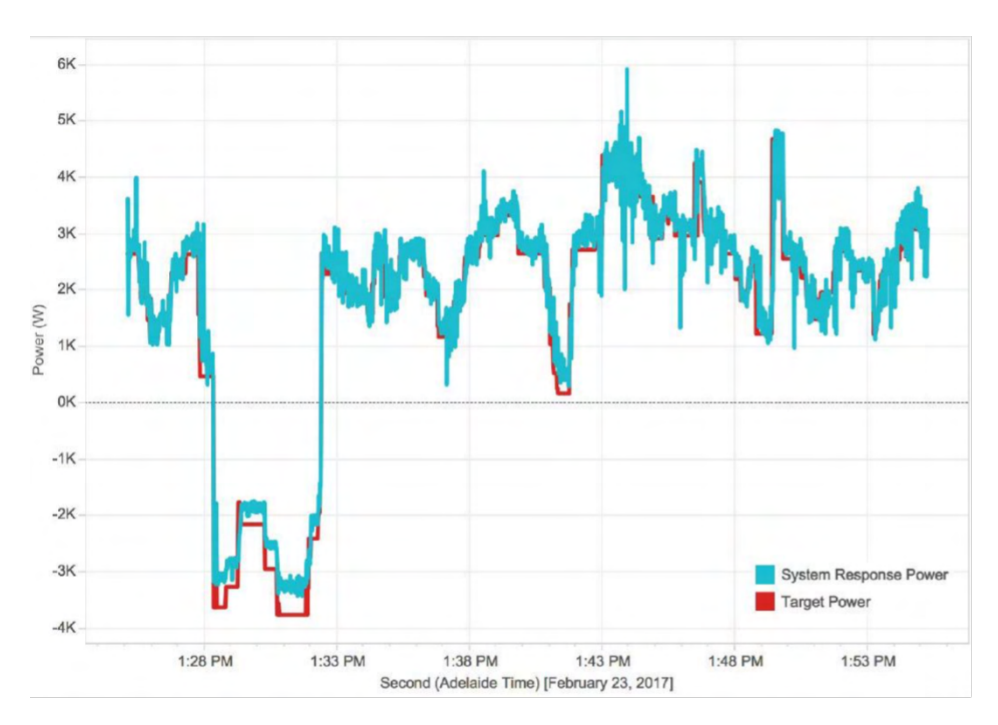


Figure 2.11: Example dispatch response from the VPP battery fleet compared to the target response [51]

A major advantage of this type of VPP design is that it unlocks several lucrative value streams, such as increasing solar self-consumption, utilising back up power during an interruption, network support during peak power, frequency control services, and the potential energy arbitrage opportunities on the spot market. Additionally, the VPP project is overseen and managed by an established energy utility company, which assists in setting up the correct stakeholder communication pathways, including end users, field installers, DSO, TSO, regulators, and the spot market. Through the dislocation of the required traditional balancing generators, the system can also be seen to significantly cut the carbon impact of energy usage.

The success of this project also highlights a deep understanding of the local regulatory environment, and that by working with existing policy mechanisms a profitable commercial opportunity can be obtained. Additionally, taking advantage of technology and service enablers that are commercially ready and well understood such as residential battery storage and smart metering hugely benefited with AGL VPP's design. These factors are certainly to be considered when designing a community-based VPP as part of the work.

#### VPPs and microgrids: In summary

Overall, VPPs and microgrids have done much to accelerate understanding of how a net-zero grid can be achieved, and that by combining the strengths of several renewable assets, one is able to successfully provide a clean, commercially viable energy opportunity.

The AGL VPP in Australia and sonnen VPP in Germany provide examples of successfully commercialised opportunities. On the regulatory side, there has been a clear understanding and ability to work with existing policy mechanisms, most notably shifting and shedding customer load to allow for direct revenue for the power market. In terms of technology enablers, both systems use readily available assets such as rooftop PV solar and residential battery systems. It is possible that investing in a diverse fleet of assets rather than centralised ones reduces the risk of whole system failure, leading to increased overall robustness. From a societal perspective, installing rooftop solar and batteries in homes allows citizens to have some control over their energy usage, reducing the risk of price premiums with market fluctuations. There is also less reliance on utility scale installs, such as wind farms, which can be viewed negatively due to the impact on the local environment.

Unfortunately, there are examples that see less technical success overall. The Fenix VPP was one of the first VPP concepts, and considered to be the conceptual beginning of decentralised energy systems of this nature. The system was, however, unable to capitalise on the available services, and the process of siloing commercial and technical system responsibilities to fit within current energy market policy proved too complex to be commercially viable at the time. The VPP was also made up of utility scale generators. These generators will naturally increase the complexity of managing various stakeholder objectives, particularly when there are several other opportunities for securing revenue outside VPPs; PPAs and government-backed Contracts for Difference being the most common.

This case studies review suggests that VPPs can maximise their impact by moving to a decentralised, local approach, where more power is given to households and businesses to actively participate in the market. Outside of frequency balancing services, the ability of demands to shift their loads to reduce grid stress is of enormous value to operators. This conclusion naturally turns the attention towards RECs, which promote local participation in order to achieve emission reduction targets.

# 2.4 Renewable Energy Communities

The term 'Energy Communities' has many definitions. Traditionally, community energy refers to collective energy actions that foster citizens' participation across the energy system. It has received increased attention in recent years, developing a wide range of practices to manage community energy projects [52]. Energy communities are described as

a non-commercial type of market actors, combining non-commercial economic aims with environmental and social community objectives [53]. Particularly, they have been defined in their 'grassroots' efforts to improve the sustainability and energy security, and therefore fostering a close community atmosphere.

An energy community has traditionally been separated by definition to a VPP as it usually describes the socio-economic environment in which stakeholders have shared ownership and investment in the system to fund the project, rather than the technical operation of the system itself. There is, however, research currently being conducted into integrating these two concepts in addition to smart control systems, such as community shared energy storage [54], virtual net metering and Distributed Ledger Technology (DLT) based platforms for community flexibility provision [55], supported by cloud based services [56]. The combination of a community driven VPP is defined as a Community VPP (cVPP) [57].

There are clear benefits for the development of energy community driven Virtual Power Plants (VPPs) including carbon emissions reduction for selected community stakeholders, potential cost reductions (dependent on revenue streams), stronger sense of community involvement, increased energy security, and even land value improvements [58]. The services delivery to realise these benefits are also well researched and understood, but often held back by energy market regulation and uncertainties [59, 60]. Similar to that of the VPP in general, many challenges are centred around the current regulation which limits the potential revenue from installing renewable energies which are community shared and owned. Increasing local energy system capacity still leads to a problem of energy imbalance and potential congestion within the distribution system.

The majority of citizen-led initiatives are cooperatives. Cooperatives are a socio-economic enterprise in which citizens can collectively own and manage local renewable energy installations and projects. Local residents can buy shares in the cooperative to fund projects to supply energy to participants such as local businesses, residents, and community buildings. Participants with investments in the local project then receive a form of dividend from any profits made through sales of electricity, license agreements, and feed in tariffs. Most profits, however, are usually fed directly back into the cooperative to fund new sustainable projects. This is the oldest type of energy community (first developed over 40 years ago), but has progressed to focus on the reduction on emissions by publicly funding the installation of PV solar, wind turbines, etc. The conversion of a passively operated energy community to a virtually managed VPP system will require the addition of several other stakeholders, increasing the complexity of the cooperative. These stakeholders include a VPP management system to control energy flows and optimal services dispatch, energy aggregators, utilities management, and access to the energy trading markets if required.

## **Energy Community Case Studies**

According to analysis conducted in [52], approximately 3,500 different energy cooperatives are in existence in Europe, that is, decentralised and sustainable energy production projects set up to increase consumer empowerment and community-driven initiatives for the benefit of local citizens and the environment. The data in Figure 2.12 displays the locations of the different local energy initiatives in European countries. It can be seen that a high concentration exists in northern European countries such as Germany and Denmark, where the energy policy and regulation has allowed for these types of partnerships for many years. Table 2.2 contains an overview of the REC examples explored in detail, due to there structure and scope similarities with the case study of this work.

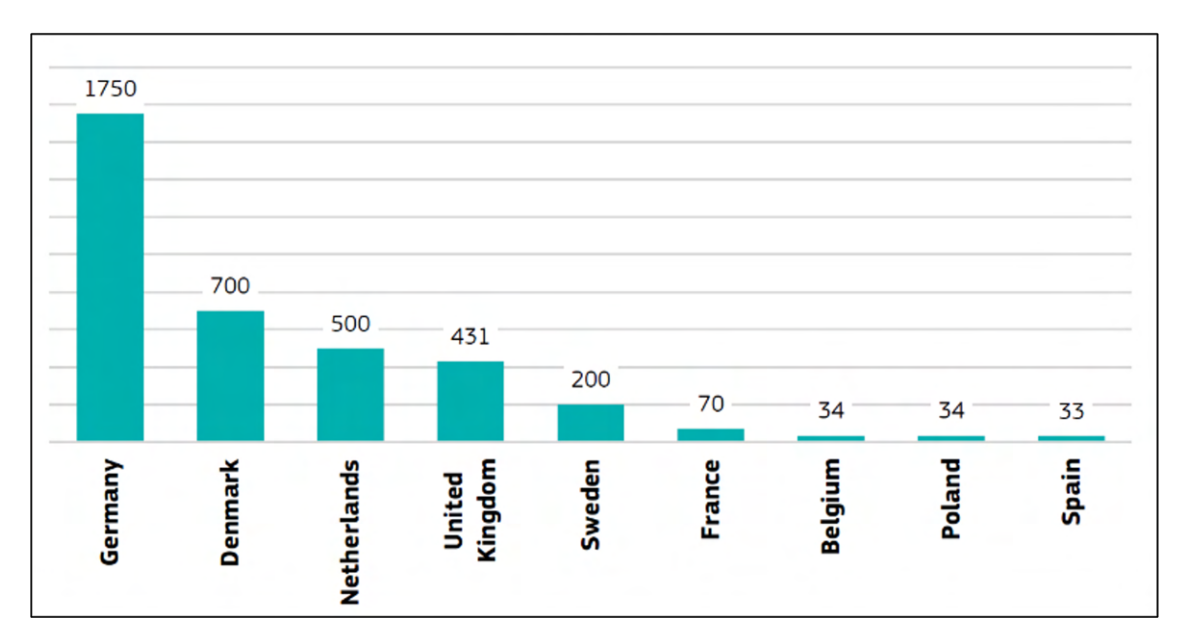


Figure 2.12: Approximate number of community energy initiatives from nine countries within Europe [52]

| TD 11 00 TD 1  | 1 10 11      |           | <b>~</b>  | • ,      | . 1      | •   | 1 , •1  |
|----------------|--------------|-----------|-----------|----------|----------|-----|---------|
| Table 2.2: Tab | de Kenewahle | Energy    | Community | projects | reviewed | ın  | detail  |
| 1001C 2.2. 10C | ne remembre  | LIICI S.y | Community | projects | icvicwca | 111 | actair. |

| Name           | Type | Location  | Summary                | Services             |
|----------------|------|-----------|------------------------|----------------------|
| Sonnen         | REC  | Germany   | Sharing excess DER     | -peer-to-peer energy |
| Community      |      | & Austria | generation among       | trading -mutual      |
| (2017-present) |      |           | over 10,000 end-users. | DER value increase   |
| [61]           |      |           | Energy value is traded | -Shared Virtual      |
|                |      |           | for the mutual benefit | Energy Storage       |
|                |      |           | of all those in the    | System (VESS)        |
|                |      |           | community.             | -Optimal real time   |
|                |      |           |                        | energy balance       |

| Edinburgh      | REC | UK      | Collective generation    | -Mutual DER           |
|----------------|-----|---------|--------------------------|-----------------------|
| Solar          |     |         | and use of solar power   | value increase        |
| Cooperative    |     |         | throughout the city of   | -Shared DER           |
| (2013-present) |     |         | Edinburgh.               | assets -Community     |
| [62]           |     |         |                          | ownership             |
| Isle of Eigg   | REC | UK      | Community run power      | -Shared energy        |
| [63]           |     |         | distribution network     | storage -Local asset  |
|                |     |         | for the remote Scottish  | ownership -Optimal    |
|                |     |         | island of Eigg           | operation             |
| Repsol         | REC | Spain   | Creation of solar energy | -Mutual DER           |
| Solmatch       |     |         | communities to promote   | value increase        |
| (2019-present) |     |         | self-consumption and     | -Peer-to-peer energy  |
| [64]           |     |         | cooperative ownership    | trading -DER          |
|                |     |         |                          | renumeration          |
| NEOOM          | REC | Austria | Commercial energy        | -Mutual DER value     |
| Energy         |     |         | communities available    | increase -Shared      |
| Communities    |     |         | to residential and       | energy storage -Local |
| (2020-present) |     |         | commercial customers     | energy market         |
| [65]           |     |         | to receive credit for    |                       |
|                |     |         | renewables and storage.  |                       |

#### sonnen VPP

The German sonnen community is one of the largest VPPs in the world. It was announced that the virtual system has reached a capacity of 250 MWh, consisting of thousands of decentralised batteries throughout the country. Similar to the AGL VPP concept, the effective battery fleet can be controlled in real time to provide frequency balancing services to the grid. The company has approximately 25,000 sonnenBatteries connected to the system as of 2023, and plans to have a capacity of over 1 GWh in the coming years. The VPP can also perform load shifting, by absorbing excess solar generation during the day and supporting the grid during peak load hours.

This VPP design is a good example of a decentralised system design, in that by allowing small-scale solar and battery systems to participate in the market, far more control is available to the system operators to provide grid services. The ability to effectively smooth out changes in demand-side load will also become vital given the shift towards more non-dispatchable renewable generation. This type of service provision should be a priority for VPPs in order to remove flexible though carbon emitting fossil fuel generators from the grid.

#### **Edinburgh Community Solar Cooperative**

Edinburgh Community Solar Cooperative Limited (ECSC) is a solar cooperative set up in 2013 in the UK which supplies PV solar energy to 24 of the City of Edinburgh's council buildings. With 541 members, the funded PV solar installations supply power to the buildings, for which the council pays the cooperative through a license agreement, with any excess generation renumerated through the UK's feed-in-tariff. The total generation is approximately 2 MW and is therefore the largest energy community of its kind in the UK [62]. According to the cooperative, £1.4 million has been invested so far in the various sustainable projects, with 1.1 GWh of clean energy supplied each year, leading to a saving of over 1,000 tonnes of CO2 as of 2019. Figure 2.13 shows the locations of the council PV installations.



Figure 2.13: Locations of the 24 council and community ECSC PV solar installations

This cooperative has been able to provide low carbon and low-cost energy to a number of buildings. However, it does not yet take advantage of the potential benefits that a VPP system would allow, such as the storage and temporal shift of excess PV solar and participating in energy trading markets. This is largely due to policy and regulatory limitations of the energy market in the UK.

#### Energy4All

Energy4All is a Private Limited Company (PLC) established in 2002 and supports 27 independent renewable energy cooperatives, including the ECSC initiative. As a social enterprise PLC, Energy4All can raise funds through a number of methods, including public shares and bond offers, and through industrial connections being able to bring in

appropriate expertise to support local initiatives financially and technically with project needs. The technologies can range from small scale PV solar to large hydro and community heating networks. A total of 30 MW capacity has been delivered by various Energy4All funding and projects, and over £71 million in community funds raised as of 2020 [66].

## Isle of Eigg

Eigg Electric Ltd [63] is a PLC located on the Isle of Eigg, UK supplies and distributes renewable energy to the residents of the small island. The Isle of Eigg is cut off from the mainland, so the community run energy distribution is responsible for supplying all power to the 96 local residents. Given the isolation from the mainland, all parameters have to be managed by the island operators. The electricity is generated from a mixture of hydro, wind, and solar power. A large hydro power plant of 100 kW supplies the majority of the demand, with two smaller 6 kW hydro turbines. Four small 6 kW wind turbines and a 50 kW PV solar array also supply power to the grid. Residents have an energy usage cap of 5 kW for residential and 10 kW for commercial buildings. With these constraints, the 184 kW is enough to supply all buildings on the island, but there are also two 64 kW diesel generators for emergencies and use during maintenance to the other generators.



Figure 2.14: small-scale hydroelectric generator located on the Isle of Eigg [63]

During times when energy is being produced in excess a bank of 96 4V (48V series) batteries located in the control building absorb the power to regulate the AC frequency and

can be released when required. If there is a scenario when the batteries are fully charged and power is still being produced, a signal is sent to switch on thermal loads in the community, such as community hall and church heaters to shed power. Most excess power generation events occur in the winter, but at other times if space heaters are not required, external thermal loads are used to dump heat to the atmosphere. The hydroelectric generators can also be restricted to limit the power output. It can be noted from the resulting energy grid that removing the reliance on diesel generators and instead using energy from renewable resources would have significantly reduced the environmental emissions of the island.

#### Repsol Solmatch

Solmatch is a commercial solar energy community concept offered by the Spanish multinational energy company, Repsol. The company has created dozens of individual solar RECs within Spain the owners of PV solar installations can join. When a customer signs up to an REC, they qualify to receive a lower charge for their amount of community-based self-consumption. This effectively reduces the energy cost when part of the REC, and through a valid Guarantee of Origin (GoO), they are guaranteed that they consume only clean energy when solar is being generated. The limitations are that the customer needs to be within a 500m radius of the REC's centre, and have sufficient, suitable rooftop area available for a solar installation [64].

This solar-based EC has a number of local benefits. Through the validated GoOs, Repsol can report a net quantity of avoided emissions for those customers. The design also means that no interaction with the national energy wholesale market is required, and the customers are still able to receive a cost benefit. The promotion of local solar installation also allows for greener communities and additional clean power job creation for those areas. Figure 2.15 shows an example REC set up created through this scheme. According to Repsol, there are almost 500 different solar-based RECs currently operating in Spain since the launch in 2019, with 6,800 tonnes of CO<sub>2</sub> avoided as of 2024 [67].

## **NEOOM Energy Communities**

NEOOM is an Austrian data and AI company that provides a REC commercial offering to residential homes and Small and Medium Enterprises (SMEs). Similar to the Repsol solar community, the NEOOM system works by aggregating groups of locally generated clean energy, commercial flexible loads, and storage into an EC. The EC design takes advantage of the recent enactment of the *Renewable Energy Expansion Act Package* (EAG), which allows for the direct and localised sharing of energy system sources within the same geographical location [65].

The NEOOM EC also provides all the same local benefits as Repsol, such as lowering energy costs and promoting local awareness of climate action, whilst expanding the asset



Figure 2.15: Example solar Energy Community created as part Repsol Solmatch [67]

scope. By allowing flexible loads and storage to participate in local balancing, the system is not limited to clean energy generation during sun hours by releasing stored energy during the night, displacing more of the higher emissions grid use. While less information is available on exactly how NEOOM controls these flexible assets, it is assumed that the system is designed to minimise dependence on grid imports over the course of the day.

Through the company knowledge base, NEOOM is one of the few EC providers to publish how the renumeration between community members works. The key element of the EC cost is that any community member should be able to sell energy into the EC at the same price as would be purchased. This ensures that the incentive to provide energy to the system remains high, and keeps the agreed price low, as local PV solar generation is often much cheaper than retail grid energy in Europe [68].

The costs and revenues can be categorised into the following:

- Electricity consumed from the grid or the EC
- Electricity generated and delivered to the grid or the EC
- Service charges and fees for use of the EC

On the consumption side, a typical European grid has a retail purchase price of 44 ct/kWh (gross), compared to the EC price of 23 ct/kWh (as of 2024). In this case it is clearly beneficial to consume from the EC rather than relying on grid energy. On the generation side, European countries such as Austria typically offer a solar Feed-in-Tariff (FiT) of 5-10 ct/kWh. When compared to the ECs agreed price of 23 ct/kWh, there is again a clear advantage to selling energy back to the community [69].

There are also service charges for the operation and maintenance of the EC itself, which NEOOM publish. The community members pay an annual service fee based on the size of the EC, starting from €7.50 per year for less than 10 members, to €3 per year for a community of more than 100 members. Additionally, there is an internal EC FiT that scales inversely depending on the quantity of energy that is delivered. The tariff starts at 2.4 ct/kWh for the first 500 kWh, to 1.2 ct/kWh for volumes over 1,500 kWh. This is to promote community members to install larger generation and storage systems to incur a smaller charge. Table 2.3 below shows an example costing for an EC community member with an annual consumption of 4,500 kWh and PV solar generation of 3000 kWh. It is assumed that the grid FiT is 5 ct/kWh. The resulting difference in annual cost shows that there are advantages resulting from this type of EC, and that with an increasing number of members the cost decreases further.

Table 2.3: Simplified example of the renumeration process of the NEOOM Energy Communities. Adapted from [69]

|                   | Total energy (kWh) | Grid-only cost (€) | EC-only cost (€) |
|-------------------|--------------------|--------------------|------------------|
| Self-consumption  | 2000               | 200                | 200              |
| Import            | 1500               | -75                | -345             |
| Export            | 1000               | 440                | 230              |
| Service fees      |                    |                    | 54               |
| Operational costs |                    |                    | 14               |
| Annual costs      |                    | 565                | 153              |

This type of cost distribution, while simple in its design, promotes growth in the distribution energy generation volume and ensures that all community members get fair renumeration for their investment regardless of system size. It is also an advantage if members shift their consumption to times when the EC generation is highest (peak sunlight hours), to receive the highest volume of cheaper electricity.

NEOOM EC is also an excellent example of using recent energy policy to its advantage in order to reduce investment risk and maximise participation.

#### VPP and Energy Community Concepts Analysis

This section presents a review of the state-of-the-art VPP systems within literature. It can be seen from the research presented that the design can vary significantly depending on a

number of environmental factors and constraints.

The Fenix VPP system is unique as the first true concept to be explored and have real pilot studies conducted. One of the first key differentiating characteristics is the distinction between the TVPP which handles the technical control and scheduling processes, and the CVPP which handles commercial and market interactions with stakeholders. Communication and integration between these two architectures is vital to the smooth operation of the VPP. The available services and commercial success of a VPP depended heavily on the market regulation and policies of the local region. The availability of a standalone Balancing Responsible Party (BRP) to aggregate services into a single energy flow schedule would significantly benefit the commercial operation of the VPP and allow for additional streams of revenue.

The commercially successful concepts including the Australian AGL VPP have been able to display the economic viability of this type of technology. The AGL VPP itself is relatively simple in principle and only has a few output services that are delivered. The first key service is demand and supply balancing for the Fast Frequency Response market in Australia, and the second is the available of emergency energy storage of thousands of energy customers with the required PV solar and battery system installed. The success of the system is due in part to the management of the project by the DSO, AGL. It is therefore more reasonable to be able to access the appropriate technical measurement data and market pathways to integrate the VPP into the traditional energy grid.

Switching from a traditional VPP definition, as is the case with Fenix and Edison, to a localised view of services delivery, removes many of the associated regulatory, technical, and investment risks. By understanding the policy environment, providing a transparent renumeration platform, and supporting system monitoring through smart monitoring and IoT control, the NEOOM Energy Communities concepts performs very well in promoting prosumer participation, clean energy awareness, and electricity cost reduction.

From reviewing these different VPP and EC options, it is clear that the supporting data behind the decision making processes is vital to commercial success. Particularly in the case of NEOOM and Repsol ECs, where data sharing and monitoring is a key value driver. This makes a case for understanding accurately the system design boundaries, control requirements, and services provision through modelling and optimisation, such that risks to the community members can be minimised.

What follows in this work is a review of energy system modelling, control and design optimisation to support the monitoring requirements and long-term decision making of the REC operators and the members.

## 2.5 Asset Modelling, Control, and Design Optimisation

It is clear from the current state of renewables ECs that in order for the positive returns to be realised over the project lifetime, accurate and insightful energy systems design and modelling is a requirement. Given the nature of the problem at hand, which is to design and operate an EC to maximise a single of multiple performance objectives, the problem can be discretised into an energy system model. This type of approach is well-researched over a number of years, some of which have been directly applied to community-based systems.

Research often consists of a defined energy demand over a given period of time, and variable system asset capacities that must be optimised within a set of technical constraints to provide the best possible desired outcome. The work in [70] presents an in depth review of trends, modelling and optimisation of RECs. The review also stipulates that commonly the system assets are grouped into lumped models, represents the loads, generation (often PV solar and wind turbines) and ESS (e.g. battery, thermal, and hydrogen storage). For each of these asset types, their performance characteristics can be represented as a series of mathematical formulae based on the governing principles of the technology. Several research articles present methods for modelling the operation of these assets within a decentralised community energy setting [71–74]. Vujanovic et al. [71] highlights that hybridising many generation and storage assets allows the system to utilise synergies between technologies and achieve the best performance. Some of which combine the dual demand of HVAC and electricity when optimising for a particular objective. Alluraiah et al. [72] in particular assessed an integrated remote microgrid design consisting of mixed wind, solar, battery, and an integrated hydrogen load. There is, however, a clear research gap when assessing energy community systems for islanded, rural locations, particularly when considering different hybrid storage options including regenerative hydrogen generation, storage, and use. This work will explore how the integration of such an asset can contribute directly towards increased energy independence, sustainability and climate transition resilience.

The modelling fidelity of the generation and storage assets also needs to be considered. For example, a solar system could be modelled based on first principles, as described in [75], which considers the physical diode interaction between voltage and current passing through the panel. At the other end of the scale, the solar asset could be considered a simple static model where the rated capacity is multiplied by a load factor profile [74]. The choice of model resolution is again decided by the role of the model and the most important set of the results desired by the system designer.

Finally, commonly used design and control optimisation methods are reviewed in detail. Approaches are often categorised into Linear Programming (LP) problems [76], which are fully deterministic in their outcome, and heuristic optimisation [77], which follows a stochastic procedure to arrive at the optimal result. Both of these are critically reviewed,

before presenting the chosen methodology for this work.

## 2.5.1 Renewable Energy Assets

The following section details the background, modelling techniques, and challenges to the integration of solar and wind generation systems, paying close attention to applications in rural and remote islands.

## Photovoltaic (PV) Solar Systems

PV solar systems are one of the most widely adopted renewable energy generators globally, with over 700 GW of capacity installed globally from 2 billion solar panels as of 2023 [78]. The photovoltaic effect is based on a fundamental physical process in that energy from photons that make up the sun's light can be used to excite electrons in within solar cells, and produce flowing electrical current. Solar, or photovoltaic cells, were first invented in the 1870s and have been studied extensively for use a renewable energy resource. In the 1940s and 50s pure crystalline cells were produced, but only used in exotic instances due to the prohibitively high cost. It was not until the late 20th century that the production cost reduced enough to make solar panels suitable for terrestrial use [79].



(a) PV solar system deployed on NASA's shuttle spacecraft [79].



(b) Commercial large-scale solar farm development made up of individual solar panels

Figure 2.16: The applications of solar cells and panels have progressed significantly over the past 50 years, from space exploration to energy production at scale.

A simple solar cell is made of an n-type layer and a p-type layer of semiconductor. When the energy from photons is absorbed into the n-type layer, electrons are able to break free from the atomic structure. This creates a charged junction between the now positively

and negatively charged layers, and electrical current flows when a circuit is applied across the layers. Modern solar panels are made up of many individual cells connected in series and parallel to produce the desired power output.

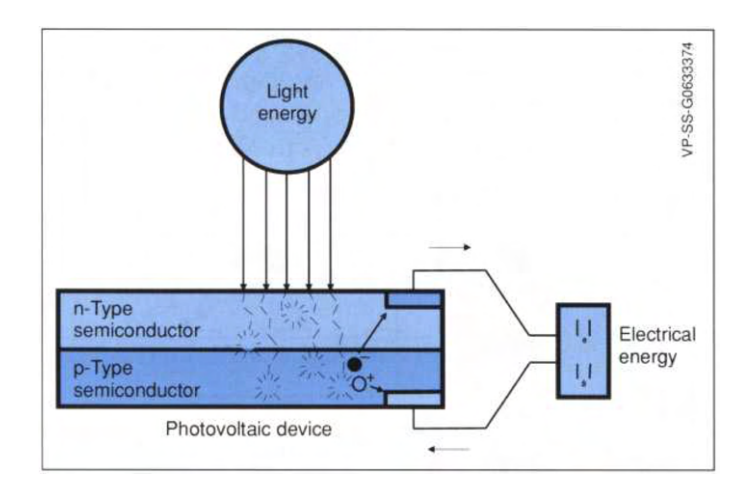


Figure 2.17: The electrical field induced by free electrons in the n-type layer produces flowing current when a circuit is applied [79].

The most common cell chemistries are poly- and mono-crystalline, of which the mono-crystalline variant is most efficient due to less induced resistance within the cell structure [80]. There are also a number of novel chemistries currently being researched, including single junction gallium arsenide cells, multi-junction cells, thin film chemistries, and emerging technologies most notably pervoskite and other tandem cells [81].

For the common mono-crystalline silicon solar panels, the cells can be mathematically represented as a simple circuit, containing a photodiode as a variable current source, as shown in 2.18. This is known as the De Soto PV model, building on the well known works of Duffie and Beckman [82] and is widely considered to be one of the most accurate approaches to simulating the physical properties of a solar cell [83].

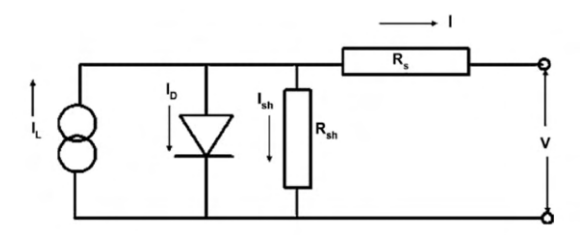


Figure 2.18: A lumped model diagram showing the mathematically modelled components of the solar cell. Source: [83]

Figure 2.18 can be represented as the following equations:

$$I = I_l - I_0 \left[ e^{\frac{V + IR_s}{a}} - 1 \right] - \frac{V + IR_s}{R_{sh}}$$
 (2.1)

where:

$$\alpha = \frac{N_s n_i k T_c}{q} \tag{2.2}$$

in which q is the electron charge, k is the Boltzmann constant,  $n_i$  is the ideality factor,  $N_s$  is the number of series cells and  $T_c$  the cell temperature. The method is also known as the '5 parameter model', as there are five unknown variables to derive numerically, and are often not shared by the manufacturer. These are the following:

- The photodiode current  $I_l$ ,
- the diode reverse saturation current  $I_0$ ,
- the series resistance  $I_s$ ,
- the shunt resistance  $I_r s$ ,
- and the diode ideality factor  $\alpha$ .

The typical current-voltage characteristics of the solar cell is shown in Figure 2.19. The open circuit voltage condition is met when no net current is following, and is instead flowing through the diode. When a load is introduced, the net current is able to flow through the external circuit, but has the inverse effect of lowering the cell voltage. This implies that the power output given the relation P = IV will have a maximum value across the IV range. This is known as the Maximum Power Point (MPP), and changes depending on the resistive load, total solar irradiance, and the cell temperature.

As stated by Duffie and Beckman [82], a solar panel can be considered as an energy balance, where light is either converted into useful electricity or thermal energy. The latter is then absorbed into the cell, raising the temperature, or dispersed through come natural dissipation. This energy balance can be defined by the following equation:

$$(\tau \alpha)G_T = \eta_c G_T + U_L (T_c - T_a) \tag{2.3}$$

Where  $\tau \alpha$  is the effective transmittance-absorptance product that when multiplied by the irradiance  $G_T$  gives the energy absorbed into the solar module.  $\eta_c$  is the cell electrical efficiency,  $U_L$  is the loss factor describing the rate at which energy is lost to the surround ambient temperature  $T_a$ .

To solve the energy balance, the cell temperature set at a consistent ambient condition is needed, known as the Nominal Operating Cell Temperature (NOCT). NOCT is measured at an irradiance of 800  $W/m^2$ , and wind speed of 1 m/s and under no load conditions. Substituting this back into the original equation yields the following:

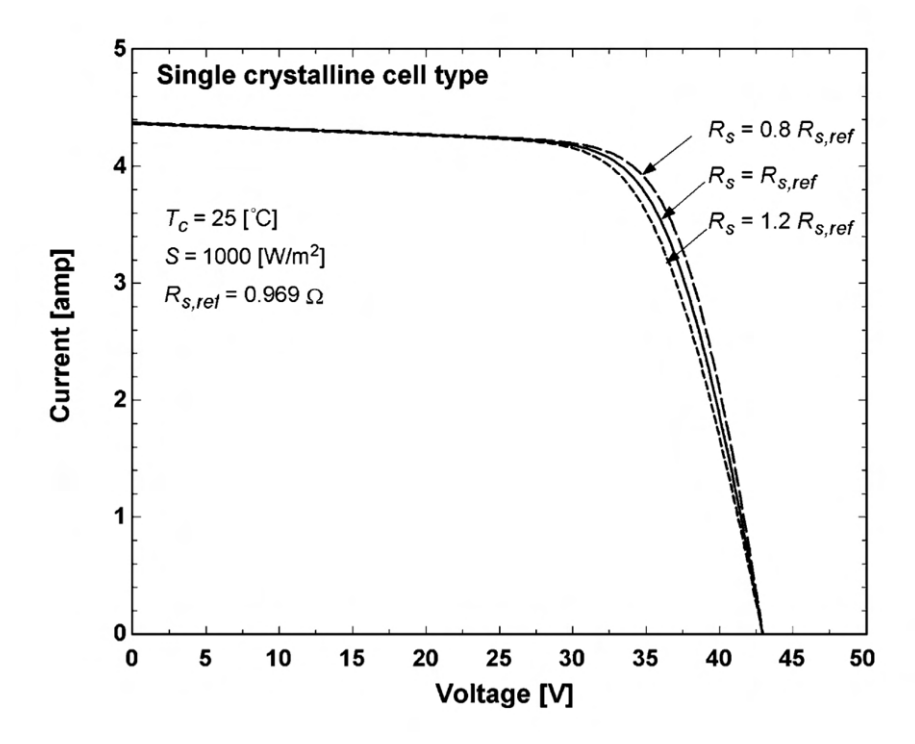


Figure 2.19: A PV solar IV curve showing the impact of changing the series resistance on the output power voltage and current

$$\frac{T_c - T_a}{T_{NOCT} - T_{a,NOCT}} = \frac{G_T}{G_{NOCT}} \frac{U_{L,NOCT}}{U_L} \left[ 1 - \frac{\eta_c}{(\tau \alpha)} \right]$$
 (2.4)

The constants  $\frac{\eta_c}{(\tau\alpha)}$  are considered small compared to the other elements, so is often estimated as 0.9 without significant loss in fidelity [82]. A major consideration is the accuracy of different modelling techniques. Decentralised energy systems, such as PV solar panels and wind turbines rely on switching converters for DC-DC voltage regulation, DC-AC conversion, and frequency regulation with the grid [84]. This includes, for example, the MPPT system required to maintain maximum power output of the system across the range of solar irradiance levels [85]. Given the grid frequency needs to be matched at 50Hz in Europe, the switching frequency of such converters is often in the order of 20-80kHz. It would be computationally impractical to model a system at such a frequency over a 10-20 year lifetime period, and therefore more common to represent the assets' average performance over an hour, day or month. The exact level of granularity is decided by the use case of the model, balancing result accuracy with computational performance.

To overcome this problem, another energy balance approach is used based on the solar cell fundamentals, as described in Equation 2.1:

$$P_i = A_c G_{T,i} \eta_{mp} \eta_e \tag{2.5}$$

Where  $P_i$  is the cell power output (W),  $A_c$  is the cell area  $(m^2)$ ,  $G_{T,i}$  is the average solar irradiance over time i,  $\eta_{mp}$  is the efficiency at MPP and  $\eta_e$  is the cell electrical efficiency. Known manufacturer data can then be substituted into Equation 2.5, in addition to the operating cell temperature based on Equation 2.4. A fully worked example is provided in the methodology section.

Another key challenge with modelling and integrating PV solar systems into a remote EC system is monitoring module derating. Derating factors can come in many forms, including a measure of dust and dirt build-up on the modules, natural degradation of the cells, and wire corrosion. The expected annual derating factor is often provided by the manufacturer, and gives a measure of how much % power output will be lost. This can be integrated into the long-term modelling to determine the actual lifetime operation of the PV solar system. The other challenges to solar integration in islands, including space requirements, and managing excess power generation will be discussed in later chapters.

This simplified model representation of solar systems is well documented in its applications in the techno-economic analysis of decentralised energy systems. Research conducted in [72] used the approach to optimise a remote microgrid design for the lowest system cost, where the entire lifetime cashflow must be considered.

## Wind Turbines

A wind turbine simply describes an electricity generating technology that is powered solely by the movement of wind to provide rotational energy [86]. The two primary wind turbine designs are horizontal- and vertical-axis variants, which describe the orientation of the generator rotation. Different wind turbine designs are chosen based on the wind characteristics of the local environment, space and cost constraints. Comprehensive comparisons between turbine technologies are laid out in [87–90]. The instantaneous power that can be extracted from a fluid flow is the integral of the mass flow rate, which itself is a function of the fluid density  $\rho$ , area A, and fluid speed U:

$$P = \frac{1}{2} \frac{dm}{dt} U^2 = \frac{1}{2} \rho A^3 \tag{2.6}$$

However, not all energy can be converted into power due to the Betz limit, which is the theoretical maximum power coefficient  $c_p$  [91] that any wind turbine is able to achieve from the air flowing past the blades. [92]. The graph in Figure 2.20 that vertical-axis turbines tend to operate at a lower tip speed ratio  $\lambda$ , that is, the ratio of the rational speed and the length of the blades. This work will focus primarily on the modelling and integration of the three-blade horizontal-axis turbine as it is the most commercially available and well-researched, and also generally achieves the highest  $c_p$ .

When considering the  $c_p$  and electrical losses  $\eta$  from conversion equipment, Equation 2.6 can be updated to the following where  $\underline{U}$  is the average wind speed over the given time

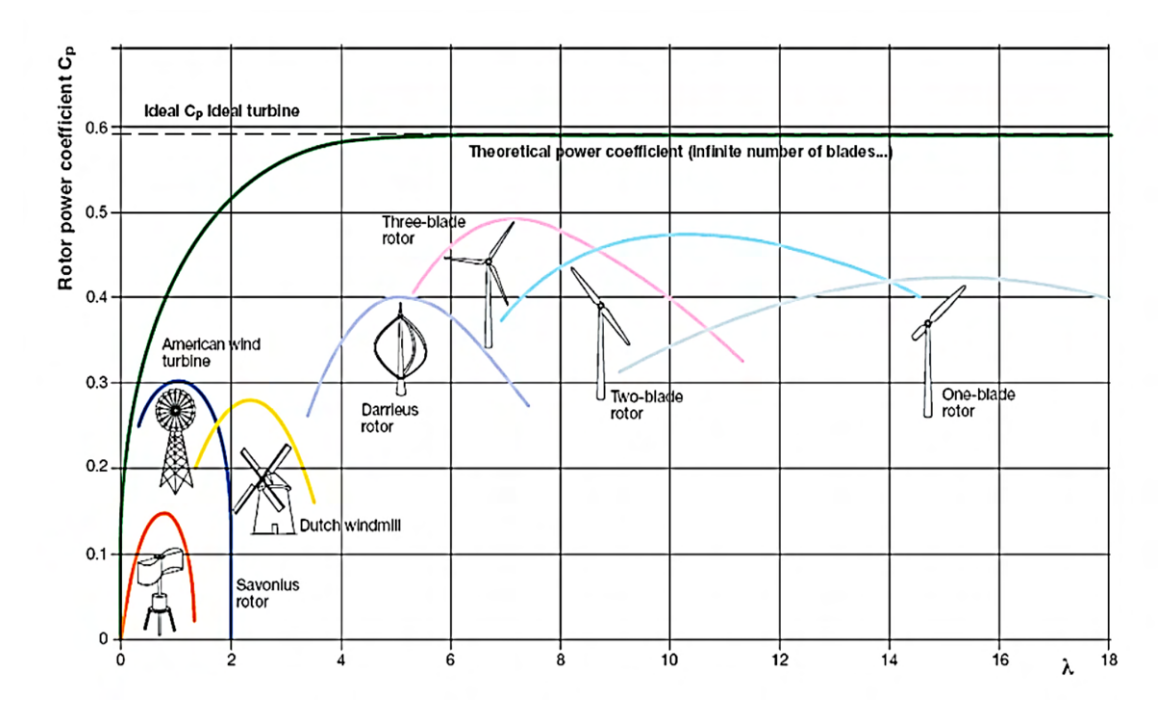


Figure 2.20: Diagram showing some types of wind turbines and their rotor power coefficient and tip speed ratio [93]

interval:

$$P_w(\underline{U}) = \frac{1}{2} A c_p \eta \underline{U}^3 \tag{2.7}$$

The type and design of the wind turbine depends on the conditions of the installation location. For geographical island applications, there are a number of local factors to consider. For horizontal axis wind turbines, these can be broadly categorised into onshore and offshore. The placement of the turbine primarily impacts the average wind speed that is met by the turbine blades, and so is directly proportional to the energy generated [86].

Onshore: Onshore wind turbines are designed for use on land, so take advantage of the specific weather conditions of different land formations. The interaction between the land and air over mountains, valleys, plains or plateaus will impact the average wind speed and variation over the year. Onshore turbines will therefore, on average, produce less energy than their offshore counterparts. Onshore turbine size is also often a limiting factor to energy generation, but increased reliability and maintainability is expected to reduce overall investment cost [94]. Onshore wind is therefore more commonly considered for use in RECs due to their low cost and smaller-scale.

Offshore: Offshore turbines are increasing being deployed at significant scales. Wind farms installed in seas benefit from a stable wind speed without any obstacles, so can generate more energy on average, while also allowing land to be freed up for cultivation

and inhabitation [95]. However, the harsh environmental conditions and salt water mean turbines are more likely to experience failures and therefore require regular maintenance [96], with accessibility to perform such maintenance being challenging [97].

### Wind Speed Variability with Height

Wind will naturally interact with obstacles on the ground, creating a velocity gradient that increases with elevation. This phenomenon is known as wind shear, and the relationship between wind speed and measurement height can be approximated using the log law [98]. The relationship is defined by a roughness length  $z_0$ , which is a function of the terrain type. It can be seen in Table 2.4 below that the wind speed impact due to land obstacles can be significant.

Table 2.4: Values of surface roughness length for various types of terrain [86]

| Terrain Description                   | $z_0 \text{ (mm)}$ |
|---------------------------------------|--------------------|
| Very smooth, ice or mud               | 0.01               |
| Calm open sea                         | 0.20               |
| Blown sea                             | 0.50               |
| Snow surface                          | 3.00               |
| Lawn grass                            | 8.00               |
| Rough pasture                         | 10.00              |
| Fallow field                          | 30.00              |
| Crops                                 | 50.00              |
| Few trees                             | 100.00             |
| Many trees, hedges, few buildings     | 250.00             |
| Forest and woodlands                  | 500.00             |
| Suburbs                               | 1,500.00           |
| Centres of cities with tall buildings | 3,000.00           |

The Log Law is defined as the following, in which z is the turbine height, k is the Von Karmen constant, U\* is the friction velocity, U(z) is the speed measured at turbine height:

$$ln(z) = \left(\frac{k}{U^*}\right)U(z) + \ln(z_0)$$
(2.8)

Wind speed measurements from an anemometer are often at a different height to the actual turbine hub height, so the equation can be reformatted such that the wind speed at any height U(z) can be modelled if the reference height  $z_r$ , reference wind speed  $U(z_r)$  and roughness length  $z_0$  are known:

$$U(z) = U(z_r) \left( \frac{\ln \frac{z}{z_0}}{\ln \frac{z_r}{z_0}} \right)$$
 (2.9)

Statistical methods can also be utilised to evaluate the theoretical total energy generated at a given site. This approach is commonly based on two probability distributions: Rayleigh

and Weibull. As discussed in [86], Rayleigh is more commonly used as only the average wind speed over the time period is needed, whereas the Weibull distribution requires both a shape and a scale factor to determine the outcome.

It is also common for wind turbines to be modelled numerically with a full CFD analysis. A review by [99] details the advancements in CFD analysis of turbines of different scales. The interactions between the blades and variable wind speeds, in addition to wakes created by nearby rotating turbines produces an extremely complex series of interconnected factors that will ultimately impact the power generation, control characteristics, ware, and potential failure modes of the assets. This type of modelling is also often considered when designing the turbine itself, including the blade profile, tip speed ratio and hub height, or to investigate the applicability for different installation sites. Since this work is focused primarily on the techno-economic performance of wind generation at the energy community level, it is vital to choose an appropriate level of modelled complexity for the application. It was therefore chosen not to explore this facet of wind turbine modelling, and to assume that a small amount of error will exist in the approach explained above.

## 2.5.2 Energy Storage Systems

ESSs are vital to balancing the intermittency of the non-dispatchable renewables discussed [100]. According to BloombergNEF, total storage capacity globally could pass 400 GW by 2030, indicating an enormous demand for grid balancing in the face of increasing volumes of wind and solar [101]. Without storage balancing assets, the service provision is left to traditional, flexible oil, coal and gas plants, significantly increasing the carbon emissions of energy use. While this work has previously reviewed ESS service provision within VPPs more broadly, it is key to also understand the applicability for energy communities, and the advantages of modelling such assets for optimal decision making. Different ESSs have varying strengths and weaknesses which must be taken into account. These are usually categorised as (1) their average discharge time at rated power and (2) their total potential storage capacity. The graph in figure 2.21 below shows the range of potential ESS options.

This work aims to compare the applicability of lithium-ion battery chemistries, as one of the most commonly researched and implemented storage types, to a novel hybrid hydrogen storage system. The technologies are compared in terms of their fundamental storage processes, common modelling approaches, strengths, and weaknesses when applied to power grids and energy communities. This review also explores the ways in which ESS in general are vital to the success of RECs if aiming for energy independence and security, in addition to system stability. The modelling of these systems can support complex design decision making as well as future renewable development for remote communities.

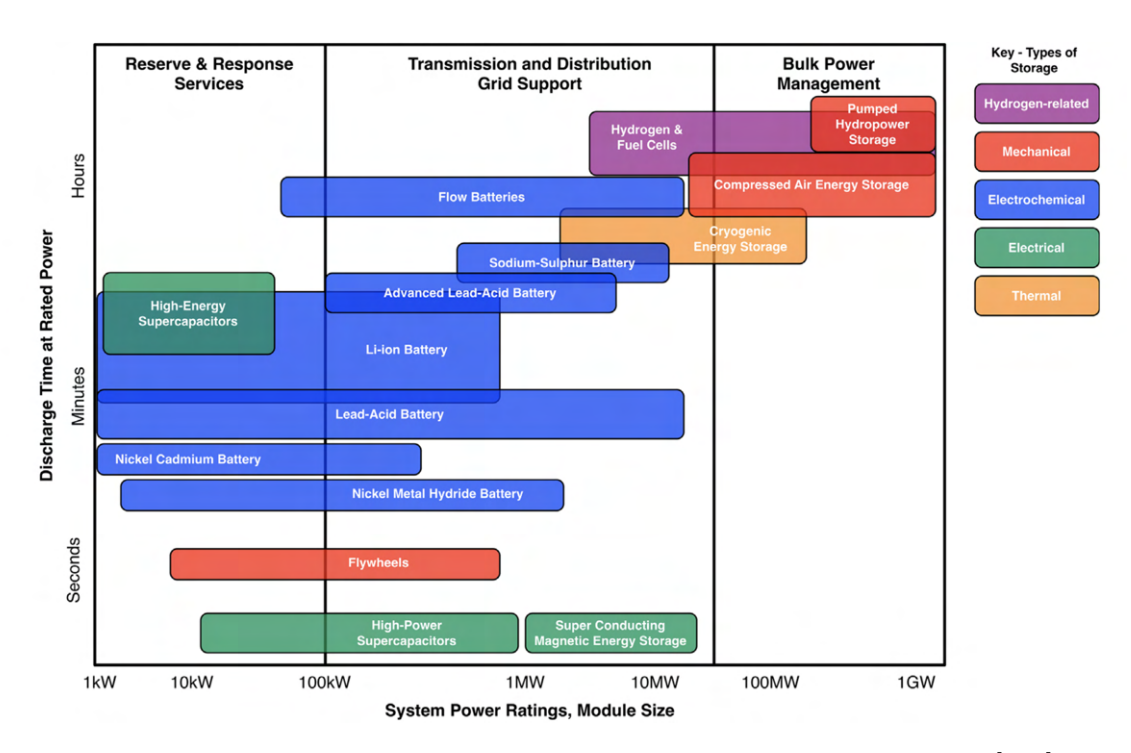


Figure 2.21: Suitability of various ESS technologies for grid applications [102]

#### **Battery Energy Storage**

Electrochemical batteries are one of the most critical components of model technological advancements. TA broad range of battery chemistries exist, including commonly used lead-acid and nickel cadmium varieties, to novel sodium sulphur and flow batteries. The most common of all, particularly those touted for electrical grid storage applications are lithium-ion technology.

Li-ion batteries have already seen huge commercial success in mobile phones, laptop computers, watches, and other small-scale applications. The need for a significant reduction in transport emissions globally has also seen the demand of li-ion batteries in electric vehicle applications grow exponentially since the start of the 21st century, with an estimated 27 million new EVs globally by 2026 [103]. For this reason, there are a number of literature sources considering battery modelling techniques specific to EV applications [104–106].

The chemical principle of li-ion batteries is the redox reaction that occurs between the anode and cathode materials that make up the cell, involving the lithium ions and electrons. The lithium ions move between the cathode and anode through the electrolyte through the separator, while electrons travel through the external circuit [107].

A common approach to modelling electro-chemical batteries is to consider the dynamics of the charge/discharge curve at different current levels. MATLAB and other popular dynamic modelling software use a modified version of the Shepard battery model [108], which describes the charge and discharge based on the terminal voltage, open circuit

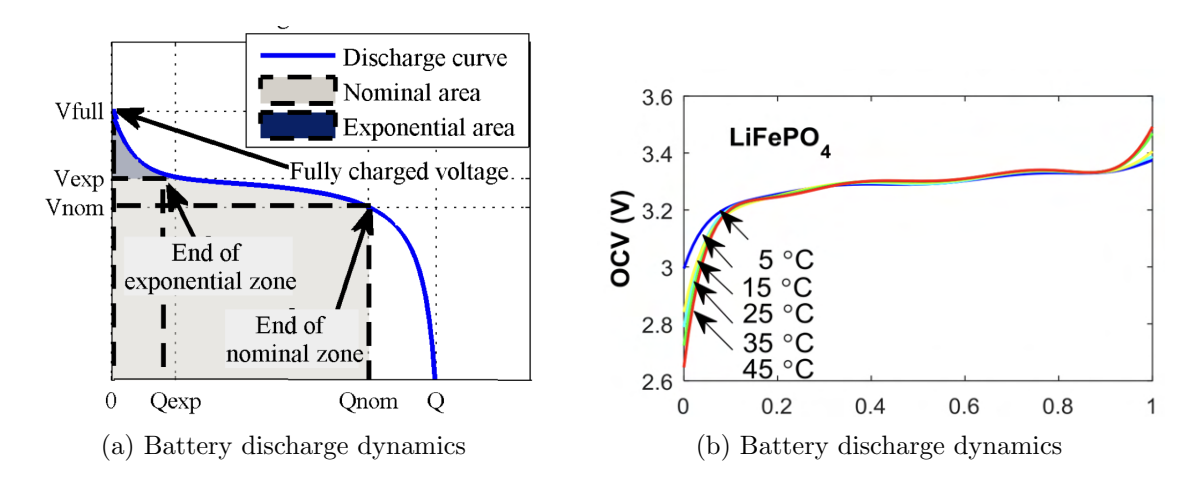


Figure 2.22: The charge in discharge characteristics of lithium ion batteries. [108]

voltage, internal resistance, discharge current and state-of-charge [109]. The model is based on an equivalent electrical circuit, similar to the PV panel methodology. The equations are as follows:

Discharge:

$$V_{batt} = E_0 - Ri - K \frac{Q}{Q - it} (it + i*) + Ae^{-Bit}$$
 (2.10)

Charge:

$$V_{batt} = E_0 - Ri - K \frac{Q}{it - 0.1Q} \left( i * -K \frac{Q}{Q - it} \right) it + Ae^{-Bit}$$
 (2.11)

These equations are based on the non-linear cell voltage  $V_{Batt}$ , the constant voltage  $E_0$ , low-frequency current dynamics I\*, cell current I, extracted capacity it, total capacity Q, exponential voltage A, exponential capacity B, and polarisation constant K.

The formulae are arranged in the model as shown in Figure 2.23. It should be noted that li-ion batteries also do not need to consider the non-linear exponential function that factors in hysteresis effects in charge and discharge, as is for other battery chemistries.

Measuring the State-of-Charge (SOC) of the cell is another challenge, as the relationship between the cell voltage and SOC is non-linear. Equation 2.12 presents the classical approach to 'count' the current leaving the cell (A) over time to approximate the change in capacity (Ah), where  $Q_n$  is multiplied by the cells nominal capacity (Ah).

$$SOC(t) = SOC(0) - \frac{1}{Q_n} \int_0^t I(t)dt$$
 (2.12)

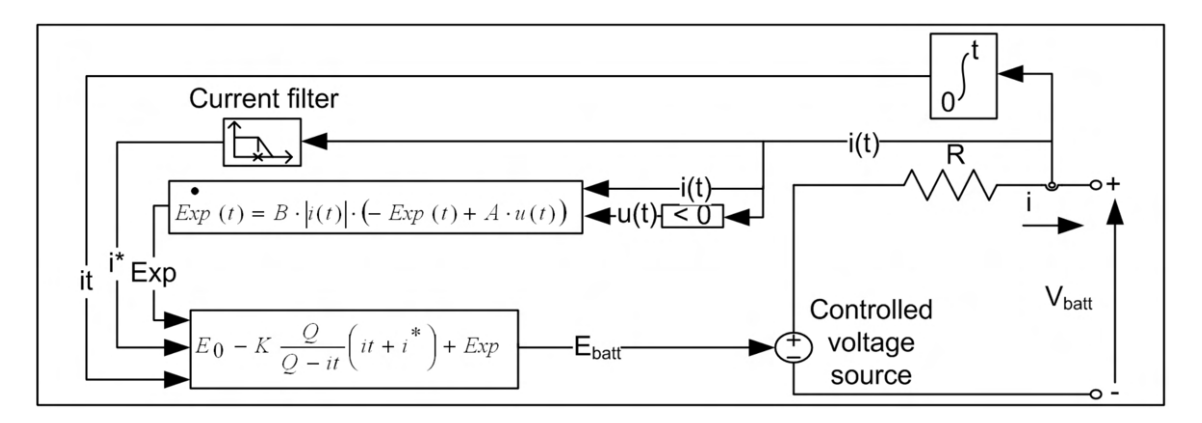


Figure 2.23: Li-ion battery equivalent circuit diagram under charging condition [108]

There are numerous examples of the application of li-ion battery chemistries in VPP and REC applications. Storing excess energy from renewable sources in a BESS not only increases the efficiency of final energy use, but also reduces the induced emissions from consuming additional grid energy. A number of resources have considered control strategies that maximise performance based on a combination of performance objectives, such as self-consumption and self-sufficiency [110–112]. The quick response time of BESS also allows for dynamic P2P energy trading markets to be created between participants of the REC [113].

One of the key market differentiators of BESS in decentralised energy applications is its low investment requirements. The cost of grid scale batteries is set to fall from a global average of 290 \$/kWh in 2022 to 175 \$/kWh in 2030 [114]. This is clearly a huge benefit to local communities that may not have the start up capital required for other ESS options. There are also potential disadvantages to using BESS in rural and remote ECs. There are concerns about the safety of battery cells [115], which if not properly monitored for heat anomalies could lead to a scenario known as thermal run away [116]. Additionally, batteries suffer from self-discharge over time when left in open circuit mode [117], which can lead to lower efficiency if only used intermittently.

While BESS will clearly have a major role to play in balancing renewables, there is a performance gap in the long-term, seasonal storage time frame. This is where hybridisation with a hydrogen-based storage system could plug this performance gap, and maximise the benefits of both technologies simultaneously.

#### Regenerative Hydrogen Storage

Hydrogen gas, being the most abundent molecule in the universe, is a versatile energy vector. Traditional uses of hydrogen have been as a feedstock for the industrial and petrochemical sectors. Hydrogen can also be combusted to produce energy directly. In recent years, there has been growing interest in hydrogen's use in storing and generating electricity.

One of the most common methods of extracting electrical potential from hydrogen is via fuel cells (FCs). FCs designs can vary in definition and internal structure, but the fundamental principle remains similar for all. The example below explains the working process of a Proton Exchange Membrane (PEM) FC, the most common and commercially available variant. A PEMFC stack consists of anode and cathode layers separated by an electrolyte. Hydrogen enters at the anode where a catalyst, typically platinum, splits the molecule into  $H^+$  protons and electrons. The protons are 'exchanged' through the electrolyte and meet the incoming oxygen molecules at the cathode side, which gives the PEMFC variant its name. The electrons flow through an externally connected circuit, meeting with the reactants at the cathode where water and heat are formed as byproducts. The chemical equations for the anode (2.13) and cathode (2.14) are given below:

Anode side:

$$H_2 \to 2H^+ + 2e^-$$
 (2.13)

Cathode side:

$$\frac{1}{2}O_2 + 2e^- + 2H^+ \to H_2O \tag{2.14}$$

The diagram in Figure 2.24 shows the typical arrangement of components within one FC stack. The central subassembly where the chemical reactions occur is known as the Membrane Electrolyte Assembly (MEA), encased by bipolar plates which aid the channeling of  $H_2$  fuel and air into the cell.

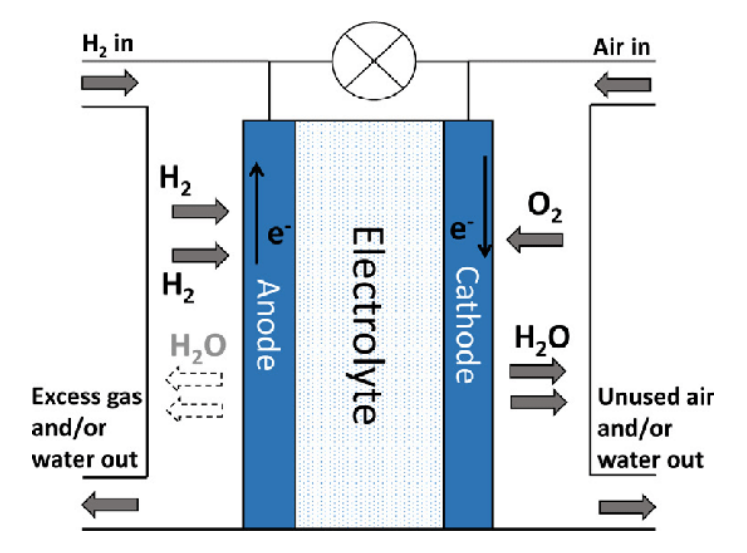


Figure 2.24: Diagram showing the working principle of a hydrogen fuel cell, specifically a PEM variant [118]

While PEMFCs are commonly assumed to be the most commercially mature of the fuel

cell designs, other options exist in the market that are more suited to certain applications. Fuel cells have been both used and touted for use in passenger cars [119], heavy transport [120], shipping [121], aerospace [122], industrial processes [123], and off-grid Uninterruptable Power Supplies (UPS) [124]. This review focuses on a comparison between PEMFC and AFC variants, though the full range of hydrogen fuel cell options is as follows:

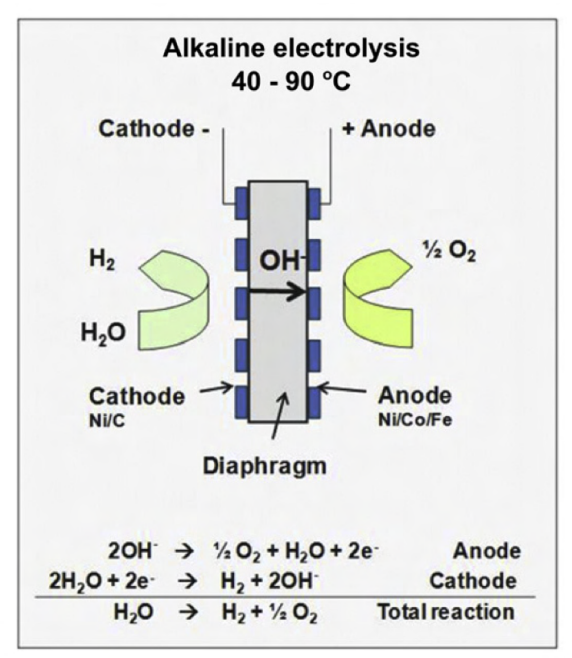
- 1. Proton Exchange Membrane Fuel Cell (PEMFC)
- 2. Alkaline Fuel Cell (AFC)
- 3. Phosphoric Acid Fuel Cell (PAFC)
- 4. Molten Carbonate Fuel Cell (MCFC)
- 5. Solid Oxide Fuel Cell (SOFC)

PEMFCs are the most dominant design due to their simple design, low operating temperatures that allow for a quick start-up, and high power density per active area. Disadvantages include the need to carefully control the moisture levels in the MEA to ensure optimal ionic conductivity, and the required platinum catalyst which can be costly. AFCs by contrast, allow the  $OH^-$  anion to travel through a liquid membrane and react with the incoming  $H_2$  at the anode. A potassium hydroxide electrolyte is used to allow transit of the anions. The operating temperatures range from 30-250C. Advantages of this design include a simpler cell structure, no required catalyst leading to lower costs, and fast start-up. However, the projected lifetime is approximately half that of the PEMFC. A comparison between these and the other options is given in Table 2.5. This work will focus primarily on PEMFCs due to their prevalence and competitiveness for applications in decentralised energies and grid storage support.

Table 2.5: A comparison table displaying the key characteristics of different hydrogen fuel cell variants [121, 125]

| Variant | Operating   | Electrolyte  | Efficiency | Power/Module |
|---------|-------------|--------------|------------|--------------|
|         | temperature |              |            |              |
| PEMFC   | 60-120°C    | Nafion       | 45-55%     | 200 kW       |
|         |             | membrane     |            |              |
| AFC     | 30-250°C    | KOH          | 40 - 50%   | 100 kW       |
| PAFC    | 160-220°C   | $H_3PO_4$    | 30-42%     | 400 kW       |
| MCFC    | 600-800°C   | $Li_2CO_3$ - | 43-55%     | 250 kW       |
|         |             | $K_2CO_3$    |            |              |
| SOFC    | 800-1000°C  | YSZ (yttria  | 50-60%     | 250 kW       |
|         |             | stabilized   |            |              |
|         |             | zirconia)    |            |              |

The next key component of the regenerative hydrogen storage system is the electrolyser. The electrolysis of through PEM technology is, in principle, the opposite process of electricity generation from a PEMFC. Water flows in at the anode, splitting into  $H^+$  and  $OH^-$  when current is supplied. Ions travel through the electrolyte to the cathode and are released has hydrogen gas. In anion exchange or alkaline electrolysis, water is instead supplied at the cathode, and  $OH^-$  anions flow through the liquid hydroxide electrolyte leaving the ions to be released as hydrogen gas. The diagrams in Figure 2.25 below show the process of electrolysis for both PEM and Alkaline types.



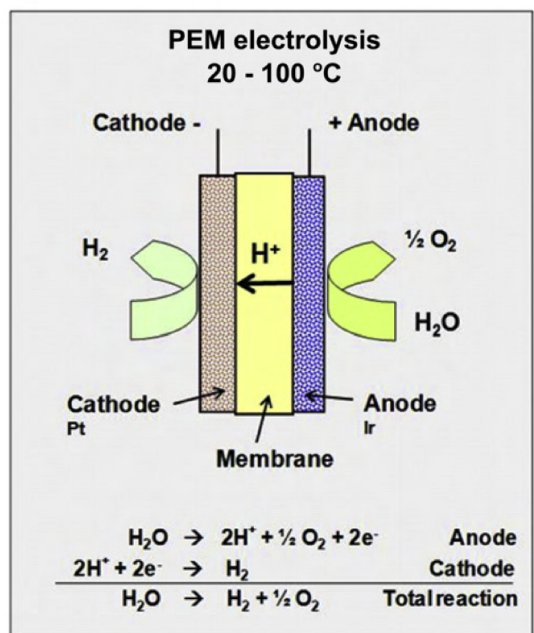


Figure 2.25: Diagram displaying the operating principles of PEM and Alkaline electrolysis [126].

When it comes to modelling, the electricity production within a PEMFC can be represented using a very similar approach to electrolysis. The assumption is that the internal resistances apply a negative (voltage decrease) effect in the FC and a positive (voltage increase). For an electrolyser, this is represented as follows:

$$V_{el} = E_{Nerst} + V_{act} + V_{ohm} + V_{conc} \tag{2.15}$$

The voltage of the cell  $V_{el}$  is equal to the open circuit or Nerst voltage  $V_{Nerst}$  plus the activation voltage  $V_{act}$ , the voltage loss arising through driving the electrochemical reaction, the ohmic voltage losses  $V_{ohm}$ , caused by linear electrical resistance through the elements of the cell, and the concentration voltage loss  $V_{conc}$ , caused by flow restrictions inside the MEA as the volume of ionic/anionic flow rises [126]. The graph in Figure 2.26 displays where the impact of the different losses occurs along a common electrolyser polarisation curve.

The approach to model these voltage loss components will be discussed in the methodology

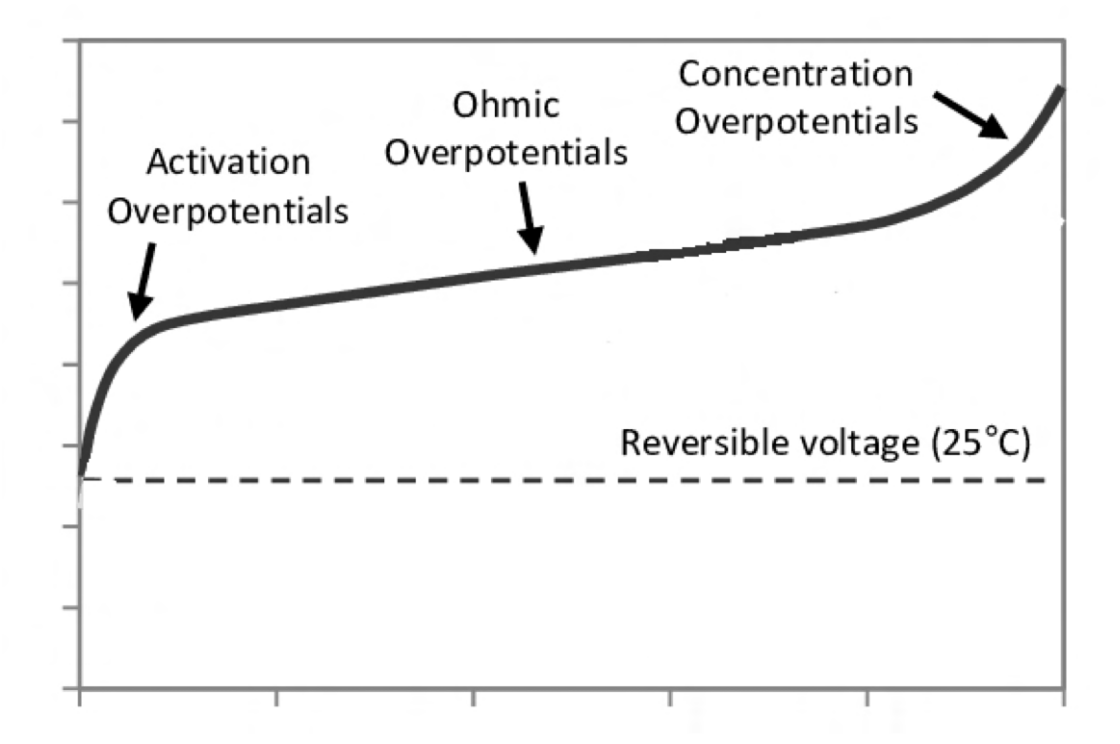


Figure 2.26: A typical polarisation curve of a PEM electrolyser [127]

section. For the energy system modelling approach, it is critical to understand the overall efficiency of conversion for both fuel cell and electrolyser at different operating regimes. There are a number of methods that can be used to approximate this value, including for electrolysers a variation of the Butler-Volmer equation [128]. For this work, an equations 2.16 and 2.17 used to first determine to hydrogen flow rate (in either production or consumption), which can be combined with the voltage output in equation 2.15 and operating current to find the overall efficiency. For both technologies, the hydrogen flow rate  $f_{H_2}$  is found by the following:

Fuel Cell:

$$f_{H_2} = S\left(\frac{IN_p}{nF}\right) \tag{2.16}$$

Electrolyser:

$$f_{H_2} = N_p \eta_f \left(\frac{I}{nF}\right) \tag{2.17}$$

For the stoichiometric air-fuel ratio S, operating current I, number of parallel cells  $N_p$ , number of electrons per hydrogen molecule n (2), Faraday constant F, and Faraday efficiency  $\eta_f$  for which the derivation is shown in equation 2.18.

$$\eta_f = 96.5 \exp\left(\frac{0.09}{i} - \frac{75.5}{i^2}\right) \tag{2.18}$$

While there are a number of examples of the use of BESS and other storage types in rural and remote energy communities, far less research has been conducted on the potential cost and emissions benefits of hybridising the ESS with a regenerative hydrogen system. A study in [129] sets out a hybrid hydrogen-battery-biomass energy community with wind and solar power generation, and results in a Levelised Cost of Energy (LCOE) of 0.084 €/kWh, five times lower than the equivalent thermal plant. A very similar community system design, also in Italy, with integrated solar, wind, battery and hydrogen storage, produced a far higher result of 0.455 €/kWh [130], showing the range of potential uncertainty. Research in [131] presents a much larger scale remote energy community with integrated hydrogen storage, resulting in a cost of 0.128 \$CAD/kWh.

Furthermore, there is limited to no knowledge of the impacts when applied to geographical island locations. A model of hybrid hydrogen and battery energy storage system in combination with renewable generation is used to provide electrical, as well as fresh water and gas heating demand for a remote island in Bangladesh [132]. This work also uses Non-Dominated Sorting Genetic Algorithm (NSGA-II); a type of multi-objective a type of evolutionary algorithm that has a number of advantages over common deterministic methods. These optimisation approaches are discussed in detail in the following section. The optimal solution resulted in an LCOE of 0.17 \$/kWh, which is in the range of similar designs for this type of application. However, this work does not consider a grid-connected case and local energy trading between community members. The system also uses the hydrogen system for CO<sub>2</sub> methanation rather than direct electrification via a fuel cell.

The work presented in this thesis aims to plug the gaps in knowledge across applications of a hybrid regenerative hydrogen system for rural or islanded RECs, and how to optimise the design for best performance.

# 2.5.3 Optimisation Approaches

Determining the design and size of the REC can be thought of as a complex optimisation problem. In previously discussed works, almost all cases use some form of optimisation routine, commonly consisting of a set of decision variables, system constraints, and an objective function. In simple terms, the values of the decision variables are set by the algorithm through some arithmetic means such that the objective function can be minimised or maximised.

In the case of energy systems, the decision variables often consist of design criteria, for example, the size of the solar system or total volume of battery storage, but can also include the individual control inputs at each timestep of the model.

In this review, the two main optimisation approaches used in energy system modelling applications are discussed. First, deterministic algorithms with particular focus on Linear Programming (LP), followed by heuristic algorithms, making the primary focus NSGA-II. Both options are attempting to solve a global optimisation problem, that is, a design

problem where the objective function may have multi-extremal solutions within the design domain [133], but ultimately a best solution for which the objective function is at its global minima. This is critical for energy system applications with potential non-linearities, where multiple good design options exist, subject to the necessary constraints.

For both categories, an assessment of applications in REC design from literature is detailed, highlighting key strengths and limitations in the context of renewable energy systems. Finally, the decision to utilise one of these optimisation methods is presented, with a rationale for following the said approach.

Included at the end of the section is an analysis of commonly used software and tools to carry out this type of modelling, and reasoning why a novel modelling framework programmed in Python over other commercial options was chosen for this work.

# **Exact Methods: Linear Programming Optimisation**

LP is a simple yet widespread deterministic optimisation method that represents a physical design or planning problem as a series of linear equations and relationships. LP itself is a historical significant area of mathematical study dating back to its use by Fourier in the 19th century. It was not until the advent of commercial computing in the 1960s and 1970s that LP models were finding applications in power system planning and design optimisation [134]. One of the first examples of this was an optimal loading and dispatch of power plants in order to meet network security constraints presented in [135].

LP and its related methods, including Mixed Integer Linear Programming (MILP) and Non-Linear Programming (NLP), have become significant enabling algorithms in the fields of engineering and design, having moved from an academic interest to a major element of modelling in industrial and commercial practice. The relationships between different assets and processes are summarised into the objective function, which is then minimised or maximised to find the result. LP has an extensive history in energy system modelling applications [136], and is still one of the most common modelling methods due to the breadth of applications and transparency.

To describe the optimisation problem, continuous LPs, that is, a problem where the input variables can take any value, can be expressed as this general algebraic form [137]:

$$minZ = f(x, y)s.t. \begin{cases} h(x, y) = 0 \\ g(x, y) \le 0 \\ x \in X, y \in Y \end{cases}$$
 (2.19)

f(x,y) is the objective function definition, for example to minimise total energy system cost. h(x,y) are system conditions that describe the overall performance, for example the power output of a solar array at given temperature, irradiance and sun angle conditions. g(x,y) are constraints applied to the system, which could be to limit the size of the solar array due to space constraints. In this example, the x and y variables are continuous

(denoted by  $x \in X, y \in Y$ ), whereas for MILP problems the y outputs would be limited to integer form  $(\{0,1\}^m)$ , which can be beneficial when considering control systems with discrete modes. Setting up this problem produces a multi-dimensional domain of potential feasibility, in which the optimal solution will exist. The graph in Figure 2.27 below shows a simple two-dimensional example of the use of constraints to define a feasible region.

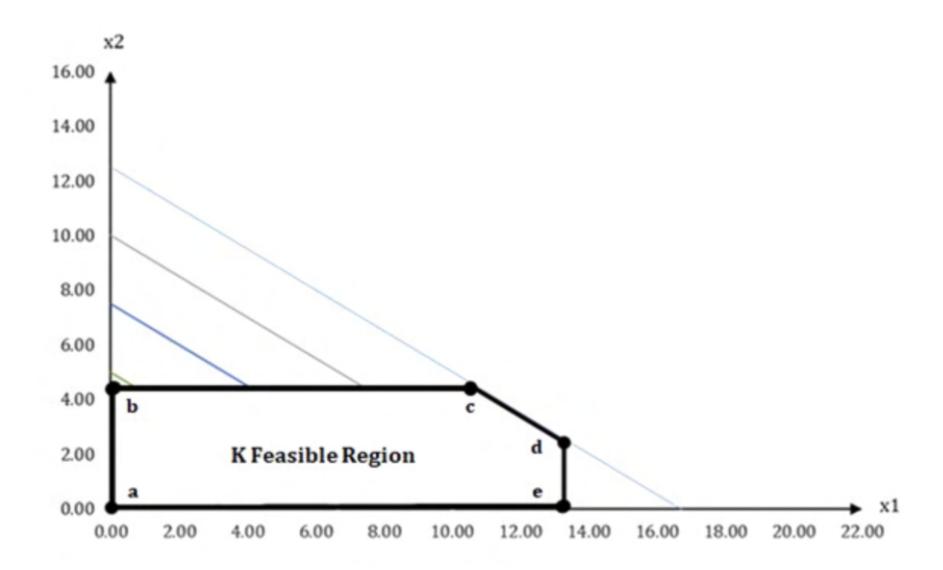


Figure 2.27: Example of a constrained LP problem illustrating the feasible region [138].

The second element of the approach is the optimisation routine itself used to find the solution, commonly designed to search out the optimal value from within a feasible design region.

The algorithm popularised by this application is the simplex method, invented in the mid-20th century. The simplex method follows a simple premise that given a feasibility region, the linear structure can be used to determine the 'worst' objective function outcome, also known as the basic feasible solution (BFS). The BFS will exist on one of the extreme vertices of the region. With the solution now limited to just feasible possibilities, the algorithm simply walks through each connected vertex, checking whether the objective function has improved with iterations. Because the problem is linear, this process will eventually result in finding the optimal solution [139].

While other algorithms, including gradient descent and interior point methods, have been proven to operate much more efficiently in certain applications, the premise of iteratively evolving the objective function towards the optimal results remains.

Due to the maturity of LP (as well as MILP and NLP), there is an extensive collection of research into their uses across decentralised energy system design, planning and optimisation. A review conducted in [136] notes 145 different tools to assess the design and operation of mixed energy use community districts that deploy some form of deterministic optimisation. The linear model produced in [74] considers the optimal deployment of wind and solar, and

ultimately results in an LCOE of less than 0.1 €/kWh. A similar deterministic modelling approach in [140] is used to determine the cost savings for members investing in the renewable EC, and found that working cooperatively the community can save considerable energy cost compared with the grid only scenario. The key strength of deterministic algorithms is that, based on the input assumptions, the result can be resolved completely to produce a single analytical solution. This process removes ambiguity in modelled outcomes and ensures accuracy.

A number of commercial energy system design software employ LP and MILP algorithms due to their prevalence and ability to provide defined and repeatable results. These softwares commonly include HOMER energy [141], iHOGA [142], Plexos [143] and MATLAB/Simulink [144].

However, there are downsides to the LP approach. One key disadvantage is that, as the model is resolved as one solution, it is more challenging to explore the feasible domain space and form relationships between competing objective functions. This can be proxied using the weighted sum method to produce a scalar objective, as shown in Equation 2.20 [145], however it limits the utility, and providing the suitable weightings can be challenging. For example, while combining the competing objectives of lowest cost and carbon emissions is possible, describing the relationship between these objectives and relative negative impact is not trivial.

$$f(x) = w_1 f_1(x) + w_2 f_2(x) + w_3 f_3(x) + \dots$$
(2.20)

where:

$$\sum_{i=1}^{M} w_i = 1, w_i \in (0, 1)$$
(2.21)

The other disadvantage is that because the model is exact, all timesteps are resolved completely, which vastly increases computational complexity for hourly simulations over a one year period, and limits the ability to create user defined control and trading logic. Conducting a stochastic sensitivity analysis, such as Monte Carlo [142] or SOBOL [146] analysis on the results to determine the reliance on specific inputs is also difficult (but not impossible) to perform with such a large, fully defined model. All relationships and model definitions also need to be linearised in order to solve, which is not always possible for renewable energy assets because of the inherent non-linearities between environmental inputs and power production. This is where the concept of heuristic modelling can fill a number of performance gaps.

# Heuristic Methods: Machine Learning and Genetic Algorithms

The invention of heuristic and meta-heuristic algorithms was motivated by a need by researchers to provide solutions to optimisation problems that were either too complex to be fully defined or too large to return an exact result. The formed hypothesis was that for most problems, a mathematically exact solution could be estimated by approximation and remain accurate enough to be credible, which gave rise to robust heuristic search algorithms.

Many heuristic algorithms are inspired by biological process, swarm/colony behaviors or physical phenomena. These can be broadly categorised into single-solution or population based as shown in Figure 2.28, with the latter consisting of the likes of Particle Swarm Optimisation (PSO) and Genetic Algorithms (GA), of which GA will be the main focus of this work. The two search schemes instilled in these procedures are the concepts of exploration (diversification) and exploitation (intensification) [147]. Exploration generally describes the procedure's ability to efficiently search the feasible domain space, while exploitation collects knowledge as the optimisation proceeds to guide the following iterations. This idea was first applied to tabu search, one of the oldest heuristic approaches [148], but perfectly encapsulates what GA is aiming to achieve.

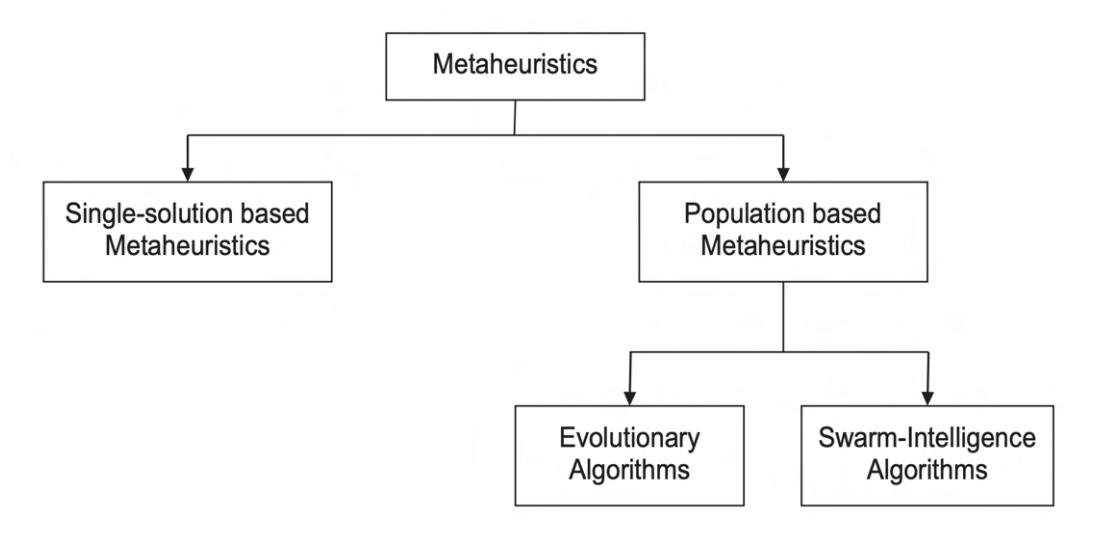


Figure 2.28: The classification of metaheuristic algorithms [149]

GAs are based on the evolutionary nature of living beings, and their ability to adapt over time to their surroundings [150], following Darwin's "survival of the fittest" law. The optimal design of an energy system can be considered analogous to a natural system or behavior, in that the assets are working together to produce the best outcome based on the environmental factors and constraints. In the algorithm, new populations are produced after each iterative generation that take on some of the characteristics of the previous generation, through the concepts of crossover, mutation, and elitism which improves the

value of the fitness function (objective function) over time. A visual illustration of the generational progression of GAs is shown in Figure 2.29. Katoch et al. [149] produced a thorough review of GAs and produced the following description of the procedure. A population Y containing unique chromosomes n is initialised, where the chromosomes are made up of a random spread of variables. Well performing chromosome sets are combined according to the crossover probability  $C_p$  to produce offspring O. Mutation, commonly induced through random gaussian noise, is also applied to offspring, which ensures a degree of diversity in the population. Some well-performing 'elite' chromosomes are passed straight through to the next generation, and the process continues until the termination criterion is met.

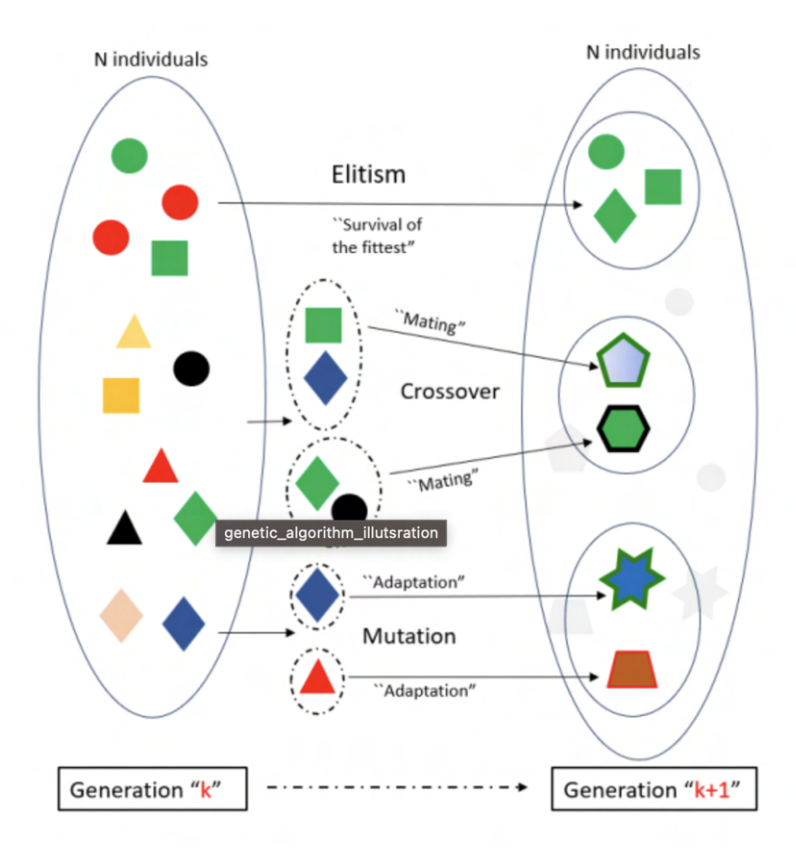


Figure 2.29: Components of a Genetic Algorithm [151].

It can be noted how, when applied to a system design problem, the combination of selection, crossover and mutation aids the algorithm as it can effectively explore the search space while ensuring the exploitation of information learned from previous generations. This reduces the probability of the optimisation result settling in a local minimum, as shown in Figure 2.30, which can be the case for other search algorithms. The additional benefit from a resource perspective is that each chromosome's model can be run in parallel, significantly improving the overall computation time.

While they are applied less often to decentralised energy system models through

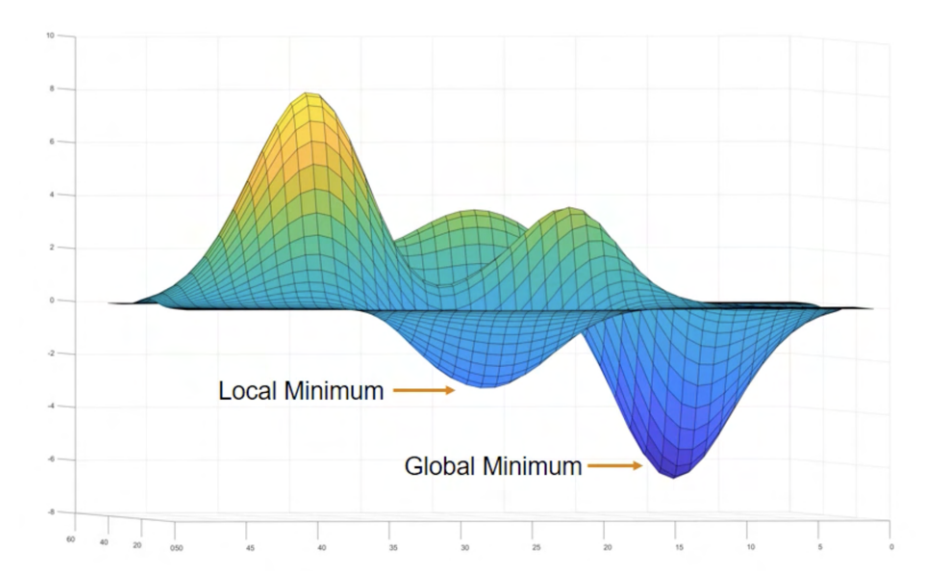


Figure 2.30: A 2D search plane illustrating the existence of both a local and global minimum. [152]

commercial software, there are still a number of GA optimisation examples within the literature. A particularly strong area of study is where GAs can be used to optimise battery storage size for an energy community [153, 154], leading to reduced operational costs and environmental impact. Ismail et al. [155] provided some of the earliest research to suggest that a decentralised energy system of combined renewable power and battery optimised via GA could be a viable source of power for a remote community. The optimal consumption of shared PV solar generation using GA has also been presented [156, 157] and illustrated the potential to optimise for multiple community agents.

While there are several advantages to GA application for decentralised energy community design, there are also disadvantages when compared to more traditional LP/MILP optimisation.

# **Approach Comparison**

Table 2.6 outlines the common performance and user considerations that must the factored in when chosen a model optimisation methodology, qualitatively assessed from excellent to poor. It can be seen that the deterministic and heuristic approaches have their own respective strengths and weaknesses, and literature shows that both options have been successfully applied in some form to energy systems design.

The key capabilities of the final approach need to include the following:

- 1. The ability to model complex asset dynamics and community trading logic quickly and efficiently,
- 2. to resolve to a solution when the model may not be fully observable over the time

period,

- 3. to represent storage asset charging and discharging characteristics,
- 4. to observe the hypothesised trade-off relationship between energy cost savings and emissions reduction,
- 5. to ensure the model can be run quickly and efficiently so as to perform ensemble sensitivity analysis.

Because of these reasons, it was decided to opt for the heuristic NSGA-II optimisation process. Although the LP/MILP is a comprehensive, industry standard approach to system design, the potential for performance issues and lack of multi-objective optimisation availability in particular it means that the approximate method is more favourable.

Table 2.6: Comparison of key performance and usability considerations between the two model and optimisation approaches.

| Factor          | Deterministic (LP/MILP)                  | Heuristic (GA)                           |  |
|-----------------|--|--|--|
| Accuracy and    | <b>Excellent</b> : Problem is resolved   | Good: Result is an                       |  |
| convergence     | to a single solution                     | approximation of the actual              |  |
|                 |  | result with high accuracy                |  |
| Computational   | Good: Energy models are                  | Excellent: Much lower resource           |  |
| simplicity      | usually fast to run, but an hourly       | requirement, and processes and           |  |
|                 | system model is highly resource          | can parallelised                         |  |
|                 | intensive                                |  |  |
| Modelling       | Good: Highly flexible in                 | <b>Excellent</b> : Can handle complex,   |  |
| flexibility     | domain and asset modelling, but          | non-linear relationships with            |  |
|                 | relationships must be linearised         | multiple variables                       |  |
|                 | for LP/MILP                              |  |  |
| Result          | <b>Excellent</b> : Problem will evaluate | <b>Poor</b> : Random inputs to starting  |  |
| repeatability   | to the same solution every time          | condition and mutation will result       |  |
|                 |  | in slightly different outcomes each      |  |
|                 |  | time                                     |  |
| Multi-objective | <b>Poor</b> : Only a weighted scalar     | Excellent: NSGA-II algorithm             |  |
| support         | multi-objective can be formed            | allows two or more objectives            |  |
|                 | using independent objectives             | to be evaluated to observe the           |  |
|                 |  | pareto front                             |  |
| Sensitivity     | Good: Some sensitivity analysis          | <b>Excellent</b> : Can run sensitivities |  |
| analysis        | is possible, but all solutions will      | on independent parameters and            |  |
| implementation  | be optimal                               | produce non-optimal solutions            |  |

In addition, the aim of this work is to show that an optimised energy community system can not only have the potential to save both cost and emissions for rural or islanded communities, but to also create a bottom-up, open-source modelling tool that will allow those communities to plan their own systems and investments. It therefore made logical

sense to create the model and optimisation routine in Python, using openly available products rather than commercially available software requiring licensing to operate.

The potential uncertainty induced through use of the approximate NSGA-II method will be assessed through a sensitivity analysis of key parameters.

# 2.6 Review Summary

The objective of this chapter is to critically explore the barriers, opportunities, and implications of VPP-based renewable energy systems deployment for rural and remote islanded communities. This review highlights the major role that RECs can play in the energy transition, and how energy system modelling and control of decentralised assets can optimise the system design to minimise cost and maximise decarbonisation impact.

It has been noted throughout the earlier sections that VPP systems can play a vital role in integrating decentralised, intermittent clean power into a coherent and commercially viable energy asset. Their role in providing grid flexibility and the possibility of integrating into the existing energy market has huge potential to reduce grid congestion to improve resilience. The development of digital connectivity and smart-grid system allows for enhanced grid visibility for operators, with more data feedback to optimise control decisioning making. The aggregation of small-scale assets also allows small-scale operators and cooperatives to enter the energy market more easily. The process of reviewing several VPP and related microgrid case studies reveal that the concept is not without challenges. There are several policy barriers associated with integrating into the power market, including asset size limits, day-ahead prediction uncertainty, and lack of incentives. There are also societal concerns regarding reliability, future government support, and cost benefits for local citizens who are most impacted by decentralised energy assets.

The solution to several of these problems is to instead to the REC which, most importantly, removes the requirement to navigate the energy market policy landscape at a regional and national level. Focus can instead be turned towards realising the system benefits at a local level. RECs are also recognised in the RED-II policy documentation, meaning an existing framework can be used to form the REC design architecture. From this point, the review begins to consider how an REC system model could be used in a to shine a light on the optimal cost and environmental performance of a potentially deployable system.

The review then covers several commonly associated renewable generation and storage assets, assessing design choices and modelling approaches. The storage assets in particular have complementary roles in which they operate most efficiently: batteries are excellent at short-term response applications whereas hydrogen storage excels in seasonal and long-term storage.

The energy system control and optimisation can take on a number of forms, and

most commonly either a linear programming model or a heuristic optimisation is applied. It was decided to follow a heuristic approach due to the opportunity to evaluate the system performance on a multi-objective basis, pitting the cost benefits directly against the emissions reduction potential. Alteratively, it is possible to combine these objectives by means of a carbon price, however, the uncertainties regarding carbon pricing both currently and in the future inspire considerable research and debate, so it was decided to not include this in the approach, and keep system cost and emissions separate.

The topic of RECs is being widely discussed in the research community, particular due to the possibilities of increased energy independence and equity among citizen cooperatives, so exists a wide-array of methods and results in the literature. However, this work aims to sit in the gap between REC technical design studies and what would be needed to widespread uptake of such systems. What was identified here was a lack of an approach to quantify uncertainty regarding the performance of such systems, particular when considering energy storage configurations and investment risk attributed to decentralised assets, as well as how modelling could be used to guide supportive policy frameworks for future REC deployment.

These insights and identified novel research areas are brought forward and expanded in the following methodology chapter. Emphasis is placed on balancing environmental and economic performance for the REC field test location, and modelling the most effective storage configuration in an accurate and computation resource efficient manner. The literature review has been vital to identifying the challenges and opportunities of RECs and VPPs, and how the gaps in the literature will positively contribute to the energy sustainability goals of Europe and the rest of the world.

# Chapter 3

# Case Study Definition and Modelling Methods

# 3.1 Overview

This section presents the materials and methodology of this research, starting with an overview of the field study location around which the Energy Community system will be designed and modelling. Collection of local energy demand and weather data is used to guide and optimise the design of the remote energy system.

The modelling approach is then laid out in detail, presenting the asset model definitions, governing equations and assumptions. A description of the system control follows, and how the integration with the genetic algorithm-based optimisation logic was achieved. The objective function formulations are also discussed, considering the techno-economic metrics of Present Value (PV) and Internal Rate of Return (IRR) of the Renewable Energy Community (REC) system, and decarbonisation potential against the counterfactual. These outcomes can then be compared against the counterfactual, grid-only scenario.

The purpose of the model is to allow analysis of the REC system's performance without the need to test or deploy the assets in the field, significantly reducing the associated risks and costs of such activities. One of the key novel elements of this work is the analysis of a hybrid battery and hydrogen energy storage system to trade-off the benefits of both technologies. When considering high power, remote energy systems, there are also safety factors to be taken into account, in addition to the clear cost benefits. These safety regulations can be difficult and costly to meet, particularly when deploying systems in remote and rural locations. Model-based design allows for significant knowledge to be gained about the potential performance of the system without having to manage the risks associated with large-scale batteries and stored hydrogen.

The sensitivity analysis method is laid out, as well as plausible ranges of uncertainty across key modelling assumptions of each of the assets. This approach employs Sobal

sensitivity analysis to provide the statistical range of uncertainty against the central, optimised result.

# 3.2 Field Test Location

The characteristics of the final deployment location dictate several aspects of the final Energy Community design. The number of solar hours and average wind speed will naturally impact the degree to which renewable energy can be produced. Additionally, the local demographic and the way power is consumed over the course of the year will influence the system design decisions of the energy storage system to maximise performance.

# 3.2.1 Location Overview, Geography, and Climate

In this case study the location of the Energy Community deployment is the island of Formentera; a remote and largely rural location south of Ibiza and in the Mediterranean Sea.

Formentera is the smallest of the Balearic Island chain, measuring just 19 km across at its widest point, and with its main civic centre being Sant Francesc Xavier towards the north of the island. The island has approximately 11,000 inhabitants as of 2023.

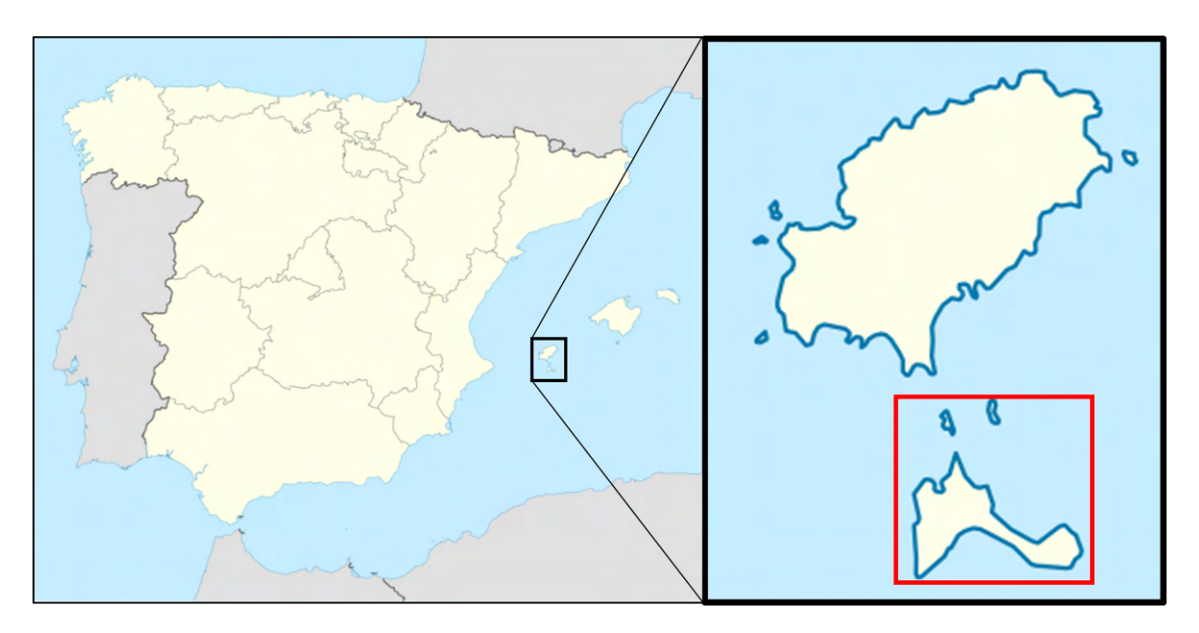


Figure 3.1: Map showing the location of Formentera in relation to the Iberian peninsula.

While Formentera's economy has been historically one of fishing, agriculture and maritime trade, like the other Ballearic islands it has shifted towards a dependence on tourism, particularly during the summer months. The move to a tourism focused economy has caused a huge change in the resource consumption habits of the island. In the case of electricity, demand can grow from a base load of 4 MW in early spring to over 16 MW during peak summer months.

The island has a local power grid connected in the north to Ibiza via a sea-cable, and renewable generation on the island in the form of a 2 MW solar farm. These two

sources combined are able to support power demand needs during times of low demand. However, the island also has an 18 MW diesel generator and 13 MW open cycle gas turbine (OCGT) to provide peaking power. Not only are these generators incredibly costly, with this particular OCGT known to be one of the most expensive in all of Spain, they also produce thousands of tonnes of CO2 annually.

In recent years, the island has recognised the growing need to reduce the emissions from energy consumption. In 2019, the local 'consel insulae de Formentera' announced plans to reduce emissions by 40% by 2030, in line with the EU's net-zero ambition. To maintain a strong tourism economy, the island will need to consider how best to manage the varying daily and annual power demand while also removing the dependence on flexible fossil fuel generators. This is where a hybrid renewable energy storage system could play an important role in the island's net-zero future.

### **Local Climate**

Like much of the mainland Iberian peninsula, Formentera has a warm, arid-like climate. The island enjoys a high level of solar irradiance throughout the year, reaching an average 4.6 Sun Peak Hours (SPH), that is, the number of hours per day that the irradiance exceeds the nominal  $1000 \text{ W/m}^2$ . The hourly solar irradiance of the island in 2023 is shown in Figure 3.2, along with the hourly temperature and wind speed.

It should be noted that the island generally sees lower average wind speeds than much of Europe, which could make the possibility of wind generation less attractive for potential EC developers. The current environmental laws surrounding the protection of migrating birds also hampers current deployment. Despite this, the model will test the cost effectiveness of wind generation to present a scenario where the environmental protections are lifted for small-scale wind turbine generation only.

The weather data is collected via API from Global Solar Atlas and NASA's Power LARC database [158].

# Power Grid Emissions

When considering the impact a potential energy community system and measurable benefits, it is key to define the current status of induced emissions through the current energy grid. All centralised power grids will have a value of embedded emissions at each node of consumption, due to the variety and location of generators providing electricity. Formentera has a mix of local generation from both renewable and fossil origins, but relies heavily on the sea-cable from Ibiza, which itself is connected via the island of Majorca to mainland Spain. To get an accurate measurement of the emissions intensity of at the REC node on Formentera, an analysis of the emissions via interconnection has to be included, considering the connection back to the mainland.

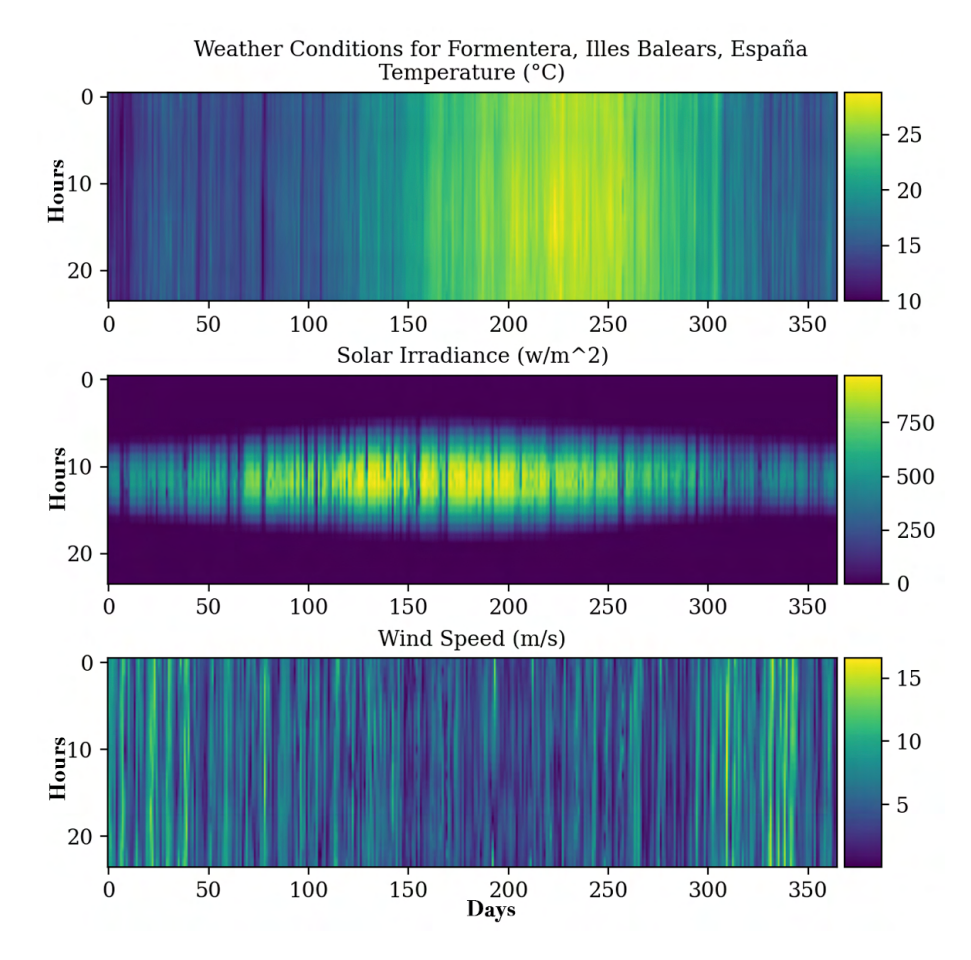


Figure 3.2: The meteorological conditions by hour of day and day of year for the proposed EC location.

Generation and demand data collected from the Spanish Transmissions System oPerator (TSO) RED Electrica de Espana (REE) has been used to build up a dataset for the local grid emissions at the REC node for each hour over one year [159]. This is achieved by first calculating the emissions intensity of the mainland, then applying this value to the interconnection activity in combination with local generation in Majorca. This process continues for each island until an accurate value for emissions intensity for Formentera is derived. The diagram in Figure 3.3 displays the flow of interconnections from the mainland to the proposed EC.

The reason why this analysis is so critical is that while strides have been made towards providing the Balearic Islands with more renewable energy, the remote nature and extreme seasonal differences in demand mean that all the islands still rely heavily on unabated coal and gas generators. This is to provide flexibility, and, although interconnection from the mainland can theoretically provide a vast majority of clean power, there are reliability and maintenance factors to consider that ultimately mean the islands cannot rely solely on them.

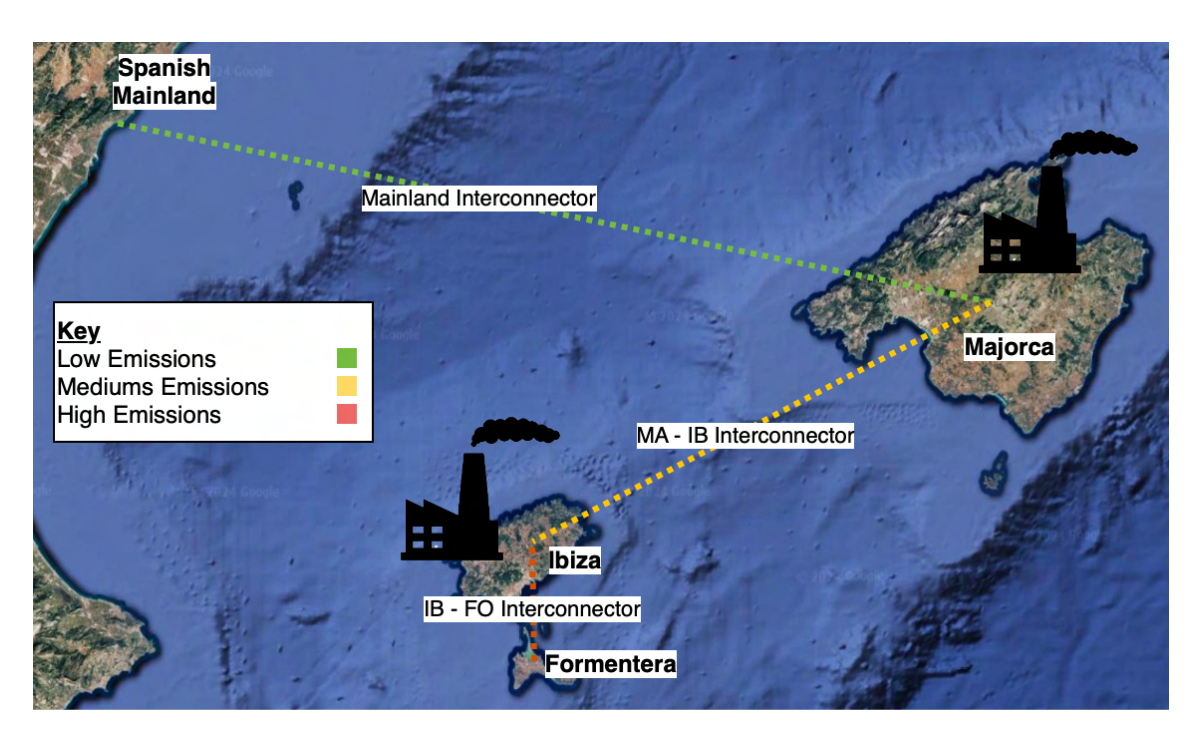


Figure 3.3: The interconnections between the mainland and Formentera, illustrating the increase in emissions intensity of the island communities.

The graph in Figure 3.4 shows the historical emissions intensity of the island based on the data from the Distribution System Operator (DSO). Emissions have remain very high compared to the Spanish mainland, peaking at over 600 gCO<sub>2</sub>e/kWh during the summer tourist season. While the emissions remain high until 2019, the COVID 19 pandemic in 2020 caused a significant reduction in tourist activity, which can be observed as a dip in the maximum emissions. This was because a lower demand for electricity from lower island occupancy led to less need for the local diesel and gas turbine engines to provide peaking power, and hence less emissions were released.

The challenge with defining a suitable baseline for the grid emissions intensity is that it is always likely to vary, not only throughout the year but also into the future as more decarbonisation efforts are taken to reduce reliance on the heavy emitters on the island of Formentera. However, such research regarding the projection of future emissions intensity of nations is a field of study in itself, and has therefore not been considered as part of this work. Instead, it was chosen to adopt a conservative view of the average emissions in recent years to provide a trade-off between the historically high emissions of the island, and what will likely be a steady reduction in emissions over the coming years. Therefore, it was decided to take the 2020 emissions intensity average as the baseline for this work. The reasons for this are that, firstly, the data has been actually measured so is a historically accurate representation of the island, and secondly the COVID 19 pandemic induced a scenario in which lower reliance on fossil fuels occurred. Therefore, one could argue that

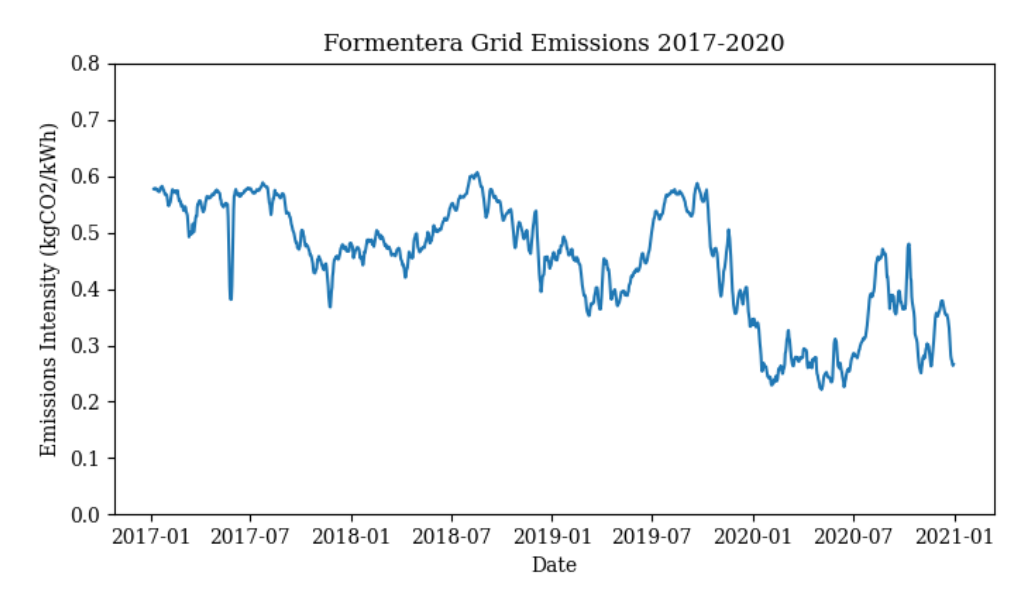


Figure 3.4: Historical emissions intensity on the Island of Formentera 2017-2020, obtained from REE.

it is most representative of a near future grid emissions state of the island of Formentera under normal tourist demand and local activities.

Figure 3.5 shows the emissions in 2020 with the average emissions intensity plotted. Based on this analysis, an average intensity value of  $325~\rm gCO_2e/kWh$  was chosen as a conservative view of the grid emissions on the island.

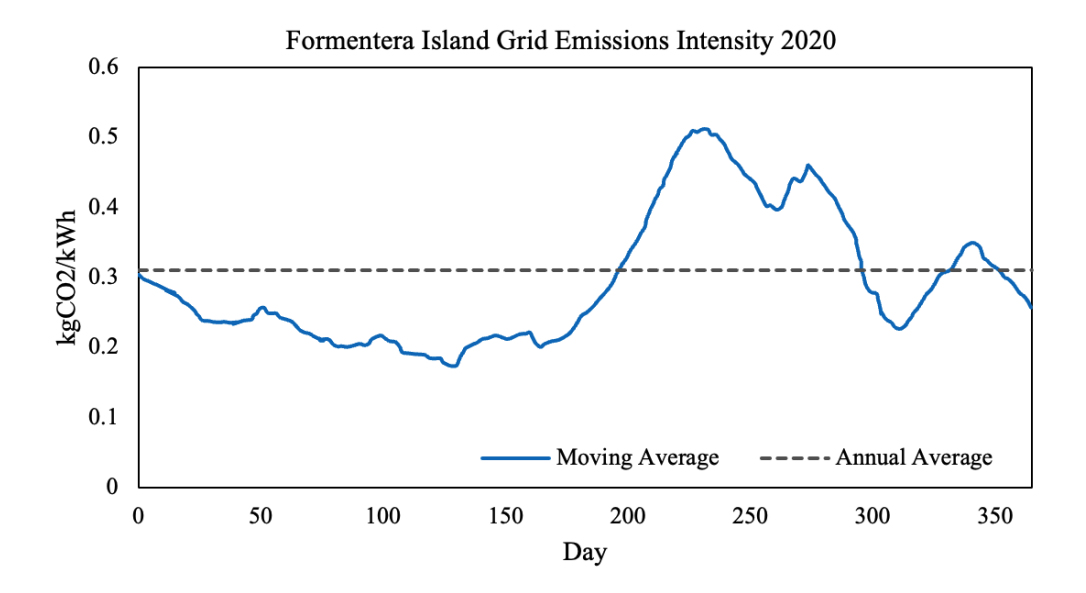


Figure 3.5: Daily and annual average emissions in 2020 for Formentera, obtained from REE.

# 3.2.2 Energy Community Definition and Building Load Profiles

# **Proposed Energy Community**

The proposed energy community test site is located north of the civic centre of St Francesc, and consists of a number of community owned and private buildings. The selection is shown in Figure 3.6.

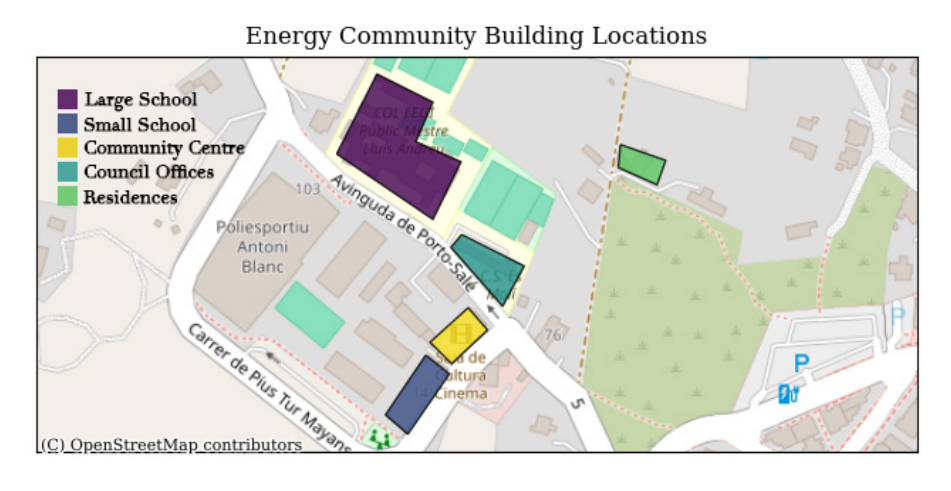
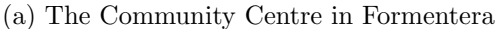


Figure 3.6: Locations of the individual buildings

The first is the 'Culture building', named here as the community centre, a community-owned hub consisting of a library and small cinema; the second a primary school; the third are council offices and a youth centre; and the fourth a secondary school. For this work the







(b) Current solar capacity installed on the roof of the small school

Figure 3.7: Proposed REC location on the island of Formentera

inclusion of three residential properties nearby were also considered as they consist of different load and demand requirements for power.

All buildings are located within 500m of one another, and are connected downstream of the same secondary substation. The total renewable energy generation volume will be restricted such that it does not exceed 200 kW. These prerequisites ensure that the REC design complies with the latest EU decree law 199-2021 for energy communities, and allows the creation of a local, virtual energy trading layer on top of the existing power utility market.

The chosen renewable and storage assets include decentralised solar arrays installed on each of the roofs of the buildings, one or more micro-wind turbine generators, and a hybrid battery and hydrogen storage system that is shared between the community members. The conceptual design on the system is shown in Figure 3.8.

### **Building Load Profiles**

A number of approaches can be employed to determine the building load of the REC model. Energy demand is highly impacted by the timing of various activities and the level of occupancy, and can therefore vary significantly for different building roles and services.

A common option is to take a bottom-up approach to building a composite view of different buildings demands. Osman at el. [160] proposed a model to investigate the impact of different household activities and behaviours on the timing and volume of demand across lighting, appliance loads and hot water use. The model uses a probablistic methodology calibrated to historical data and is able to generate stochastic yet realistic load profiles. However, a key downside of this approach is the availability of input data, which for

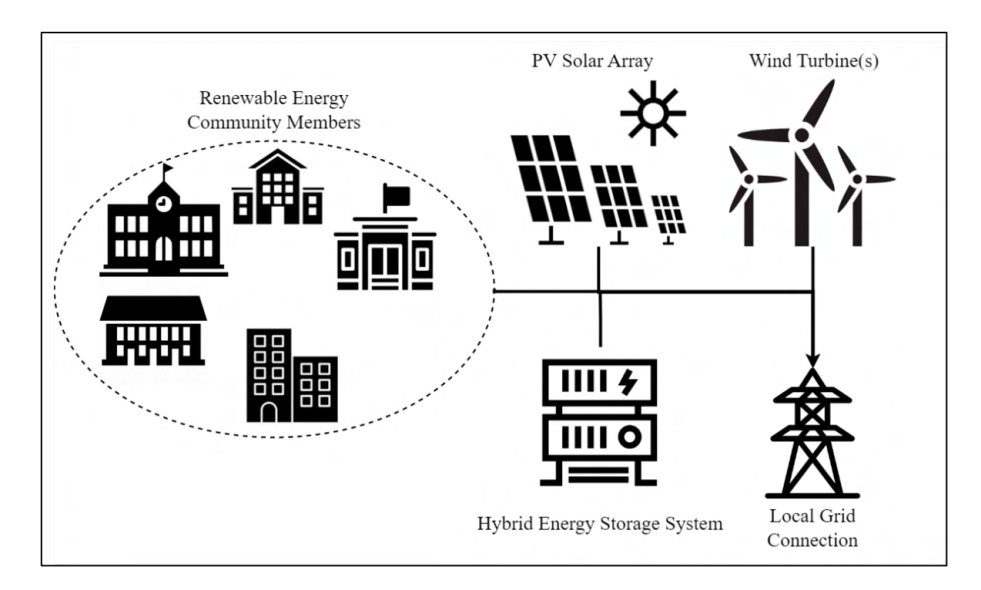


Figure 3.8: A simplified overview of the Energy Community design highlighting key assets.

building types outside of residential is scarce. Additionally, the authors not that modelling short, sharp demands such as water boiling are largely overlooked. Thirdly, there is limited consideration for location and demographic effects, including the characteristics of households and local climate conditions outside of the time of day.

Another option is to collect real data about the buildings in question and fill any gaps in the knowledge with a categorised data profile for the building type. This approach can be used to fill gaps in pre-existing load knowledge about the building types to build up a complete picture of the hourly profile. The methodology implemented in this work is similar to that used by Lage et al. [161], who used building load classifications at an hourly granularity to determine the techno-economic benefits of energy communities in Italy and Portugal.

Because of the nature of this data collection exercise, and privacy restrictions on the use of personal consumption information, some buildings' data profiles have been part synthesised using a combination of real monthly data and an archetypal daily load profile of that building.

For example, while annual data was available for the residential buildings, it was not possible due to privacy reasons to collect hourly data. Where this has occurred, the definition of the local climate in Formentera has been used to match the assumed consumption profile with load profile data from the National Renewable Energy Laboratory (NREL) building stock database. The approach to data collection and quantification of building profiles for the US, including those used here, is explained in detail in a report published by the US Department of Energy and produced by NREL in 2022 [162].

It can be seen in Figure 3.9 that Formentera is located in a hot, semi-arid climate or category Bsh according to the Köppen Climate Classification system [163]. This

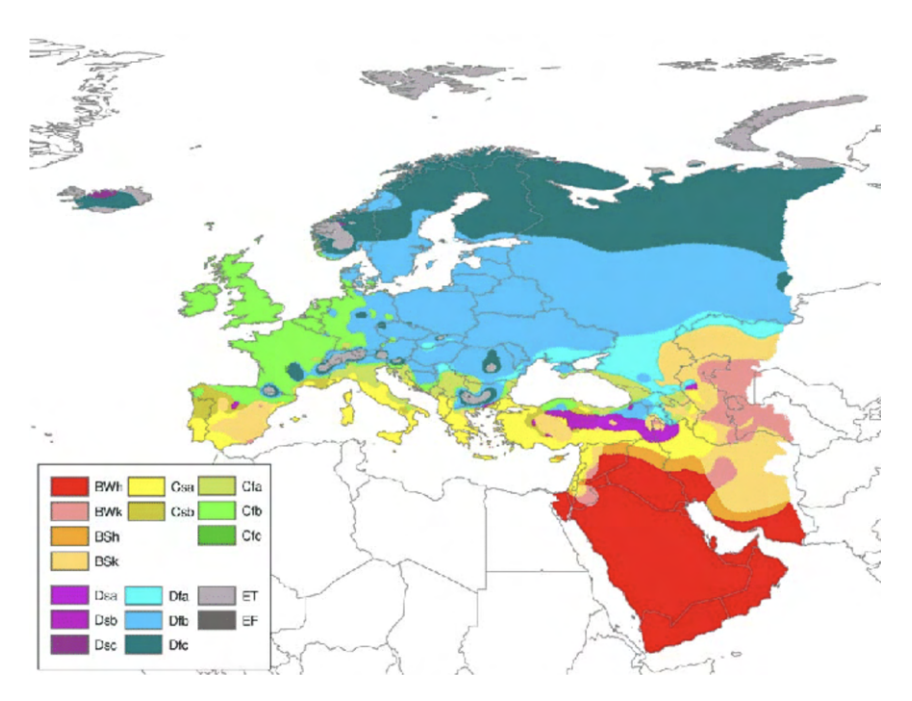


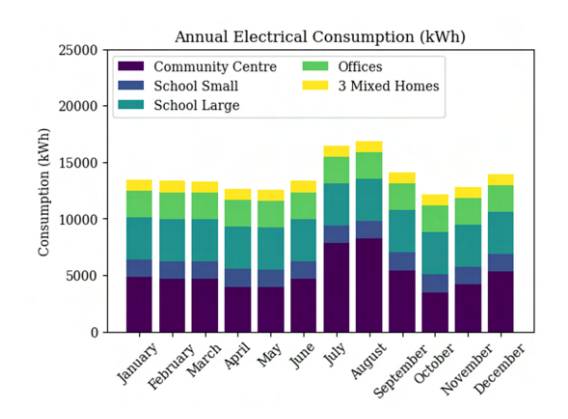
Figure 3.9: Map displaying the classification of Köppen climate regions in Europe [163].

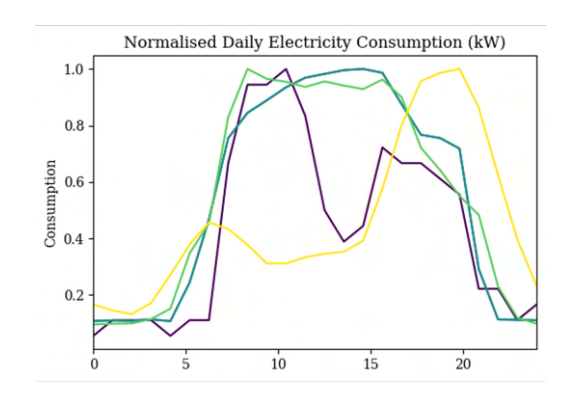
classification can be cross referenced with equivalent climate from the NREL database to get archetypal load profiles for residential properties, as well as commercial properties including schools, hospitals, community centres, hotels and offices. It should be noted that while this provides a great estimation for the true hourly profile, the NREL data is measured from US buildings stock, so will naturally differ slightly from the equivalent European variant. The database is classified by US state, and suggests that the climate of Formentera most closely matched the classification of Arizona, so those profiles have been used for this work.

The graphs in Figure 3.10a and 3.10b display the monthly and daily load profiles for the REC members grouped by building type. The monthly demand is based on true data collected from the site, whereas the hourly load profiles are supplied by archetypal buildings within the same climate classification, for both weekday and weekend loads.

Table 3.1 shows the different granularities of load data that has been successfully collected for the participating buildings within the proposed REC. The community centre has the most data available, with almost one year's worth of hourly load profile data. For the other building types, including the schools, offices and residences, only an annual total could be collected due to privacy restrictions. Therefore, the NREL data has been used to estimate the daily load profile, which is then projected over the course of the year such that the total annual load is equal to the true value collected from the field. The normalised tabular data for the building loads used, in hourly increments, is included for reference in Table B.1 of the Appendix.

Where the monthly load data is available, as in the case of the community centre, a





- (a) Real load profile data collected from proposed EC buildings.
- (b) Archetypal hourly building load profiles over the course of one day.

Figure 3.10: The composite components of the load input assumptions for EC members.

Table 3.1: A summary of load data available for each of the Energy Community Buildings in Formentera

| Building Name    | Daily load | Monthly Load | Annual Load |
|------------------|------------|--------------|-------------|
| Community Centre | Measured   | Measured     | Measured    |
| Small School     | NREL data  | Static       | Measured    |
| Large School     | NREL data  | Static       | Measured    |
| Council Offices  | NREL data  | Static       | Measured    |
| Three Residences | NREL data  | Static       | Measured    |

spline function is used to scale the daily load profile data such that it will sum up to the total annual measured load. Figure 3.11 shows this methodology applied to the community building monthly load. The next step is then to scale the daily load profile to follow this curve.

Once the appropriate NREL load profiles are matched to the building definitions as shown in Figure 3.10b and the monthly data is splined where needed, the loads can then be summed to provide a representation of the total electrical load expected from the REC in Formentera of the course of one year, as shown in Figure 3.12. The peak demand occurs in the summer period between July and early September, caused by the increase electrical load in the Community Building. Daily peak demand occurs at the same time throughout the year between 8:00 and 11:00 when building occupancy grows to its maximum level. The second peak can be seen in the evening, when occupants are leaving the buildings or are more likely to be operating appliances, for cooking purposes in the case of the residential buildings.

It can be noted from the data in Table 3.2 that the community building has the highest load of all the REC members, peaking at 34.5 kW during the peak summer period. This is because of the various uses that the building performs, including a public library, cinema,

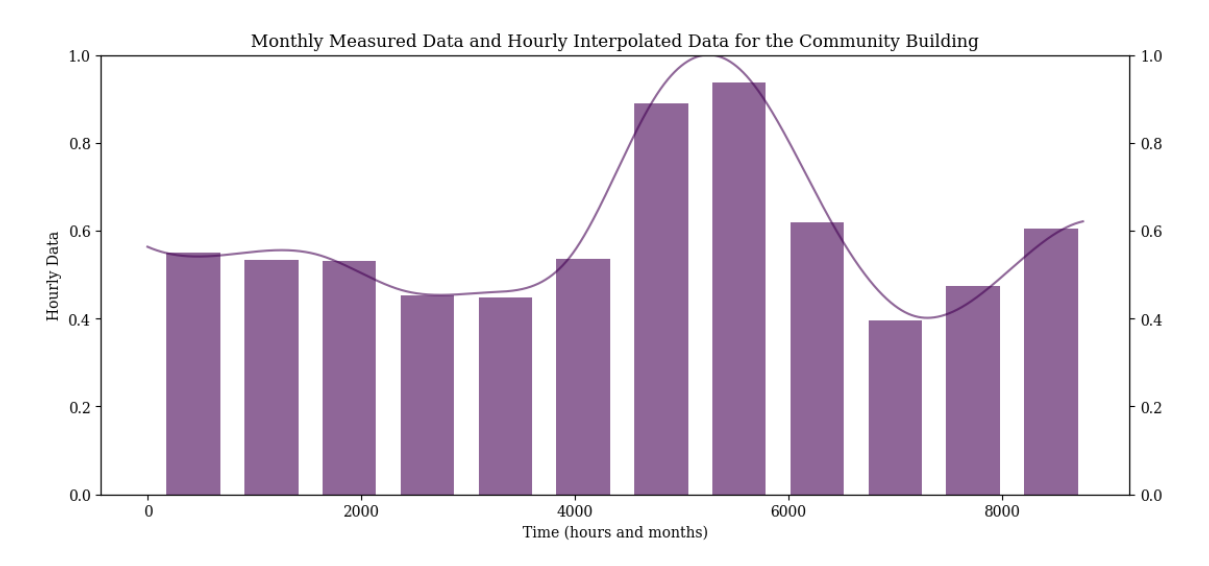


Figure 3.11: Illustration of the spline function used to fit the daily and monthly measured load profiles into the annual total load expectation

Table 3.2: Building load statistics for the different members of the REC

| Building Name    | Minimum | Maximum | Average | Annual Total (kWh) |
|------------------|---------|---------|---------|--------------------|
| Community Centre | 0.77    | 34.5    | 6.9     | 61,100             |
| Small School     | 0.4     | 3.9     | 2.1     | 18,800             |
| Large School     | 1.0     | 9.2     | 5.1     | 44,800             |
| Council Offices  | 0.5     | 5.7     | 3.2     | 28,300             |
| Three Residences | 0.4     | 3.0     | 1.4     | 12,000             |

and social centre hosting various community activities. The schools, though stated as primary and secondary schools, are both small even by urban standards, leading to a lower average and peak power requirement. The residential buildings have a peak demand of approximately 1 kW per household and a total of 4,000 kWh per year, which is common of average family households in Europe. Note that for this work, the service demands are fixed for each hourly time slice, and flexible loads based on time or price signals are not being considered.

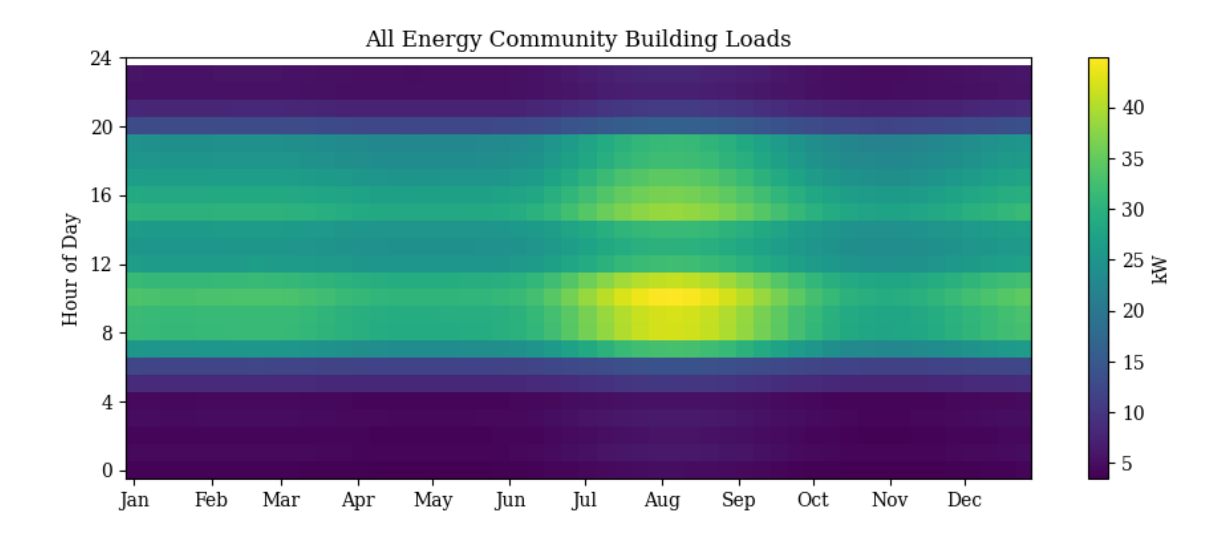


Figure 3.12: Heat map illustrating the total daily load for all buildings in the REC

# 3.3 Energy Community Asset Models

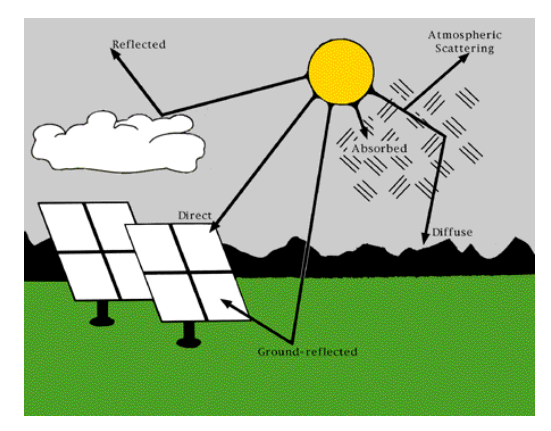
The creation of an REC model begins with the definition of the individual asset models that will be used in the final deployed system. As expressed in the literature, this work follows the process consistent with research by selecting the most commonly used decentralised renewable generation assets: PV solar arrays and micro wind turbines. Where this work diverges from other current research is in the exploration of energy storage options. Several works have modelled the use of battery storage systems for use in RECs, but very few, if any, have performed a direct comparison with a hybrid battery and hydrogen storage system across a number of competing cost and emissions reduction objectives. This thesis aims to fill this gap in the research.

In order to balance the additional competing demands of high-quality modelling results with limits to computation complexity, it was decided to create what is known as 'grey box' lumped models. These models exist between completely transparent equations and assumptions based on first principles, which are very complex to represent, and 'black box' models, which use a set of simplifying relationships to limit the quantity of inputs required to produce an accurate outcome.

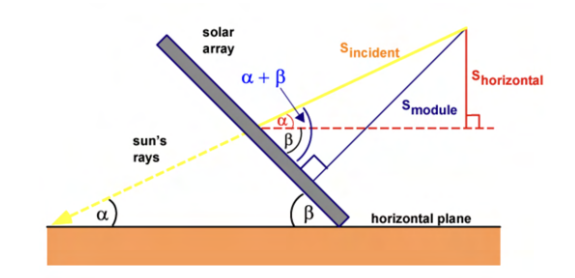
Within this work, a critical assessment of this approach with be performed in the discussion section, debating whether this technical trade off was necessary and worth reducing model fidelity in place of program usability, commercial potential, and use of understanding. First an outline is presented detailing the principles and equations used in the photovoltaic (PV) solar and wind turbine models, before moving onto the battery and hydrogen storage systems.

# 3.3.1 PV Solar Array

The lumped model is based on the equations laid out in section 2.5.1. The PV solar array model uses the previously defined inputs of irradiance and temperature along with some additional constants to calculate the expected power output from the generator. A crucial assumption made in this case is that the array is fixed at a particular tilt angle, which is optimised based on the latitude of EC location. Irradiance measured from the sun is often given as Global Horizontal Irradiance (GHI), which is equal to the total of all instances of irradiance on a flat surface, as shown in Figure 3.13a. This always includes Direct Normal Irradiance and Diffuse Horizontal Irradiance (DHI), and often will consider ground reflected radiation, although this is always very small compared to the other components. Since the solar array will be tilted, the GHI must be adjusted to account for the Plane-of-Array (POA) irradiance.



(a) Diagram displaying the different irradiance components that make up GHI. [164]



(b) A vector diagram showing the relationship between horizontal and model (POA) irradiance. [165]

Figure 3.13: The impact of different irradiance measures on the power output of a solar module

The relationship between GHI and POA is as follows:

$$S_{POA} = \frac{S_{GHI}\sin(\alpha + \beta)}{\sin(\alpha)}$$
(3.1)

In this equation,  $\alpha$  is the elevation angle and  $\beta$  is the panel tilt angle. It should be noted here that some solar arrays have active solar tracking, however, for this model a fixed tilt angle is assumed to minimise additional system costs.

The elevation angle  $\alpha$  is a function of the installation location's latitude  $\phi$  and the sun's declination angle  $\delta$  as it changes with time throughout the year.

$$\alpha = 90 - \phi + \delta \tag{3.2}$$

where:

$$\delta = 23.45 \sin \left[ \frac{360}{365} (284 + d) \right] \tag{3.3}$$

with  $23.45^{\circ}$  being the angle of the earth's tilt about its rotational axis relative to the sun, 284 signifies the day of solar equinox, and d is the input day of the year.

The PV solar array model uses the newly derived POA irradiance in combination with the ambient temperature data along with some additional constants to calculate the expected power output from the generator. The overall relationship is summarised in the equation below:

$$P_{PV} = P_r D_f \left(\frac{G_T}{G_{T,STC}}\right) \left[1 + \alpha p(T_c - T_c, ST_c)\right]$$
(3.4)

The derating factor  $D_f$  is the impact on the power output of factors such as soiling and natural cell degradation. As discussed in the literature review section, the key unknown in this case is the cell temperature  $T_c$ , which ultimately determines the impact to which natural heating the panel from solar energy is degrading the photovoltaic effect. This can be derived using the Nominal Operating Cell Temperature (NOCT) condition, which is to measure against a standard amount of heating at a known irradiance, ambient temperature and wind speed to estimate the impact. The NOCT condition (usually between 40-45°C) is given by the panel manufacturer.

$$T_c = T_a + \left(T_{c,NOCT} - T_{a,NOCT}\right) \left(\frac{G_T}{G_{T,NOCT}}\right) \left(1 - 1\frac{\eta_{mp}}{\tau\alpha}\right)$$
(3.5)

The final unknown in this equation is the panel efficiency at Maximum Power Point Tracking (MPPT)  $\eta_{mp}$ , which can be found by substituting in the following:

$$\eta_{mp} = \eta_{mp,STC} [1 + \alpha_p (T_c - T_{c,STC})] \tag{3.6}$$

 $\eta_{mp,STC}$  is given by the manufacturer as the rated power in W of the panel or array. Performing this final substitution results in this equation describing the power output of the solar array for a set of given input conditions:

$$T_{c} = \frac{T_{a} + (T_{c,NOCT} - T_{a,NOCT}) \left(\frac{G_{T}}{G_{T,NOCT}}\right) \left[1 - \frac{\eta_{mp,STC}(1 - \alpha_{p}T_{c,STC})}{\tau \alpha}\right]}{1 + (T_{c,NOCT} - T_{a,NOCT}) \left(\frac{G_{T}}{G_{T,NOCT}}\right) \left[\frac{\alpha_{p}\eta_{mp,STC}}{\tau \alpha}\right]}$$
(3.7)

 $P_{PV} = PV$  power output (W)

 $D_f = \text{derating factor } (\%)$ 

 $G_T = \text{POA irradiance (W/m}^2)$ 

 $G_{T,STC}$  = irradiance under standard conditions (1000 W/m<sup>2</sup>)

```
\begin{split} &\alpha_p = \text{thermal power coefficient (\%)} \\ &T_c = \text{PV cell temperature (°C)} \\ &T_{c,STC} = \text{PV cell temperature under standard test conditions (25°C)} \\ &T_a = \text{ambient temperature (°C)} \\ &T_{c,NOCT} = \text{NOCT (40-45°C)} \\ &T_{a,NOCT} = \text{NOCT ambient temperature (20°C)} \\ &G_{T,NOCT} = \text{NOCT irradiance (800 W/m}^2) \\ &\eta_{mp} = \text{efficiency at MPP (\%)} \\ &\tau\alpha = \text{solar transmittance } \tau \text{ and absorptance } \alpha \text{ of the cell} \end{split}
```

# 3.3.2 Wind Turbine

Similar to the PV solar model, the assumptions for the wind turbine power output are built upon those laid out in Section 2.5.1, and use a 'grey box' approach to balance model performance and usability.

The first step of the model formulation is determining the true wind speed met by the turbine blades at the hub height. The wind speed data from NASA powerLARC is measured at 10m above ground level (not mean sea level) at the coordinate location. This is achieved using the log law as introduced in equation 2.9.

From studying Formentera's local area and considering the rural nature of the environment even near to the main town of St Francesc, it is logical to give a roughness height  $z_0$  of 0.05 metres. This aligns with Table 2.4 suggestion of some obstacles including crops and small trees, but overall surface impact is low.

From here, the modelling approach diverges slightly from the literature, as instead of using a combination of blade swept area and the coefficient of performance to find the output power, IEC standard power curves are used to approximate the output of a range of turbine types across the entire operating range.

The Wind Integration National Dataset (WIND) tool created by NREL [166] uses the IEC standards and assesses a range of installations across the USA to correlate the performance output by wind speed to the standards. The IEC 61400 turbine design standards specify the requirements to operate a certain ranges of wind speeds to provide the optimal power output. Below, Table 3.3 describes the classes used in this model, and the average corresponding wind speed requirements for maximum performance. To protect the turbine from damage at higher wind speed, each classification is given a cut-out speed as also shown in the table.

Table 3.3: Wind turbine IEC class for corresponding average wind speeds used in modelling turbine power output. [167]

| Turbine class | Wind conditions       | Rated average speed | cut-in           | cut-out           |
|---------------|-----------------------|---------------------|------------------|-------------------|
| IEC-I         | High winds            | 10 m/s              | 3  m/s           | $25 \mathrm{m/s}$ |
| IEC-II        | Medium/variable winds | 8.5  m/s            | 3  m/s           | 25  m/s           |
| IEC-III       | Low winds             | 7.5  m/s            | 3  m/s           | 22  m/s           |
| Offshore      | High winds            | 10 m/s              | $4 \mathrm{m/s}$ | $25 \mathrm{m/s}$ |

The choice of IEC class is linked to the local average wind speed, so will be chosen automatically by the model to optimise performance. There is also a final class provided for offshore wind turbines, so is not a function of wind speed, but rather the location of installation. The performance curves for each of the different classes are shown in Figure 3.14. The full dataset from which the performance is interpolated is included in Table B.2 of the Appendix.

By simplifying the initial Equation 2.7 the estimation of the wind power output  $P_{wt}$  is

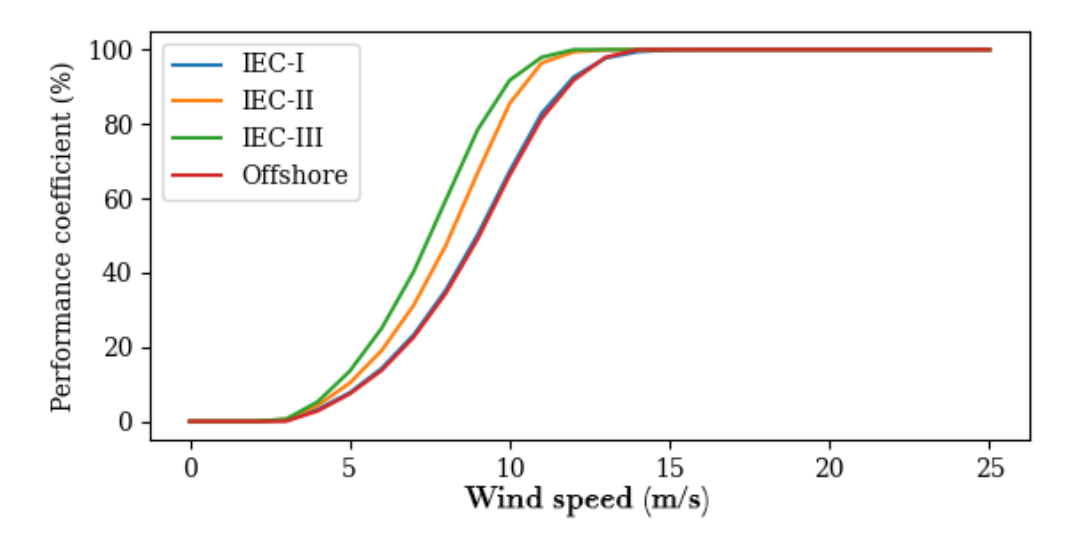


Figure 3.14: Graph showing the performance characteristics of the IEC classes.

as follows:

$$P_{wt} = P_r p_{coeff} \eta_e \tag{3.8}$$

 $P_{wt}$  = turbine output power (kW)  $P_r$  = turbine rated power (kW)  $p_{coeff}$  = power coefficient (%)  $\eta_e$  = electrical efficiency (%)

The electrical efficiency  $\eta_e$  can be approximated from literature, particularly an in-depth study produced by researchers at NREL in 2021. The result showed that among other potential external factors that can cause losses, including degradation, icing, mechanical failure, electrical losses in inversion and connection to the grid which can be significant [168]. For this work, a  $\eta_e$  value of 97% is assumed.

While this model does not explicitly consider the complex nature of fluid flows around the turbine blades, the  $p_{coeff}$  value being based on real measured output from turbine assets goes some way to describing, in aggregate, the various forces and turbulent behaviours that are acting.

# 3.3.3 Battery Storage System

The main role of the battery storage asset is to provide short term, fast response to demand when the generation assets are not generating power. The approach here uses a similar but simplified version of the Shepard battery model discussed in the literature review.

In essence, since the model does not need to have direct visibility of the voltage and current levels in the system (as it is assumed that a DC control system will manage this), only the state of charge needs to be accurately tracked to provide a signal to the rest of the Energy Community system as to whether the asset is available to provide or store energy. The battery system contains two parts: a charge model and a discharge model. The models take the power requirement from the battery and outputs the resulting State-of-Charge (SOC) for the end of the time step, as shown in Equations 3.9 and 3.10 below.

Charge phase:

$$SOC_{t+1} = \frac{Q_t + \int_t^{t+1} P_{charge} \eta_{charge}, dt}{Q_i} \bullet 100$$
 (3.9)

Discharge phase:

$$SOC_{t+1} = \frac{Q_t - \int_t^{t+1} P_{discharge} \eta_{discharge}, dt}{Q_i} \bullet 100$$
 (3.10)

Battery systems often specify a maximum charge and discharge power, due to the current limits through connecting cables and to minimise thermal risks. This model also has the ability to limit the volume of energy in kWh that can be absorbed or released by the battery asset.

 $SOC_{t+1}$  = battery SOC in next timestep (%)  $Q_t$  = battery current state of change (%)  $Q_i$  = battery initial state of charge (%)  $P_{charge}$  = maximum charge power (kWh)  $P_{discharge}$  = maximum discharge power (kWh)  $\eta_{charge}$  = charging efficiency (%)  $q_{discharge}$  = discharging efficiency (%)

These outputs are subject to the minimum and maximum SOC limits. The model can also include degradation in the battery capacity linearly as a function of charge cycles, as shown below:

$$Q(l) = Q_i - \alpha l \tag{3.11}$$

Where Q(l) is the dynamic capacity (kWh) as a function of charge cycles l (cycles) and alpha is the aging factor (kWh/cycle).

# 3.3.4 Regenerative Hydrogen Storage System

In contrast to the battery storage, the regenerative hydrogen system's main role is to provide long-term balancing of the energy system, smoothing demand fluctuations between weekdays and weekends, and seasonal shifts in power generation. The model consists of a Proton Exchange Membrane Fuel Cell (PEMFC) and an Anion Exchange Membrane (AEM) electrolyser capable of consuming and producing hydrogen, respectively. The system also considers a hydrogen storage module with its own rated capacity and efficiency. The overall equations are similar to those of the simplified battery model in that the electrolyser and fuel cell analogously represent the charge and discharge elements. The system can therefore be shown as the following:

Electrolyser phase:

$$Q_{H2,t+1} = Q_{H2,t} + \int_{t}^{t+1} P_{el} \eta_{el} \eta_{stor}, dt$$
 (3.12)

Fuel cell phase:

$$SOC_{H2,t+1} = Q_{H2,t} - \int_{t}^{t+1} P_{fc} \eta_{fc} \eta_{stor}, dt$$
 (3.13)

 $Q_{H2,t+1} = \text{next time step hydrogen energy stored (kWh)}$ 

 $Q_{H2,t} = \text{current time step hydrogen energy stored (kWh)}$ 

 $P_{el}$  = electrolyser rated electrical power (kW)

 $P_{fc}$  = fuel cell rated electrical power (kW)

 $\eta_{el} = \text{electrolyser efficiency } (\%)$ 

 $\eta_{fc}$  = fuel cell efficiency (%)

 $\eta_{stor} = \text{pressurised storage efficiency } (\%)$ 

Also similar to the battery model, the regenerative hydrogen system is also subject to SOC minimum and maximum constraints and will not operate beyond these limits even when considering the fuel cell, electrolyser and storage efficiencies.

The asset models as described are implemented in coded form to the overall REC modelling framework. Sample code for the PV solar and Battery Energy Storage System (BESS) assets is included in Appendix C.1 for reference, showing where the design assumptions are inputted and processed to provide the power measures for each simulation timestep. In particularly, the power and SOC control of the BESS can be seen in the function findNextStep, which is explained in more detail in next section.

# 3.4 System Control Logic and Trading

All REC designs require a specific control logic that will maximise the performance of the available renewable assets and benefits (increased reliability, reduced cost and emissions) to the community members. In this section the fundamentals of the control logic are outlined, highlighting the roles of each asset and how the power is delivered to the consumer.

In this model, the low-level control of system assets including voltage regulation, inversion, rectification, and other embedded properties are not included. This is because these technologies often operate on a MHz switching frequency, and as the model here is built to assess long-term annual to lifetime performance, it is computationally impractical to model these processes completely. It is therefore assumed that the losses incurred are included in the efficiencies of the individual assets that use them, such as the MPPT inverter needed for solar installations.

Here, the macro decision-making of the energy management system hour-by-hour is discussed, and the data collected about the states of the individual components needed to provide robust, reliable control.

Since it is common for RECs to have multiple, independent members, it is also vital to consider how energy flows between production and consumption during each hour. A simple energy trading logic has been designed to manage which load is consuming which asset at any given moment, how much grid energy is consumed, and what is the effect cost of electricity at every time step. Using this method, it is possible to evaluate, on a load-by-load basis, the cost and decarbonisation benefits of connecting to the REC system.

# 3.4.1 Energy Management Strategy

The Energy Management Strategy for the hybrid storage system is shown in Figure 3.15.

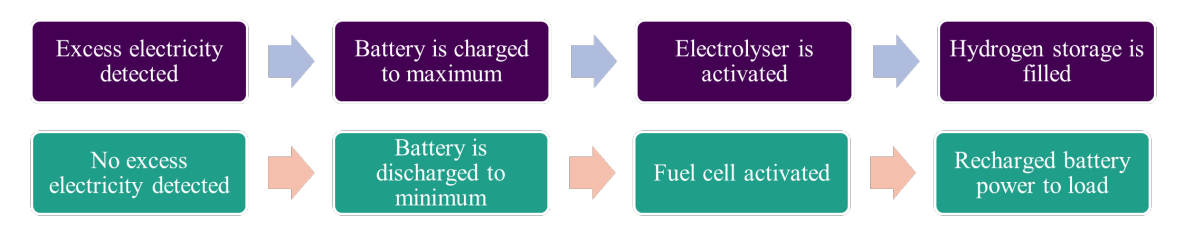


Figure 3.15: Flowchart with a simplified view of the energy management control logic

The control logic is simple in its design, but can also be nuanced in its bias towards different technologies based on capacity and availability. The system adheres to a load following approach, in that renewable generation will always be used first to satisfy the current REC demand, then, if in excess of demand, will either be absorbed by the hybrid storage system or sent to the grid. When renewable generation is not available in excess of demand, the system will dynamically switch to the storage systems to balance the load, or use grid power.

A challenge here is in choosing when to activate the battery and hydrogen storage system to prioritise best performance. Because the battery performs well in fast response applications and can quickly match demand, it is most logical for it to be used first. Then when the battery is running low, the hydrogen system activates to provide a lasting, firm response to the demand. The hydrogen storage is not as fast responding as batteries, and usually take 2-3 minutes to warm up to operating conditions. In practical terms, the battery is actually being charged by the fuel cell while the hydrogen system is active, as the fuel cell cannot modulate its output without incurring performance losses. Batteries also suffer from current leakage over long periods, so it also may make practical sense to install a smaller battery and trade-off against a larger hydrogen system if extended storage is needed. This performance trade-off is to be tested in this thesis.

Therefore, under excess supply conditions the battery charges first to be ready for the next demand response, followed by the long-term hydrogen storage, with any remaining supply sold to the grid at the specified feed in tariff. Then, when supply is no longer in excess, the battery discharges first, followed by the hydrogen storage system. If all storage systems are empty, grid power is imported.

For completeness, the management strategy was tested in reverse, with the hydrogen system responding first, followed by the battery system. It was found that this provided worse performance overall, so was decided to proceed with the chosen strategy. Ideally, and like similar approaches from the literature, the storage operation would be directly optimised, in which every hour of operation acts as a design variable, controlling the levels of charge and discharge. However, this process is very computationally intensive, particularly for non-linear models, so was impractical to implement based on the objectives of this work.

A complete view of the energy management system including flow within the optimisation process is shown in Figure 3.18 later in this chapter.

# 3.4.2 Community Energy Trading

There a numerous methods for modelling and simulating decentralised energy trading logic applicable to an REC. The most commonly cited is the P2P energy trading approach, in which the REC members are able to autonomously calculate the energy shared among the system independently of a system operator or centralised power market. In this scenario, community members collectively benefit from a series of bilateral transactions in which energy is virtually transferred from its supply source to the demand. Under this approach, it is assumed that all REC members collectively invest in generation and storage assets, and that competition is not considered, similar to the way in which cooperatives are managed in the UK and Europe. The objective is to therefore reduce the system cost as much as possible, while not necessarily providing the lowest cost on a per member basis.

Another approach is to create a local energy market, which follows a structure more

similar to that of the standard power market mechanism, except that it is controlled and managed by the energy community. Members submit supply bids and demand bids to a pool, then the price is set where the two supply and demand curves cross, otherwise known as the marginal price. This is generally thought of as a good approach to represent consumer competitive behaviours and to reflect the opportunity cost for prosumers for investing in their respect assets. This method therefore allows a small degree of market competition between members with the view that this will bring down the opportunity cost, reducing the effective energy price for all members.

One of the questions surrounding RECs is the level to which competition between community members should be allowed, and to what extent this would mutually benefit the overall system investment cost and returns. The main results of this work will consider the non-competitive trading arrangement of the EC only, but will also test, as a sensitivity, the behaviour of the model when a competitive market is applied.

#### **Non-Competitive Trading**

In this approach, it is assumed that while members have physical renewable installation on the property, they all share the same access to the virtual 'pool' of generation and storage at any given moment. Energy available in excess will be provided in equal measures to all members with a demand. This can be thought of as filling up 'buckets', where each members demands can be represented as buckets of different sizes.

While the demands are being satisfied equally at first, once the smaller demand buckets are 'full', then the larger demands will continue to be filled. Once all the excess supply has been used, it is likely that the members with the largest excess demand remain unsatisfied by the REC. A small excess demand is therefore beneficial to a given community member, which would encourage either the installation of additional renewables, or to reduce demand through efficiency measures. It can be noted that there is no direct market competition between members. This process is illustrated in Figure 3.16.

The process can also be broken down into three distinct stages:

Stage 1 - Equal energy distribution For each timestep t, the process begins by dividing the total renewable supply  $E_t$  equally among all member demands.

$$E_{m,t} = \min\left(\frac{E_t}{M}, D_m\right) \tag{3.14}$$

Where:

- $\bullet$  *M* is the total number of demand buckets.
- $D_m$  is the demand capacity of bucket m.

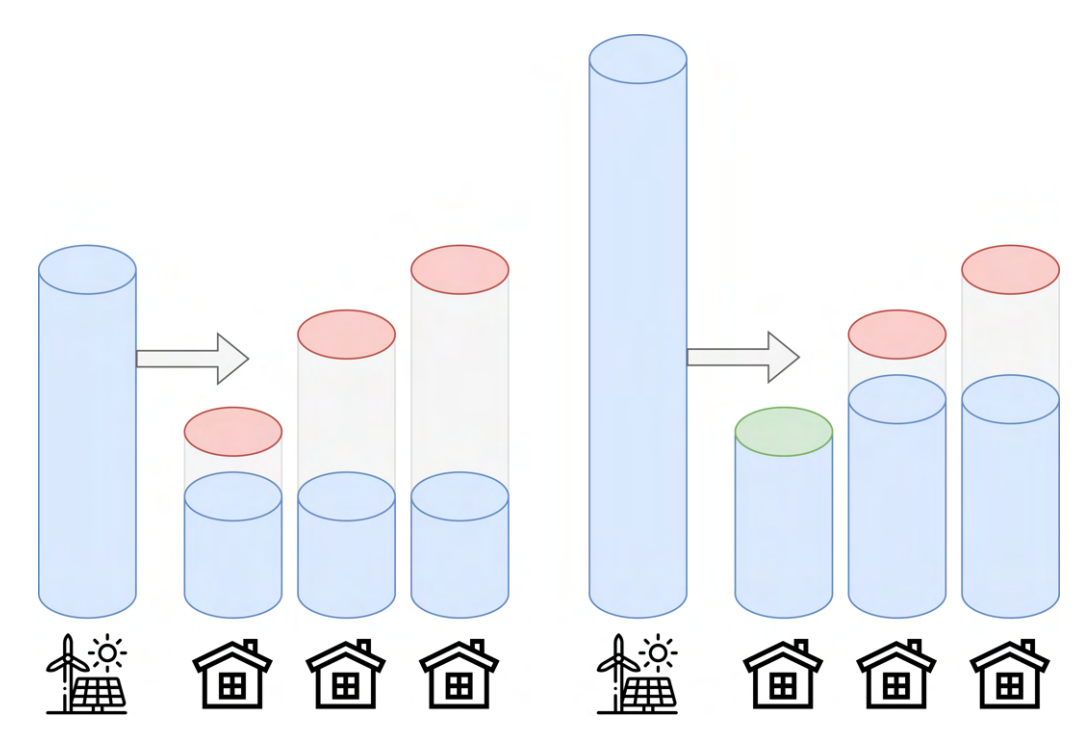


Figure 3.16: Simple energy trading concept of the EC, showing (left) an example with low generation and (right) high generation.

Stage 2 - Allocate the residual After the initial step, any remaining demand gets distributed to the other, unfilled demands in an iterative procedure.

$$E_{m,t} = \min\left(\frac{E_{t,remaining}}{M_{remaining}}, D_m\right)$$
(3.15)

Where:

- $\bullet$   $E_{t,remaining}$  is the remaining renewable supply after filling the previous buckets.
- $M_{remaining}$  is the number of remaining unfilled buckets.

Stage 3 - Termination condition The process continues until all  $E_t$  is allocated.

$$\sum_{m=1}^{M} E_{m,t} = E_t \tag{3.16}$$

### Market-based Trading

This sensitivity tests the behaviour of the system design when, instead of a collaborative trading environment, a competitive logic is applied across the REC. The simple market

clearing process considers the battery, renewable supply bids, and the grid. The grid only supplies energy when REC offers are uncompetitive or unavailable, and after all feasible renewable energy and battery storage have been used.

**Energy Storage Considerations**: For this sensitivity it is assumed that, unlike the generation assets, the hybrid energy storage system is still a shared asset which operates independently of the community members. Essentially, the storage will still absorb any excess renewable generation by default, and release energy to supply community demand in any given hour. The storage therefore submits offers for supply and bids for demand that are equal to the known excess supply or demand, such that the SOC limits are not exceeded.

Stage 1 - Supply offers: Each renewable installation submits an offer  $S_i$  with an associated price  $P_i$ , and the offers are sorted by price:

$$P_1 \le P_2 \le \dots \le P_n \tag{3.17}$$

Where:

- $S_i$  is the volume of energy submitted by community member i as an offer.
- $P_i$  is the price of the renewable energy offer from community member i.
- $\bullet$  *n* is the number of renewable installations submitting offers.

**Stage 2 - Clearing price:** The marginal clearing price is determined by the last offer used to meet demand:

$$P_{marginal} = P_k \quad \text{where} \quad \sum_{i=1}^{k-1} S_i < D_{total} \le \sum_{i=1}^k S_i$$
 (3.18)

Where:

- $P_{marginal}$  is the clearing price of the market, determined by the last supply offer  $P_k$ .
- k is the index of the last offer used in the market clearing process.
- $\sum_{i=1}^{k-1} S_i$  is the sum of all offers before the marginal offer.
- $D_{total}$  is the total demand from all members.

In situations where assets, such as similar PV solar, offer in at the same price, a very small random number (order of  $10^{-3}$ ) is added to each supply offer to resolve tie-breaks.

**Stage 3 - Market balance**: The total energy supplied (from renewable offers and battery discharge) must meet the total demand:

$$\sum_{i} S_i + St_{discharge} + S_{grid} = D_{total} \tag{3.19}$$

Where:

- $\sum_{i} S_{i}$  is the total energy supplied by all renewable installations.
- $St_{discharge}$  is the energy supplied by the storage.
- $S_{qrid}$  is the energy supplied by the grid.
- $D_{total}$  is the total demand from all community members.

The market then 'clears' and is assumed to operate on a pay-as-cleared approach, where all participants pay the same price, which is equal to the marginal supply offer. An illustration of how the marginal clearing price is set is shown in Figure 3.17. It can be seen that the total demand when netting off self-consumption for this EC is 16 kWh in the sample timestep. Given the offers of each prosumer, this points to a marginal price of the decentralised market of 0.17 €/kWh. Any bids under the marginal price will receive renumeration at that set price, whereas any over the margin are only able to sell energy back to the grid at the feed-in-tariff rate. It should be noted that under this scheme, certain prosumer offers will be able to receive a profit over and above their assumed LCOE costs, but also means that all demand bids pay a higher rate compared to if the total demand was lower.

This type of market design is known as a post-delivery LEM pool market [169], as it assumes that the energy has already been fairly distributed among community members as in section 3.4, and is aiming to evaluate the cost renumeration structure that follows. However, since the cost savings/profits are also evaluated, the outcome can be harnessed as an objective function in the design optimisation loop to determine the optimal system sizing for maximum market opportunity.

### 3.5 Design Optimisation and Performance Analysis

Once the asset models and control logic has been determined, the REC model can be simulated over the course of a one-year period. The final step is to implement a design optimisation logic such that the system size and performance can be optimised for the one year simulation period.

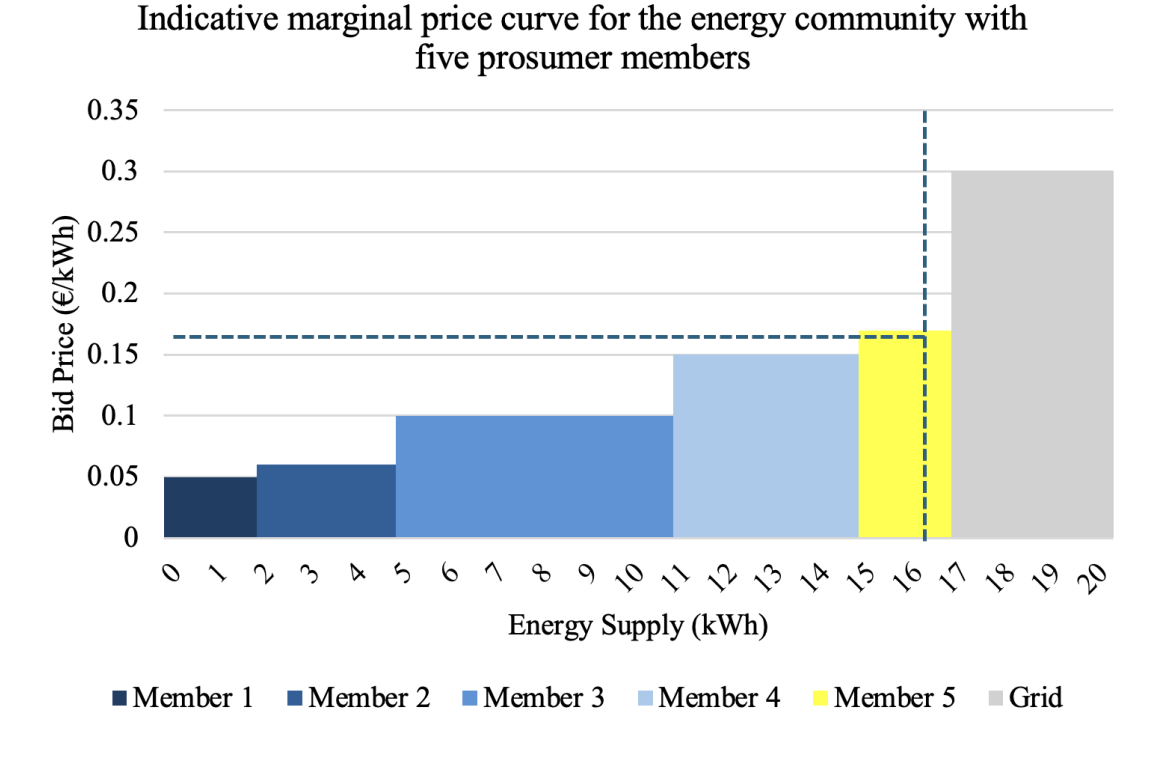


# Figure 3.17: Graph illustration of how the marginal price is set under the simple decentralised energy market scheme.

The first part of the section describes the economic and environmental objective functions used to drive the optimisation routine towards the optimal outcome. The second part details how the Non-Dominated Sort Genetic Algorithm (NSGA-II) is integrated with the model and executed, as well as the assumptions and setting for the procedure.

### 3.5.1 Economic and Environmental Objective Functions

The objective functions can be broadly categorised into being economically or environmentally driven. Economic objectives concern the financial viability of the REC as a project to be undertaken by location stakeholders compared to other energy delivery methods, whereas environmental objectives measure the extent to which the system is able to reduce the quantity of embedded carbon emissions produced from energy consumption.

Like any new technology or process, a comprehensive economic evaluation is required to ensure confidence that the design will provide the required level of return for the community. Often the Net Present Value (NPV) of a given investment is used to measure its returns. The NPV is derived to represent the value of an investment to the REC as a business. The investment is considered worthwhile (producing returns) if the NPV is more than zero at the end of the investment terms, which for the community-based systems is 20 years, and is evaluated using equation 3.20 below:

$$-C_0 + \frac{-C_1 - O_1}{1 + R} + \dots + \frac{-C_T - O_T}{(1 + R)^T}$$
(3.20)

Where:

- $C_0$  is the initial capital investment (CAPEX)
- $C_T$  is the capital investment for year T
- $O_T$  is the operations costs (OPEX) for year T
- ullet is the discount rate of the investment

It can be noted here that given the CAPEX and OPEX values are measured as positive here, they are subtracted from the system value year-on-year such that under this current definition, there is no path to producing a positive return. This is because the cost of the REC system is effectively behind compared to a counterfactual scenario in which only the grid is used to provide electrical power. This equation therefore needs to be modified to evaluate the effective opportunity cost of grid only use when the REC is instead being operated. This can be achieved with the following:

$$-C_0 + \frac{-C_1 - O_1 + G_1}{1+i} + \dots + \frac{-C_T - O_T + G_T}{(1+i)^T}$$
(3.21)

Where  $G_T$  is the counterfactual opportunity cost of grid use only. This effectively values the REC as an alternative system and will produce a positive NPV if the discounted investment cost is less than the discounted grid-only utilisation. This can be rewritten simply in equation 3.22 below, where  $R_t$  is the total in and out cashflow of the system.

$$NPV = \sum_{T=0}^{n} \frac{R_T}{(1+i)^T}$$
 (3.22)

In this form, it can now be noted that if the in- and outflows as well as discount rates were valued in such a way as to produce a NPV of zero, the project would break even. The CAPEX and OPEX and grid costs are a function of the system boundaries, whereas the discount rate is a measure of the capital risk or cost of capital for the investment, and can vary based on the type of system. The equation can therefore be rearranged to evaluate the maximum discount rate, or Internal Rate of Return (IRR) possible from a system still capable of breaking even. The IRR is another popular approach to economic analysis as it measures the allowable volume of risk undertaken by the project and gives confidence in the return.

$$0 = NPV = \sum_{T=0}^{n} \frac{R_T}{(1 + IRR)^T}$$
 (3.23)

Another key metric in the financial analysis that can be sources from this equation is the payback period, which is the term over which the system is assumed to be able to return its investment. This is found by solving Equation 3.23 for the time period T when NPV is equal to zero.

The final metric is the LCOE, which, as discussed in the literature review, is key to comparing single generation assets and entire integrated systems on a like-for-like basis. Particularly when comparing storage assets, it is important to present their economic performance within the REC on a common basis. LCOE is defined as the total lifetime cost of the asset divided by the total electricity delivered to the consumer in  $gCO_2/kWh$ , where  $E_{T,j}$  is the energy delivered per asset j over the one-year time period T. The investment quantities are also discounted over the system lifetime.

$$LCOE_{j} = \frac{\sum_{T=0}^{n} C_{T,j} + O_{T,j}}{\sum_{T=0}^{n} E_{T,j}}$$
(3.24)

A range of different assessments exist for the economics of renewables assets, as it is highly dependent on the capital requirement, location, weather conditions, delivery and connection costs, and available labour at the installation site. The results for CAPEX, OPEX and lifetime parameters are included in the subsequent section, and are assumed to include the Balance of Plant (BOP) costs, such as DC-AC inverters, wiring, connection costs, and Internet of Everything (IoT) control equipment. A range of literature sources are used to determine the final economic assumptions, and the sensitivity analysis will be used to test the credible range of outcomes.

For the optimisation routine, it is most consistent to adopt NPV as the economic objective function, as it includes the assumed discount rate of 5%, though the payback period could equally be used to provide the same optimal input signal to the model.

The environmental objectives are mostly concerned with using the embedded emissions of the EC system, including any generation assets and storage, and comparing this with the embedded grid energy carbon, also known as the scope 2 emissions. This section previously discussed how analysis of the local grid of the Balearic Islands is used to evaluate the emissions, which will be compared to the life cycle emissions of the REC. The environmental impact was estimated through the Global Warming Potential (GWP) of the assets, which when summed up together and divided by the total energy delivered over the system lifetime derives the emissions intensity.

$$EI_{system} = \frac{\sum_{j=1}^{m} EI_j \bullet E_j}{\sum_{j=1}^{m} E_j}$$

$$(3.25)$$

Where:

- $EI_{system}$  is the emissions intensity of the system
- $EI_j$  is the embedded emissions intensity of asset j

### • $E_i$ is the energy delivered by asset j

The embedded emissions values were extracted from studies in the literature, and provide an up-to-date view of the carbon produced during the material extraction, manufacturing and installation process (cradle-to-gate), but do not include the end-of-life transport and disposal/recycling impacts. There is far less reliability information available for the life cycle emissions of the regenerative hydrogen system, so where necessary, assumptions based on emissions from similar technologies are used. This will again be tested as part of the sensitivity and uncertainty propagation analysis.

The created modelling tool can also calculate the percentage of self-consumption achieved by each building within the energy community, which is a measure of the extent to which the community member has used REC generation energy as a percentage of their total consumption. This is useful when comparing the effective environmental performance on a member-by-member basis as it is known how much clean energy is used.

### 3.5.2 Genetic Algorithm Implementation

Designing and configuring the optimal system sizing for a hybrid decentralized energy system is a complex process. There are a number of non-linear phenomena being simulated, and many potential design objectives and constraints. The chosen objective functions considering both cost and carbon reduction are the NPV and the annualised system emissions intensity. The objective functions rely on varying the capacities of the PV solar, wind, battery, and hydrogen storage installations at the site.

The NSGA-II uses a heuristic evolutionary learning algorithm with a population of potential design solutions within the defined constraints. It then ranks the population based on a non-dominated sorting, producing a Pareto front of optimal solutions by minimising both objective functions. Each individual in the population was determined based on the simulation of the model of a one-year period and evaluating the two objectives. The best performing individuals are passed to the next generation, whereas a combination of mutations and created offspring (crossover) determines the remaining individuals. The solving process for NSGA-II implementation, including the overall REC control logic is shown in Figure 3.18. The software implementation of the algorithm within the model is shown in Python code form in Appendix B, showing the input variables described within this section.

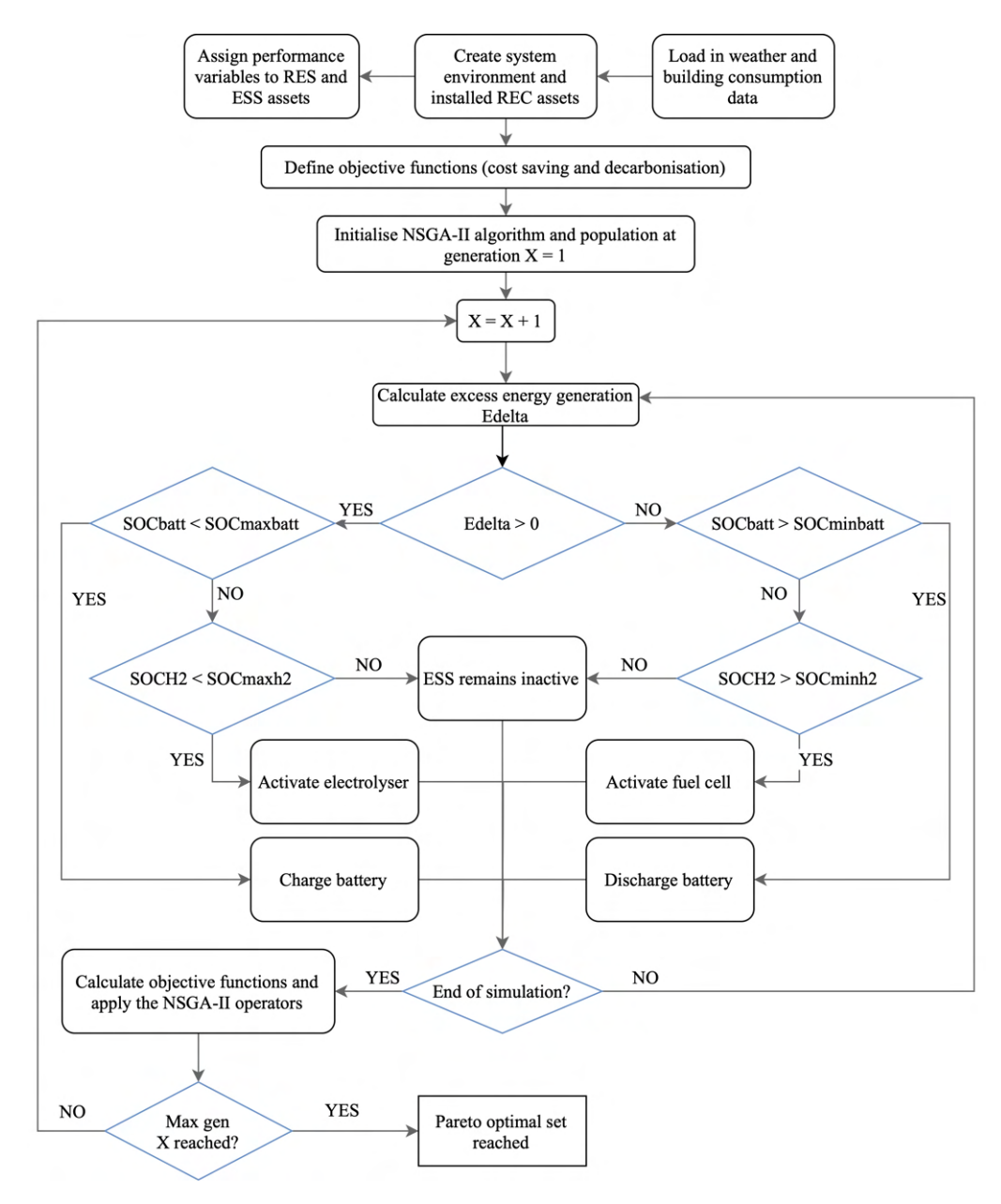


Figure 3.18: Hybrid energy system model approach with multi-objective optimisation algorithm NSGA-II solving process.

It is well known that the NSGA-II algorithm, like all meta-heuristic optimisation processes, provides a highly accurate estimation of the exact solution, rather than the solution itself. This is because finding the exact solution for a highly non-linear problem like the REC design model set out would be too computationally complex and impractical to implement, as discussed in the literature review of optimisation approaches. Therefore, the algorithms parameters need to be chosen such that they will accurately and repeatably produce a solution to the problem. For the NSGA-II algorithm, the main parameters that are adjusted are the population, number of generations, mutations rate, and crossover rate.

The population is the number of individual model solutions in each generation that are able to evolve over time. Generally speaking, the greater the population size, the more genetic variations are available, leading to a more global solution and avoids the population getting 'stuck' in a local minimum. This comes at a higher computation cost, and can lead to diminishing returns at higher population sizes.

A generation represents a single iteration of the procedure, so 'maximum generations' is the highest number of iterations that can proceed before the algorithm terminals. Like population size, more generations will allow more time for the population to search the design domain for the best solution, but too many will take more time to solve and have diminishing returns.

The 'mutation rate' is the probability of a random mutation in the design variables happening for a given member of the population. A lower mutation rate can be more stable when executing, but a higher mutations allows for more randomness and better searching of the design domain.

'Crossover' is the rate at which parents which produce offspring with a combination of their genetic data. This allows for better searching by combining information gained about the design domain by well-performing individuals when high, but can also lead to solution instability.

To find the settings used in this analysis, a spread of settings for each of the variables presented was inputted into the program and tested in isolation. Table 3.4 below shows the spread of variable values used.

Table 3.4: Spread of parameters values tested to determine the best operation of the NSGA-II

| Parameter                 | Upper sensitivity | Lower sensitivity |
|---------------------------|-------------------|-------------------|
| Population Size           | 200               | 50                |
| Max Number of Generations | 250               | 100               |
| Mutation Rate             | 0.9               | 0.1               |
| Crossover Rate            | 1.0               | 0.5               |

The resulting Pareto fronts of all tested parameters are shown in Figure 3.19. It can be noted towards the upper end of the curve that a lower population certainly has a negative

impact on the result, as the values are dominated by other, better solutions in the region. This indicates that this setting has not allowed the algorithm to search the domain as effectively. Low generations and low crossover also appear to have lowered the optimisation performance significantly, with a high crossover also seeming sub-optimal. The mutation results impact was less clear, so setting the value to the default central value would be a reasonable choice.

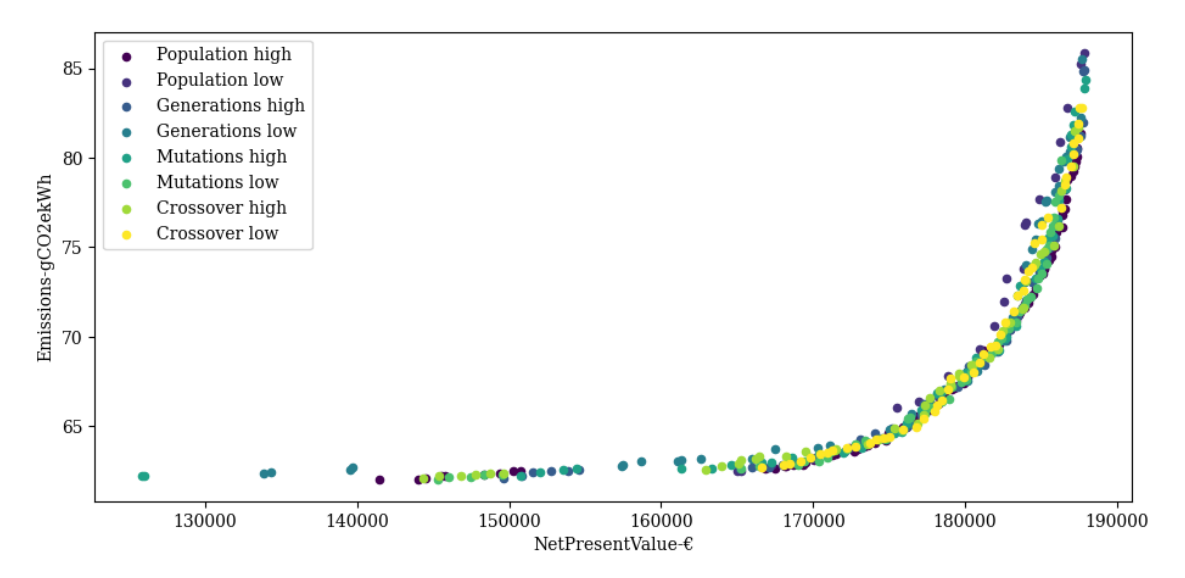


Figure 3.19: Resulting Pareto optimality fronts used to find the best NSGA-II settings

Based on this analysis, the chosen optimisation parameters were set as given below in Table 3.5. The lower limit for all system assets was set to zero, while the upper limit as set to 200 kW in line with the adopted REC regulation as discussed in the literature review. The *pymoo* module created and maintained by Blank et al. [170] was used to implement the NSGA-II algorithm in Python.

Table 3.5: Table showing the main NSGA-II algorithm control setting used in determining the design solution

| Parameter                 | Value       |
|---------------------------|-------------|
| Population Size           | 100         |
| Max Number of Generations | 200         |
| Mutation Rate             | 0.5         |
| Crossover Rate            | 0.9         |
| Lower Bounds (all assets) | 0  kW/kWh   |
| Upper Bounds (all assets) | 200  kW/kWh |

The input parameters were set into the simulation model with the selected objective functions and run within the NSGA-II algorithm. The optimisation ran to the maximum allowed number of generations before terminating. Due to the bound nature of the problem, the component capacity variables start as a random distribution, from which the

non-dominated solutions on the Pareto front are derived. Well-performing individuals are moved forward to the next generation, as well as a selection of offspring and individuals that have experienced random mutation. As the generations progress, the population steadily converges on a large set of non-dominated solutions that align with the Pareto front between best system economics and decarbonisation performance, denoted by the objective functions of cost savings and emissions intensity. The graph in Figure 3.20 shows the convergence of the objective function products during the progression through the first 200 generations of the hybrid system optimisation, which will converge towards a single value.

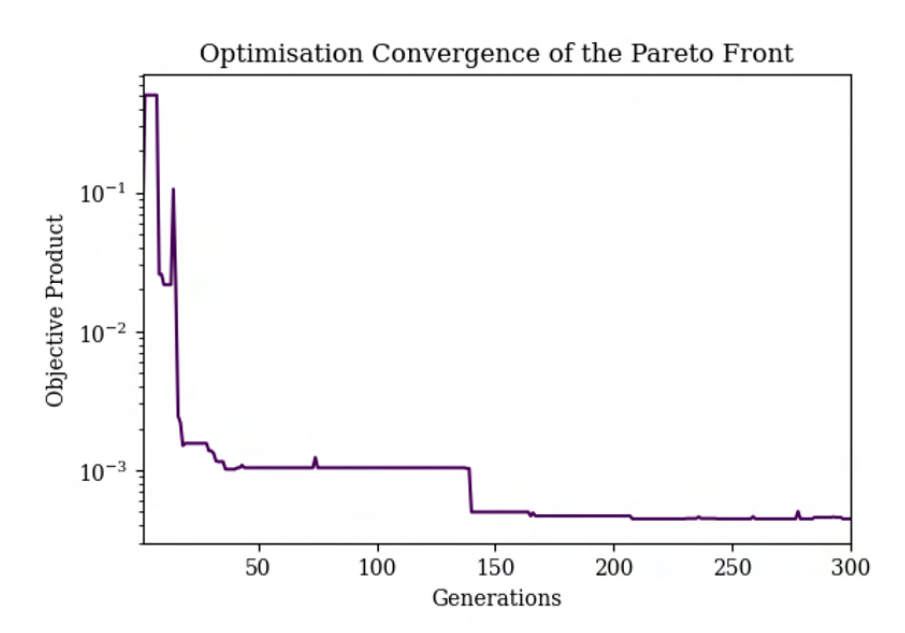


Figure 3.20: Convergence of the optimisation pareto front as shown by an aggregated scalar objective function minimising towards a single value

### 3.6 Model Assumptions

This sections documents all the model variables and assumptions made to produce the results presented in this thesis. Where available, a number of literature sources have been used to determine a credible value for each assumption and included in the Table 3.6 to Table 3.10 below. Also included are the ranges for variables that will be utilised in the analysis of error propagation within the results. Many factors, such as the embedded carbon of different assets are far less certain overall. For this reason, embedded emissions values have had a 30% standard uncertainty applied to the central expectation, in line with the approach taken by Arowolo et al. [171] assessing a similar, decentralised PV solar mixed asset model. Additional references are also added to support the stated range of uncertainties.

Table 3.6: Table of the global model assumptions

| Variable             | Value                   | $\mathbf{Unit}$ | Sensitivity Range |
|----------------------|-------------------------|-----------------|-------------------|
| Project location     | St Francisc, Formentera |                 |                   |
| Coordinates          | 38.706, 1.4335          |                 |                   |
| Base data year       | 2023                    | year            |                   |
| Project period       | 20                      | years           |                   |
| Discount rate        | 5%                      |                 | 2%                |
| Inflation rate       | 2%                      |                 | 1%                |
| Local grid emissions | 325                     | $gCO_2/kWh$     |                   |
| Local grid cost      | 0.3                     | €/kWh           |                   |

Table 3.7: PV technical parameters and assumptions

| Variable                  | Value  | Unit                 | Source          | Sensitivity range |
|---------------------------|--------|----------------------|-----------------|-------------------|
|                           |        |                      |                 | (+/-)             |
| CAPEX                     | 2,500  | €/kW                 | [124, 171, 172] | 250               |
| OPEX                      | 30     | €/kW/year            | [124, 171, 172] | 15                |
| Power per panel           | 400    | W                    | [124]           | 5                 |
| Panel area                | 2      | $\mathrm{m}^2$       | [173]           | 0.05              |
| Derate factor             | 0.40%  | V/year               | [173]           | 0.05%             |
| Power thermal coefficient | -0.35% | W/°C                 | [173]           | 0.05%             |
| Lifetime                  | 20     | years                | [173]           | 0                 |
| NOCT                      | 45     | $^{\circ}\mathrm{C}$ | [174]           | 1                 |
| Embedded carbon           | 1826   | $kgCO_2/kW$          | [175]           | 30%               |
| emissions                 |        |                      |                 |                   |
| Tnoct                     | 25     | $^{\circ}\mathrm{C}$ | [174]           | 0                 |
| Gnoct                     | 800    | W/m                  | [174]           | 0                 |
| Tstd                      | 25     | $^{\circ}\mathrm{C}$ | [174]           | 0                 |
| $\operatorname{Gstd}$     | 1,000  | W/m                  | [174]           | 0                 |
| Taualpha                  | 0.9    | •                    | [176]           | 0                 |

Table 3.8: Wind Turbine technical parameters and assumptions

| Variable         |        | Value | Unit         | Source          | Sensitivity range (+/-) |
|------------------|--------|-------|--------------|-----------------|-------------------------|
| CAPEX            |        | 2850  | €/kW         | [177]           | 250                     |
| OPEX             |        | 16    | €/kW/year    | [177]           | 0.5                     |
| Hub height       |        | 20    | m            | Author estimate | 0.5                     |
| Roughness height |        | 0.05  | $\mathbf{m}$ | Author estimate | 0.01                    |
| Lifetime         |        | 20    | years        | Author estimate | 0                       |
| Embedded         | carbon | 1,800 | $kgCO_2/kWp$ | [178]           | 30%                     |
| emissions        |        |       |              |                 |                         |

Variable

CAPEX OPEX Round trip

Lifetime

Max cycles

Embedded

emissions

Depth of discharge

|            | Value | ${f Unit}$ | Source | Sensitivity range |
|------------|-------|------------|--------|-------------------|
|            |       |            |        | (+/-)             |
|            | 328   | €/kWh      | [179]  | 100               |
|            | 22    | €/kWh/year | [179]  | 3                 |
| efficiency | 95%   | , , , ,    | [179]  | 2%                |

Author estimate

Author estimate

Author estimate

0

0

0

30%

[180]

Table 3.9: Battery technical parameters and assumptions

|             |          | ~       | -      |           |                |              |
|-------------|----------|---------|--------|-----------|----------------|--------------|
| Table 3.10· | Hydrogen | Storage | Energy | technical | parameters and | Lassumptions |

kgCO<sub>2</sub>/kWh

years

cycles

| Variable                | Value | Unit            | Source          | Sensitivity range |
|-------------------------|-------|-----------------|-----------------|-------------------|
|                         |       |                 |                 | (+/-)             |
| CAPEX fuel cell         | 1,250 | €/kW            | [179]           | 250               |
| OPEX fuel cell          | 13    | €/kW/year       | [179]           | 5                 |
| CAPEX electrolyser      | 1,500 | €/kW            | [181]           | 250               |
| OPEX electrolyser       | 14    | €/kW/year       | [181]           | 5                 |
| CAPEX hydrogen storage  | 20    | €/kWh           | [182]           | 0.5               |
| Efficiency fuel cell    | 46%   |                 | [179]           | 5%                |
| Efficiency electrolyser | 68%   |                 | [179]           | 5%                |
| Depth of hydrogen       | 95%   |                 | Author estimate | 0                 |
| discharge               |       |                 |                 |                   |
| Embedded carbon         | 73.3  | $\rm kgCO_2/kW$ | [183]           | 30%               |
| emissions fuel cell     |       |                 |                 |                   |
| Embedded carbon         | 239   | $kgCO_2/kW$     | [183]           | 30%               |
| emissions electrolyser  |       |                 |                 |                   |
| Embedded carbon         | 5.2   | $kgCO_2/kWh$    | [184]           | 30%               |
| emissions hydrogen      |       |                 |                 |                   |
| storage                 |       |                 |                 |                   |
| Lifetime                | 20    | years           | [185]           | 0                 |

### 3.7 Technical Structure and Execution

95%

8,000

254

10

carbon

This final section of the methodology describes how an REC model instance is created and executed as with the designed software architecture. One of the novel developments explored in this work is a energy system modelling tool using open-source software, rather than the more restrictive and less novel approach of using existing, commercially available software packages. Not only are there far more limited areas of exploration within the literature, but most commercial packages are unable to perform flexible, multi-objective modelling and simulation of a decentralised, renewable energy community. The choice to develop the tool in Python gives the freedom to explore a number of different options and configurations.

The diagram in Figure 3.21 displays the model architecture as designed in Python.

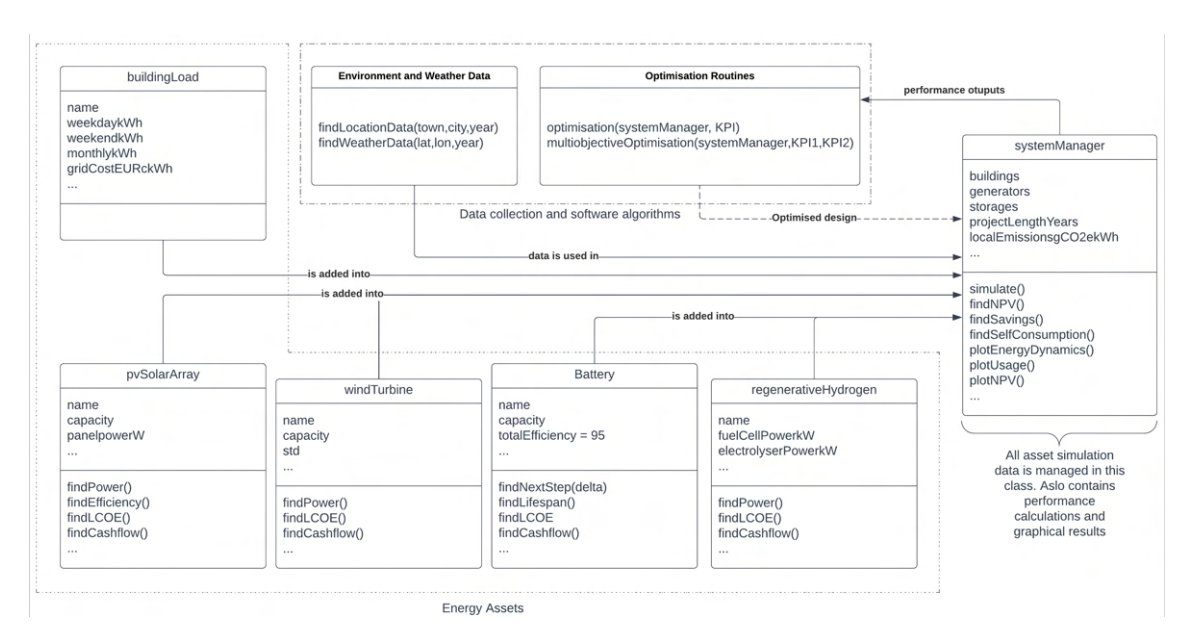


Figure 3.21: The object-based architecture of the system model implemented in Python

The model consists of different object entities which contain all the data and functions to model the generation and storage assets, collect local weather data, compile the full energy system, and execute the optimisation procedure. An REC model is created by the following steps:

- Define location and collect local meteorological data: The user must start by simply defining the town and city of the desired EC location, then the program uses an open-source geolocator tool to get the coordinate location and begin downloading wind speed, temperature and solar irradiance data from the NASA PowerLARC database for the chosen base year.
- Define the generation and storage assets: The user must then create instances for the assets that will be included in the EC design. When creating an instance, the initial asset type (i.e. wind turbine, solar panel, etc.), including capacity and type, is also defined. This process is the same for the energy storage assets (Battery and hydrogen storage).
- Define the building loads: The user can either input custom electrical loads or choose from one of the preset load profiles from the NREL dataset discussed in the previous section. To define a custom profile, the hourly weekday and weekend load profile must be added, as well as the monthly average total consumption. The model then uses this information to synthesise the building load profile over the course of one year. When using the archetypal profiles, only the annual energy consumption must be specified.

- Create the energy system instance: Once all sub-systems have been defined, they are then added to an energy system instance. This object manages all aspects of the model, including the main model execution, storing input assumptions and recording outputs, and visualising the results.
- Run the optimisation routine: The model can be executed independently of the optimisation routine to ensure no errors are present. Once complete, the optimisation model is started, and terminates once the termination criteria are met. This is usually defined as a maximum number of NSGA-II generations.

Once all steps have been completed, the model's output provides the multi-objective optimisation routine, which is in the form of a pareto front describing the non-dominating relationship between the two chosen objective functions of cost and decarbonisation. It is then the decision of the user whether to explore the design domain further and run simulations for specific optimal results.

# Chapter 4

# Results

This chapter presents the results of the REC system model created in this thesis. The primary objective is to support the climate transition objectives of the local community on the island of Formentera, whilst ensuring low-cost, secure energy availability. The creation of an energy system model, capable of testing and optimising several renewable assets and load profiles to assess the routes to commercial deployment of REC systems is essential for the energy transition of any geographical island.

The first part of this chapter details the asset validation process, ensuring that the performance is representative of the real world technology. The second introduces and evaluates the optimal REC system design achieved through multi-objective, evolutionary optimisation. The major result presented is the true impact in terms of cost and decarbonisation potential that could be attained via the REC design, including the relevant design choices and trade offs to achieving either optimal performance outcome.

The third part of this chapter defines and tests a couple of scenarios that could affect the design and operation of the REC. The first scenario test provides an analysis of the hybridisation of battery and hydrogen storage technology compared to their standalone counterparts, to quantify any benefits in combining assets to minimise drawbacks of the storage options. The second scenario test presents a comparison of two potential trading policies that could be utilised by the REC members, a 'friendly' trading logic and a 'competitive' local market design, as outlined in Chapter 3.

Finally, this chapter concludes with a detailed investigation into the potential error propagation in the model due to input parameter uncertainty. The variable sensitivities outlined in Tables 3.7 to 4.1 state the sensitivities used in a Monte Carlo assessment, followed by a Sobol sensitivity analysis to identify the inputs driving the maximum uncertainty.

### 4.1 Asset Model Validation

The motivation for the creation of a Renewable Energy Community (REC) model is to accurately and credibly project the energy system performance under a number of different scenarios. It is therefore crucial to understand the accuracy of the individual asset models that are providing hourly power generation to the EC. The concept of the approach is that the developed software is location and system size agnostic, in that any volume of solar and wind generation can be applied and in any technically feasible location around the world.

This section includes a validation of the photovoltaic (PV) solar and wind turbine asset models. The results include a sample annual dataset consisting of real measured performance and environmental conditions, measured against the simulation to determine a representative error. As discussed in the previous section, the chosen asset parameterisation methodologies are based on a trade-off between performance and practically of a 'white-box' fully resolved model and a 'black-box' simplified model. Understanding the potential simulation error can be used in the analysis to determine if further model enhancements are required.

### 4.1.1 PV Solar

The PV solar is a crucial generation technology in the field test location of Formentera due to the high solar potential of the Balearic Islands. Accessing PV solar test data, including the measured power and environmental conditions for southern Spain is challenging, so data provided by the The National Renewable Energy Laboratory (NREL) is used to for validation.

NREL performed a variety of PV solar tests of the course of several years, and have included all the required technical parameters to recreate the asset in the model, as shown in Table 4.1 below. The test system is an amorphous tandem junction solar cell technology, with a rated power output of 40 W.

| Parameter                              | Value                            | $\operatorname{Unit}$ |
|--|----------------------------------|-----------------------|
| Location                               | Golden, Colorado                 |                       |
| Coordinates                            | $39.74^{\circ}, -105.18^{\circ}$ |                       |
| Rated power $(P_r)$                    | 40                               | W                     |
| Cell area $(A)$                        | 0.079                            | $\mathrm{m}^2$        |
| Thermal power coefficient $(\alpha_p)$ | -0.22                            | %/°C                  |
| Efficiency $(\eta)$                    | 20%                              |                       |
| Tilt angle $(\beta)$                   | $40^{\circ}$                     |                       |
| Azimuth angle $(\alpha)$               | 180°                             |                       |

Table 4.1: The technical cell parameters of the PV solar test set-up [186].



Figure 4.1: NREL PV solar test set up in Golden, Colorado.

The data covers a one-year period in 15-minute intervals starting in August 2012 over the daylight periods, equating to 12,070 validation points total. The global horizon irradiance (GHI), ambient temperature, wind speed, and measurement time stamp are recorded in addition to the cell temperature and power output. The assumptions in the table above are set into the model and the asset is simulated over the same period and in

the same geographical location.

Figure 4.2 displays a sample 5-day period comparing the recorded test data with the asset simulation output. As can been seen, the model performance shows good agreement with the test data, even accurately reflecting the tips and changes in power output due to clouding effects. When analysing the error histogram in Figure 4.2 it can also be seen that the absolute error mode is 0.4-0.7 W, or just over 1% error. Considering the mean error, this increases to approximately 5%.

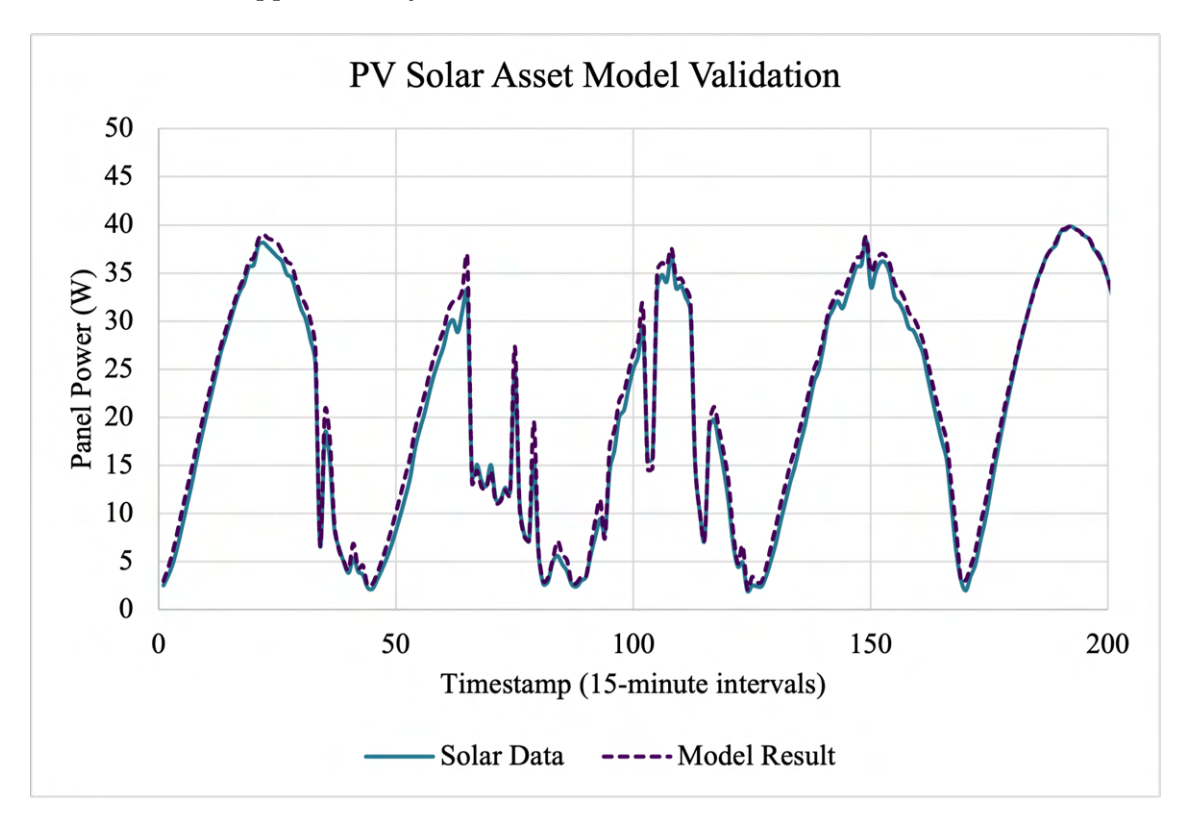


Figure 4.2: A portion of the solar validation data compared to the modelled result.

While an error is observable between the measured and simulated data, an effective 95% confidence is an acceptable result over a one year period. Changes in light scattering, reflections, heat transfer due wind speed variation, and manufacturing defects in the solar cell are among a number of factors not directly captured in the model that may be causing the variation observed.

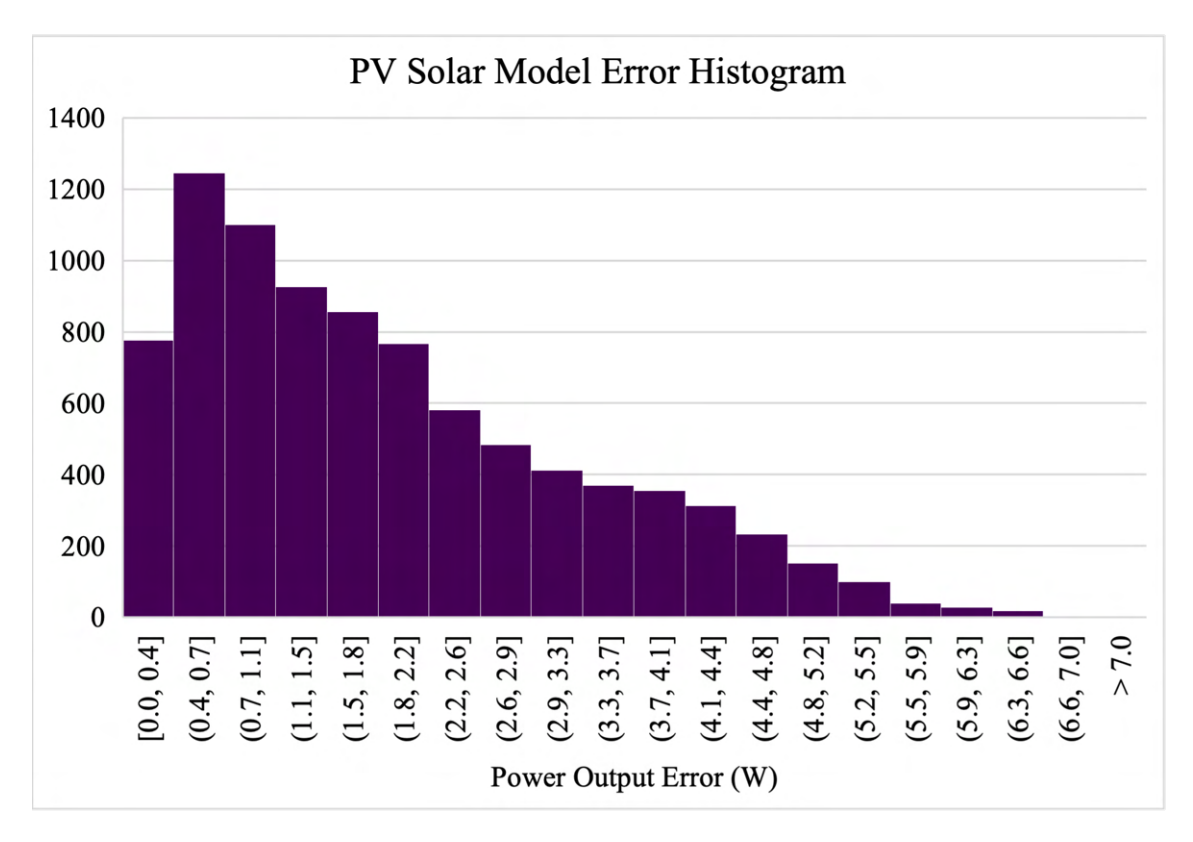


Figure 4.3: Histogram illustrating the error distribution and variance over the validation time horizon (one year).

### 4.1.2 Wind Turbine

Like the PV solar validation approach, the wind turbine asset model is validated against real measured performance and environmental conditions. Since there are currently no wind turbine installations on Formentera, wind power generation results are taken from another island, Gökçeada, in Turkey. This island has two 900 kW wind turbines installed that supply power directly to the local grid. The data was provided from one of the turbines in hourly increments for 2019.

Table 4.2 below includes the model parameterisation employed to align the simulation with the physical test data. The average wind speed at the installation site is 7.5 m/s which matches the design requirements of the on-shore IEC-II type turbine, so the corresponding performance profile is chosen for the model test.

Figure 4.5 shows a sample 10-day period of the asset model performance comparison against the Gökçeada wind turbine. It can be seen as with the PV solar result that the model shows good overall agreement with the measured power generation. The model is able to successfully capture the changes in generation output with the change in wind speed, and considers the difference in wind speed measurement height (10m) with the hub height (m) using the log law Equation 2.8.



Figure 4.4: The Gökçeada installation site of the wind turbines used for model validation.

Table 4.2: The technical parameters required for the wind turbine model [187]

| Parameter                | Value                          | Unit         |
|--------------------------|--------------------------------|--------------|
| Location                 | Gökçeada, Turkey               |              |
| Coordinates              | $40.18^{\circ}, 25.94^{\circ}$ |              |
| Rated power $(P_r)$      | 900                            | kW           |
| Hub height $(z_h)$       | 40                             | $\mathbf{m}$ |
| Roughness length $(z_0)$ | 0.03                           | $\mathbf{m}$ |
| Turbine classification   | IEC-II                         | (low winds)  |

The error over the one-year test period is less than 1% on average, which is reassuring given the complexity of wind turbine operation, and the fact that the model does not explicitly consider the hugely complex fluid dynamics and energy transfer. The error histogram affirms the low error margin, with a mode of 0-2.6 kW of error, or 0.26% of the rated asset power. This result gives a good degree of confidence that the modelled result will be minimally impacted by potential induced errors in the wind turbine asset. In terms of the representation of the wind generation in the asset model, it is assumed that the generation could consist of multiple micro-wind turbines of the same technical specification as opposed to a single, large turbine generator. For example, if the optimal deployment is equal to 100 kW of wind capacity, it is assumed for practical installation purposes that the true system would consist of 3-4 smaller wind turbines of suitable size to be deployed within or near the rural energy community, and as such the generator can be connected down stream of the same secondary substation.

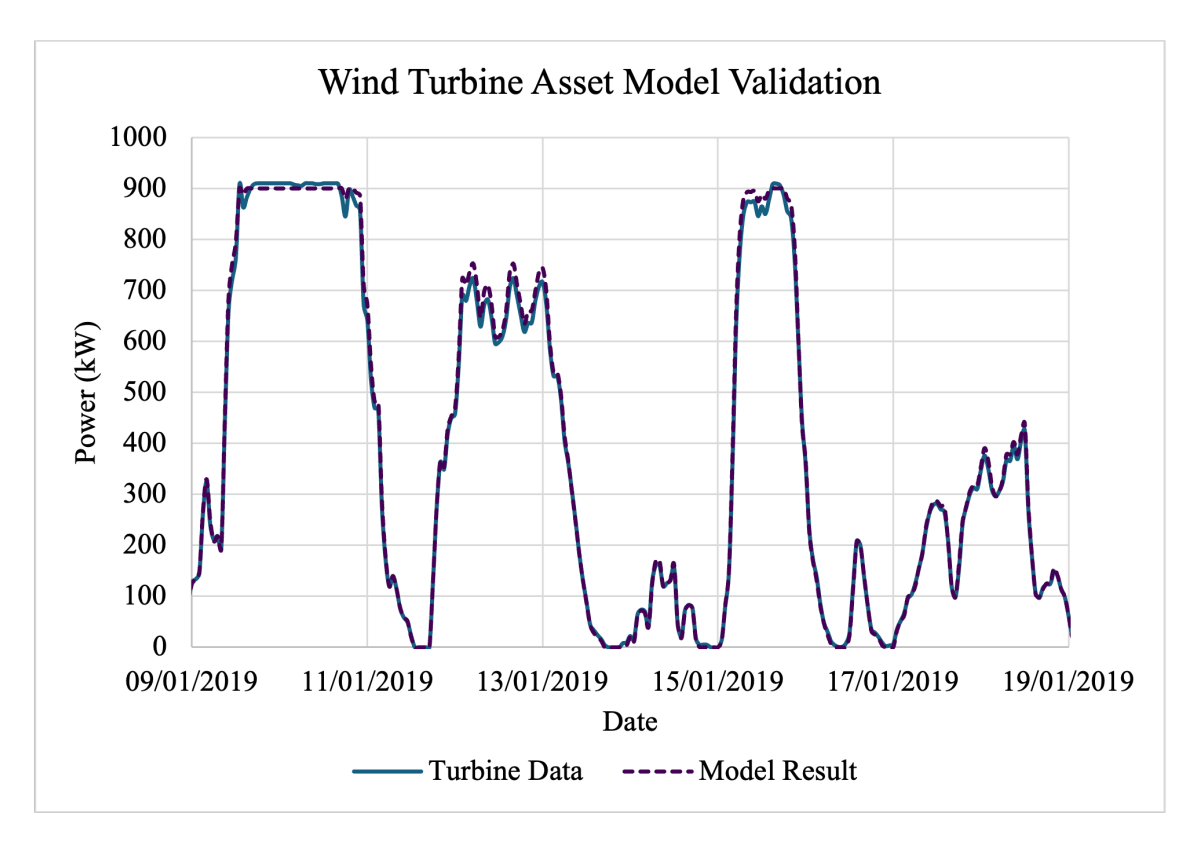


Figure 4.5: An example section of wind validation data compared to the modelled outcome.

### 4.2 Multi-Objective Optimisation of the Renewable Energy Community System

The assumptions outlined in the methodology section were inputted into the model, including the five fixed building electrical loads. The variables consist of the optimised capacities for PV solar, wind generation, battery storage and hydrogen storage. The optimisation has a maximum restriction on asset size of 200 kW in line with the RED-III policy framework. The NSGA-II algorithm was run with the following settings:

Table 4.3: NSGA-II optimisation settings

| Parameter             | Value |
|-----------------------|-------|
| Population size       | 100   |
| Crossover probability | 50%   |
| Mutation probability  | 90%   |
| Max generations       | 200   |

The input parameters were set into the simulation model with the selected objective functions over maximum system present value and minimum emissions intensity. The optimisation ran to the maximum allowed number of generations before terminating. Due to the bound nature of the problem, the component capacity variables start as a random distribution, from which the non-dominated solutions on the Pareto front are derived. Well-performing individuals are moved forward to the next generation, as well as a selection of offspring and individuals that have experienced random mutation. As the generations progress, the population steadily converges on a large set of non-dominated solutions that align with the Pareto front between best system economics and decarbonisation performance.

The primary case studied was the hybrid architecture consisting of a lithium battery and a hydrogen storage system. Within the resulting Pareto front in Figure 4.6, each point on the graph represents a different combination of design choices to be made by the REC developers to achieve the highest economic returns and lowest net carbon output. The lifetime cost savings potential ranges from approximately  $150,000 \, \text{©}$  to  $190,000 \, \text{©}$ , while the emission intensity ranges from 59 to 93 gCO<sub>2</sub>e/kWh.

Within this Pareto front exists the information and insight required to design and build the optimal REC system for the island of Formentera. It is interesting to note that the savings do not start at zero, implying that below 150,000€ returns the configuration was able to increase in economic performance as well as decarbonisation before reaching an inflection point. At this point, it becomes clear that the net savings were able to continue increasing, while the net emissions reached their minimum and began to climb again. At the other end of the front, the gradient began to increase as the returns increase but also the emissions intensity. This continued up to the point where the system can no longer

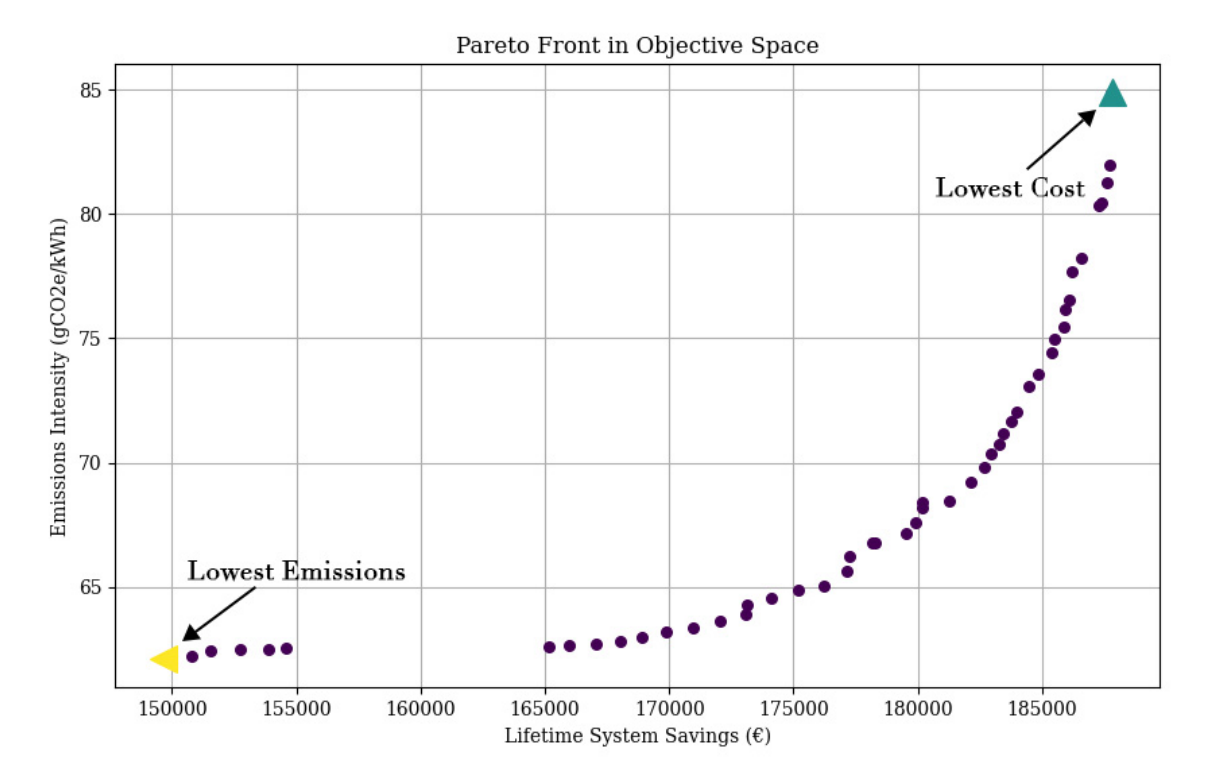


Figure 4.6: The set of Pareto optimal solutions for the REC system design

provide additional savings without an exponential increase in embedded emissions and therefore environmental impact.

Deeper analysis can be conducted of the various system design choices by graphing the change in asset sizing that corresponds to each side of the objective space, that being the range of design choices to achieve the best cost savings and/or best decarbonisation.

It can be seen more clearly in Figure 4.7 that the renewable generation and storage sizing choices has a direct impact on the performance objective. The graph displays the capacities of PV solar, wind power, battery, fuel cell, and electrolyser systems with the final population arranged by the two objective functions. The best economic outcome is on the left, while the best environmental outcome is on the right. It can be observed that all systems generally tend towards an increase in capacity as the emissions improve. This is most likely because a larger total off-grid capacity has a higher self-consumption rate, and therefore is relying less on the grid which has a high emissions intensity of 325 gCO<sub>2</sub>e/kWh. The REC was consequently able to reduce emissions to a greater extent. This, of course, negatively impacts on the economics of the REC as more capital has to be invested into a more substantial design. It appears from the graph that the wind power, as well as the fuel cell and electrolyser, which make up the RHFC and are most sensitive to changes in the objective function. The following section explores the chosen optimal design, and details why the capacities affect the objective functions in this way. As the Pareto efficient solutions move towards the lowest emissions objective, most assets increase

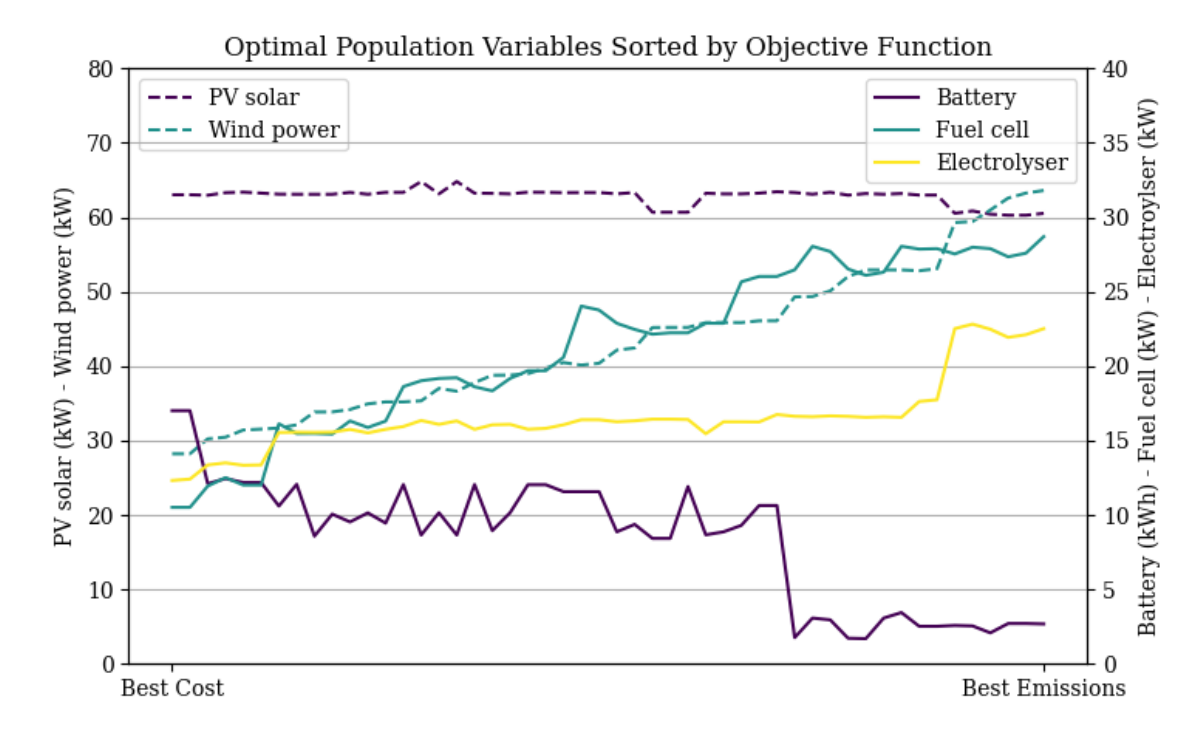


Figure 4.7: The change in renewable asset size with specific performance target

in size, with the exception of solar energy generation, which appears to remain relatively stable at approximately 60-65 kW of rated power. Wind generation, by contrast, increases from 28 kW under optimal savings conditions to over 65 kW.

The changes in storage system asset sizing are more nuanced as there are a number of second order decision making processes going into the final capacity. The battery storage sees a decrease as the design moves away from best cost and towards best emissions reduction, with a notable step change. The battery sizing peaks at approximately 17 kWh before steadily declining towards the right of the graph. An analysis of this behaviour is explored further in the discussion section on this thesis. The fuel cell and electrolyser sub-models increase in size between best cost and best emissions reduction. This result makes logical sense as both assets are required and in the correct proportionality to create a fully utilised and efficient hydrogen storage system. The fuel cell size ranges between 10-28 kW and the optimal electrolyser size lies between 17-23 kW. The pressurised hydrogen storage tank is not optimised directly, but is instead sized based on the maximum seasonal storage requirement over the one-year simulation period based on the optimal fuel cell and electrolyser combination.

### 4.2.1 Optimal System Design

While the Pareto front is a useful tool to understand the range of potential optimal solutions, a system design must be chosen such to allow an investigation of the dynamics of the system and the internal decision-making. There are several methods that can be used to choose a 'best' trade-off system from the population to perform further analysis. Based on the research conducted by Wang and Rangaiah [188], it was chosen to use Simple Additive Weighting (SAW). SAW normalises both objective function values, where zero is the worst possible result and one is the most improved. The values are then summed up for each member of the population to find the best overall solution.

$$F_{ij} = \begin{cases} \frac{f_{ij}}{f_j^+}, & \text{for a maximisation criterion, where } f_{j^+} = \max_{i \in m} f_{ij}, \\ \frac{f_{ij}}{f_j^-}, & \text{for a minimisation criterion, where } f_{j^-} = \min_{i \in m} f_{ij}. \end{cases}$$
(4.1)

$$A_i = \sum_{j=1}^n F_{ij} \tag{4.2}$$

 $F_{ij}$  is the normalised set of objective functions j for Pareto population i,  $f_{ij}$  is the initial set, and  $f_{j^+}$  is and  $f_{j^-}$  is the maximum and minimum criteria of the set, respectively.  $A_i$  then provides the best set of design variables to use in the hybrid REC. The system was then simulated to perform analysis of all performance indicators.

By performing the calculation over all multi-objective results, a feasible design is derived that attempts to trade-off the relationship equally between cost and decarbonisation. The resulting asset sizes are shown in Table 4.4 below. It should be noted here for clarity that this REC combination of system design choices will, by definition, exist somewhere within the pareto front approximately on the apex between the two objective functions.

Table 4.4: Optimal decentralised asset sizing for the Formentera REC

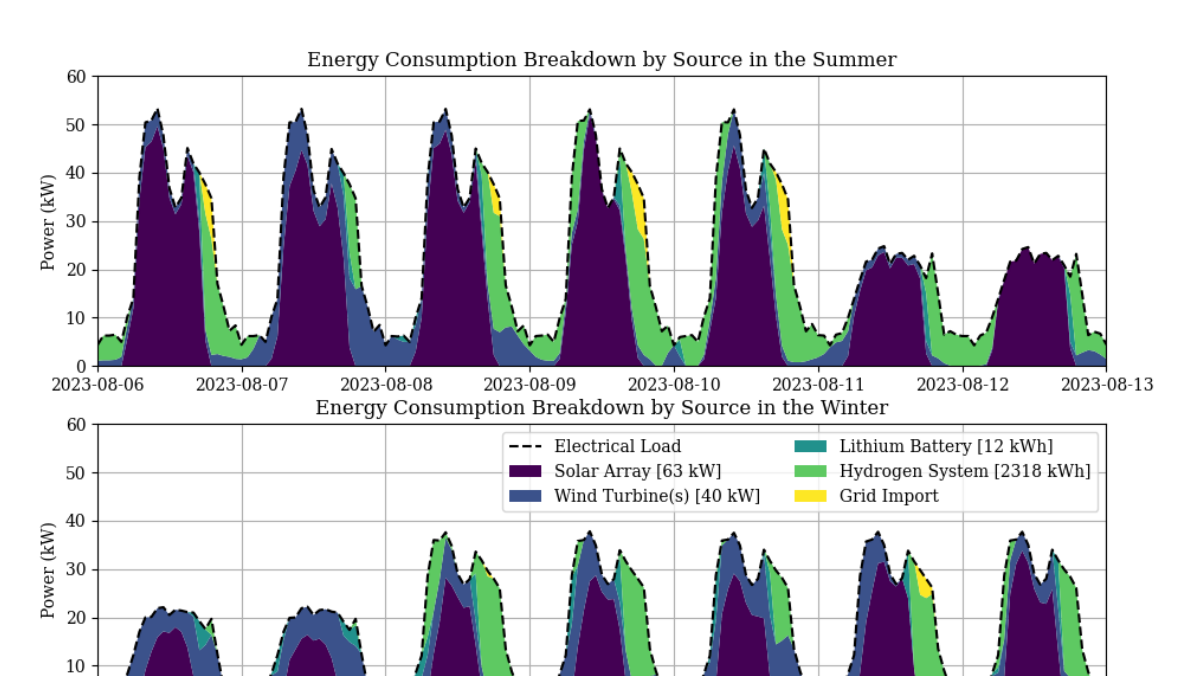
| REC Asset             | Value            |
|-----------------------|------------------|
| PV Solar              | 63 kW            |
| Wind $Turbine(s)$     | 40  kW           |
| Battery Storage       | 12  kWh          |
| Fuel Cell             | $24~\mathrm{kW}$ |
| Electrolyser          | $16~\mathrm{kW}$ |
| Hydrogen Storage Tank | 2,318  kWh       |

Figure 4.8 contains two one-week sample periods obtained from the simulation, displaying the balance of each asset and their contribution to balancing the total REC load. Typical summer and winter periods are used to observe the seasonal variation in the system's response. The REC load was higher on average during the summer period. The higher seasonal demand is due in part to the increased use of air conditioning to ensure comfortable habitation in the climate of Formentera. The higher load leads to increased reliance and the energy grid to fill gaps in the consumption requirement when the Energy Storage System (ESS) was unavailable. The winter period, by contrast, was able to satisfy the load

2023-02-10

2023-02-11

2023-02-12



requirement with the exception of some short periods.

Figure 4.8: Energy generation hour-by-hour breakdown by source. Example shown includes a typical summer (August 2023) and winter (February 2023) week.

2023-02-14

2023-02-15

2023-02-16

2023-02-17

2023-02-13

It can be seen from the graph that the PV solar generation provides the majority of the renewable power during the summer due to the high average peak sun hours. The battery and hydrogen system can then use the excess solar to charge or generate hydrogen. Once the peak sun hours have past, the battery, supplemented by any available wind generation, discharges to balance the load. Once the battery has been discharged completely, the hydrogen fuel cell is then activated to provide baseline power. Grid power is only used in instances when both the battery and hydrogen systems cannot provide enough power output to balance the load. Occurrences of this nature can be seen during late evening periods where building loads across the Renewable Energy Systems (RES) can be almost at their peak. This shows that although the REC can operate largely off-grid, it is still beneficial from an economic and emissions perspective to remain grid-connected from the short period when the REC generation and hybrid storage cannot fully balance the consumption.

The hydrogen system requires a maximum storage of 2,318 kWh, which was evaluated from the simulation as the storage required to avoid any state-of-charge limits. The value therefore is a worst-case scenario for the system, as it is likely that a smaller storage would be chosen in accordance with the installation space available within the REC. Given the Lower Heating Value (LHV) of hydrogen and the average fuel cell efficiency of 46%, the

system would require approximately  $21.9~\mathrm{m}^2$  volume of hydrogen stored at 35bar, to supply the required quantity of a one-year period.

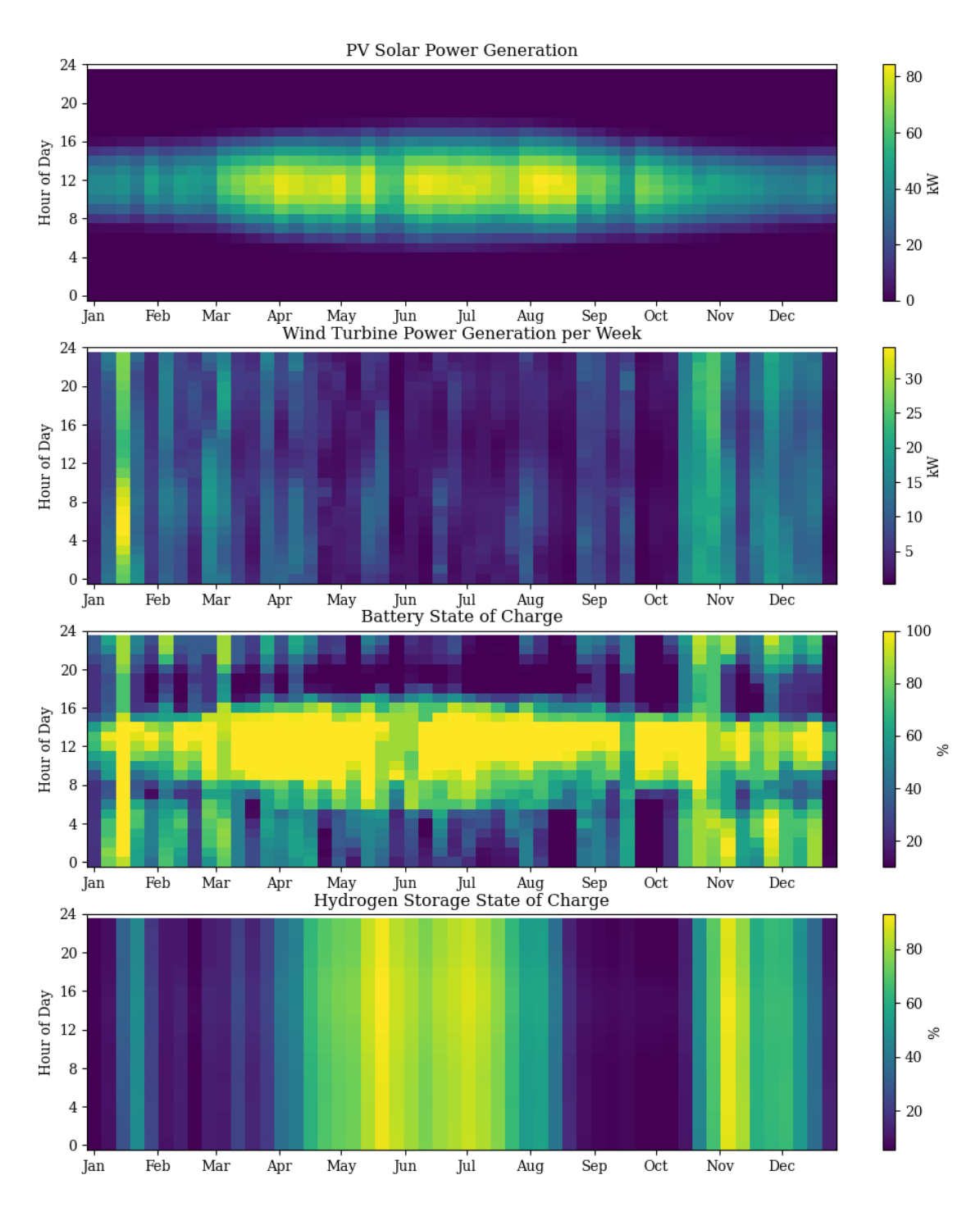


Figure 4.9: The annual weekly-averaged daily operation of the hybrid combined storage, and PV solar and wind generation.

The heat maps in Figure 4.9 illustrate the daily generation of the wind and solar assets, and the SOC of the battery and hydrogen storage. SOC here is also used to refer to the so-called 'state-of-hydrogen', a measure of the volume of chemical storage available compared to the maximum possible stored. The hourly data is aggregated into one-week average results over the course of a day to create maps that display the weekly average 24 hours period on the y-axis, and the weeks of the year on the x-axis.

Starting with the solar generation data, it can be observed that the majority of the solar potential increases in the late-spring to early autumn-period, in line with the seasonality in the northern hemisphere. This dynamic has a direct impact on the excess generation availability that can be used to charge the battery or generate hydrogen. There is also, as expected, a huge dependence on the time of day which correlates to when solar power is available, and, although to a lesser degree, across the year. By contrast, the wind generation is far more evenly spread over the year. There does appear to be a correlation between the winter months and higher wind generation, possibly due to the higher probability of seasonal storms and changing weather, resulting in higher average wind speeds. A small increase in power output in the afternoon can also be seen in the summer months. This phenomenon is common to warm, coastal climates as warming of the lands surface during the day causes uneven patches of air pressure, inducing localised breezes in the afternoon and evening.

It is interesting to note that the characteristics of the generation activities over the one-year simulation period have a direct impact on storage State-of-Charge (SOC). Starting with the battery storage system, the SOC commonly reaches a maximum over the midday period. This is due to the daily utilisation of the excess solar generation to charge the battery system. The hourly building load also drops significantly after the early morning period, allowing for additional excess charging power. When the battery is then required in the evening period, it discharges to satisfy the load, reducing the average state-of-charge. The lowest average state of charge occurs in the very early morning period, particularly during low wind generation volumes in the summer months. In the winter period, the building loads are lower on average, and wind generation is higher, so the BESS is more likely to maintain charge throughout a 24-hour period.

The hydrogen system performs a different energy storage role to the battery, in that it allows for the seasonal shift of stored generation to annual costs. This is a role commonly associated with natural gas, pointing to a potential opportunity for hydrogen in the future. The hydrogen storage volume is much larger by energy potential than the battery; a difference that is reflected in the state of storage graph, in that the level of stored hydrogen changes very little on average throughout a 24 hour period. However, over the course of a number of weeks, the storage volume can change significantly. The period from January to February, and in October, are the average low points for hydrogen storage. This observation is due to the requirement for storage energy in the months before these periods, causing

an overall deficit. Essentially, high building power demand in August and September leads to larger volumes of storage withdrawal. Similarly, the December to January period sees lower solar and wind potential. The storage volume peaks in the period from June-July and again in November. The graph in Figure 4.10 shows the direct comparison between the two storage systems, directly illustrating the different roles that the hydrogen and battery technologies are playing in balancing the needs of the energy community.

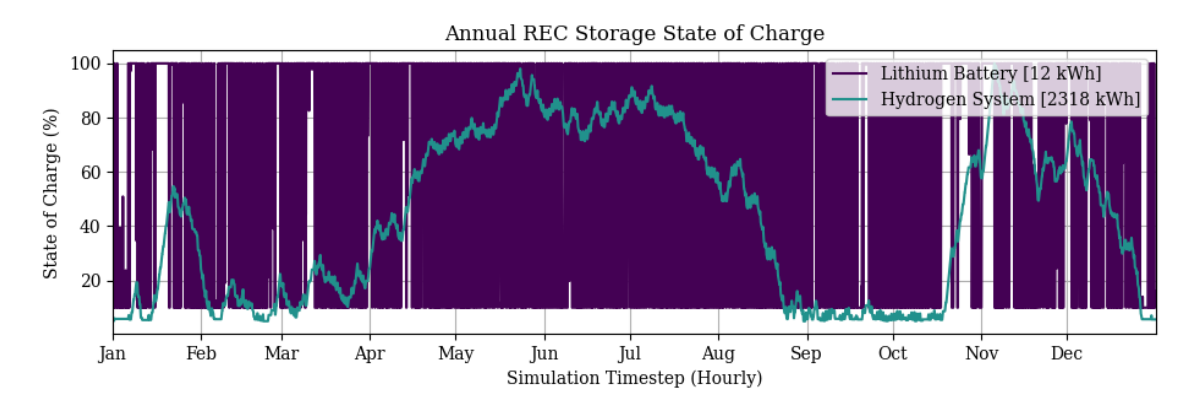


Figure 4.10: A comparison of the state of charge between the hydrogen and battery storage systems on an hourly basis.

#### Techno-economic Assessment

Table 4.5 below shows a full breakdown of the economic and environmental performance of each grouped asset. The solar array was able to deliver the most energy to the REC due to the high capacity of 63 kW, but also the higher solar potential on the island of Formentera of 4.8 kWh/m², compared to London, UK, of 2.9 kWh/m². Energy generated from wind provides the next greatest portion of over 24%, the benefit of which is that energy is generated during the night period as well as the day to charge the battery and a steady quantity of hydrogen. The battery itself was relatively small compared to the other components and responds only when energy generated is no longer available in excess of supply. The fuel cell and electrolyser were sized at 24 kW and 16 kW, respectively. It is interesting to note that the electrolyser was smaller in power input capacity than the fuel cell, even though the efficiencies would dictate the fuel cell would need to approximately half the rated power of the electrolyser to achieve the same capacity factor. The increased generation from wind power over a longer simulation period may allow the electrolyser to operate at increased capacity factors and make up the fuel cell's lower efficiency.

It is important to analyse each component on an individual basis to fully understand their contribution to the economic and emissions performance within the system. This not only would help confirm the results seen in the Pareto optimality, but also assist a potential system designer to identify the most important assets, any particularly sensitive parameters, from a practical perspective while allowing for the assessment of the risks associated with each.

| Table 4.5: Optimal REC | system | design l | key tec | hnoeconomic results |
|------------------------|--------|----------|---------|---------------------|
|------------------------|--------|----------|---------|---------------------|

| Technology  | Energy          | Capacity                 | CAPEX   | OPEX     | LCOE    | Emissions      |
|-------------|-----------------|--------------------------|---------|----------|---------|----------------|
| Asset       | Delivered (kWh) | $\mathbf{Factor}$ $(\%)$ | (€)     | (€/year) | (€/kWh) | $(gCO_2e/kWh)$ |
| PV Solar    | 116,000         | 21                       | 158,000 | 1,900    | 0.08    | 48.7           |
| [63 kW]     | 110,000         | 21                       | 155,000 | 1,900    | 0.08    | 40.1           |
| Wind        | 68,400          | 19                       | 91,200  | 1,300    | 0.10    | 15.2           |
| Turbine(s)  |                 |                          |         |          |         |                |
| [40  kW]    |                 |                          |         |          |         |                |
| Lithium     | 3,900           | 8                        | 3,800   | 250      | 0.08    | 75.5           |
| Battery [12 |                 |                          |         |          |         |                |
| kWh]        |                 |                          |         |          |         |                |
| Hydrogen    | 26,600          | 13                       | 99,800  | 570      | 0.15    | 33.3           |
| System      |                 |                          |         |          |         |                |
| [2318  kWh] |                 |                          |         |          |         |                |

The solar array has the largest capital and operational costs compared with the wind power alternative due to the higher unit costs per kW. Despite this, since the PV solar was able to achieve a greater capacity factor, which is the measure of energy output as a ratio of the total potential output of the same period. PV solar is naturally limited by the hours of solar available, while wind power is limited by the average wind speed and distribution. The higher capacity is the main mechanism which produced a lower Levelised Cost of Electricity (LCOE) for the PV solar of 0.08 €/kWh compared with wind power of 0.10 €/kWh, despite the higher CAPEX and OPEX costs. This result also implies that although wind power is possible with the REC, it may be beneficial from a financial point of view to study a PV solar generation only option due to the potential impracticalities of local wind turbines. The inverse was then observed for the environmental impact, in that the PV solar has considerably higher embedded emissions of 48.7 gCO<sub>2</sub>e/kWh compared with 15.2 gCO<sub>2</sub>e/kWh expected from equivalent wind energy. These results show good agreement with reported embedded emissions from the IPCC AR5 report [189] of 40-45 gCO<sub>2</sub>e/kWh and 13 gCO<sub>2</sub>e/kWh for solar and wind, respectively.

At €100k, the hydrogen system CAPEX was a twenty times that of the battery system. This trend carries over into the LCOE results, where an approximate doubling of the levelised cost was observed for hydrogen compared with lithium batteries. These outcomes are in line with similar hydrogen system results found in the literature [190], where the investment required results in a significantly higher cost. It is widely known that hydrogen technology is a less financially viable alternative for many applications, so this result was somewhat expected. This could change in the near future as costs of hydrogen technology reduce.

The emissions output from the battery per kWh delivery was far higher than the hydrogen solution at 76 gCO<sub>2</sub>e/kWh and 33 gCO<sub>2</sub>e/kWh, respectively. The trend is also supported by the population variables in Figure 4.7, in which its noted that as the hydrogen assets increase in capacity, the emissions result improved, while the net savings deteriorated.

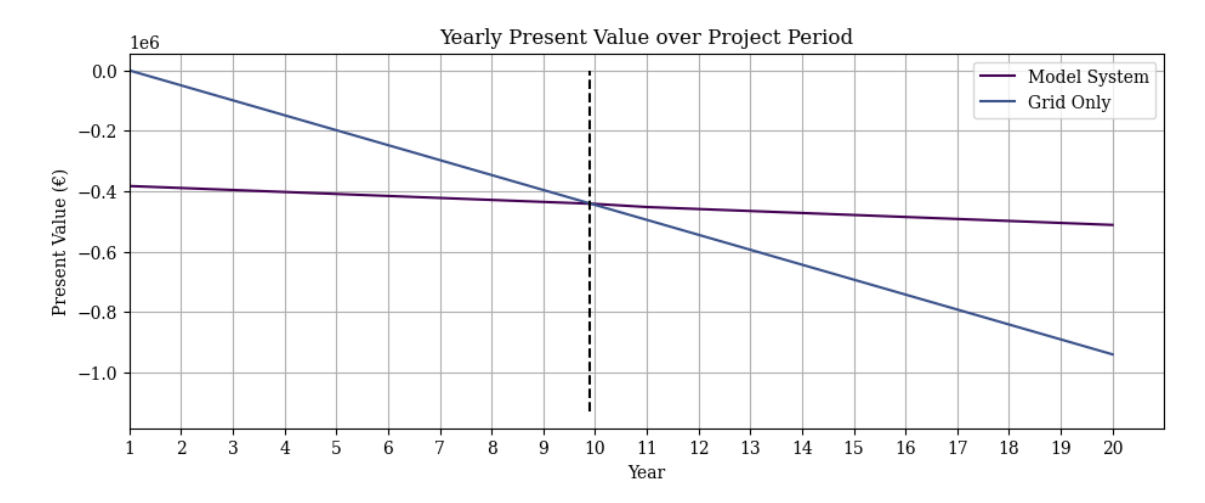


Figure 4.11: Present value curve for the central scenario compared to grid-only use.

Figure 4.11 contains the present value curve of the grid-only case, that is when electricity cost is paid to the utility company over the project period. The curve starts at zero as there is no capital cost associated with grid usage, but the operational cost per year is high. By contrast, the modelled REC requires an initial investment of  $353,000\mathfrak{C}$ . However, the lower year-on-year cost means that the system can pay off the investment cost, described as the payback term, in 9 years (start year is to the base of 1). The project ends with a final total savings of  $180,000\mathfrak{C}$  when the inflation and discounts rates of 2% and 5%, respectively, are considered. The result produces an IRR of 11.1%, annualised savings of 9.7%, and an average system LCOE of  $0.155\mathfrak{C}/\mathrm{kWh}$ .

Considering the historical and currently observed trends in renewable energy generation and energy storage equipment cost, it is projected that by 2030 and beyond there will continue to be a substantial decrease in the financial requirements for this type of system. The results shown here are therefore towards the upper bounds in terms of uncertainty about the future cost of an REC implementation.

#### REC members' net savings and environmental impacts

The model not only provides a global view of the potential impact of an REC configuration but is also able to analyse the reduction in cost and emissions on a per load basis. There were five discretised loads within the model, with each being able to mutually accept and trade energy with the decentralised assets. The REC provided a considerable degree of self-consumption, ranging from 91.1% for the largest load to over 98% for the smallest. In terms of impact on the energy cost, the new LCOE ranged between 0.16-0.17  $\mbox{\ensuremath{\mathfrak{C}}/kWh}$  compared to 0.30  $\mbox{\ensuremath{\mathfrak{C}}/kWh}$  for grid-only. The decarbonisation of energy usage was also seen to be in the range 75-77% in the first year of installation.

### 4.2.2 REC System Performance at the Extrema

During the study, it was vital to understand not only the characteristics of the system at the 'best' result, denoted in this work as the central optimal case, but also the performance at the extremes of the multi-objective optimisation. The result gives an indication as to how sensitive the result was to changing parameters. In place of using a weighted approach, the generation and storage asset capacity variables were found by simply evaluating the Non-dominated Sorting Genetic Algorithm (NSGA-II) optimisation individual's results at both end of the Pareto front, as shown in Figure 4.6. Table 4.6 contains the results of the three chosen REC configurations in terms of hybrid generation and storage capacities.

Table 4.6: Comparison REC configurations for extreme cases for net savings and decarbonisation potential compared with the central optimal case.

|                          | Best net savings | Central Optimal | Best emissions savings |
|--------------------------|------------------|-----------------|------------------------|
| REC Delivered            | 81,000           | 153,000         | 160,000                |
| (kWh)                    |                  |                 |                        |
| Self-Consumption         | 51%              | 95%             | 99.9%                  |
| LCOE (€/kWh)             | 0.149            | 0.155           | 0.180                  |
| Net Savings (€)          | 188,000          | 180,000         | 150000                 |
| Simple Savings           | 10.1%            | 9.7%            | 8.3%                   |
| IRR                      | 14.1%            | 11.1%           | 7.4%                   |
| Payback Term (years)     | 7.7              | 8.9             | 11.6                   |
| Emissions $(gCO_2e/kWh)$ | 85               | 68              | 62                     |

Under the lowest cost scenario, the energy community reaches a net saving of 187,000€, compared to the lowest emissions which sees a drop to 156,000€. The clear reason for this is the increase in investment in the system to size up both the generation and storage systems, as shown in Table 4.7. The LCOE is similar between the low cost and central optimal outcome, though the emissions see a wider gap emerge between outcomes, with 85 gCO<sub>2</sub>e/kWh and 62 gCO<sub>2</sub>e/kWh achieved for the former and latter, respectively. The lowest emissions scenario displays a far higher LCOE at 0.180 €/kWh, an increase of 13%. One of the most prominent changes between the extrema scenarios is the Internal Rate of Return (IRR) which ranges from 7.4-14.1%. It is often suggested that an IRR of at least 12% for an emerging energy product of service is desired as a minimum, considering potential investment risk, indicating that an optimal system towards the optimal cost end of the Pareto front would be more desirable for commercial deployment.

As explained in Figure 4.7, the optimal asset sizing can vary considerably depending on the target objective function. The system sees considerable emissions benefit from deploying additional wind generation and hydrogen storage to squeeze out the requirement for grid imports and maximise self-consumption. The challenge with reaching 100% energy independence is that it is observed to get almost exponentially more expensive due to the moments of high load and low intermittent generation that need to be balanced via long-term storage.

| Table 4.7: Energy | community | asset siz | zing at t | the optim | isation | extrema |
|-------------------|-----------|-----------|-----------|-----------|---------|---------|
|-------------------|-----------|-----------|-----------|-----------|---------|---------|

| Technology       | Lowest cost size   | Lowest emissions size |
|------------------|--------------------|-----------------------|
| PV Solar         | $63.0~\mathrm{kW}$ | $60.5~\mathrm{kW}$    |
| Wind Turbine(s)  | $28.2~\mathrm{kW}$ | $63.6~\mathrm{kW}$    |
| Battery          | 17.0  kWh          | $2.70~\mathrm{kWh}$   |
| Fuel Cell        | $10.5~\mathrm{kW}$ | $28.7~\mathrm{kW}$    |
| Electrolyser     | $12.3~\mathrm{kW}$ | $22.5~\mathrm{kW}$    |
| Hydrogen Storage | 1,312  kWh         | 4,365  kWh            |

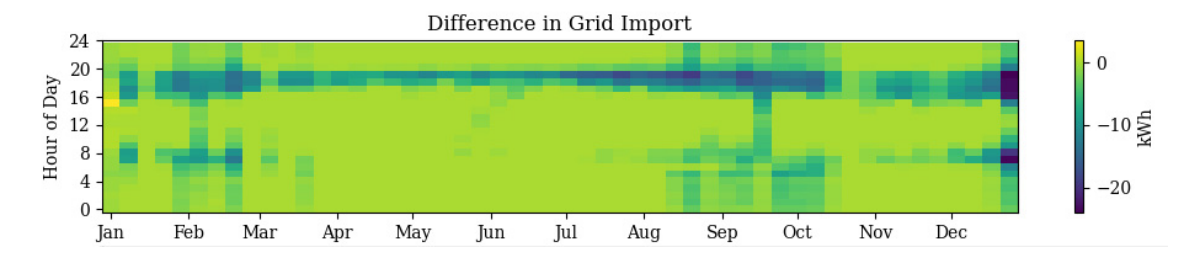


Figure 4.12: The absolute change in power import volume between the lowest cost and lowest emissions scenarios

Figure 4.12 shows the change in import volume in each hourly time slice between the two extrema scenarios. Negative values indicate more import and positive indicate less. It can be seen here that the system experiences particular moments or periods throughout the year when it is very challenging to ensure independence from the grid. When evaluated together with the power generation and storage heat maps in Figure 4.9, the lowest overall periods of energy independence are the periods of September-October and January-February. This is due to the lower wind and solar generation, and the lower hydrogen reserves after high levels of withdrawal over the peak summer period. This dynamic shows the importance of long-term grid storage for ensuring energy security, as well as that hydrogen could play a potential role in providing this service. There is also a pattern in grid requirement needed, particularly during the evening period throughout the year, which is commonly a peak time of high power demand, and hence more challenging and more costly to cover with storage availability.

A side-by-side comparison of the energy delivery dynamics between the scenarios brings further understanding to the points of highest stress throughout the year.

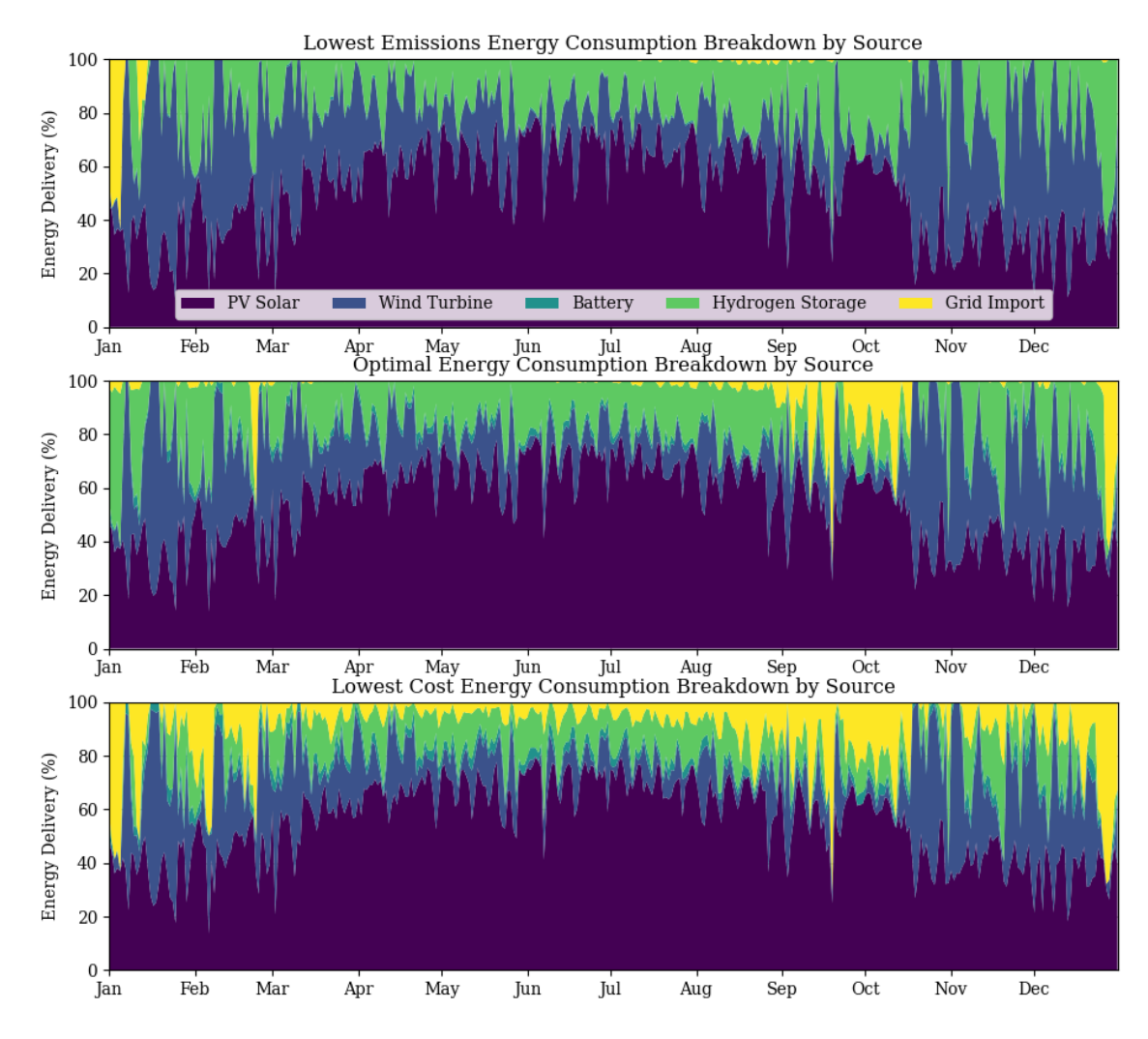


Figure 4.13: Percentage of demand delivered by each of the renewable asset classes over the three scenarios.

# 4.3 Sensitivity Scenarios

This section documents the results of the two main sensitivity scenarios that were tested as part of the multi-objective design optimisation of the REC in Formentera. There are understandably a number of potential configurations, both in terms of the physical system planning as well as the energy system integration and trading policy that might impact the ultimate performance of the energy community and the way in which it is managed by local stakeholders. The first of these scenario sensitivities tests the storage configuration options, and whether it is beneficial to hybridise the electrochemical battery and hydrogen technologies to maximise performance. The second, more policy driven scenario, is considering the energy trading regime of the community, and how the resulting optimal energy community design may in reality be driven differently if a competitive trading regime is implemented, as opposed to the standard cooperative sharing that has

been assumed.

### 4.3.1 Scenario Set 1: Battery and Hydrogen Storage Comparison

As detailed in the motivation of this section, the key contributor to the decarbonisation of the energy grid is the efficient utilisation of storage technologies. This sensitivity aims to answer the question of how much benefit does the hybridising battery and hydrogen storage bring to the daily operation of the REC. The hypothesis is that, under normal load conditions, the battery is able to provide short-term, high-power and quickly respond to demand, whereas the hydrogen system, with a lower round-trip efficiency, is advantageous when covering long durations of storage requirement.

For this test set-up, the model was configured such that only battery or hydrogen storage could be used independently. These were then run through the multi-objective optimisation routine to observe the impact and to compare with the hybrid result.

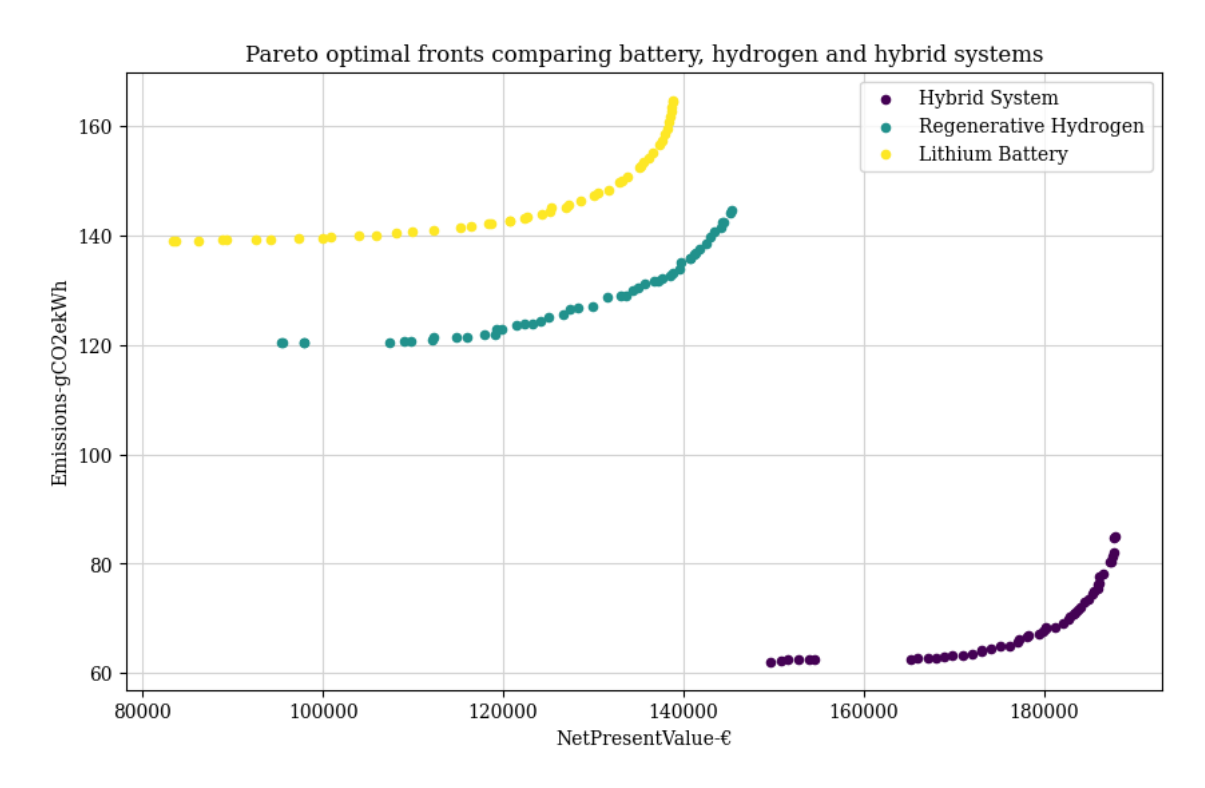


Figure 4.14: A Pareto front comparison between battery-only, hydrogen-only, and the hybrid storage system set up

Figure 4.14 illustrates the Pareto fronts produced with binary storage choices. For both cases, a single storage technology performs worse overall compared to the hybrid approach. The reason for this is again due to the nuanced relationship between storage and excess power generation throughout the model year, as well as the technical limitations of the individual technology.

Starting with the battery only scenario, the result indicates that this configuration produces the lowest overall performance. Breaking down the simulation dynamics, it is observed that the battery is generally being sized to perform well in providing response to high demand during or right after a balanced period between the load and the generation. This means that over a longer period, the battery suffers more from degradation and leakage current, and therefore does not perform as well in this role. Additionally, the embedded carbon of the battery, at 75 gCO<sub>2</sub>e/kWh, is much higher than that of the generation technologies and hydrogen storage over its lifetime. The ability to decarbonise to the same extent as the hybrid storage is significantly reduced when working alone, achieving the lowest emissions intensity of 140 gCO<sub>2</sub>e/kWh compared with the hybrid solution of less than 70 gCO<sub>2</sub>e/kWh.

The plot in Figure 4.15a shows the range of Pareto optimal design solutions when considering only battery as the storage option. As expected, the battery size is far higher than it otherwise would need to be if the hybridisation with hydrogen is considered, reaching over 90 kWh to ensure optimal performance in the low emissions objective. The limited factor in this case is the embedded carbon. In the cost optimal scenario, the optimisation elects to have almost no storage, to rely on the intermittent renewable to provide cost benefit. This significantly increases grid dependence and would suggest that the system has no means of balancing demand during daily and seasonal variation.

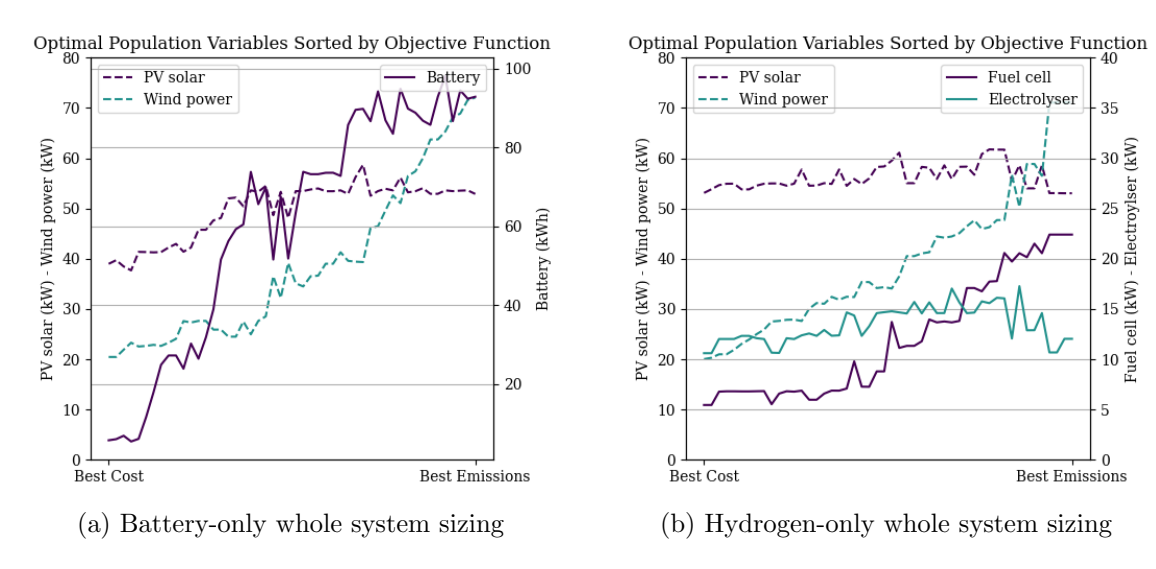


Figure 4.15: The optimal system sizing with binary storage choice ranging from best cost to best decarbonisation performance

The hydrogen-only scenario, by contrast, has a different set of reasons for why the performance is less than that of the hybrid system. While the fuel cell and electrolyser assets benefit from having lower embedded carbon, they are significantly more expensive, with an LCOE of 0.15~€/kWh compared to 0.10~€/kWh of the battery. The cost is therefore the first significant barrier.

The second limitation is due to the operational limits of the fuel cell and electrolyser. The battery is assumed to be able to charge and discharge energy up to twice its rated capacity, whereas the fuel cell and electrolysers are limited to their rated outputs. This indicates that, under normal operating conditions, the hydrogen storage system has far lower flexibility. This, combined with the higher capital and operational expenditure of the hydrogen technology, leads to a natural optimal limit for its deployment. In the hybrid scenario, the battery is able to fill the gaps in between the hydrogen system utilisation, such that the operational limits are less of a problem.

The graph in Figure 4.15b illustrates the optimal hydrogen only system sizing, where it can be observed that the optimisation routine actually deploys less hydrogen capacity than the hybrid result. This could be due to the fact that the hydrogen system working alone is less efficient overall at valley-filling gaps in renewable energy generation compared to the flexibility of the battery storage. The hydrogen assets also need more excess generation to make up for the inflexibility, adding to the cost and embedded carbon of the energy community.

Overall, the hybrid approach provides the best solution, due to the following observations:

- 1. The battery asset, while flexible, is not able to perform the same long duration storage duties as hydrogen due to current leakage that limits efficiency.
- 2. The battery model has a much higher embedded emissions originating from the manufacture of the lithium polymer chemistry.
- 3. While the hydrogen asset excels in long-duration storage, it is limit by its peak rated operation.
- 4. The fuel cell and the electrolyser assets both have a high capex and opex, leading to a higher levelised cost.

### 4.3.2 Scenario Set 2: REC Energy Trade Policies

The trading policy in the base REC design scenario is based on a friendly regime in which community members share a 'pool' of RES and storage assets. It is assumed, therefore, that the community is working together to minimise the total system cost and produce the best performing system. This scenario tests the case where competitiveness between community members is assumed. In this latter case, each member has their own generation asset and offers into the locally created energy market.

The social and economic implications sit at the heart of any REC policy design, so assessing the impact of different energy trading regimes is crucial. In the friendly trading regime, there is a better opportunity for energy equity among members, as all participants are sharing their assets, and it ensures that smaller, lower consumption members still benefit. However, there may be some additional complexity regarding the way in which

the community is governed and renumeration and reinvestment volumes are managed. By contrast, in the competitive market trading regime, members act far more independently, and it is up to their individual investment decision making to provide the optimal asset sizing. While this simplifies the management of the REC from the top-down, in reality it could lead to potentially unequal access to REC benefits, with larger, lower cost systems extracting higher value. The market is modelled as pay-as-cleared, where the price paid and received is equal to the marginal offer. This was done to simplify the model, and ensure scalability as it reflects the process of national wholesale markets, but could have the downside of providing significant profits for low cost participants.

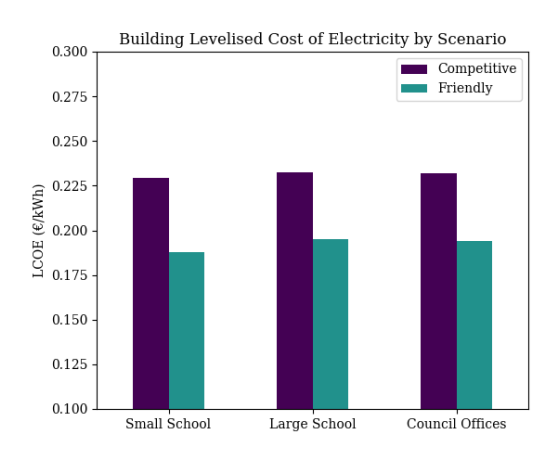
For this test, the community size was reduced from five to three members to simplify the approach, and rather than the option for both wind or solar generation, it is assumed that only PV solar is available to deploy. The three community members included are the large school, small school, and council offices, as shown in Figure 4.16.

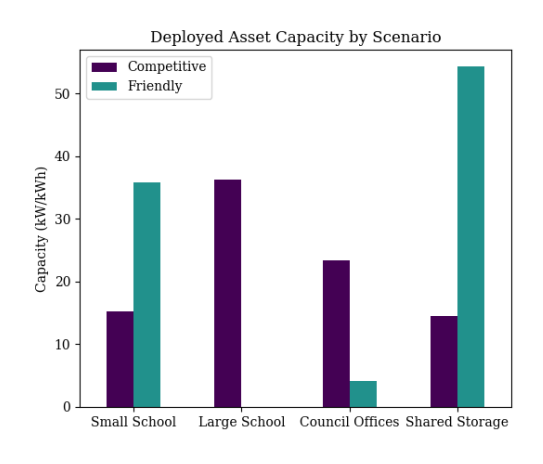


Figure 4.16: Reduced set of community buildings to test trading impacts

The optimisation for the sensitivity was switched to a single objective function to minimise cost, as this is primarily a test of market-driven decision-making by the model. The baseline 'friendly' case uses the standard lowest system cost objective, whereas the 'competitive' policy regime tries to reduce the total energy price including import costs. The results of the optimisation routine are shown in Figure 4.17a and 4.17b below:

It can be seen in Figure 4.17a that there is a notable reduction in LCOE across all buildings when the shared trading logic is used over the competitive local market simulation. The market model results in an LCOE of approximately 0.23~€/kWh across all three





- (a) Building Levelised Costs
- (b) Building and shared storage capacities

Figure 4.17: The impact on system sizing and LCOE performance under different local trading regimes.

buildings, reducing to between 0.19-0.20 €/kWh for the friendly trading case.

The main difference between the two is in the optimisation objective, in that the base scenario uses the system cost, so has an aggregated view of the entire system and is therefore aiming to achieve mutual benefit across all the community members. The competitive trading, by contrast, is only able to observe the recorded prices in each hour that the buildings are required to pay or receive in renumeration based on their position in the market merit order. If the member is lower in the order, they are able to sell their excess energy and receive the dual benefit of self-consumption and payment for sold volumes. However, if the members asset is further up the merit order, they risk their excess generation falling outside of the margin, not receiving renumeration, and damaging their perceived energy equity.

Based on this dynamic, it is more beneficial under the competitive scenario for the community members to maximise self-consumption and minimise the risk of grid export. This can be seen in the choice of asset size to be deployed, in that each building utilises a PV solar capacity that is proportional to their specific annual building load, and any excess generation is not as useful. This phenomenon may also explain the choice to deploy a lower capacity of storage compared with the baseline 'friendly' scenario, in that the availability of excess generation to be used for storage is lower, as the members are not as easily able to observe the global benefit for higher storage capacity due to the objective function used.

The baseline case by comparison deploys a much higher volume of PV solar generation and storage, as the global cost benefit is greater when considering the combined impact for all community members. It can be noted that, even though PV solar can be deployed across each building, the volumes are uneven. This is because the objective function considers all assets to be shared equally, and so the physical location of deployment is

not as important. The observed outcome could be crucial of this type of REC, as some buildings may have more or less space available to install generation and storage assets. An assumptions of shared, cooperatively owned systems could be of huge benefit to locations such as Formentera, or more built-up areas with strict environmental policies. Additionally, the total cost impact increases the visibility and utility of the battery energy storage system, which can be seen to increase in size considerably under the default trading scheme.

This scenario comparison shows that the choice of trading policy in an REC is not just an operational decision, but impacts the distribution of economic benefit. It has shown that the 'friendly' trading regime tends to promote greater equity and storage resilience, whereas competitive markets, as the principle suggests, can still maximise individual gain but at the cost of community energy sharing and fairness.

## 4.4 Results Uncertainty Analysis

Like all modelling techniques, a certain degree of uncertainty in the input assumptions exists, leading to varying results and outcomes. The acceptability of this uncertainty is ultimately a decision made by the REC developers, including the extent to which investment risk can be absorbed by the local community if the system was to provide a slightly different level of performance.

The factors that will impact uncertainty can be broadly categorised into the following groups:

- 1. System assets sizes and achievable performance
- 2. Uncertainty in asset investment needed and operational costs
- 3. External forces impacting the community

Starting with the system performance itself, variation in actual energy generated or stored, even if only minor, could have a measurable impact on the total system performance over its projected lifetime. Variations in manufacturing quality are commonly cited as contributing to different output efficiencies. For example, in the case of PV solar panels, a process of 'binning' is used to categorise the power output of the silcon-based cells with the aim to somewhat account for performance differentials, though cannot fully remove the uncertainty. Similarly for the battery and hydrogen storage technologies, small changes in the internal chemistries, age and condition could change the storage potential. For batteries, slight differences in electrolyte concentration, electrode thickness and condition of the contacts would affect the internal resistance, causing alternative responses to thermal variations and self-discharge rate. The PEMFC and AEM Electrolyser, while consisting of slightly alternate design characteristics, share the same fundamental principles internally. Differentials in the membrane thickness, the distribution of catalytic compounds, and exposure to different thermal and humidity conditions would all contribute to a change in the overall efficiency of the regenerative hydrogen storage system. Performance assumptions including the power output, efficiency, and derating factors have been used to represent uncertainty in performance.

Current and future uncertainty in technology costs is an intuitive factor to consider when designing a renewable system of this scale. The research conducted in this study has aimed to consider up-to-date technology costs data, but the renewable landscape is ever changing as new manufacturing methods and increasing market sizes will naturally move the cost assumptions. Accounting for future uncertainty is also challenging, due to the range of possible climate transition outcomes for a given country, or even localised area in which the REC is established. In this work, variations in the CAPEX and OPEX are both considered.

Additionally, the impact of differing weather conditions are tested on the optimal REC system design. Uncertainty in the weather conditions are handled separately to the design variable set, as they are less controllable and predictable compared to the impacts of manufacturing and system losses. Ten weather years from 2014 to 2023 are used to evaluate potential uncertainty produced, both in the current year and in future.

This section provides the resulting uncertainty based on two approaches. The first is a simple Monte Carlo analysis, which takes a random sample of the variation in inputs assumptions between the specified upper and lower limits, and provides a statistical analysis based on the impact of the uncertainty. The second approach goes a step further in decomposing the variance observed in the Monte Carlo assessment to implement a Sobol sensitivity analysis. The aim of Sobol is to quantify how much of the observed variation in the result can be attributed to a given variable, the implications of which could be hugely beneficial in understanding where uncertainty is having the biggest impact in the model.

The definition of the variation in each input used in the uncertainty analysis is given in Tables 3.7 to 3.10. Some definitions are informed by research into the relevant literature, manufacturer specifications, and discussions with industry experts, while all others are defined as a suitable standard error in based on the variable magnitude.

### 4.4.1 Parameter Uncertainty Propagation

The analysis was produced using a Monte Carlo analysis approach implemented in Python. Firstly, extreme case scenarios were produced where all model uncertainties were set to their best and worst possible outcomes in terms of cost and carbon reductions. The objective was to produce the total feasible range of uncertainty that could be measured using the REC model configuration. This is useful for understanding the bounds of the problem, and identifying the credibility of the central result based on the measured variation.

Figure 4.18 shows a recreation of the present value and payback curve of the central optimal scenario compared to the grid-only counterfactual, as in Figure 4.11. This new graph includes error bas to represent the maximum variation in returns measured based on the uncertainty definition. Also illustrated is the range of payback period expected given the propagation of this uncertainty throughout the lifetime of the REC system. In the worst case scenario, the REC investment results in a lifetime savings of 151,000€, compared to the central optimal case of 180,000€, or a potential downside investment risk of -16%. However, in the best case scenario, the system returns a net saving of 211,000€ over the 20 year period, or a percentage upside of 17%. The aggregate LCOE follows a similar trend, with a downside of 15% compared to the nominal 0.155 €/kWh cost, and an upside of -16% reduction. The NPV graph indicates that the difference in the payback period for the project could be delayed in excess of one year under the downside risk scenario, but on the other hand experience an advance of one year and three months in the upside case. A summary of the key performance indicators between scenarios is available

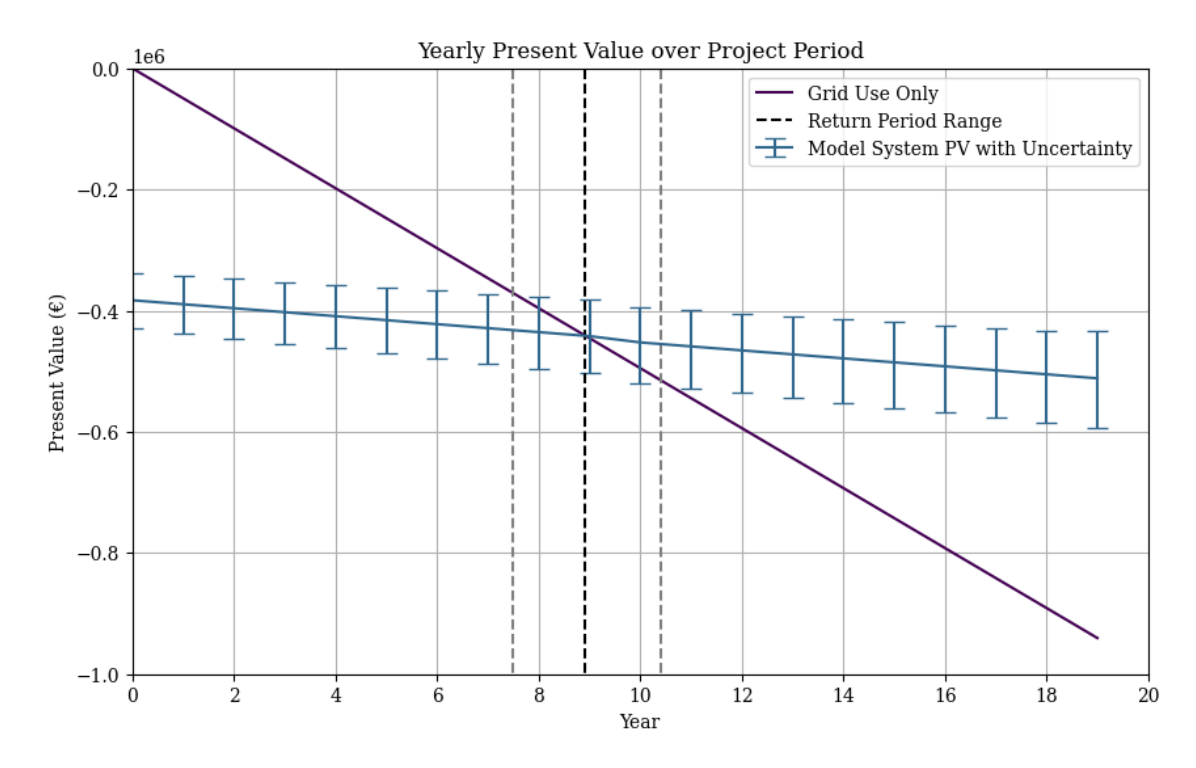


Figure 4.18: REC system NPV graph with the included maximum impact of parameter uncertainty.

in Table 4.8, where it can be noted that there is a similar variation in the system emissions intensity, with a symmetrical -19% reduction on the upside and 19% increase in carbon on the downside.

Table 4.8: Summary of key performance parameters considering the maximum degree of uncertainty propagation in the REC model.

| Parameter                                    | Worst Case | Central Optimal | Best Case |
|--|------------|-----------------|-----------|
| Savings (€)                                  | 151,000    | 180,000         | 221,000   |
| Aggregate LCOE (€/kWh)                       | 0.179      | 0.155           | 0.130     |
| Payback Period (years)                       | 10.4       | 8.9             | 7.5       |
| IRR (%)                                      | 8.6%       | 11.1%           | 14.3%     |
| Emissions Intensity (gCO <sub>2</sub> e/kWh) | 81.9       | 68.4            | 55.0      |

While it is useful to observe and understand the total range of possible uncertainty produced in the model, in reality the statistical likelihood (assuming a linear distribution of uncertainty in each parameter) of all values of a given parameter sample being at the lower or upper end of the uncertainty is extremely small. Understanding the impact of the parameter distribution would go a step further to shining a light on the true result of uncertainty in the model.

The Monte Carlo analysis was implemented by first defining the uncertainty range as

performed for the best and worst scenarios. The program would then randomly generate a parameter value within the set range for every input assumption, including asset efficiency, CAPEX, inflation rate, etc. This random sample group would then be applied to the model and simulated, storing the performance result. This process is repeated for 10,000 iterations to achieve a suitably large sample size. The results of the analysis are shown in Figures 4.19a and 4.19b.

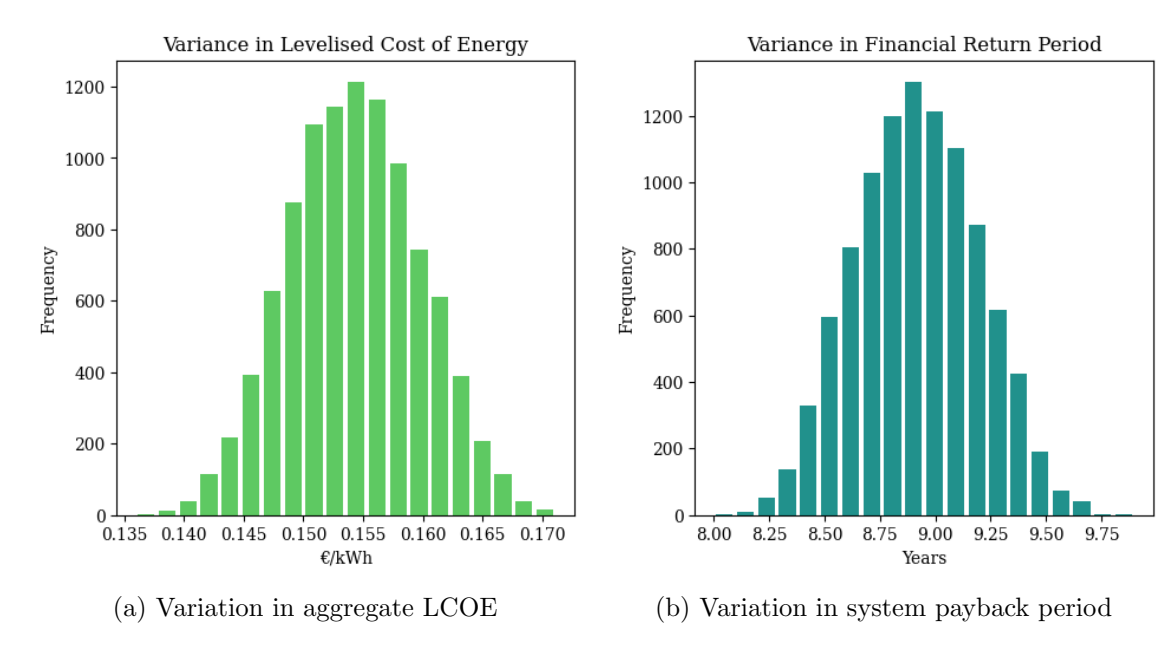


Figure 4.19: Uncertainty distribution of system LCOE and payback period resulting from the Monte Carlo assessment

As expected, even when observing the statistical distribution of uncertainty, the range of possible input assumption error has a measurable impact on the aggregate LCOE of the REC, though the expected variation is far smaller. The standard deviation reaches only 0.5 ct/kWh, with a 25th and 75th percentile of 0.150 €/kWh and 0.158 €/kWh, respectively. A similar difference is seen in the return periods, with an STD of 0.3 years of approximately 4 months, and a 25th and 75th percentile of 8.7 and 9.2 years, respectively. This result illustrates that, as expected, the true expectation of uncertainty in the result is far lower than when evaluated on absolute terms.

The emissions intensity, while a key performance metric in measuring the environmental effectiveness of the renewable energy community, has its own degree of uncertainty. The associated error margin is far smaller than that of the economic factors relative to the counterfactual grid-only scenario, with a spread between 63.1-73.7 gCO<sub>2</sub>e/kWh for the 25th and 75th percentile, respectively. This points to a firm ability of the system to provide valuable emissions reduction even when error is considered.

Assessing the uncertainty of an engineering project, such as this proposed implementation of an REC on the island of Formentera is critical for several reasons. An understanding of

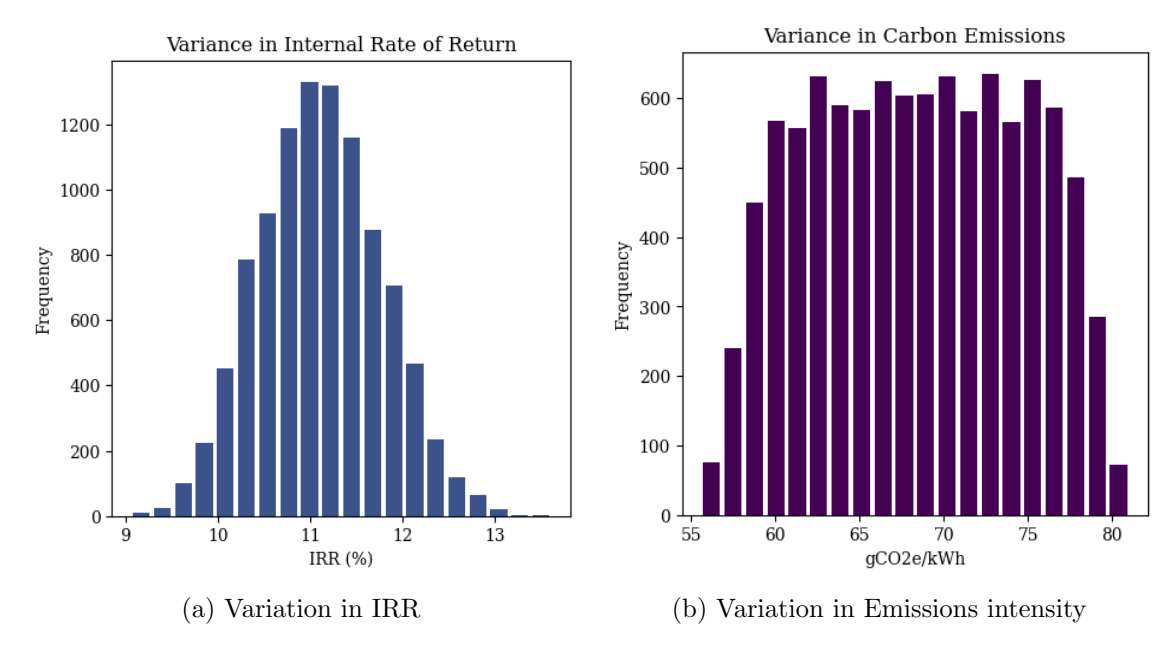


Figure 4.20: Uncertainty distribution of system LCOE and payback period resulting from the Monte Carlo assessment

modelling errors and how they may propagate is key to helping identify system weak points and improve resilience under stressful conditions. For example, evaluating whether the storage system will be available at a given time to provide power at a peak demand period would be vital to ensuring energy security. Chiefly, the error propagation approach used in this work is to support the costing and design decision-making processes, to help reduce financial risk for the energy community members and prevent costly project overruns. An assessment of uncertainty increases stakeholder confidence, ensuring due diligence has been conducted to understand the risks and building trust among all involved. These important elements will be discussed further within the context of the entire thesis in the following chapter.

#### Impact of weather conditions

In the previous uncertainty analysis, changes to the weather conditions are not included in the set of variable design parameters. There are a number of reasons for this decision.

First is the matter of predictability and variability. While variation exists within engineering designs, materials and manufacturing processes, they are often more predictable once the design parameters have been defined. Additionally, and in the case of PV solar panels for example, the performance can be statistically modelled based on historical data and performance. By contrast, weather conditions are complex, being driven by uncontrollable factors such as storms, extreme temperature events or even seismic activity. These factors are generally viewed as highly variable and challenging to predict over longer

time frames, often require their own modelling approaches.

This analysis illustrates the independent impact of changing the input weather year on the performance of the optimised REC system design. The NASA powerLARC database used in this work has historical weather data reaching back several years. To evaluate any impact on performance, the data for the 10 years between 2014 and 2023 were extracted and implemented in the model.

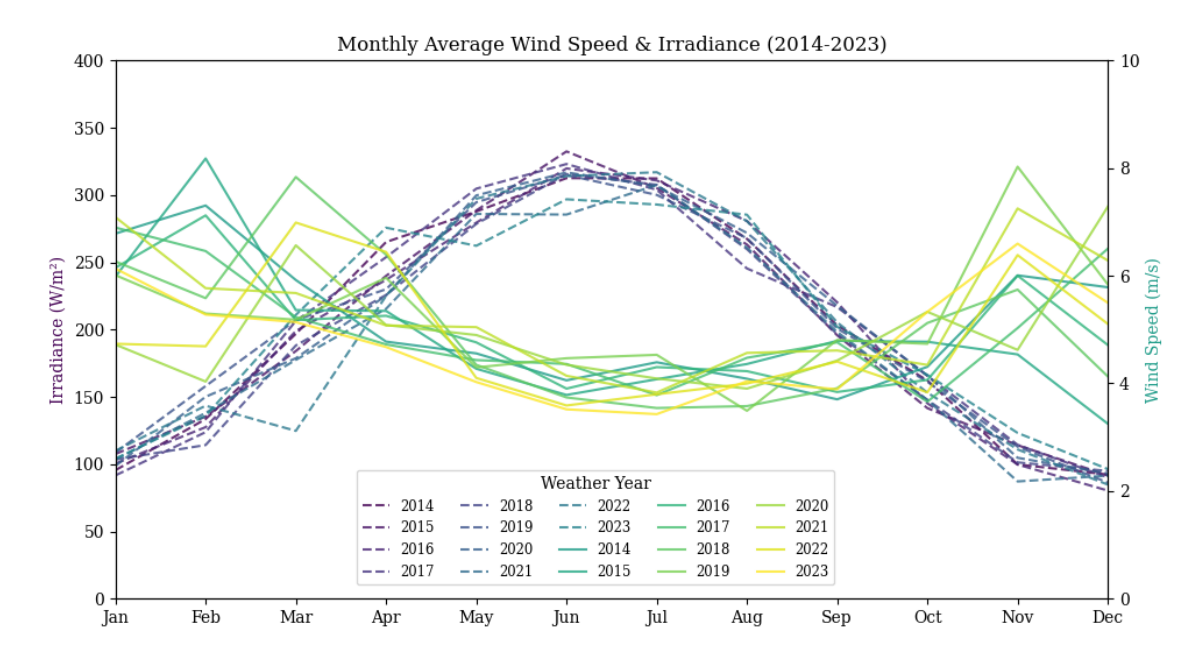


Figure 4.21: Average monthly solar irradiance and wind speed data by year from 2014-2023.

Figure 4.21 above displays the key average monthly meteorological input parameters (solar irradiance in W/m<sup>2</sup> and wind speed in m/s) over each weather year. While the solar irradiance remains relatively consistent throughout each weather year, the wind speed is far more variable. This is particularly noticeable in the autumn and winter months, when the average monthly wind speed could range from 3 m/s to over 8 m/s, easily doubling the expected monthly generation from the wind turbine. There are two years in the sample set when the solar irradiance in peak summer falls below 300 W/m<sup>2</sup>, but is relatively stable overall. The result suggests PV solar generation is likely of lower risk given the higher guarantee of stable output and returns compared to wind generation, which sees considerable variation over several years.

Figure 4.22 above contains a bar graph of the resulting LCOE and emissions intensity characteristics of the optimal system model based on the input weather year. The REC design was optimised using the weather data from 2023, so it is understandable why that year provides the best combined performance. If the system was optimised specifically for a different year, this would naturally present a different set, though still optimal, results. Interestingly, 2021 provides a slightly improved emissions intensity at 63 gCO<sub>2</sub>e/kWh

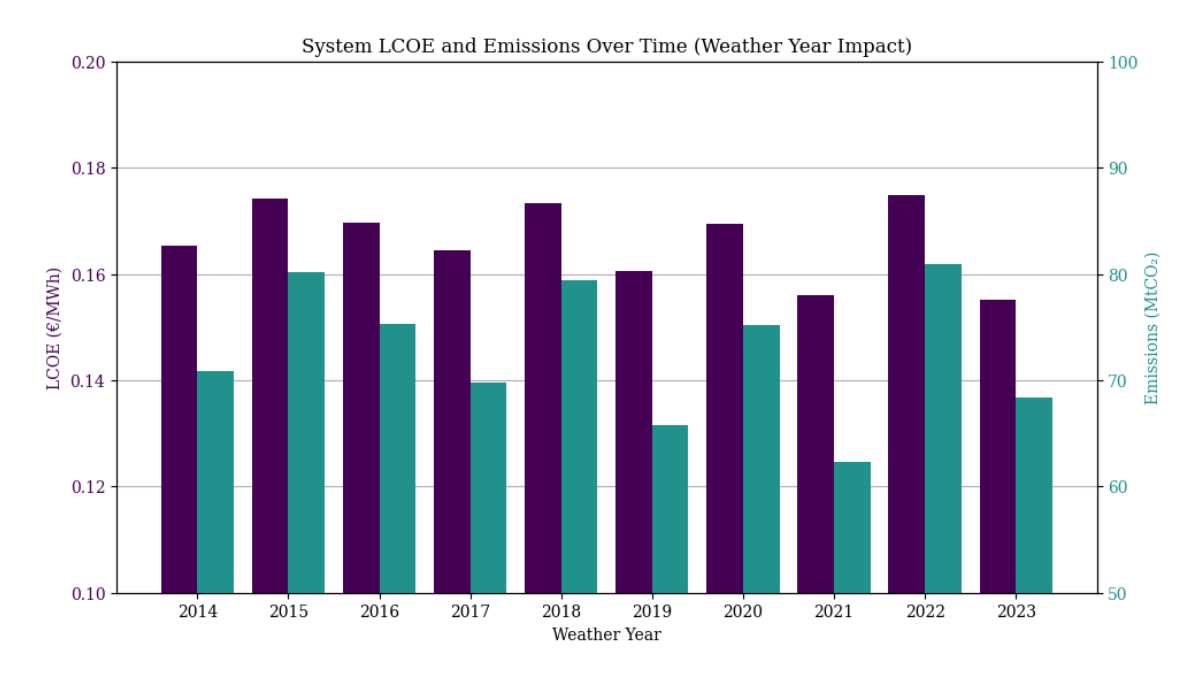


Figure 4.22: Resulting variation by weather year in the system LCOE and emissions intensity

compared to the reference 2023 at  $68~{\rm gCO_2e/kWh}$ . 2021 benefits from a marginally higher annual wind potential, which could have allowed the storage to operate more efficiently during times of lower power production, and hence lowering the total emissions of the system.

Overall, however, the system performance could worsen under different weather conditions. The mean LCOE overall all years is equal to 0.168~€/kWh; 8% higher than the optimal result based on 2023. The mean emissions intensity is  $72.8~\text{gCO}_2\text{e/kWh}$ , or 7% higher than nominal. The maximum extrema cases are even more broad, with 0.172~€/kWh reached in the weather years 2015 and 2022, and  $82~\text{gCO}_2\text{e/kWh}$  in the latter. This result shows the critical impact of weather uncertainty on the result, with analysis of how it should be incorporated into the system design process.

### 4.4.2 Sensitivity Analysis

The final build on the variance assessment approach was to conduct a sensitivity analysis using Sobol's method. As discussed in the previous section, Sobol is a commonly used tool in engineering design to estimate the importance of the input parameters and influence they have individually on the solution [191]. The Sobol method was chosen over other sensitivity analysis approaches, such as Morris and FAST, for its ability to manage non-linear relationships between parameters, and quantify their precise influence on the performance of the model. In this way, Sobol provides quantitative, policy-relevant results and robust actionable insights regarding potential design risks of the REC. Additionally,

Sobol naturally builds on the Monte Carlo simulations presented, so fits well with the overall methodology of this analysis. Using the approach, the most critical design variables can be identifying and closely controls such that their influence on the ultimate performance of the system can be minimised. Crucially for remote energy communities, they may have limited maintenance resources and monitoring equipment, so the ability to prioritise project tasks and understanding any weaknesses in the design before it is deployed could be hugely beneficial and may save cost in turn. The Sobol method was applied to the REC model using the open-source SALib [192, 193] for the selection of variables defined in Tables 3.7 to 3.10 across PV solar, wind, battery and hydrogen storage technologies, in addition to the global financial parameters.

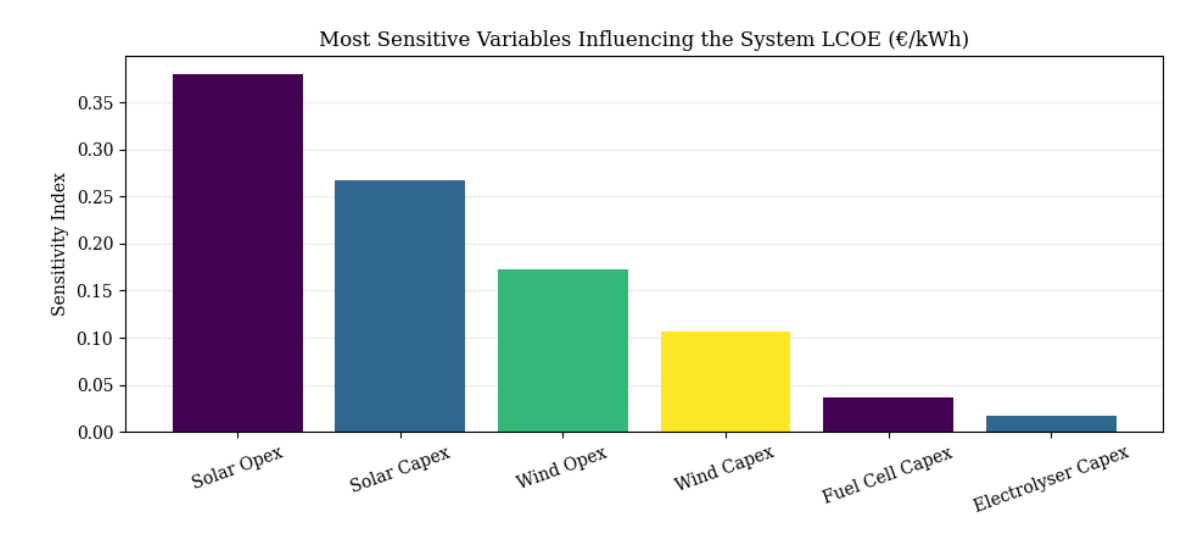


Figure 4.23: Ranking of the most sensitive variables contributing to the system LCOE derived via SOBOL method

Figure 4.23 shows a graph illustrating the top ranking most influential model variables on the resulting LCOE of the system. For the analysis, the normalised % contribution was limited to show only variables with a share above 2.5%, to avoid statistically insignificant results. It can be observed that, as somewhat expected, all of the most sensitive variables relate to the capital investment and operation of the renewable assets. However, a deeper analysis of the variable ranking reveals some interesting characteristics of the system.

The largest cost dependency in the renewable energy community is relating to the PV solar assets, with both the operational expenditure and capital investment ranking highest. This is due primarily to the PV solar being such a large portion of the total energy supply, which as shown in figure 4.13 provides approximately 50% of the total annual energy demand, and generates 164 MWh in the central optimal case. It is interesting to note that the Opex presents a higher level of cost risk to the system than the initial capital investment. This is likely due in part to the highly relative uncertainty in the assumptions provided. Literature sources on the topic, such as those presented in [124], [171] and [194]

result in a broad range of 15-45€ per kW in annual upkeep of the PV assets. A similar justification can be considered in the case of the wind assets, in which the opex and capex costs are the next most sensitive in influencing the levelised cost. Wind generation provides less of the building electricity demand overall at 68.4 MWh per year.

The final parameters that are above the sensitivity threshold are the capital investment costs for the hydrogen fuel cell and electrolyser. Hydrogen fuel cells are assumed to come at a high cost of 1,250€ in the nominal case, with an approximate uncertainty of 250€. Anion Exchange Membrane (AEM) electrolysis is assumed to be higher still, at 1,500€ per kW. Modelling results show that the regenerative hydrogen storage system provides 26.6 MWh of stored energy to the REC, or 16% of that which generated by the solar assets. It makes logical sense, therefore, that on a levelised cost basis, the hydrogen system combined would be 17% of the sensitivity share of the PV solar opex, which ranks highest in this analysis.

The battery storage system does not appear above the sensitivity threshold, likely because at just 4 MWh storage provided per year, changes in battery capex and opex may not be a high financial risk to the overall renewable energy community proposition.

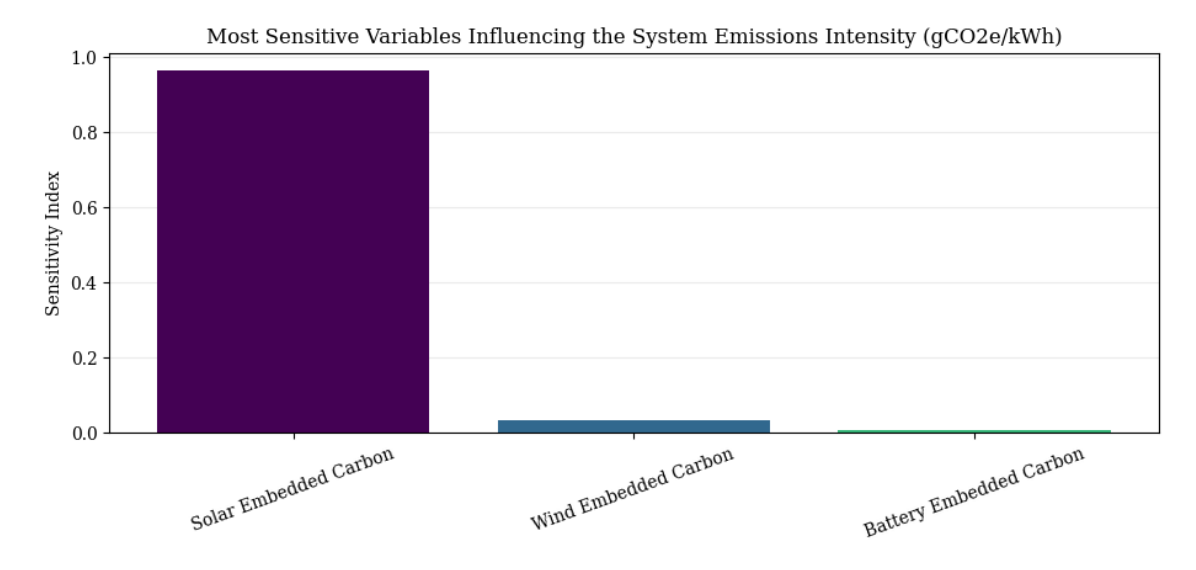


Figure 4.24: Most sensitive variables contributing to the system emissions intensity derived via SOBOL method

Figure 4.24 above shows a ranking of the most sensitive parameters to the resulting embedded and grid emissions intensity of the optimal system. Compared to the levelised cost result, the implications for increased emissions risk are far clearer. PV solar embedded carbon contributes the overwhelming majority of sensitivity to the result. When looking at the embedded carbon assumptions, the findings here make logical sense. Every kW rated capacity of PV solar, including the panels and balance of plant (BOP) equates to 1,826 kg of carbon dioxide equivalent. This assumption from literature is far higher than that of

a kW capacity of wind power, with 520 kg of carbon embedded during manufacture and distribution to installation site.

When accounting for the modelled load factors, PV solar is comparable to the emissions intensity carbon of the hydrogen ESS, at 35.2 and 33.3 gCO<sub>2</sub>e/kWh, respectively. The difference here is that, as discussed in the cost sensitivity, the high dependency on solar for the bulk of the REC operation generates a higher sensitivity to the result. By contrast, wind generation sees a far lower emissions intensity at just 15.2 gCO<sub>2</sub>e/kWh.

The Sobol sensitivity analysis highlights that there a several key risk factors to consider in specifying the RES design beyond seeking the optimal cost and environmental behaviour. Certain design parameters and variables are going to have a higher impact on the uncertainty on the system performance. Keeping track of project risks whilst aiming for the optimal trade off relationship between cost and decarbonisation could be hugely valuable in ensuring a viable energy transition for rural and remote communities such as the one on Formentera.

# Chapter 5

# Discussion

## 5.1 Research Context and Objectives

The overarching objective laid out in this study was to design, model and optimise a Renewable Energy Community (REC) for the benefit of remote and islanded locations.

Rural and geographically islanded communities face a number of energy related challenges, including energy security, higher average costs, and reliance on back-up fossil-based generation. These problems will likely compound over time as the energy transition continues in Europe towards net-zero, the risk of higher intermittency and energy security concerns mentioned will begin to compound. There is a risk, therefore, of these communities being left behind in the transition, being far from urban and industrial cores with better access to clean energy resources.

RECs, being an extension of the Virtual Power Plant (VPP) definition, offer an ability to minimise the transition risks that could impact rural living standards and maximise the benefits of clean energy resources for community members. However, existing research shows that their reach can be limited, driven by uncertain financial performance and limited policy support within the wider energy market frameworks that exist, leading to a significant societal nervousness around the proposed decentralised energy approach. A better understanding of these factors, as well as the design and optimisation of RECs could benefit hugely from comprehensive modelling and analysis.

A number of previous studies have explored renewable energy assets and their integration into energy communities. Managing the decentralised trading logic through Peer-to-Peer (P2P) contracts is also a major area of research, and is playing a key role in the commercial uptake of these systems.

Gaps remain, however, in the understanding of the performance of these systems. In particular, gauging the trade-off relationship between cost and decarbonisation, particularly under real world constraints and policy limitations. Furthermore, little research has been conducted into the performance uncertainty in these renewable assets and control systems,

and by extension the sensitivity of asset variation and influence on the REC system.

The results of this study show that, for cost reduction and decarbonisation of the energy supply, there is a benefit to introducing the conceptual REC design developed here to the case study location of Formentera, Spain. The outcome presented is in agreement with a number of supporting research pieces, that suggest RECs are a positive approach to engaging local citizens in decarbonisation activities while providing real cost benefit. Additionally, the results demonstrate a clear trade-off relationship between cost and decarbonisation; an area of study which has been explored very narrowly so far within the literature. The study also found that by hybridising the storage system by combining both electrochemical batteries and a regenerative hydrogen storage system, there is an overall net benefit for both cost and emissions reduction.

The policy definition laid out in the European RED-III documentation defines the concept of a renewable energy community, but the means of investment and payment distribution are more vague. This study considers both a cooperative approach to investment and returns, as well as a simple local energy market with a competitive element. The results show that a cooperative approach to financing and investment provides greater returns community-wide, a statement that further reinforces the findings from successful energy communities from the literature.

The use of Monte Carlo simulations and Sobol sensitivity analysis reveal two key outcomes. The first is that there is measurable uncertainty and the potential for error to propagate through the system, which if the system was to be deployed, should be managed appropriately. The second being that specific design parameters and asset variation can significantly impact overall performance, highlighting the need for robust planning and tighter controls on particular design decisions.

This work also innovates on existing REC models from the literature, including those presented by Kang et al. [112] and Fleischhacker et al. [195]. The former presents a comprehensive optimisation model, but only considers the cost element of the REC, without potential impact on emissions reductions. The multi-objective model in this work, considering both cost and emissions, opens up the potential for carbon-based policy support, such as carbon Contracts for Difference (CFDs) and other pricing structures. Both examples also do not consider the uncertainty in the results and sensitivity to particular input parameters, closing off further potential for specific analysis and contribution to future support structures. Other works also often use proprietary software, such as HOMER or MATLAB, which do not allow for the open-source scalability of Python-based development.

Table 5.1 below lists the research questions defined at the start of this work, how the research problem was addressed, and the key outcomes and novelty of the result.

From the answers to the research questions presented, the following novel contributions to the field are as follows:

| Table 5.1: Thes | is research | questions | with how | each | objective | has | been | ${\it addressed}$ | and t | he |
|-----------------|-------------|-----------|----------|------|-----------|-----|------|-------------------|-------|----|
| key outcomes    |             |           |          |      |           |     |      |                   |       |    |

| Research Question       | Approach to Addressing          | Key Outcomes                     |
|-------------------------|---------------------------------|----------------------------------|
| Summary                 |                                 |                                  |
| REC deployment for      | Literature and policy review;   | Design principles and deployment |
| rural islands           | contextual analysis using       | barriers identified; tailored    |
|                         | Formentera case study           | guidance for remote energy       |
|                         |                                 | transitions                      |
| Modelling REC           | Development of a multi-domain   | Validated, generalised model     |
| dynamics                | energy system model with real   | of REC operation under local     |
|                         | data inputs (demand, weather,   | conditions                       |
|                         | emissions)                      |                                  |
| Design exploration and  | Multi-objective optimisation    | Quantified trade-offs between    |
| optimisation            | using NSGA-II; comparison of    | cost and emissions; optimal      |
|                         | Pareto-optimal designs          | system configurations proposed   |
| Hybrid storage benefits | Scenario modelling of           | Hybrid storage shown to enhance  |
|                         | battery-only, hydrogen-only,    | flexibility and reduce unmet     |
|                         | and hybrid configurations       | demand and costs                 |
| Assess uncertainty      | Ran Monte Carlo simulations and | Identified key design risks and  |
| propagation and         | Sobol sensitivity analysis      | sensitive parameters to guide    |
| sensitivity             |                                 | future planning and support      |
|                         |                                 | potential policy development.    |

- 1. The modelling and optimisation of an REC design specifically for remote islanded communities, including the hybridisation of battery and hydrogen storage under a multiobjective framework.
- 2. The representation and comparison of two different decentralised energy trading mechanisms (cooperative and competitive trade).
- 3. The incorporation of uncertainty analysis through both Monte Carlo simulations and Sobol method to evaluate robustness of results, a key gap in current REC study.

Given the overall findings presented, the following sections will provide a detailed view at the each key insight, starting with the modelling results and validation, cost-to-emissions trade-off characteristics, asset sizing and hybrid storage configurations.

# 5.2 Multi-Objective Design Results

One of the most significant results presented in this work is the prevalence of the trade-off relationship between energy cost reductions and decarbonisation potential of the renewable energy community. The clear dichotomy has been the subject of several research pieces in the context of energy systems and microgrids, in which the objective is to achieve both a cost savings and reductions in carbon emissions.

To provide the lowest cost, similar studies employing either Mixed Integer Linear Programming (MILP) and hourly simulations with the NSGA-II procedure as adopted in this work have demonstrated a tendency towards reliance on diesel generation or other fossil options, including those presented by Zhu et al. [196] and Araoye et al. [197]. Reduction in emissions intensity alone is seldom considered a single objective function, as it can often result in overcapacity of renewable energy and storage asset capacities, leading to infeasibly large investment requirements. Results presented by Park et al. [198] and Schram et al. [199] are the closest comparison to a multi-objective optimisation considering cost and decarbonisation for an energy community. The difference in both these cases are that they do not consider the specific case for an islanded community in Europe, and that the specific definitions of the objective functions are different, which naturally will lead to alternative research outcomes in comparison to this work.

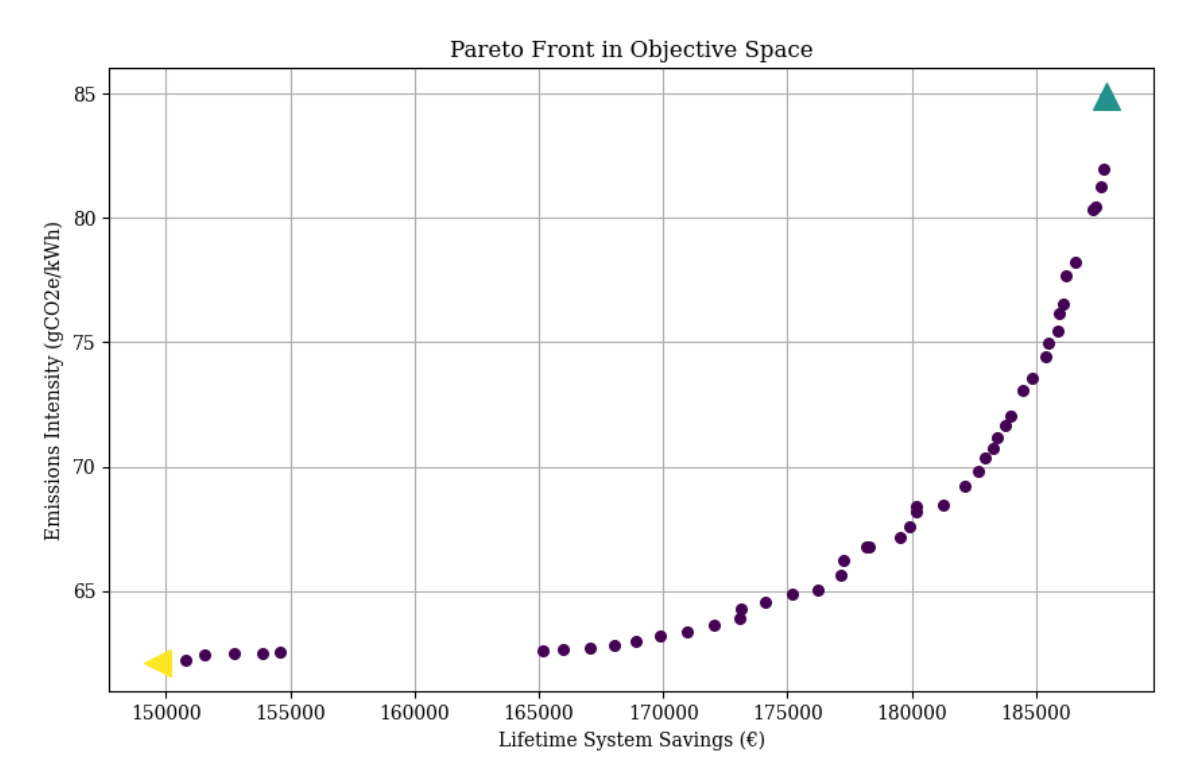


Figure 5.1: Pareto front resulting from the REC system multi-objective optimisation

The Pareto front in Figure 5.1 shows a similar overall trade-off relationship that has been observed in literature. When the system is small, a saving in both costs and emissions can be achieved, which occurs when the system savings are less than 155,000€, or to the left of the Pareto front. However, to achieve a higher level of carbon abatement, more investment has to be put in to oversize the system for events when additional renewable energy generation and storage are needed. Each component is modelled to consider the life cycle embedded carbon, which means that it is impossible to achieve zero carbon. Eventually the optimisation for lowest emissions results in an exponential level of investment, as seen on the right of the Pareto front.

This result is in line with other similar literary outcomes, including Schram et al. [199],

who showed that at emissions approaching less than 300 gCO<sub>2</sub>e/kWh the energy cost begins to climb at a faster rate exceeding 0.05 €/kWh. If the trend was to continue, the Pareto front would intersect 100 gCO<sub>2</sub>e/kWh close to 0.12 €/kWh, which would align with the outcomes of this work at 85 gCO<sub>2</sub>e/kWh and 0.15 €/kWh towards the top end of the front. Unlike this work from the literature, this study presented considers a rural location for the set up, and is not only deploying a battery storage system but is also optimising the sizing and utilisation of a hybridised regenerative hydrogen storage. The result from the literature is also considering the wholesale energy market cost, whereas the energy community created here is assumed to operate solely on the retail side, which can go some way to explain the difference in costs.

When considering the results for cost optimisation only, there exists a larger body of research to validate the outcomes of this work. Table 5.2 below summarises a range of Levelised Cost of Electricity (LCOE) results from literature with similar smart grid and renewable energy architectures, incorporating hydrogen storage where available. It should be noted that specific parameters such as renewable energy availability, local technology costs, and system sizing may induce uncertainty in the resulting total system LCOE. For example, locations with higher solar potential are naturally able to achieve a lower PV solar LCOE, and conversely, remote areas with high delivery and installation costs would experience higher project costs. The resulting average is 0.13 €/kWh, which is in good agreement with central economic and environmental trade-off case produced in this work.

Table 5.2: Comparison of the levelised cost of electricity results of similar hybrid hydrogen smart grid systems within the literature.

| Reference | Smart<br>grid<br>architecture | Assets       | Location    | Approx<br>Scale | LCOE<br>(€/kWh) |
|-----------|-------------------------------|--------------|-------------|-----------------|-----------------|
| This work | Energy                        | Solar, wind, | Formentera, | 100  kW         | 0.15            |
|           | community                     | battery/RHFC | Spain       |                 |                 |
| [190]     | DC                            | Solar,       | Sub-saharan | 100 kW          | 0.16            |
|           | microgrid                     | battery/RHFC | Africa      |                 |                 |
| [200]     | AC                            | Solar/wind,  | Morocco     | 1 MW            | 0.07            |
|           | microgrid                     | genset/RHFC  |             |                 |                 |
| [201]     | AC                            | Solar/wind,  | India       | 1  MW           | 0.08            |
|           | microgrid                     | hydrogen     |             |                 |                 |
| [202]     | Energy                        | Solar/wind,  | Ghana       | 100 kW          | 0.26            |
|           | community                     | battery/RHFC |             |                 |                 |
| [131]     | Energy                        | Solar/wind,  | Canada      | 1MW             | 0.08            |
|           | community                     | hydrogen     |             |                 |                 |

The goal for EU countries outlined in the Renewable Energy Direct (RED) policy documentation is to achieve an emissions reduction of 45% by 2030 against 1990 levels. The results here can be seen to align with this aspiration, as if the REC configuration was

to be constructed, the emissions reduction could be as high as 82% for the community, propelling them towards the future climate objectives of the region. Results from [199] and [195] suggest that RECs will eventually be vital to reducing energy costs and emissions for communities, and that modelling of these systems will assist urban planners and developers to consider the optimal trade-off arrangement between the two objective functions. The literature also consistently poses the argument that emissions reductions begin to diminish exponentially with increasing system scale, adding to the critical nature of such modelling exercises.

## 5.3 System Performance and Renewable Asset Sizing

The model was designed and created to optimally size and simulate, at an hourly granularity, the REC operation and ultimate performance over a one year period. A discounted financial evaluation is then used to determine the final system savings over the assumed 20-year lifespan. The model can efficiently size a range of renewable and storage assets for any scale of energy demand comprised of any number of REC members, and be located any where in the world. For this study, the location of Formentera was used, due to its unique set of climate and local energy security challenges, in addition to the varying degrees of renewable energy potential for wind and solar generation.

Once the Pareto front was derived using the NSGA-II algorithm, the SAW method found the theoretical optimal trade-off system between cost and carbon reduction. The results in Table 5.3 shows the central performance expectation between the best net savings and best net emissions configurations.

Table 5.3: Comparison REC configurations for extreme cases for net savings and decarbonisation potential compared with the chosen nominal case.

|                          | Best net savings | Central optimal | Best emissions savings |
|--------------------------|------------------|-----------------|------------------------|
| REC Delivered            | 81,000           | 153,000         | 160,000                |
| (kWh)                    |                  |                 |                        |
| Self-Consumption         | 51%              | 95%             | 99.9%                  |
| LCOE (€/kWh)             | 0.149            | 0.155           | 0.180                  |
| Net Savings (€)          | 188,000          | 180,000         | 150,000                |
| Simple Savings           | 10.1%            | 9.7%            | 8.3%                   |
| IRR                      | 14.1%            | 11.1%           | 7.4%                   |
| Payback Term (years)     | 7.7              | 8.9             | 11.6                   |
| Emissions $(gCO_2e/kWh)$ | 85               | 68              | 62                     |

The hourly simulation of the optimal REC system shows how the different assets contribute to meeting the building demand. PV solar, at 63 kW, provides the majority

of the renewable power, which is balanced during peak hours by the storage system. PV solar is the dominant generator due to its lower levelised cost of 0.06 €/kWh, in line with a recent International Renewable Energy Agency (IRENA) report on renewable costs [203]. Figure 4.9 shows how, during the solar peak hours, the excess energy is used to charge the battery to 100%, after which it can be discharged intermittently throughout the afternoon to smooth difference in the demand and generation curve.

Wind generation, at 40 kW, is sized smaller than the solar system, and with a lower capacity factor produces 42% less power annually at 68 MWh. Despite this, wind generation still has a key role to play in the REC operation. While the interplay between solar and battery exists to balance the short-term differences in supply and demand, the longer-term and seasonal fluctuations are handled by a combination of wind generation and regenerative hydrogen storage. When looking at Figure 4.7, one observation made was that the capacity of wind power and fuel cell output scale almost exactly. In the low cost scenario, the volumes are low, whereas in the low carbon scenario volumes climb to an optimally high level. It is clear that the additional wind generation is being used to produce hydrogen via electrolysis, which also grows in capacity with wind, which is then released when available. The fuel cell size has to scale because unlike the battery, output is limited to the rated size of the asset.

Research such as that presented in [204] evaluates the impact of co-locating battery and hydrogen Energy Storage System (ESS). While the result shows an increase in both cost savings and emissions when the system is hybridised, it does not seem to explain why this is the case, or how the roles of the storage assets are impacted. It is clear from this analysis that the hybrid ESS is taking on different roles based on the strengths and weaknesses of the technologies, with the batteries' ability to response with a high burst of power making it perfect for short-term, cost-effective smoothing, whereas regenerative hydrogen having limited output but greater capacity and lower embedded carbon, is more suited to seasonal duties.

### 5.4 Additional Scenarios

In addition to the main optimisation study, two sensitivity scenarios were also tested. The first of which was to test the performance impact of limiting the storage system to either battery or hydrogen technology. The main objective of this sensitivity was to confirm, in accordance with the literature, that the hybridisation approach to storage for decentralised energy communities would be the best option for optimal performance.

The result of the scenario testing showed a benefit to the hybridisation design route. In the case of the battery-only scenario, the system embedded carbon doubled from 68 gCO<sub>2</sub>e/kWh to over 140 gCO<sub>2</sub>e/kWh, illustrating the effect of the higher life cycle emissions of the technology compared to hydrogen which is at 75.5 gCO<sub>2</sub>e/kWh. The sub-optimal

seasonal role for batteries also limits the cost-effectiveness. Similarly, a hydrogen only system is also limited by the increased cost of the fuel cell and electrolyser components compared with battery. This result is also in line with the conclusions of [204] which demonstrated a reduction in cost and  $CO_2$  emissions by 46.2% and 11.3%, respectively, when a battery is introduced to the hydrogen storage system.

The second sensitivity was a simplified test of REC trading policy for the test design. The current policy of RECs is based on the RED II defined, which states that they must be distinct legal entities, with community members being able to participate voluntarily. The members can include anyone from individual households to local authorities and subject matter experts. The case study here considers the inclusion of a primary school, secondary school, community centre, council offices, and 3 residential buildings, representing a mixture of private entities and local government. The goal must be to maximise the environmental, social and economic welfare of those entities.

The policy does not, however, explicitly impose a financial structure to the REC, and how investments will be renumerated among members. The two main options are the cooperative approach where all investments and therefore assets are shared equally among members, and the other being the creation of a local market where members are in soft competition for the best energy price. The objective of this sensitivity was to test which policy configuration would be best for the REC in Formentera.

The results show that for all entities involved, the novel cooperative energy trading logic would provide the best outcome. Energy costs would be decreased by as much as 17% compared with the competitive trade, in which members are trying to size their individual installation such that their energy bids clear the demand margin in each hour.

While competitive energy trading is a widely researched topic among many related disciplines, such as those explored in [205], less has been dedicated to the direct comparison of competitive and non-competitive trading arrangements for this application present in this study. The cooperative trading logic implemented attempts to fairly distribute energy among the members such that all benefit equally, aligning with other cooperatives trading arrangements tested in literature. The conclusions of [206] demonstrated the benefits of a game theory-based coalition of entities provides the best overall system cost.

The topic of energy trading logic is a large and complex undertaking, and there are a number of limitations and improvements that could be applied to the implementation of the sensitivity scenario presented. Considering P2P energy trading, such as the investigation presented in [207] could be vital in ensuring a digital infrastructure for REC members to communicate and interact with the energy grid. Uncertainties around the financial policies of RECs allow for much research on this topic, and would certainly be a key contributor to the financial success of such a system.

## 5.5 Uncertainty and Sensitivity Analysis

The robustness of the REC optimal design results was subject to a Monte Carlo analysis as well as the implementation of the Sobol method to seek out the most sensitive parameters on the final performance outcome.

The Monte Carlo results concluded that based on the variable assumptions and uncertainty ranges, a possible deviation of 4% in total system LCOE between the 25th and 75th percentile values could be expected. This result is within the suitable uncertainty range of 5%. Similarly, the emissions deviation is considered up to 7% above and below the central value. This deviation is much larger, and is driven by the range of embedded carbon outcomes that are assumed from literature. The payback period is expected to by within 8.7-9.2 years within the 25th and 75th percentile, again giving confidence that the project would give reasonable returns even in a downside scenario.

Providing confidence of the project success is critical for a relatively novel endeavour such as implementing an REC. The local entities are far less likely to be able to expose themselves to financial risk, as many will be small local government entities and households. The REC therefore needs to prove it can perform as expected under the estimated level of uncertainty.

The Sobol method results in a number of interesting sensitivity outcomes. When considering the cost objective, the most sensitive parameters related to the investment costs of the assets, starting the PV solar as it was the largest total investment required for the REC, with the opex and capex variables at 37% and 26% of the total normalised sensitivity to system LCOE. This was then followed by the wind asset's opex and capex, which makes logical sense as it is the next largest asset in the system, at 17% and 11%, respectively. Finally, the regenerative hydrogen system, namely the fuel cell and electrolyser capexes were the final sensitivities that are within the significant range.

There is limited literature to compare with the uncertainty result applied to RECs, certainly when considering the hybrid storage solution. Research presented in [208] used an error propagation approach to assess the impact of parameter variability on system LCOE. The results showed that while asset investment costs were significant factors of uncertainty, the approach placed more significance on the external energy price and load factor variation, uncertainties that were not explicitly considered as part of this work. Because of this, the results illustrated are potentially wider range of uncertainty compared to that which as been presented in this work, but here the focus is more on internal design and asset decisional as opposed to external, uncontrollable forces that might affect the REC profitability.

This result highlights the need to identify these weak points in the system that could lead to great financial of environmental uncertainty, with greater care and attention can be placed on these areas in the planning and design process. The investment costs, maintenance requirements, and other high risk variables can have careful controls placed on them, such that their impact is minimised. This type of analysis could be of huge benefit to rural and islanded communities, as they may have limited resources to consider all possible elements of risk in the REC design.

## 5.6 Synthesis and Broader Implications of RECs

The results presented in this work demonstrated through system modelling that an REC is a viable solution to solving many of the climate and energy security related problems of rural and remote communities. Through the integration of multiple renewable assets, hybrid battery and hydrogen storage, flexible trading options, and a multi-objective design optimisation, the research laid out in this work outlines the building blocks for future clean energy systems for islands such as Formentera.

Initiatives such as Sonnen community, NEOMM and Repsol solar have represented various commercial strategies for maximising the positive impact of decentralised generation throughout Europe and propel those markets towards net-zero. NEOMM in particular, represents an approach to cooperative participation that promotes participation in which community members have successfully transitioned to renewable technology, with less reliance on the grid, and a measurable reduction in carbon emissions as a result.

The model presented in this work assumes a baseline grid emissions intensity in the first year of 325 gCO<sub>2</sub>e/kWh, estimated based on power market data from Spanish operator REE. The emissions intensity is reduced to 68 gCO<sub>2</sub>e/kWh in the central optimal design case. Given the annual build load of 165 MWh, this represents an emissions reduction of 42.4 tonnes of CO<sub>2</sub> in the first year of operation, equal the annual output of 27 petrol vehicles (assuming an EU average emissions 105 gCO<sub>2</sub>/km [209] and 15,000 km driven per year), or the equivalent emissions stored in one hectare of forest. It also suggests a potential 79% reduction in emissions. The system also achieved an LCOE of 0.155 €/kWh, far lower than the assumed average retail grid price of 0.30 €/kWh as of 2024, and a net lifetime saving of 180,000€.

The results confirm along with leading literature that flexible, co-located storage is the optimal choice to provide the best annual performance for the system. The combined battery and hydrogen ESS take on different roles and trade-off each others' weaknesses to ensure the best outcome. The battery is best suited to smoothing out short-term, hourly imbalances in supply and demand, whereas the hydrogen system excels at long-term, seasonal storage duties, particularly in months with higher excess renewable generation.

The concept of cooperative energy trading between community members has the possibility to further enhance energy equity within rural locations. There is limited literature on specific policies used for RECs, this is a research area that will continue to play a key role in the commercial viability and attractiveness of RECs in the future. Policy

makers should therefore shape REC regulations based on the shared goals of all members within the community, and incentivises collective investment in decentralised assets in addition to private, small-scale generation. The access to digital monitoring and visibility will also play a key part in the success of these prosumer community clusters, as it will allow grid operators to plan the network more effectively, and possibly reduce investment in local grid upgrades where it would no longer be needed.

The flexibility and breadth of potential scenarios that could be tested using the REC model produced in this work could have implications for a number of stakeholders, the key groups of which would be the REC developers/owners, the local network operators, and government policy makers.

The main utility for *REC developers* is the ability to set up the local community environment based on real demand assumptions and technology choices, then estimate the potential cost and emissions savings through various optimal design strategies. The operator could then choose to trade-off emissions reduction with available investment to design the best possible REC for the given situation. The sensitivity analysis can also be used to track higher risk investments and assets that are most likely to impact performance. The developers can also communicate the benefits of participation to the local community before installing and testing real equipment.

For *local network operators*, RECs could significantly improve visibility of decentralised generation assets, providing them with tools to better plan network maintenance and upgrades. The virtual monitoring of the different REC assets can be shared with the operators in real time so that they can make optimal choices relating to electricity delivery to minimise costs. As discussed in the literature review of barriers for VPPs, this is one of the biggest challenges facing network operation with increasing intermittent renewables.

For local government and policy makers, the capabilities of the REC model could have significant implications for future clean, decentralised network planning and support. The current policy and regulation surrounding RECs is limited but growing in different European countries as popularity increases. The results of this work point to the potential for a number of policy recommendations and support mechanisms that could accelerate the uptake of RECs in remote and rural locations. In addition to the trading arrangements, the analysis presented in this work shows that the REC system cost is particularly sensitive to the capital and operational costs of the renewable assets, as well as the discount rate of the system. A key policy could encourage renewable investment by providing targeted subsidies for technology that would be used to create an REC, easing the investment risk imposed by wind and solar requirements. Additionally, the benefits of hybridising batteries with regenerative suggest the potential for further subsidies for hydrogen generation and storage technology. As of 2024, hydrogen fuel cell and electrolyser costs remain high after many years of continued development, presenting another risk to the success of the system. And finally, while flexible loads were not considered as part of this work, it was clear that the

ability to satisfy high demand in all parts of the year was the most costly challenge for the REC, with investment costs increasing exponentially as grid independence tended towards 100%. Therefore, incentives for demand shedding within community members at times of high demand could considerable reduce overall costs whilst gaining all the emissions reduction benefits of the REC, which could be achieved through specialised tariff designs for those with flexible loads. Most of all, funding support for environmental schemes, local land protection, and supporting local skilled roles in renewable technology maintenance should all be considered potential REC policies to remove the barriers to implementation for rural members.

Institutional shifts in the way that decentralised renewables are perceived and managed would, by necessity, need to change in order for the uptake of energy communities to accelerate in future. Community-based governing structures establishing cooperative energy sharing models would provide the overall steer. These non-profit governing bodies would manage public engagement, such as town hall meetings and marketing through local media, as well as memberships and voting rights. They would also need to offer a fully transparent financial management process and reinvestment decision-making process. In Europe, interpretation of the REC definition from the RED-II documentation is growing, but more needs to be done to accelerate the regulatory frameworks and legal recognition of such systems. Operators should also simplify the process of grid connection and installation of new renewable assets. Utility company should also allow for collective self-consumption, and in return can be provided visibility on the generation and consumption activities to manage the local grid more effectively. Finally, funding and grant platforms should be set up to allow early-stage development of RECs, moving into loan arrangements for more mature community frameworks. A significant issue identified is access to technical skills needed to operate and maintain the assets. Therefore, setting up funds for local citizens to retrain and work towards qualifications in renewable systems engineering would also be beneficial. This will also tie the local community closer to the ownership and daily running of the new assets, fostering a sense of independence.

This view is supported by research presented by Taffuri et al. [210], who outline the importance of visibility, transparency and local education surrounding RECs such that the potential members understand the benefits and minimise worries regarding costs and energy security. As detailed by Slee [211], energy communities in Scotland are eligible to receive up to 100% in grant funding towards community-led renewable projects. A common issue raised in the literature is the risk of over-commercialisation of the system, where larger corporate entities may be able to own and sell REC services at a premium to those willing to pay. While this socio-political characteristic will always play a role in the energy industry, minimising the involvement of private investment and ensuring community-owned energy is incentivised will preserve the benefits and cost reductions found in this study.

If the governing frameworks and regulation surrounding RECs is successful, an ever-present

issue is the public perception of renewables in rural and aesthetic areas. In addition to transparent governing and community engagement, framing the REC around shared ownership and explaining both the risks and benefits will help to provide clarity to those with fears that the new technology may impact the economy and identity of the area. Community involvement, and in particular providing training and qualifications to local people so that they are able to manage the system will support the sense of maintained community and natural incorporation of the REC into the heart of rural identity.

In summary, the work presented here provides a novel contribution to the research field of REC through a model capable of providing the cost and environmentally optimal REC system design for remote and rural locations. The additional scenario explored and uncertainty analysis support the case for further research into community engagement models and targeted support to facilitate the growth in this promising field of energy and resources. The modelling framework is completely modular and can be easily adapted to other locations, allowing for numerous combinations of building loads, community member types, and renewable assets to be tested, unlocking a host of potential policy support programs and ultimately could assist those considering investing in a community-owned energy system. To make it more accessible to non-technical stakeholders, a simple user interface could be developed, allowing users to input their location, load and generation parameters, and allow the model to optimise for their individual REC case. The model does not use any proprietary software, and was instead developed in Python such that it can remain open-source and available to potential use and further development in the future.

# Chapter 6

# Conclusions

## 6.1 Main Conclusions of this Study

This thesis lays out the application of modelling and optimisation of decentralised renewable energy systems for rural and islanded communities. The market for decentralised renewables has continued to increase in recently years as the impacts of climate, particularly on remote citizens, begins to become a reality for many in Europe and the wider globe. Europe's policies to achieve its ambitious climate objective of a 65% reduction in emissions by 2030 are, while supportive of urban areas and connected communities, at risk of leaving rural communities and islanded locations behind in the transition. This hypothesis is due in part to lower investment, infrastructure visibility, and higher energy costs compared with larger population centres. This discussion comes at an interesting time for Europe as policymakers work to facilitate the potential benefits of aggregating decentralised renewables, one such method being the REC. The steady cost reduction in PV solar and wind power as seen over the past years has also accelerated growth in the decentralised energy sector. The rise of cost-effective battery storage and hydrogen technology is set to make considerable impact on how energy is stored and transported as a vector.

The main objective for this work was to investigate the economic and environmental performance of a Renewable Energy Community (REC) for the case study location of the island of Formentera, Spain. With a low population and economy heavily reliant on tourism, Formentera presents an archetypal community that may struggle in future to decarbonise its economic activities and support local people. Critical obstacles to the implementation of Virtual Power Plants (VPPs) were evaluated from the literature, leading to the choice to focus on research and analysis of RECs to solve the novel problem laid out.

The case study system was defined based on data collected of the local climate and building loads that would take part in the REC. The renewable assets consisted of distributed photovoltaic (PV) solar, small-scale wind turbines, and a hybridised battery and hydrogen storage system. The results from this study show that there is an inherent

trade-off relationship between cost reduction and ability to decarbonise the energy system. By using a model built in Python, several different economic and environmental scenarios can be assessed. The implementation of a multi-objective algorithm gives potential system designers and policymakers a range of possible solutions. In this case, the optimal design results in a Levelised Cost of Electricity (LCOE) of  $0.16 \, €/kWh$ , a project Internal Rate of Return (IRR) of 11.1% and a return period of 8.9 years. Greenhouse gas emissions were reduced by 79% in the first year of installation to  $68 \, gCO_{2}e/kWh$ . Analysis of similar models from the literature are in agreement with these results, which in the case of LCOE varies from  $0.08-0.26 \, €/kWh$  between different energy community and microgrid projects.

The uncertainty and sensitivity analysis revealed that there is measurable investment risk involved with the adoption of the optimal REC design, though these risks can be kept to a minimum by closely tracking the most sensitive design and decision variables, including the solar and wind capital and operational costs.

Additional scenarios tested point to significant advantages of a co-located battery and hydrogen storage system, as the combined technologies are able to compensate for each other's weaknesses, producing a 19% and 5% improvement in both emissions intensity and net savings of the system, respectively, compared to a hydrogen-only alternative.

The policy environment for decentralised renewable is constantly evolving. The abilities of the novel REC modelling framework could be used by policy makers to guide targeted incentives for deployment and protect participant from the most significant investment and operational risks. Crucially, the modelling presented in this thesis provides a quantitative guide for potential developers, government entities, and network operators on how to trade-off system cost with positive climate impact to produce the optimal REC system for a given rural and remote scenario for the benefit of the local people.

The results of this work are already being applied in a commercial setting. The core model, named the 'Smart Planning Tool', is currently being tested as part of a wider energy system modelling and optimisation software package to help key stakeholders understanding the benefits of localised clean energy deployment.

### 6.2 Recommendations for Further Work

While the flexibility and adaptability of the modelling framework has been explored in detail, there are some limitations and topics for further investigation in this field.

The operational relationship between demand requirement, generation and storage are relatively fixed in the model presented, in that the demand is not able to flex in to reduce system stress. There has been considerable research into flexible loads as a vehicle to reduce peak demand and system costs. Therefore, its implementation into a REC system could be hugely beneficial.

The approach and modelling parameters used are novel in their design, such that there

is little research and data to directly validate performance. Ideally, a system designed using this modelling framework would be deployed and tested in the field. Accompanying laboratory validation may also be used to guide the parameterisation of the renewable assets further, and could improve the accuracy of the result. Particularly in the case of the storage systems, the models were simplified to trade-off computational complexity and ensure the program remains usable. Validating the storage performance, reliability, and interactions with generation should be prioritised in future work. Particularly in the case of hydrogen which gained significant traction in the past years, but as of 2024 is facing significant investment and project hurdles in Europe. As part of this work, plans were made to validate the model performance against a real world deployment of the REC system. While a complete validation was not achievable in this study, reference materials regarding the set up and function of the REC field test system is included in Appendix A.1.

Lastly, this thesis evaluated simple implementations of energy trading policy to assess the impact of cooperative and competitive trading regimes. Future research should build on this further, perhaps through the implementation of a live Peer-to-Peer (P2P) trading logic to better analyse the benefits to individual community members. Additional to the trading policy, the model could also be improved by varying the grid parameters with time, such as the retail power price and grid emissions intensity, and how these might evolve in future. Different policy support mechanisms including feed-in-tariffs and investment grants could then be dynamically tested depending on the expected emissions reductions achieved and size of community served over a given period, and other qualification criteria, tying the analysis in with potential government support mechanisms for such an REC system.

From a model development perspective, creating the modularity to allow for flexible load testing and optimisation would be a high priority. Following on from this would be the integration of exogenous price signals for other local market services, such as local grid balancing, allowing for more value to be extracted from the REC. Finally, additional modularity to test other energy trading regimes, as these are vital to the socio-economic performance and energy equity of the system.

Further robust assessment of the external factors challenging and supporting a specific REC deployment opportunity could improve knowledge precision regarding the input assumptions. Rigorous analysis of the benefits of such system for remote and rural locations will ensure buy-in support from all related stakeholders, and most importantly, clean renewable energy for the future.

# References

- [1] The European Parliament, "Directive (eu) 2018/2021: On the promotion of the use of energy from renewable sources," Official Journal of the European Union, vol. 328, pp. 82–209, 2018.
- [2] T. Stankovic, J. Hovi, and T. Skodvin, "The paris agreement's inherent tension between ambition and compliance," *Humanities and Social Sciences Communications*, vol. 10, no. 1, p. 550, 2023.
- [3] International Energy Agency. "World energy outlook 2024." (2024), [Online]. Available: https://www.iea.org/reports/world-energy-outlook-2024.
- [4] United Nations Secretariat, Technical dialogue of the first global stocktake. synthesis report by the co-facilitators on the technical dialogue, United Arab Emirates, 2023. [Online]. Available: https://unfccc.int/documents/631600.
- [5] W. Hayes, 2023 uk greenhouse gas emissions provisional figures, London, UK, 2022. [Online]. Available: https://assets.publishing.service.gov.uk/media/6604460f91a320001a82b0fd/uk-greenhouse-gas-emissions-provisional-figures-statistical-release-2023.pdf.
- [6] European Commission Secretariat, Factsheet on 2014-2020 Rural Development Programme for Poland. Brussels, Belgium: European Commission, 2020.
- [7] European Commission Secretariat, Climate Action Progress Report Poland Profile 2023. Brussels, Belgium: European Commission, 2023.
- [8] Department for Business, Energy and Industrial Strategy, Uk energy in brief 2020, en, London, UK, 2020. [Online]. Available: https://assets.publishing.service.gov.uk/media/5f2043b4e90e071a56f934d4/UK\_Energy\_in\_Brief\_2020.pdf.
- [9] D. Candra, K. Hartmann, and M. Nelles, "Economic optimal implementation of virtual power plants in the german power market," en, *Energies*, vol. 11, no. 9, p. 2365, 2018.
- [10] S. Ahmed, A. Ali, and A. D'Angola, "A review of renewable energy communities: Concepts, scope, progress, challenges, and recommendations," *Sustainability*, vol. 16, p. 17499, 2024.

- [11] European Commission, *Prices and Costs of EU Energy*, en. Brussels, Belgium: European Commission, 2016.
- [12] D. Pudjianto, C. Ramsay, and G. Strbac, "Virtual power plant and system integration of distributed energy resources," en, *Renewable Power Generation*, *IET*, vol. 1, no. 1, pp. 10–16, 2007.
- [13] A. Marinescu, C. Harris, I. Dusparic, V. Cahill, and S. Clarke, "A hybrid approach to very small scale electrical demand forecasting," en, in *ISGT 2014*, Washington, DC, 2014.
- [14] A. Pyrgou, A. Kylili, and P. Fokaides, "The future of the feed-in tariff (fit) scheme in europe: The case of photovoltaics," en, *Energy Policy*, vol. 95, pp. 94–102, 2016.
- [15] Public-Private-Partnership Research Centre, Power purchase agreements (ppas) and energy purchase agreements (epas), Online, Aug. 2021. [Online]. Available: https://ppp.worldbank.org/public-private-partnership/sector/energy/energy-power-agreements/power-purchase-agreements..
- [16] A. Andersen, T. Erge, C. Sauer, T. Siewierski, and G. Romanovsky, "Massig: 'how to start entering the big markets as a small player'," en, in *EU-project MASSIG*, 2010.
- [17] E. Kardakos, C. Simoglou, and A. Bakirtzis, "Optimal offering strategy of a virtual power plant: A stochastic bi-level approach," en, *IEEE Transactions on the Smart Grid*, vol. 7, no. 2, pp. 792–806, 2016.
- [18] M. Barbero, C. Corchero, L. Casals, L. Igualada, and F.-J. Heredia, "Critical evaluation of european balancing markets to enable the participation of demand aggregators," en, *Applied Energy*, vol. 264, p. 114707, 2020.
- [19] D. Schwabeneder, C. Corinaldesi, G. Lettner, and H. Auer, "Business cases of aggregated flexibilities in multiple electricity markets in a european market design," en, *Energy Conversion and Management*, vol. 230, p. 113783, 2021.
- [20] P. Bertoldi, P. Zancanella, and B. Boza-Kiss, Demand Response status in EU Member States, en. JRC Science for Policy Report, 2016.
- [21] G. Plancke, K. Vos, and R. Belmans, "Virtual power plants: Definition, applications and barriers to the implementation in the distribution system," en, in *International Conference on the European Energy Market*, 2015.
- [22] C. Zhang, Y. Ding, N. Nordentoft, P. Pinson, and J. Østergaard, "Flech: A danish market solution for dso congestion management through der flexibility services," fr, J. Mod. Power Syst. Clean Energy, vol. 2, no. 2, pp. 126–133, 2014.

- [23] Y. Zhou, J. Wu, G. Song, and C. Long, "Framework design and optimal bidding strategy for ancillary service provision from a peer-to-peer energy trading community," en, *Applied Energy*, vol. 278, p. 115 671, 2020.
- [24] E. Gui and I. Macgill, "Typology of future clean energy communities: An exploratory structure, opportunities, and challenges," en, *Energy Research and Social Science*, vol. 35, pp. 94–107, 2018.
- [25] European Commission, "Regulation (eu) 2019/943 'on the internal market for electricity'," en, Official Journal of the European Union, vol. 158, pp. 54–124, 2019.
- [26] European Commission, "Directive (eu) 2019-944 on common rules for the internal market for electricity and amending directive 2012/27/eu," en, Official Journal of the European Union, vol. 158, pp. 125–199, 2019.
- [27] T. To, M. Heleno, and A. Valenzuela, "Risk-constrained multi-period investment model for distributed energy resources considering technology costs and regulatory uncertainties," *Applied Energy*, vol. 319, p. 119210, 2022.
- [28] B. Moya, R. Moreno, S. Püschel-Løvengreen, A. M. Costa, and P. Mancarella, "Uncertainty representation in investment planning of low-carbon power systems," *Electric Power Systems Research*, vol. 212, p. 108470, 2022.
- [29] D. Parra, L. Valverde, J. Pino, and M. Patel, "A review on the role, cost and value of hydrogen energy systems for deep decarbonisation," en, *Renewable and Sustainable Energy Reviews*, vol. 101, pp. 279–294, 2019.
- [30] P. Li, Z. Wang, N. Wang, W. Yang, M. Li, X. Zhou, Y. Yin, J. Wang, and T. Guo, "Stochastic robust optimal operation of community integrated energy system based on integrated demand response," en, *International Journal of Electrical Power and Energy Systems*, vol. 128, p. 106 735, 2021.
- [31] Y. Xia, Q. Xu, H. Qian, W. Liu, and C. Sun, "Bilevel optimal configuration of generalized energy storage considering power consumption right transaction," en, International Journal of Electrical Power and Energy Systems, vol. 128, p. 106750, 2021.
- [32] N. Good, K. Ellis, and P. Mancarella, "Review and classification of barriers and enablers of demand response in the smart grid," en, *Renewable and Sustainable Energy Reviews*, vol. 72, pp. 57–72, 2017.
- [33] D. Kiedanski, M. Hashmi, A. Busic, and D. Kofman, "Sensitivity to forecast errors in energy storage arbitrage for residential consumers," en, in 2019 IEEE SmartGridComm, Beijing Shi, China, 2019.
- [34] A. Paladin, R. Das, Y. Wang, Z. Ali, R. Kotter, and G. Putrus, "Micro market based optimisation framework for decentralised management of distributed flexibility assets," da, *Renewable Energy*, vol. 163, pp. 1595–1611, 2021.

- [35] J. Guerrero, D. Gebbran, S. Mhanna, A. Chapman, and G. Verbic, "Towards a transactive energy system for integration of distributed energy resources: Home energy management, distributed optimal power flow, and peer-to-peer energy trading," en, Renewable and Sustainable Energy Reviews, vol. 132, p. 110 000, 2020.
- [36] G. Calabrese, "Generating reserve capacity determined by the probability method," en, Transactions of the American Institute of Electrical Engineers, vol. 66, no. 1, pp. 1439–1450, 1947.
- [37] M. Kubli and S. Puranik, "A typology of business models for energy communities: Current and emerging design options," *Renewable and Sustainable Energy Reviews*, vol. 176, p. 113165, 2023.
- [38] S. Cafasso, *Hydropower dams threaten fish habitats worldwide*, en, Online]. Available: 2020-02-03. [Online]. Available: https://earth.stanford.edu/news/hydropowerdams-threaten-fish-habitats-worldwide#gs.wht1wd..
- [39] J. West, I. Bailey, and M. Winter, "Renewable energy policy and public perceptions of renewable energy: A cultural theory approach," en, *Energy Policy*, vol. 38, pp. 5739–5748, 2010.
- [40] G. Kallis, P. Stephanides, E. Bailey, P. Devine-Wright, K. Chalvatzis, and I. Bailey, "The challenges of engaging island communities: Lessons on renewable energy from a review of 17 case studies," *Energy Research and Social Science*, vol. 81, p. 102 257, 2021.
- [41] M. Braun, "Virtual power plants in real applications-pilot demonstrations in spain and england as part of the european project fenix," lb, in ETG-Fachbericht-Internationaler, ETG-Kongress, Düsseldorf, 2009.
- [42] TWENTIES, Twenties project: Final report, nl, 2013. [Online]. Available: https://www.ewea.org/fileadmin/files/library/publications/reports/Twenties.pdf.
- [43] Con Edison, Rev demonstration project outline, en, New York, US, 2015. [Online]. Available: http://origin-states.politico.com.s3-website-us-east-1.amazonaws.com/files/CONEDDEMO3.pdf.
- [44] A.G.L., Virtual power plant in south australia, el-Latn, Adelaide, Australia, 2017. [Online]. Available: https://arena.gov.au/assets/2020/10/virtual-power-plant-in-south-australia.pdf.
- [45] Piclo, Piclo microgrid, en, 2021. [Online]. Available: https://piclo.energy/.
- [46] Brooklyn Microgrid, Brooklyn microgrid, en, 2021. [Online]. Available: https://www.brooklyn.energy/..

- [47] F. Ruz and M. Pollitt, "Overcoming barriers to electrical energy storage: Comparing california and europe," en, *Competition and Regulation in Network Industries*, vol. 17, no. 2, pp. 123–149, 2016.
- [48] M. Marinelli, "Aces (across continents electric vehicle services) projects: Scaling up system integration," en, *DTU Electrical Engineering*, 2018.
- [49] Web2Energy, Web2energy, en, 2011. [Online]. Available: https://www.web2energy.com/..
- [50] Con Edison, Rev demonstration project: 2017 1q quarterly progress report notice of temporary suspension of the clean virtual power plant project, en, New York, US, 2017.
- [51] A.G.L., Virtual power plant in south australia: Stage 2 public report, en, 2018. [Online]. Available: https://arena.gov.au/assets/2017/02/virtual-power-plants-in-south-australia-stage-2-public-report.pdf.
- [52] A. Caramizaru and A. Uihlein, Energy communities: an overview of energy and social innovation, en. Luxembourg: Publications Office of the European Union, 2020.
- [53] J. Roberts, D. Frieden, and A. Gubina, *Energy community definitions*, 2019. [Online]. Available: https://main.compile-project.eu/wp-content/uploads/Explanatory-note-on-energy-community-definitions.pdf.
- [54] E. Barbour, D. Parra, Z. Awwad, and M. González, "Community energy storage: A smart choice for the smart grid?" en, *Applied Energy*, vol. 212, pp. 489–497, 2018.
- [55] J. Schlund and R. German, "A distributed ledger based platform for community-driven flexibility provision," en, *Energy Informatics*, vol. 2, no. 5, pp. 1–20, 2019.
- [56] A. Aldegheishem, R. Bukhsh, N. Alrajeh, and N. Javaid, "Faavpp: Fog as a virtual power plant service for community energy management," en, *Future Generation Computer Systems*, vol. 105, pp. 675–683, 2020.
- [57] L. Summeren, A. Wieczorek, and G. Verbong, "The merits of becoming smart: How flemish and dutch energy communities mobilise digital technology to enhance their agency in the energy transition," en, *Energy Research and Social Science*, vol. 79, p. 102 160, 2021.
- [58] G. Doci and E. Vasileiadou, "Let's do it ourselves" individual motivations for investing in renewablesatcommunitylevel," en, Renewable and Sustainable Energy Reviews, vol. 49, pp. 41–50, 2015.
- [59] C. Liu, R. Jing Yang, X. Yu, C. Sun, P. Wong, and H. Zhao, "Virtual power plants for a sustainable urban future," en, Sustainable Cities and Society, vol. 65, p. 102 640, 2021.

- [60] J. Cuenca, E. Jamil, and B. Hayes, "Energy communities and sharing economy concepts in the electricity sector: A survey," en, in *International Conference on Environment and Electrical Engineering (EEEIC*, Madrid, Spain, 2020.
- [61] Sonnen Community, Sonnen, en, 2021. [Online]. Available: https://sonnengroup.com/sonnencommunity/..
- [62] Edinburgh Community Solar Cooperative, Edinburgh community solar cooperative, en, 2021. [Online]. Available: https://www.edinburghsolar.coop/.
- [63] Isle of Eigg, Eigg electric, en, 2021. [Online]. Available: http://isleofeigg.org/eigg-electric/.
- [64] Repsol Solar S.A., Repsol launches solmatch the first lagre solar energy community in spain, Apr. 2020. [Online]. Available: www.repsol.com/content/dam/repsol-corporate/.
- [65] NEOOM A.G, Neoom energy communities, Aug. 2024. [Online]. Available: https://neoom.com/en/solutions-res.
- [66] Energy4All, Energy4all annual report, en, Barrow in Furness, Cumbria, 2023. [Online]. Available: https://energy4all.co.uk/wp-content/uploads/2024/07/E4A-2023-Annual-Report-low-res.pdf.
- [67] Repsol Solar S.A., Repsol solmatch, Aug. 2024. [Online]. Available: https://www.repsol.es/particulares/hogar/energia-solar/que-es-solmatch/.
- [68] S. Philipps, "Photovoltaics report," Fraunhofer Institute for Solar Energy Systems, Tech. Rep., Jul. 2024.
- [69] NEOOM A.G, Neoom example calculation of the energy community (prosumer), Aug. 2024. [Online]. Available: https://wissen.neoom.com/beispielrechnung-eg-prosumer.
- [70] E. Barabino, D. Fioriti, E. Guerrazzi, I. Mariuzzo, D. Poli, M. Raugi, E. Razaei, E. Schito, and D. Thomopulos, "Energy communities: A review on trends, energy system modelling, business models, and optimisation objectives," Sustainable Energy, Grids and Networks, vol. 36, p. 101 187, 2023.
- [71] M. Vujanović, Q. Wang, M. Mohsen, N. Duić, and J. Yan, "Sustainable energy technologies and environmental impacts of energy systems," *Applied Energy*, vol. 256, p. 113 919, 2019.
- [72] N. C. Alluraiah and P. Vijayapriya, "Optimization, design, and feasibility analysis of a grid-integrated hybrid ac/dc microgrid system for rural electrification," *IEEE Access*, vol. 11, 2023.

- [73] J. K. Kim, H. Park, S. jung Kim, J. Lee, Y. Song, and S. C. Yi, "Optimization models for the cost-effective design and operation of renewable-integrated energy systems," *Renewable and Sustainable Energy Reviews*, vol. 183, 2023.
- [74] J. Sousa, J. Lagarto, C. Camus, C. Viveiros, F. Barata, P. Silva, R. Alegria, and O. Paraíba, "Renewable energy communities optimal design supported by an optimization model for investment in pv/wind capacity and renewable electricity sharing," *Energy*, vol. 283, 2023.
- [75] M. B. Slimene and M. A. Khlifi, "Modelling and study of energy storage devices for photovoltaic lighting," *Energy Exploration and Exploitation*, vol. 38, no. 5, pp. 1932–1945, 2020.
- [76] S. Dorahaki, M. Rashidinejad, S. F. F. Ardestani, A. Abdollahi, and M. R. Salehizadeh, "An integrated model for citizen energy communities and renewable energy communities based on clean energy package: A two-stage risk-based approach," *Energy*, vol. 277, 2023.
- [77] Y. Q. Ang, A. Polly, A. Kulkarni, G. B. Chambi, M. Hernandez, and M. N. Haji, "Multi-objective optimization of hybrid renewable energy systems with urban building energy modeling for a prototypical coastal community," *Renewable Energy*, vol. 201, 2022.
- [78] P. Majewski and P. R. Dias, "Product stewardship scheme for solar photovoltaic panels," Current Opinion in Green and Sustainable Chemistry, vol. 44, p. 100 859, 2023.
- [79] G. Cook, L. Billman, and R. Adcock, *Photovoltaic Fundamentals*. NREL, 1995.
- [80] S. Sugianto, "Comparative analysis of solar cell efficiency between monocrystalline and polycrystalline," *INTEK: Jurnal Penelitian*, vol. 7, no. 12, p. 92, 2020.
- [81] M. A. Green, E. D. Dunlop, J. Hohl-Ebinger, M. Yoshita, N. Kopidakis, and A. W. Ho-Baillie, "Solar cell efficiency tables," *Progress in Photovoltaics: Research and Applications*, vol. 28, no. 1, pp. 3–15, 2020.
- [82] J. Duffie and W. Beckman, Solar Engineering of Thermal Processes, Photovoltaics and Wind. John Wiley and Sons, 1991.
- [83] W. De Soto, S. Klein, and W. Beckman, "Improvement and validation of a model for photovoltaic array performance," *Solar Energy*, vol. 80, no. 1, pp. 78–88, 2006.
- [84] S. A. Gorji, H. G. Sahebi, M. Ektesabi, and A. B. Rad, "Topologies and control schemes of bidirectional dc–dc power converters: An overview," *IEEE Access*, vol. 7, 2019.

- [85] S. Adhikari and F. Li, "Coordinated v-f and p-q control of solar photovoltaic generators with mppt and battery storage in microgrids," *IEEE Transactions on Smart Grid*, vol. 5, 3 2014.
- [86] J. F. Manwell, J. G. McGowan, and A. L. Rogers, Wind Energy Explained: Theory, Design and Application. Wiley, 2010.
- [87] H. Eftekhari, A. S. M. Al-Obaidi, and S. Eftekhari, "Aerodynamic performance of vertical and horizontal axis wind turbines: A comparison review," *Indonesian Journal of Science and Technology*, vol. 7, 1 2022.
- [88] K. Pope, I. Dincer, and G. F. Naterer, "Energy and exergy efficiency comparison of horizontal and vertical axis wind turbines," *Renewable Energy*, vol. 35, 9 2010.
- [89] P. Jamieson, Innovation in Wind Turbine Design. 2011.
- [90] A. Tummala, R. K. Velamati, D. K. Sinha, V. Indraja, and V. H. Krishna, A review on small scale wind turbines, 2016.
- [91] P. J. Schubel and R. J. Crossley, Wind turbine blade design, 2012.
- [92] M. A. Al-Rawajfeh and M. R. Gomaa, "Comparison between horizontal and vertical axis wind turbine," *International Journal of Applied Power Engineering*, vol. 12, 1 2023.
- [93] M. Ebrahimpour, R. Shafaghat, R. Alamian, and M. Safdari Shadloo, "Numerical investigation of the savonius vertical axis wind turbine and evaluation of the effect of the overlap parameter in both horizontal and vertical directions on its performance," *Symmetry*, vol. 11, no. 6, p. 821, Jun. 2019.
- [94] S. Spyridonidou and D. G. Vagiona, "Systematic review of site-selection processes in onshore and offshore wind energy research," *Energies*, vol. 13, 22 2020.
- [95] L. Kou, Y. Li, F. Zhang, X. Gong, Y. Hu, Q. Yuan, and W. Ke, Review on monitoring, operation and maintenance of smart offshore wind farms, 2022.
- [96] D. Cevasco, S. Koukoura, and A. J. Kolios, Reliability, availability, maintainability data review for the identification of trends in offshore wind energy applications, 2021.
- [97] H. Guo, W. Wang, and M. Xia, "On-line multi-objective decision model for the maintenance scheduling of offshore wind turbine group," Zhongguo Dianji Gongcheng Xuebao/Proceedings of the Chinese Society of Electrical Engineering, vol. 37, 7 2017.
- [98] C. W. Kent, C. Grimmond, D. Gatey, and J. F. Barlow, "Assessing methods to extrapolate the vertical wind-speed profile from surface observations in a city centre during strong winds," *Journal of Wind Engineering and Industrial Aerodynamics*, vol. 173, pp. 100–111, Feb. 2018.

- [99] K. Calautit, A. Aquino, J. K. Calautit, P. Nejat, F. Jomehzadeh, and B. R. Hughes, A review of numerical modelling of multi-scale wind turbines and their environment, 2018.
- [100] N. Shamarova, K. Suslov, P. Ilyushin, and I. Shushpanov, Review of battery energy storage systems modeling in microgrids with renewables considering battery degradation, 2022.
- [101] Bloomberg NEF, Global energy storage market to grow 15-fold by 2030, Online, Oct. 2022. [Online]. Available: https://about.bnef.com/blog/global-energy-storage-market-to-grow-15-fold-by-2030/.
- [102] P. Taylor, R. Bolton, D. Stone, X.-P. Zhang, C. Martin, and P. Upham, *Pathways for Energy Storage in the UK*, English. The Centre for Low Carbon Futures, Mar. 2012.
- [103] Bloomberg NEF, *Electric vehicles outlook 2023*, Online, Aug. 2023. [Online]. Available: https://about.bnef.com/insights/clean-transport/electric-vehicle-outlook/.
- [104] J. Meng, G. Luo, M. Ricco, M. Swierczynski, D. I. Stroe, and R. Teodorescu, Overview of lithium-ion battery modeling methods for state-of-charge estimation in electrical vehicles, 2018.
- [105] J. Shin, W. Kim, K. Yoo, H. Kim, and M. Han, "Vehicular level battery modeling and its application to battery electric vehicle simulation," *Journal of Power Sources*, vol. 556, 2023.
- [106] R. R. Kumar, C. Bharatiraja, K. Udhayakumar, S. Devakirubakaran, K. S. Sekar, and L. Mihet-Popa, Advances in batteries, battery modeling, battery management system, battery thermal management, soc, soh, and charge/discharge characteristics in ev applications, 2023.
- [107] Y. Zhao, P. Stein, Y. Bai, M. Al-Siraj, Y. Yang, and B. X. Xu, A review on modeling of electro-chemo-mechanics in lithium-ion batteries, 2019.
- [108] O. Tremblay and L. A. Dessaint, "Experimental validation of a battery dynamic model for ev applications," World Electric Vehicle Journal, vol. 3, 2 2009.
- [109] C. M. Shepherd, "Design of primary and secondary cells: Ii . an equation describing battery discharge," *Journal of The Electrochemical Society*, vol. 112, no. 7, p. 657, Jul. 1965.
- [110] P. E. Campana, L. Cioccolanti, B. François, J. Jurasz, Y. Zhang, M. Varini, B. Stridh, and J. Yan, "Li-ion batteries for peak shaving, price arbitrage, and photovoltaic self-consumption in commercial buildings: A monte carlo analysis," Energy Conversion and Management, vol. 234, p. 113 889, 2021.

- [111] G. Sæther, P. Crespo del Granado, and S. Zaferanlouei, "Peer-to-peer electricity trading in an industrial site: Value of buildings flexibility on peak load reduction," *Energy and Buildings*, vol. 236, p. 110737, 2021.
- [112] H. Kang, S. Jung, J. Jeoung, J. Hong, and T. Hong, "A bi-level reinforcement learning model for optimal scheduling and planning of battery energy storage considering uncertainty in the energy-sharing community," Sustainable Cities and Society, vol. 94, p. 104538, 2023.
- [113] A. Lüth, J. M. Zepter, P. Crespo del Granado, and R. Egging, "Local electricity market designs for peer-to-peer trading: The role of battery flexibility," *Applied Energy*, vol. 229, pp. 1233–1243, 2018.
- [114] International Energy Agency, Batteries and Secure Energy Transitions. Paris, France: IEA, 2022. [Online]. Available: https://www.iea.org/reports/batteries-and-secure-energy-transitions.
- [115] T. Chen, Y. Jin, H. Lv, A. Yang, M. Liu, B. Chen, Y. Xie, and Q. Chen, "Applications of lithium-ion batteries in grid-scale energy storage systems," *Transactions of Tianjin University*, vol. 26, no. 3, pp. 208–217, 2020.
- [116] S. Shahid and M. Agelin-Chaab, "A review of thermal runaway prevention and mitigation strategies for lithium-ion batteries," *Energy Conversion and Management:* X, vol. 16, p. 100310, 2022.
- [117] H. Liao, B. Huang, Y. Cui, H. Qin, X. Liu, and H. Xu, "Research on a fast detection method of self-discharge of lithium battery," *Journal of Energy Storage*, vol. 55, 2022.
- [118] M. Yue, H. Lambert, E. Pahon, R. Roche, S. Jemei, and D. Hissel, "Hydrogen energy systems: A critical review of technologies, applications, trends and challenges," Renewable and Sustainable Energy Reviews, vol. 146, p. 111 180, Aug. 2021.
- [119] A. Pramuanjaroenkij and S. Kakaç, The fuel cell electric vehicles: The highlight review, 2023.
- [120] A. Ferrara, S. Jakubek, and C. Hametner, "Cost-optimal design and energy management of fuel cell electric trucks," *International Journal of Hydrogen Energy*, vol. 48, 43 2023.
- [121] A. G. Elkafas, M. Rivarolo, E. Gadducci, L. Magistri, and A. F. Massardo, Fuel cell systems for maritime: A review of research development, commercial products, applications, and perspectives, 2023.
- [122] A. Baroutaji, T. Wilberforce, M. Ramadan, and A. G. Olabi, "Comprehensive investigation on hydrogen and fuel cell technology in the aviation and aerospace sectors," *Renewable and Sustainable Energy Reviews*, vol. 106, 2019.

- [123] B. Salehi and L. Wang, Critical review on nanomaterials for enhancing bioconversion and bioremediation of agricultural wastes and wastewater, 2022.
- [124] G. Jansen, Z. Dehouche, and H. Corrigan, "Cost-effective sizing of a hybrid regenerative hydrogen fuel cell energy storage system for remote and off-grid telecom towers," *International Journal of Hydrogen Energy*, vol. 46, 35 2021.
- [125] L. Giorgi and F. Leccese, "Fuel cells: Technologies and applications," *The Open Fuel Cells Journal*, vol. 6, pp. 1–20, 2013.
- [126] M. Carmo, D. L. Fritz, J. Mergel, and D. Stolten, "A comprehensive review on pem water electrolysis," *International Journal of Hydrogen Energy*, vol. 38, no. 12, pp. 4901–4934, 2013.
- [127] S. Niroula, C. Chaudhary, A. Subedi, and B. S. Thapa, "Parametric modelling and optimization of alkaline electrolyzer for the production of green hydrogen," IOP Conference Series: Materials Science and Engineering, vol. 1279, no. 1, p. 012 005, Mar. 2023.
- [128] K. Hu, J. Fang, X. Ai, D. Huang, Z. Zhong, X. Yang, and L. Wang, "Comparative study of alkaline water electrolysis, proton exchange membrane water electrolysis and solid oxide electrolysis through multiphysics modeling," *Applied Energy*, vol. 312, p. 118 788, 2022.
- [129] E. Gul, G. Baldinelli, A. Farooqui, P. Bartocci, and T. Shamim, "Aem-electrolyzer based hydrogen integrated renewable energy system optimisation model for distributed communities," *Energy Conversion and Management*, vol. 285, p. 117 025, Jun. 2023.
- [130] P. Marocco, D. Ferrero, E. Martelli, M. Santarelli, and A. Lanzini, "An milp approach for the optimal design of renewable battery-hydrogen energy systems for off-grid insular communities," *Energy Conversion and Management*, vol. 245, 2021.
- [131] M. Temiz and I. Dincer, "Development of solar and wind based hydrogen energy systems for sustainable communities," *Energy Conversion and Management*, vol. 269, p. 116 090, Oct. 2022.
- [132] M. M. Ahmed, B. K. Das, P. Das, M. S. Hossain, and M. G. Kibria, "Energy management and sizing of a stand-alone hybrid renewable energy system for community electricity, fresh water, and cooking gas demands of a remote island," *Energy Conversion and Management*, vol. 299, 2024.
- [133] D. E. Kvasov and M. S. Mukhametzhanov, "Metaheuristic vs. deterministic global optimization algorithms: The univariate case," *Applied Mathematics and Computation*, vol. 318, 2018.

- [134] J. A. Monoh, M. E. Ei-Hawary, and R. Adapa, "A review of selected optimal power flow literature to 1993 part ii: Newton, linear programming and interior point methods," *IEEE Transactions on Power Systems*, vol. 14, 1 1999.
- [135] D. Wells, "Method for economic secure loading of a power system," *Proceedings of the Institution of Electrical Engineers*, vol. 115, 8 1968.
- [136] C. Klemm and P. Vennemann, Modeling and optimization of multi-energy systems in mixed-use districts: A review of existing methods and approaches, 2021.
- [137] L. T. Biegler and I. E. Grossmann, "Retrospective on optimization," *Computers and Chemical Engineering*, vol. 28, 8 2004.
- [138] G. Romeo, "Chapter 7 linear programming," in *Elements of Numerical Mathematical Economics with Excel*, G. Romeo, Ed., Academic Press, 2020, pp. 383–415.
- [139] G. B. Dantzig, "Linear programming and extensions," in 2021.
- [140] M. Zatti, M. Moncecchi, M. Gabba, A. Chiesa, F. Bovera, and M. Merlo, "Energy communities design optimization in the italian framework," *Applied Sciences* (Switzerland), vol. 11, 11 2021.
- [141] L. Uwineza, H. G. Kim, and C. K. Kim, "Feasibilty study of integrating the renewable energy system in popova island using the monte carlo model and homer," *Energy Strategy Reviews*, vol. 33, 2021.
- [142] K. A. Kavadias and P. Triantafyllou, "Hybrid renewable energy systems' optimisation. a review and extended comparison of the most-used software tools," *Energies*, vol. 14, 24 2021.
- [143] E. Zafeiratou and C. Spataru, "Sustainable island power system scenario analysis for crete under the energy trilemma index," *Sustainable Cities and Society*, vol. 41, 2018.
- [144] T. Nasir, S. Raza, M. Abrar, H. A. U. Muqeet, H. Jamil, F. Qayyum, O. Cheikhrouhou, F. Alassery, and H. Hamam, "Optimal scheduling of campus microgrid considering the electric vehicle integration in smart grid," Sensors, vol. 21, 21 2021.
- [145] X. S. Yang, Nature-Inspired Optimization Algorithms. Elsevier, 2014.
- [146] G. Mavromatidis, K. Orehounig, and J. Carmeliet, "Uncertainty and global sensitivity analysis for the optimal design of distributed energy systems," Applied Energy, vol. 214, 2018.
- [147] C. Blum and A. Roli, "Metaheuristics in combinatorial optimization: Overview and conceptual comparison," *ACM Computing Surveys*, vol. 35, pp. 268–308, 3 2003.

- [148] F. Glover, "Discrete diversity and dispersion maximization," in R. Martí and A. Martínez-Gavara, Eds. Springer, 2023, ch. Tabu Search, pp. 137–149.
- [149] S. Katoch, S. S. Chauhan, and V. Kumar, "A review on genetic algorithm: Past, present, and future," *Multimedia Tools and Applications*, vol. 80, 5 2021.
- [150] B. Webb, "Swarm intelligence: From natural to artificial systems," *Connection Science*, vol. 14, pp. 163–164, 2 2002.
- [151] Y. Matanga, *Genetic algorithms*, Online, Nov. 2024. [Online]. Available: https://mlinsightscentral.com/index.php/genetic-algorithms/.
- [152] MATLAB, Surrogate optimization, Online, Sep. 2018. [Online]. Available: https://uk.mathworks.com/videos/surrogate-optimization-1535996187824.html.
- [153] Y. Li, F. Qian, W. Gao, H. Fukuda, and Y. Wang, "Techno-economic performance of battery energy storage system in an energy sharing community," *Journal of Energy Storage*, vol. 50, 2022.
- [154] M. Secchi, G. Barchi, D. Macii, D. Moser, and D. Petri, "Multi-objective battery sizing optimisation for renewable energy communities with distribution-level constraints: A prosumer-driven perspective," *Applied Energy*, vol. 297, 2021.
- [155] M. Ismail, M. Moghavvemi, and T. Mahlia, "Genetic algorithm based optimization on modeling and design of hybrid renewable energy systems," *Energy Conversion* and Management, vol. 85, pp. 120–130, Sep. 2014.
- [156] F. Lazzari, G. Mor, J. Cipriano, F. Solsona, D. Chemisana, and D. Guericke, "Optimizing planning and operation of renewable energy communities with genetic algorithms," *Applied Energy*, vol. 338, 2023.
- [157] P. Huang, Y. Sun, M. Lovati, and X. Zhang, "Solar-photovoltaic-power-sharing-based design optimization of distributed energy storage systems for performance improvements," *Energy*, vol. 222, 2021.
- [158] National Aeronautics and Space Administration, Nasa prediction of worldwide energy resources, Online, Apr. 2025. [Online]. Available: https://power.larc.nasa.gov.
- [159] Red Electrica de Espana, *Power grid transparent platform*, Online, Apr. 2025. [Online]. Available: https://www.esios.ree.es/en.
- [160] M. Osman, M. Ouf, E. Azar, and B. Dong, "Stochastic bottom-up load profile generator for canadian households' electricity demand," *Building and Environment*, vol. 241, p. 110490, 2023.
- [161] M. Lage, R. Castro, G. Manzolini, V. Casalicchio, and T. Sousa, "Techno-economic analysis of self-consumption schemes and energy communities in italy and portugal," *Solar Energy*, vol. 270, p. 112 407, 2024.

- [162] National Renewable Energy Laboratory, End-Use Load Profiles for the U.S. End-Use Load Profiles for the US Building Stock: Methodology and Results of Model Calibration, Validation, and Uncertainty Quantification. Boulder, Colorado: US Department of Energy, 2022.
- [163] M. C. Peel, B. L. Finlayson, and T. A. McMahon, "Updated world map of the köppen-geiger climate classification," *Hydrology and Earth System Sciences*, vol. 11, 5 2007.
- [164] HOMER Energy, Global horizontal irradiance (ghi), Nov. 2024. [Online]. Available: https://homerenergy.com/products/pro/docs/3.15/global\_horizontal\_irradiance\_ghi.html#:~:text=Global%20Horizontal%20Irradiance%20(GHI)%20is,Photovoltaic%20Panels%20(PV).
- [165] PVEducation, Solar radiation on a tilted surface, Online, Nov. 2024. [Online]. Available: https://www.pveducation.org/pvcdrom/properties-of-sunlight/solar-radiation-on-a-tilted-surface.
- [166] C. Draxl, A. Clifton, B.-M. Hodge, and J. Mccaa, "The wind integration national dataset (wind) toolkit," *Applied Energy*, vol. 151, pp. 355–366, Aug. 2015.
- [167] International Electrotechnical Commission, "Wind turbines-part 1 : Design requirements," *IEC61400-1*, 2005. [Online]. Available: https://cir.nii.ac.jp/crid/1574231875236217984.
- [168] J. C. Y. Lee and M. J. Fields, "An overview of wind-energy-production prediction bias, losses, and uncertainties," Wind Energy Science, vol. 6, no. 2, pp. 311–365, 2021.
- [169] J. Mello, C. de Lorenzo, F. A. Campos, and J. Villar, "Pricing and simulating energy transactions in energy communities," *Energies*, vol. 16, no. 4, 2023.
- [170] J. Blank and K. Deb, "Pymoo: Multi-objective optimization in python," *IEEE Access*, vol. 8, pp. 89497–89509, 2020.
- [171] W. Arowolo and Y. Perez, "Rapid decarbonisation of paris, lyon and marseille's power, transport and building sectors by coupling rooftop solar pv and electric vehicles," *Energy for Sustainable Development*, vol. 74, pp. 196–214, 2023.
- [172] P. K. Sahu, C. Chakraborty, and J. Roy, "Comparative economic analysis of bifacial roof-top pv systems," *Energy for Sustainable Development*, vol. 83, p. 101593, 2024.
- [173] JA Solar, 400w perc half-cell black module, Jan. 2020. [Online]. Available: https://www.jasolar.com/uploadfile/2020/0619/20200619040057517.pdf.
- [174] M. Muller, Measuring and Modeling Nominal Operating Cell Temperature (NOCT) NREL Test and Evaluation. Albuquerque, NM: National Renewable Energy Laboratory, Sep. 2010.

- [175] M. Carvalho, V. L. Menezes, K. C. Gomes, and R. Pinheiro, "Carbon footprint associated with a mono-si cell photovoltaic ceramic roof tile system," en, Environmental Progress and Sustainable Energy, vol. 38, no. 4, p. 13120, 2019.
- [176] J. Duffie and W. Beckman, Solar Engineering of Thermal Processes, en. Hoboken: Wiley, 1991.
- [177] T. Stehly, P. Beiter, and P. Duffy, 2019 Cost of Wind Energy Review, en. Golden, Colorado: National Renewable Energy Laboratory, 2019.
- [178] Intergovernmental Panel on Climate Change, Climate Change 2021: The Physical Science Basis Contribution of Working Group I to the Sixth Assessment Report of the Intergovernmental Panel on Climate Change, en. Cambridge, UK: Cambridge University Press, 2021.
- [179] K. Mongird, 2020 Grid Energy Storage Performance Assessment, en. Richland, Washington: US Department of Energy, 2020.
- [180] M. Romare and L. Dahllöf, The Life Cycle Energy Consumption and Greenhouse Gas Emissions from Lithium-Ion Batteries, en. Stockholm, Sweden: IVL Swedish Environmental Research Institute, 2017.
- [181] E. Department for Business and I. Strategy, Hydrogen Production Costs, en. London, UK: HM Government UK, 2021.
- [182] K. Reddi, A. Elgowainy, N. Rustagi, and E. Gupta, "Techno-economic analysis of conventional and advanced high-pressure tube trailer configurations for compressed hydrogen gas transportation and refueling," en, *International Journal of Hydrogen* Energy, vol. 43, no. 9, pp. 4428–4438, 2018.
- [183] Ballard, Fuel Cell Life cycle Assessment, Burnaby, en. Burnaby, Canada: Ballard, 2018.
- [184] A. Agostini, N. Belmonte, A. Masala, J. Hu, P. Rizzi, M. Fichtner, P. Moretto, C. Luetto, M. Sgroi, and M. Baricco, "Role of hydrogen tanks in the life cycle assessment of fuel cell-based auxiliary power units," en, *Applied Energy*, vol. 215, pp. 1–12, 2018.
- [185] T. Salameh, A. Al-Othman, A. G. Olabi, S. Issa, M. Tawalbeh, and A. H. Alami, "Comparative life cycle assessment for pemfc stack including fuel storage materials in uae," en, in 2020 Advances in Science and Engineering Technology International Conferences (ASET), 2020, pp. 1–5.
- [186] W. Marion, A. Anderberg, C. Deline, S. Glick, M. Muller, G. Perrin, J. Rodriguez, S. Rummel, K. Terwilliger, and T. Silverman, *User's manual for data for validating models for pv module performance*, Boulder, Colorade, 2014.

- [187] Enercon, Enercon e-44 datasheet, Online, 2025. [Online]. Available: https://en.wind-turbine-models.com/turbines/531-enercon-e-44.
- [188] Z. Wang and G. P. Rangaiah, "Application and analysis of methods for selecting an optimal solution from the pareto-optimal front obtained by multiobjective optimization," en, *Industrial & Engineering Chemistry Research*, vol. 56, no. 2, pp. 560–574, 2017. eprint: https://doi.org/10.1021/acs.iecr.6b03453.
- [189] Intergovernmental Panel on Climate Change, Climate Change 2014: Synthesis Report, en. Geneva, Switzerland: IPCC Secretariat, 2014.
- [190] G. Jansen, Z. Dehouche, and H. Corrigan, "Cost-effective sizing of a hybrid regenerative hydrogen fuel cell energy storage system for remote and off-grid telecom towers," en, *International Journal of Hydrogen Energy*, vol. 46, no. 22, 2021.
- [191] R. Zhao, N. Zhu, X. Zhao, Z. Luo, and J. Chang, "Multi-objective optimization of a novel photovoltaic-thermoelectric generator system based on hybrid enhanced algorithm," *Energy*, vol. 319, p. 135046, 2025.
- [192] J. Herman and W. Usher, "SALib: An open-source python library for sensitivity analysis," *The Journal of Open Source Software*, vol. 2, no. 9, Jan. 2017. [Online]. Available: https://doi.org/10.21105/joss.00097.
- [193] T. Iwanaga, W. Usher, and J. Herman, "Toward SALib 2.0: Advancing the accessibility and interpretability of global sensitivity analyses," *Socio-Environmental Systems Modelling*, vol. 4, p. 18155, May 2022.
- [194] J. Park, S. Kang, S. Kim, H. Kim, H.-S. Cho, C. Lee, M. Kim, and J. H. Lee, "The impact of degradation on the economics of green hydrogen," *Renewable and Sustainable Energy Reviews*, vol. 213, p. 115472, 2025.
- [195] A. Fleischhacker, G. Lettner, D. Schwabeneder, and H. Auer, "Portfolio optimization of energy communities to meet reductions in costs and emissions," *Energy*, vol. 173, pp. 1092–1105, 2019.
- [196] X. Zhu, C. Peng, and H. Geng, "Multi-objective sizing optimization method of microgrid considering cost and carbon emissions," in 2022 4th International Conference on Smart Power and Internet Energy Systems (SPIES), 2022, pp. 2278–2283.
- [197] T. Araoye, E. Ashigwuike, A. Sadiq Umar, E. Eronu, T. God, I. Ozue, E. Sochima Vincent, J. Muncho, Mbunwe, M. Odo, G. Nnaemeka, and N. Ajah, "Modeling and optimization of pv-diesel-biogas hybrid microgrid energy system for sustainability of electricity in rural area," *International Journal of Power Electronics and Drive Systems (IJPEDS)*, vol. 14, pp. 1855–1864, Sep. 2023.

- [198] S.-H. Park, Y.-S. Jang, and E.-J. Kim, "Multi-objective optimization for sizing multi-source renewable energy systems in the community center of a residential apartment complex," *Energy Conversion and Management*, vol. 244, p. 114 446, 2021.
- [199] W. L. Schram, T. AlSkaif, I. Lampropoulos, S. Henein, and W. G. van Sark, "On the trade-off between environmental and economic objectives in community energy storage operational optimization," *IEEE Transactions on Sustainable Energy*, vol. 11, no. 4, pp. 2653–2661, 2020.
- [200] S. El Hassani, F. Oueslati, O. Horma, D. Santana, M. A. Moussaoui, and A. Mezrhab, "Techno-economic feasibility and performance analysis of an islanded hybrid renewable energy system with hydrogen storage in morocco," *Journal of Energy Storage*, vol. 68, p. 107853, 2023.
- [201] N. C. Alluraiah and P. Vijayapriya, "Optimization, design, and feasibility analysis of a grid-integrated hybrid ac/dc microgrid system for rural electrification," *IEEE Access*, vol. 11, pp. 67013–67029, 2023.
- [202] P.-F. Pai, A. Acakpovi, P. Adjei, N. Nwulu, and N. Y. Asabere, "Optimal hybrid renewable energy system: A comparative study of wind/hydrogen/fuel-cell and wind/battery storage," *Journal of Electrical and Computer Engineering*, vol. 2020, p. 1756 503, 2020.
- [203] IRENA, Renewable power generation costs in 2023. Abu Dhabi: International Renewable Energy Agency, 2024.
- [204] A. Jahanbin, L. Abdolmaleki, and U. Berardi, "Techno-economic feasibility of integrating hybrid battery-hydrogen energy storage system into an academic building," *Energy Conversion and Management*, vol. 309, p. 118 445, 2024.
- [205] F. Bandeiras, E. Pinheiro, M. Gomes, P. Coelho, and J. Fernandes, "Review of the cooperation and operation of microgrid clusters," *Renewable and Sustainable Energy Reviews*, vol. 133, p. 110311, 2020. [Online]. Available: h.
- [206] Y. Du, Z. Wang, G. Liu, X. Chen, H. Yuan, Y. Wei, and F. Li, "A cooperative game approach for coordinating multi-microgrid operation within distribution systems," *Applied Energy*, vol. 222, pp. 383–395, 2018.
- [207] C. Zhang, J. Wu, Y. Zhou, M. Cheng, and C. Long, "Peer-to-peer energy trading in a microgrid," *Applied Energy*, vol. 220, pp. 1–12, 2018.
- [208] L. Pagnini, S. Bracco, F. Delfino, and M. de-Simón-Martín, "Levelized cost of electricity in renewable energy communities: Uncertainty propagation analysis," *Applied Energy*, vol. 366, p. 123 278, 2024.

- [209] European Environment Agency, Co2 emissions performance of new passenger cars in europe, Online, Dec. 2024. [Online]. Available: https://www.eea.europa.eu/en/analysis/indicators/co2-performance-of-new-passenger?activeAccordion=ecdb3bcf-bbe9-4978-b5cf-0b136399d9f8.
- [210] A. Taffuri, D. Padovan, O. Arrobbio, A. Sciullo, D. Grasso, and A. Grignani, "Energy commoning: The politicization of energy collective action in southern europe," Rassegna Italiana di Sociologia, Rivista trimestrale fondata da Camillo Pellizzi, no. 2/2024, pp. 315–342, 2024.
- [211] B. Slee, "Collaborative action, policy support and rural sustainability transitions in advanced western economies: The case of scotland," English, *Sustainability*, vol. 16, no. 2, p. 870, 2024.

### Appendix A

## Supplementary Analysis

#### A.1 Solution Deployment and Test

Another aim of this work that has not been stated in detail was to deploy a test REC system to the island of Formentera to validate the renewable asset performance. A test system was procured alongside this thesis and was eventually installed within the defined energy community, however, due to time and cost constraints the validation was not possible. However, this section briefly described some of the technical aspects of the REC storage design, highlighting the practical design considerations and challenges.

Due to cost restrictions, the full optimal system could not be realised for the project, so a smaller but still cost and environmentally effective system was designed using the modelling framework. The REC consisted of 15kW PV solar installation in two 7.5kW parallel strings connected to a 15kW three phase inverter. A battery stack made up of three 4.8kWh units equating to 14.4kWh was also chosen, to be combined with the hydrogen system. The PEM fuel cell was a 4kW air-cooled unit which consumed hydrogen from a 1,000 litre cylindrical pressure vessel where it is stored at 30 bar and generated from the connected electrolyser. The AEM electroylser stack consisted of three 2.4kW units wired into the same three phase supply as the PV solar array. The full schematic is shown in Figure 5.1

The specific energy community policy requirements in Spain, based on Real Decreto 244/2019, dated 5 April and itself based on the RED-II directive, instructs that less than 50,000 citizens and assets less than 2,000 meters apart can be designated as an REC.

Figure A.2a shows the new solar installation on the roof of the community centre building. This solar array is addition to the existing capacity installed at the small and large schools as well as the council offices. Figure A.2b includes images of the battery storage stack connected in series to the 48V DC terminals of the distributor bus at a recommended discharge current of 75A.

Figure A.3a then shows the main hydrogen storage system cabinet, complete with (1)

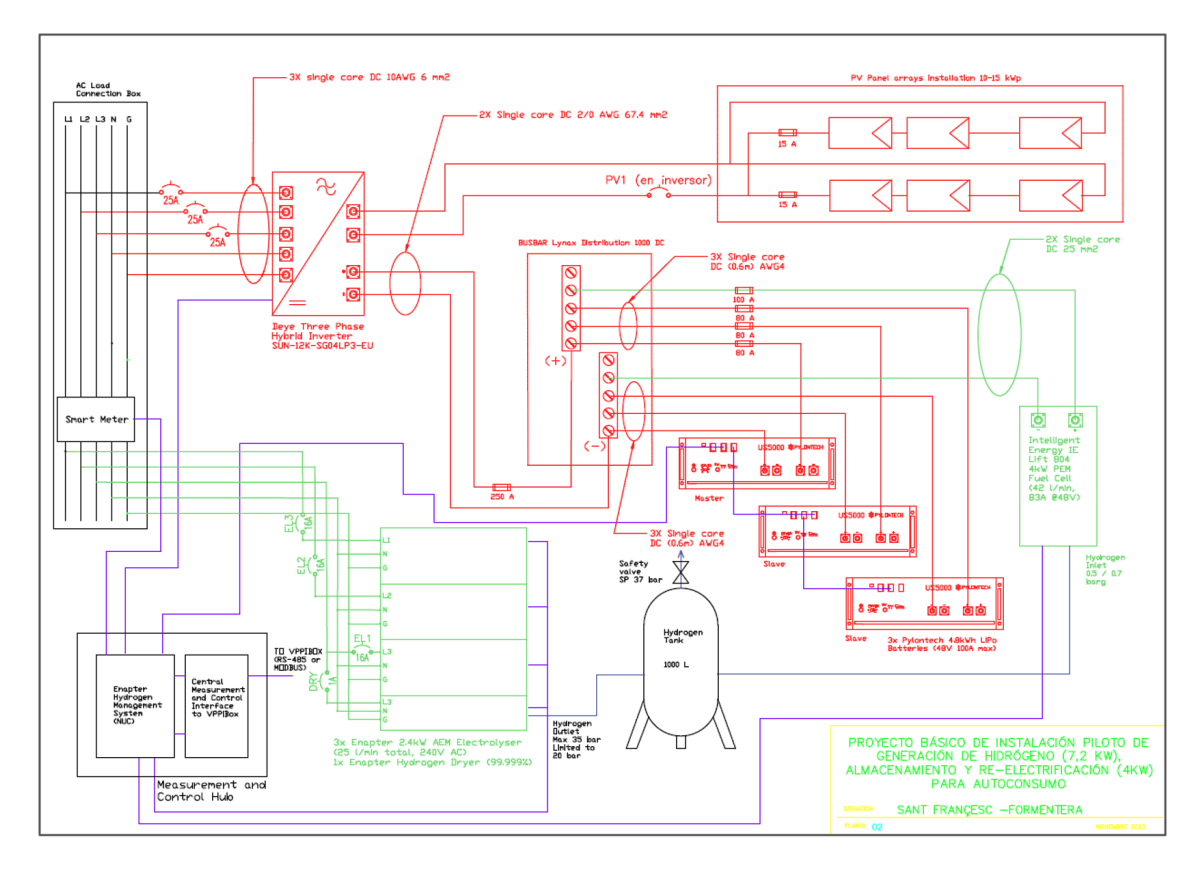


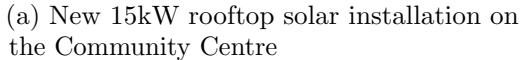
Figure A.1: REC asset schematic for the installation on Formentera

the 4kW PEM fuel cell and (2) the 7.2kW electrolyser stack. In addition to the electrolysers, there is a water treatment tank to ensure the conductivity of the input water is at an acceptably low range and remains at a constant input pressure of 1.5-4 bar, and a hydrogen dryer to ensure a purity of 99.9% H2. The fuel cell is connected to the 48V distributor bus in parallel to the battery storage, whereas the electrolysers are fed power via the mains 230V AC, producing hydrogen at 35 bar for the pressure vessel, shown in Figure A.3b. All pressures are carefully monitored and controlled by a series of pressure regulation valves for each input and output of the hydrogen system.

All systems are monitored and controlled by the central hydrogen management system, provided by the electrolyser manufacturer, Enapter. There is then an MQTT messaging system that allows the measured system data to be passed to the energy management and trading platform to make decisions regarding charge and discharge states to optimise the virtual flow of energy to the different community members. Much of the electrical monitoring is also handled by the three-phase inverter system and 48V lynx DC bus, which are shown in Figure A.4.

Due to project time constraints a direct performance validation was not able to be performed, but the output of the system can be measured and seen as operating effectively on the island. Figure A.5 illustrates the operation of the system for a portion of the month







(b) Battery cabinet housing the 14.4kWh stack

Figure A.2: Solar and battery installations for the REC in Formentera

of July 2024. It can be seen that the storage system is making use of the excess PV solar generation when available and charging the battery system first, before producing hydrogen for storage via the electrolyser stack. Like the model simulation, the battery handles hourly and daily differences between supply and demand, whereas the hydrogen storage fills over a longer period to be used for long-term balancing.

The result of this deployment shows that even as a smaller, simplified version of the optimal system modelled in this work, the proposed REC design is able to successfully operate and provide benefits by reducing dependence on the grid for electricity, therefore increasing energy security and embedded emissions.



(a) The hydrogen system cabinet consisting of the [1] the 4kW fuel cell and [2] the 7.2kW electrolyser stack.



(b) Installation of the 1,000 litre hydrogen pressure vessel.

Figure A.3: The hydrogen system installation showing the cabinet and storage tank.



Figure A.4: The 15 kVA three-phase inverter and 48 V DC bus to manage the DC power generation and battery storage for the REC system.

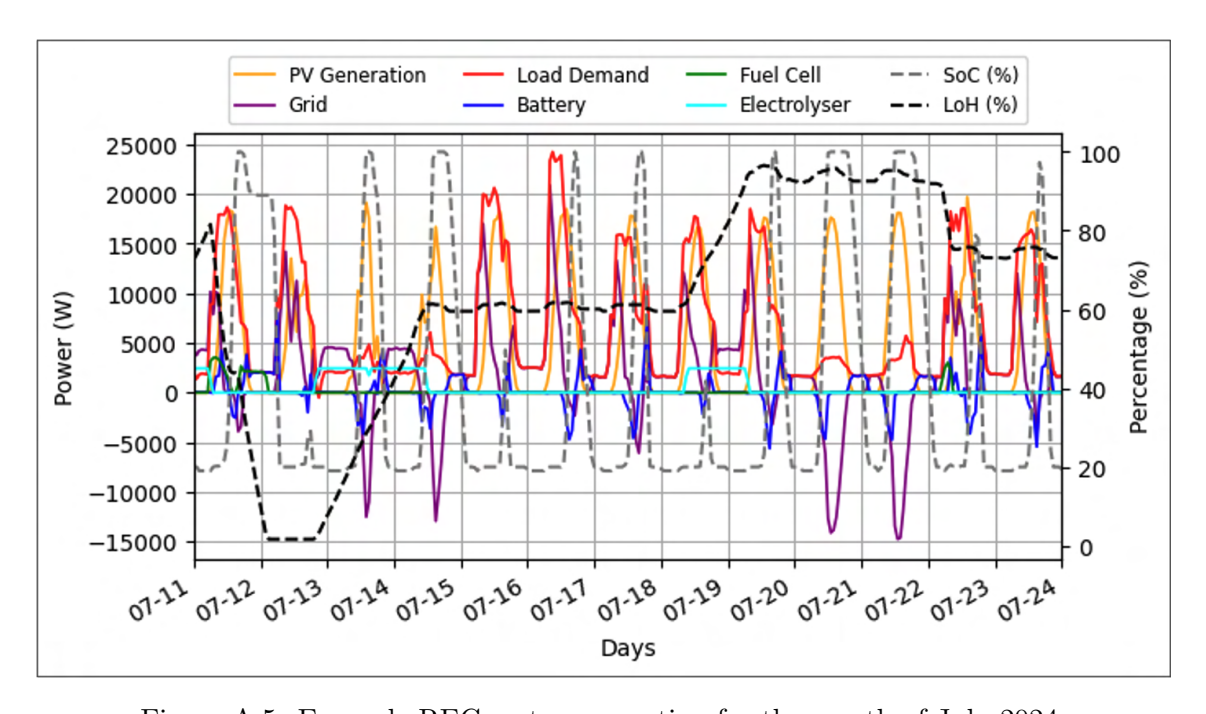


Figure A.5: Example REC system operation for the month of July 2024.

# Appendix B

# Input data tables

Table B.1: Adopted building power load profiles for the hourly simulation [normalised]

| Hour | Hospital | Hotel | Office | Residenc | e School | Commerc | cendustry |
|------|----------|-------|--------|----------|----------|---------|-----------|
| 0    | 0.19     | 0.21  | 0.10   | 0.17     | 0.11     | 0.14    | 0.37      |
| 1    | 0.19     | 0.16  | 0.10   | 0.15     | 0.11     | 0.13    | 0.37      |
| 2    | 0.18     | 0.14  | 0.10   | 0.13     | 0.11     | 0.14    | 0.36      |
| 3    | 0.28     | 0.15  | 0.11   | 0.17     | 0.11     | 0.17    | 0.37      |
| 4    | 0.33     | 0.20  | 0.15   | 0.27     | 0.11     | 0.18    | 0.36      |
| 5    | 0.54     | 0.43  | 0.35   | 0.38     | 0.24     | 0.34    | 0.35      |
| 6    | 0.77     | 0.68  | 0.45   | 0.46     | 0.47     | 0.42    | 0.30      |
| 7    | 0.87     | 0.70  | 0.83   | 0.43     | 0.76     | 0.61    | 0.30      |
| 8    | 0.94     | 0.61  | 1.00   | 0.38     | 0.84     | 0.81    | 0.85      |
| 9    | 0.98     | 0.47  | 0.96   | 0.31     | 0.89     | 0.88    | 0.91      |
| 10   | 1.00     | 0.41  | 0.95   | 0.31     | 0.94     | 0.97    | 0.98      |
| 11   | 0.97     | 0.42  | 0.94   | 0.33     | 0.97     | 1.00    | 1.00      |
| 12   | 0.98     | 0.40  | 0.96   | 0.35     | 0.98     | 0.99    | 0.91      |
| 13   | 1.00     | 0.39  | 0.94   | 0.35     | 1.00     | 0.97    | 0.92      |
| 14   | 0.99     | 0.40  | 0.93   | 0.39     | 1.00     | 0.96    | 0.99      |
| 15   | 0.99     | 0.45  | 0.96   | 0.58     | 0.99     | 0.95    | 1.00      |
| 16   | 0.98     | 0.54  | 0.90   | 0.80     | 0.87     | 0.94    | 0.35      |
| 17   | 0.72     | 0.76  | 0.72   | 0.96     | 0.77     | 0.89    | 0.35      |
| 18   | 0.60     | 0.90  | 0.64   | 0.99     | 0.76     | 0.83    | 0.35      |
| 19   | 0.46     | 1.00  | 0.55   | 1.00     | 0.72     | 0.74    | 0.37      |
| 20   | 0.37     | 0.98  | 0.48   | 0.86     | 0.29     | 0.53    | 0.36      |
| 21   | 0.27     | 0.79  | 0.23   | 0.62     | 0.11     | 0.22    | 0.38      |
| 22   | 0.22     | 0.50  | 0.12   | 0.40     | 0.11     | 0.20    | 0.37      |
| 23   | 0.20     | 0.30  | 0.10   | 0.23     | 0.11     | 0.20    | 0.38      |

Table B.2: Wind turbine performance profiles by IEC classification

| Speed (m/s) | $\mathbf{IEC}_{-}1$ | $\bf IEC_{-2}$ | ${f IEC\_3}$ | $off\_shore$ |
|-------------|---------------------|----------------|--------------|--------------|
| 0           | 0                   | 0              | 0            | 0            |
| 1           | 0                   | 0              | 0            | 0            |
| 2           | 0                   | 0              | 0            | 0            |
| 3           | 0.0043              | 0.0052         | 0.0054       | 0            |
| 4           | 0.0323              | 0.0432         | 0.053        | 0.0281       |
| 5           | 0.0771              | 0.1031         | 0.1351       | 0.074        |
| 6           | 0.1426              | 0.1909         | 0.2508       | 0.1373       |
| 7           | 0.2329              | 0.3127         | 0.4033       | 0.2266       |
| 8           | 0.3528              | 0.4731         | 0.5952       | 0.3443       |
| 9           | 0.5024              | 0.6693         | 0.7849       | 0.4908       |
| 10          | 0.6732              | 0.8554         | 0.9178       | 0.6623       |
| 11          | 0.8287              | 0.9641         | 0.9796       | 0.815        |
| 12          | 0.9264              | 0.9942         | 1            | 0.9179       |
| 13          | 0.9774              | 0.9994         | 1            | 0.9798       |
| 14          | 0.9946              | 1              | 1            | 1            |
| 15          | 0.999               | 1              | 1            | 1            |
| 16          | 0.9999              | 1              | 1            | 1            |
| 17          | 1                   | 1              | 1            | 1            |
| 18          | 1                   | 1              | 1            | 1            |
| 19          | 1                   | 1              | 1            | 1            |
| 20          | 1                   | 1              | 1            | 1            |
| 21          | 1                   | 1              | 1            | 1            |
| 22          | 1                   | 1              | 1            | 1            |
| 23          | 1                   | 1              | 0            | 1            |
| 24          | 1                   | 1              | 0            | 1            |
| 25          | 1                   | 1              | 0            | 1            |
| 26          | 0                   | 0              | 0            | 0            |

## Appendix C

# Sample Model Code

This appendix section contains some of the model code that is referenced in the methodology section.

### C.1 Energy System Model Classes

```
class energySystem:
       """ parent to all model classes (base that can have more global variables
       Args:
           name
       11 11 11
       def __init__(self,name,capacity):
           self.initialName = name
           self.capacity = capacity
           self.unit = "kW"
           self.name = self.initialName+" ["+str(round(self.capacity))+"
            11
       def updateName(self):
           self.name = self.initialName+" ["+str(round(self.capacity))+"

    "+self.unit+"]
"

14
   class pvSolar(energySystem):
15
       """ Create a PV solar array class (either solar or wind asset is REQUIRED)
16
       Args:
           capacity (kW)
19
           panel (W)
20
           panel_a (m2) Defaults to 2.
21
           tilt: panels tilt angle from horizontal (°) Defaults to 35.
22
```

```
derate: power derate factor (%/yr) Defaults to 0.004.
23
            alpha: thermal coefficient (%/°C) Defaults to -0.003.
24
            noct: Nominal Operating Cell Temperature (°C) Defaults to 2.
25
            lifetime: system lifetime (years) Defaults to 20.
            capex: capital cost (€/kW) Defaults to 1500.
            opex: operational cost (€/kW/year) Defaults to 18.
28
            emissions: emissions intensity (qCO2e/kWh) Defaults to 43.
29
            lat: latitude of installation (°) Defaults to location latitude
30
        ,, ,, ,,
31
        def __init__(self, name, capacity, panelPowerW,
        panelAream2=2,tiltAngle=False,powerDerate=0.004,thermalCoefficient=-0.0022,
33
34
           NOCT=50,lifetimeYears=20,capexEUR=2500,opexEURkW=30,emissionsgCO2ekWh=43,embedded=1826):
            super().__init__(name,capacity)
35
            self.energykWh = np.zeros(8760)
36
            self.capacity = capacity
            self.panelPowerW = panelPowerW
38
            self.panelAream2 = panelAream2
39
            self.powerDerate = powerDerate
40
            self.thermalCoefficient = thermalCoefficient
41
            self.NOCT = NOCT
42
            self.lifetimeYears = lifetimeYears
            self.capexEUR = capexEUR
            self.opexEURkW = opexEURkW
45
            self.emissionsgCO2ekWh = emissionsgCO2ekWh
46
            self.latitude = globalConfig.lat
47
            self.efficiency = self.panelPowerW/(self.panelAream2*1000)
48
            self.embedded = embedded
            if tiltAngle == False:
51
                self.tiltAngle = globalConfig.lat
52
            else:
53
                self.tiltAngle = tiltAngle
        All energy classes contain methods to calculate performance measurements,
57
        → these include:
        - efficiency (%)
58
        - direct irradiance (W)
        - power output (given specific environmental conditions)
        - Levelised Cost of Energy (€/kWh)
61
        - project cashflow
62
        - yearly energy delivery (for simulation)
63
64
```

```
def updateCapacity(self, value):
65
             self.capacity = np.around(value,2)
66
67
        def findEfficiency(self):
             return self.panelPowerW/(self.panelAream2*1000)
70
        def findPOA(self):
71
             """ output the point of incidence of solar irradiance using the solar
72
             → array tilt, latitude, asumuth angle and time of year
74
             Args:
                 G: irradiance (W/m2)
75
76
             def d2r(d):
77
                 return d*np.pi/180
79
             day =
80
             np.linspace(0,365*len(globalConfig.irradianceWm2)/8760,
81
             → len(globalConfig.irradianceWm2))
             delta = 23.45*np.sin((360/365)*(284+day))
82
             alpha = 90 - self.latitude + delta
83
             return np.array(globalConfig.irradianceWm2*np.sin(d2r(alpha +

→ self.tiltAngle))/np.sin(d2r(alpha)))
85
        def findPower(self):
86
             """ finds the output power of solar asset, taking into account the
87
             \hookrightarrow thermal coefficient (alpha) and the NOCT conditions
             Args:
89
                 G: global irradiance
90
                 T: ambient temperature
91
92
             Returns:
93
                 self.p_vals: array of power output values for the given inputs
95
             Gp = self.findPOA()
96
97
             def load_irr_from_file():
98
                 df = pd.read_excel('inputs/Golden_aSiTandem90-31.xlsx',skiprows=2)
                 Gp = df['POA irradiance CMP22 pyranometer (W/m2)'].to_numpy()
100
                 return Gp
101
102
             noctT = 20
103
             noctG = 800
104
```

```
stdT = 25
105
             stdG = 1000
106
             tauAlpha = 0.9
107
109
             e = self.findEfficiency()
             num = globalConfig.temperatureC + (self.NOCT - noctT)*(Gp/noctG) *
110
                (1-((e*(1-self.thermalCoefficient*stdT))/tauAlpha))
             den = 1 + (self.NOCT - noctT)*(Gp/noctG) * ((self.NOCT*e)/tauAlpha)
111
             cell_t = num/den
112
             thermal_impact = 1 + (self.thermalCoefficient)*(cell_t - stdT)
             irradiance_ratio = self.capacity*(Gp/stdG)
114
             out = irradiance_ratio * thermal_impact
115
             self.energykWh = out
116
             # out = pd.DataFrame({'Power': self.energykWh, 'Cell temp': cell_t,
117
                'Irradiance': globalConfig.irradianceWm2, 'Temp':
             \rightarrow globalConfig.temperatureC})
             # out.to_csv('outputs/PV_model_power.csv')
118
             return self.energykWh
119
120
         def findLCOE(self):
121
             """ finds the Levelised cost of Energy (must run find power first!)
122
123
             Returns:
124
                 LCOE value
125
126
             energy = np.sum(np.abs(self.energykWh))*self.lifetimeYears
127
             self.lcoe = (self.capacity*(self.capexEUR+self.lifetimeYears *
128

    self.opexEURkW))/(energy)

             return self.lcoe
129
130
         def findCashflow(self):
131
             """ determines the asset cashflow over the system lifetime, taking into
132
                account CAPEX and annual OPEX
133
             Returns:
134
                 cashflow: value for each year as an array
135
136
             cashflow = np.zeros(20)
137
             for index, x in enumerate(cashflow):
                 cashflow[index] = cashflow[index]-(self.opexEURkW*self.capacity)
139
                 if (index % self.lifetimeYears) == 0:
140
                     cashflow[index] = cashflow[index]-(self.capexEUR*self.capacity)
141
             return cashflow
142
143
```

```
def findYearlyEnergy(self):
144
             """ calculates the yearly energy output for performanc assessment
145
146
             Returns:
                 yearly energy generated
148
149
             self.yearlyOutput = np.sum(self.energykWh[self.energykWh > 0])
150
             return self.yearlyOutput
151
152
        def findEmissions(self):
153
             self.emissionsgCO2ekWh = (self.embedded*self.capacity*1000) /
154
                 (self.findYearlyEnergy()*self.lifetimeYears)
             return self.emissionsgCO2ekWh
155
156
        def findCostPerYear(self):
157
             cf = self.findCashflow()
158
             self.costPerYearEUR = np.sum(cf[0:self.lifetimeYears])/self.lifetimeYears
159
             return self.costPerYearEUR
160
161
        def findCapacityFactor(self):
162
             self.capacityFactor = (self.findYearlyEnergy()/(365*24*self.capacity))
163
             return self.capacityFactor
164
165
        def finalResults(self):
166
             self.results = {
167
                 'Name': self.name,
168
                 'Energy-Delivered-kWh': self.findYearlyEnergy(),
169
                 'Capacity-Factor': self.findCapacityFactor(),
170
                 'Capital-Cost': self.capexEUR*self.capacity,
                 'Operational-Cost': self.opexEURkW*self.capacity,
172
                 'Levelised-Cost': self.findLCOE(),
173
                 'Emissions': self.emissionsgCO2ekWh
174
             }
175
             return self.results
177
        def terminateStep(self):
178
             self.findEmissions()
179
180
181
    class Battery(energySystem):
182
         """ Create a battery energy storage asset class instance. Lithium battery is
            used, but lead acid or other could be similarly implemented if data is
             known.
184
```

```
Args:
185
             name:
                         battery asset name
186
             capacity:
                         battery capacity (kWh)
187
             eff:
                          efficiency (%) Defaults to 90.
188
                          initial state of charge (%) Defaults to 100.
             soc:
189
             dod:
                          depth-of-discharge (%) Defaults to 90.
190
             max_cycles: maximum lifetime cycles Defaults to 5000.
191
                         maximum lifetime age (years) Defaults to 8
             max_age:
192
                          capital cost (€/kWh) Defaults to 350.
             capex:
193
                         operational cost (€/kWh/yr) Defaults to 22.
             opex:
                         emissions intensity (gCO2e/kWh) Defaults to 89.
195
             emissions:
             lifetime:
                         battery maximum lifetime (years) Defaults to 8.
196
         ,, ,, ,,
197
         def __init__(self, name, capacity, totalEfficiency=95, stateOfCharge=100,
198
            depthOfDischarge=90,
             maximumCycles=8000, maximumAge=10, capexEURkwh=328, opexEURkWhYear=22,
199
                emissionsgCO2ekWh=89,
             lifetimeYears=10, embedded=254):
200
             super().__init__(name,capacity)
201
             self.energykWh = np.zeros(8760)
202
             self.capacity = capacity
203
             self.totalEfficiency = totalEfficiency
             self.stateOfCharge = stateOfCharge
205
             self.depthOfDischarge = depthOfDischarge
206
             self.maximumCycles = maximumCycles
207
             self.maximumAge = maximumAge
208
             self.capexEURkwh = capexEURkwh
209
             self.opexEURkWhYear = opexEURkWhYear
210
             self.emissionsgCO2ekWh = emissionsgCO2ekWh
             self.socValues = np.zeros(8760)
212
             self.socStart = np.zeros(8760)
213
             self.lifetimeYears = lifetimeYears
214
             self.yearlyOutput = 0
215
             self.maxOutput = self.capacity
216
             self.kWh = np.zeros(8760)
             self.unit = "kWh"
218
             self.embedded = embedded
219
220
         def updateCapacity(self,value):
221
             self.capacity = np.around(value,2)
222
         def findNextStep(self, value):
224
             """ This method is used to step forward the model simulation for the
225
                lithium ion battery
```

```
226
             Args:
227
                 value: the energy determined to be available to be sent to/from the
228
                 \rightarrow battery (kWh)
229
             Returns:
230
                 energy: the actual hourly energy sent to/from the battery (kWh)
231
232
             kwhRemaining = np.around(self.capacity *
233
                 (self.stateOfCharge/100-(1-self.depthOfDischarge/100)) *
                 (self.totalEfficiency/100),2)
             kwhToFull = np.around(self.capacity*(1-self.stateOfCharge/100) /
234
             self.kWhSet.append(kwhRemaining)
235
             # Initial check to make sure storage can operate, if not then no energy
236
             \hookrightarrow is converted
             # Battery Discharge Model
237
             if value > 0:
238
                 if value >= kwhRemaining:
239
                     energy = copy.deepcopy(kwhRemaining)
240
                     self.stateOfCharge = 100-self.depthOfDischarge
241
                 else:
                     energy = value
243
                     self.stateOfCharge = self.stateOfCharge -
244
                      → 100*(energy*(100/self.totalEfficiency)/self.capacity)
             # Battery Charge Model
245
             else:
246
                 if -value >= kwhToFull:
                     energy = -copy.deepcopy(kwhToFull)
248
                     self.stateOfCharge = 100
249
                 else:
250
                     energy = value
251
                     self.stateOfCharge = self.stateOfCharge +
252
                      → 100*(-energy/(100/self.totalEfficiency)/self.capacity)
             return energy
253
254
         def initialStep(self):
255
             """Initial simulation function (mostly for resetting important
256
             \rightarrow parameters)
             ,,,,,,
257
             # TODO move initial functions from simulation function to here
258
             self.socValues = np.zeros(8760)
259
             self.socStart = np.zeros(8760)
260
             self.kWh = np.zeros(8760)
261
```

```
self.yearlyOutput = 0
262
            self.kWhSet = []
263
            return
264
266
        def terminateStep(self):
            """final simulation function (used to perform final processes and
267
            \hookrightarrow cleanup)
            11 11 11
268
            self.kWh = np.array(self.kWhSet)
269
            self.findEmissions()
270
            return
272
        def findLifespan(self):
273
            """ Defines the lifespan of the battery based on cycle usage and the
274
            275
            Returns:
276
                self.lifetime: the lifetime of the asset (years)
277
278
            cycles = np.sum(np.abs(self.energykWh))/(self.capacity)
279
            self.lifetimeYears = round(self.maximumCycles/(cycles+1))
280
            if self.lifetimeYears > self.maximumAge:
                self.lifetimeYears = self.maximumAge
282
            return self.lifetimeYears
283
284
        def findLCOE(self):
285
            """ finds the Levelised cost of Energy (must run find power first!)
286
287
            Returns:
288
                LCOE value
289
290
            lifespanYears = self.findLifespan()
291
            num = (self.capexEURkwh*self.capacity +
292
            den = (np.sum(np.abs(self.energykWh))*lifespanYears)
293
            self.lcoe = num/den
294
            return self.lcoe
295
296
        def findCashflow(self):
297
            """ determines the asset cashflow over the system lifetime, taking into
298
             → account CAPEX and annual OPEX
299
            Returns:
300
                cashflow: value for each year as an array
301
```

```
,, ,, ,,
302
             cashflow = np.zeros(20)
303
             for index. x in enumerate(cashflow):
304
                 cashflow[index] = cashflow[index]-(self.opexEURkWhYear*self.capacity)
306
                 if (index % self.lifetimeYears) == 0:
                      cashflow[index] =
307
                          cashflow[index]-(self.capexEURkwh*self.capacity)
             return cashflow
308
309
         def findYearlyEnergy(self):
             """ calculates the yearly energy output for performanc assessment
311
312
             Returns:
313
314
                 yearly energy output
315
             self.yearlyOutput = np.sum(self.energykWh[self.energykWh > 0])
316
             return self.yearlyOutput
317
318
         def findEmissions(self):
319
             self.emissionsgCO2ekWh = (self.embedded*self.capacity*1000) /
320
                 ((self.findYearlyEnergy()+0.001)*self.findLifespan())
             return self.emissionsgCO2ekWh
321
322
         def findCostPerYear(self):
323
             cf = self.findCashflow()
324
             self.costPerYearEUR = np.sum(cf[0:self.lifetimeYears])/self.lifetimeYears
325
             return self.costPerYearEUR
326
327
         def findCapacityFactor(self):
328
             self.capacityFactor = (self.findYearlyEnergy()*2)/(365*24*self.capacity)
329
             return self.capacityFactor
330
331
         def finalResults(self):
332
             self.results = {
                 'Name': self.name,
334
                  'Energy-Delivered-kWh': self.findYearlyEnergy(),
335
                  'Capacity-Factor': self.findCapacityFactor(),
336
                  'Capital-Cost': self.capexEURkwh*self.capacity,
337
                  'Operational-Cost': self.opexEURkWhYear*self.capacity,
338
                  'Levelised-Cost': self.findLCOE(),
339
                  'Emissions': self.emissionsgCO2ekWh
340
341
             return self.results
342
343
```

### C.2 Multi-objective Optimisation Routine

```
def multiOptimise(sys,pop=100,gens=250,mutation=0.5,crossover=0.75):
        sys.totalCost = []
        with open(r"optimsys.pkl", "wb") as file:
            pickle.dump(sys,file)
        class myProblem(ElementwiseProblem):
            # initial, upper, lower, idx = processObjects.initials(system)
            def __init__(self, sys, **kwargs):
10
                super().__init__(sys,
11
                                 n_{obj} = 2,**kwargs)
12
                initial, upper, lower, index = initials(sys)
                self.xl = np.asarray(lower)
                self.xu = np.asarray(upper)
15
                self.n_var = index
16
            def _evaluate(self, x, out, *args, **kwargs):
                with open(r"optimsys.pkl", "rb") as file:
                    system = pickle.load(file)
                idx = 0
22
                for generator in system.generator:
                    generator.updateCapacity(x[idx])
                    idx += 1
                for storage in system.storage:
                    if isinstance(storage,energyObjects.Battery) is True:
                        storage.updateCapacity(x[idx])
                        idx += 1
29
                    else:
                        storage.fuelCellPowerkW = np.around(x[idx],2)
                        storage.electrolyserPowerkW = np.around(x[idx],2)
33
                        idx += 1
35
                system.simulation()
36
                F1 = system.findSavings()
                F2 = system.findGlobalDecarbonisation()
                out["F"] = [F1,F2]
39
40
        class MyCallback(Callback):
41
            def __init__(self) -> None:
42
```

```
super().__init__()
43
                 self.data["best"] = []
44
45
        problem = myProblem(sys)
48
        algorithm = NSGA2(
49
            pop_size=pop,
50
            sampling=FloatRandomSampling(),
51
            crossover=SBX(prob=crossover, eta=15),
            mutation=PM(prob=mutation, eta=20),
            eliminate_duplicates=True
54
        )
55
56
        termination = get_termination("n_gen", gens)
57
        print("Running multi-objective optimisation routine...")
59
60
        res = minimize(problem,
61
                     algorithm,
62
                     termination,
63
                     seed=1,
                     save_history=True,
65
                     callback=MyCallback(),
66
                     verbose=True)
67
68
        return res
69
```